UNIVERSITY OF KWAZULU-NATAL

COLLEGE OF AGRICULTURE, ENGINEERING AND SCIENCE

STUDY OF A SOLAR-ASSISTED AIR CONDITIONING SYSTEM FOR SOUTH AFRICA

Jerusha Sarah Joseph

Dissertation submitted in fulfilment of the degree, MSc Eng in Mechanical Engineering, School of Engineering, University of KwaZulu-Natal

Durban

20th December 2012

Supervisor

Dr Freddie L. Inambao

As the candidate's Supervisor I agree to the submission of this thesis.

Dr Freddie L. Inambao

……. ……..

NAME OF SUPERVISOR SIGNATURE

COLLEGE OF AGRICULTURE, ENGINEERING AND SCIENCE

DECLARATION 1 – PLAGIARISM

I, Jerusha Sarah Joseph, declare that:

(i) The research reported in this dissertation/thesis, except where otherwise indicated, is my original work.

(ii) This dissertation/thesis has not been submitted for any degree or examination at any other university.

(iii) This dissertation/thesis does not contain other persons' data, pictures, graphs or other information, unless specifically acknowledged as being sourced from other persons.

(iv) This dissertation/thesis does not contain other persons' writing, unless specifically acknowledged as being sourced from other researchers. Where other written sources have been quoted, then:

a) their words have been re-written but the general information attributed to them has been referenced;

b) where their exact words have been used, their writing has been placed inside quotation marks, and referenced.

(v) Where I have reproduced a publication of which I am an author, co-author or editor, I have indicated in detail which part of the publication was actually written by myself alone and have fully referenced such publications.

(vi) This dissertation/thesis does not contain text, graphics or tables copied and pasted from the Internet, unless specifically acknowledged, and the source being detailed in the dissertation/thesis and in the References sections.

Signed

……..

COLLEGE OF AGRICULTURE, ENGINEERING AND SCIENCE

DECLARATION 2 – PUBLICATIONS

DETAILS OF CONTRIBUTION TO PUBLICATIONS

Publication 1: Joseph J.S. and Inambao F.L., "Utilizing Solar Energy for Air Conditioning", Botswana Institution of Engineers (BIE), 12th Biennial Conference, 3rd -5th September 2011, pp 272-276.

In this paper, I, Jerusha Sarah Joseph was the main and corresponding author, whilst Dr Freddie L. Inambao was the co-author and my research supervisor.

Signed

……..

ACKNOWLEDGEMENTS

I acknowledge my supervisor, Dr Freddie L. Inambao for all of his guidance with regards to the MScEng research study and the inspiration received from his high expectations of me. I also acknowledge my family for their support and patience with me in regard to my absence due to the dedication required for this degree.

Special thanks to my employer, Airports Company South Africa, especially the management of King Shaka International Airport for allowing me time off from work duties to complete my testing at Netcare's Pretoria Moot Hospital Solar Powered Absorption Cooling Plant in Gauteng.

I acknowledge the management of Voltas Technologies, Cristian Cernat and Frank Major for affording me the opportunity to do a study on their first ever installed Solar Powered Absorption Cooling Plant in South Africa, together with Flip Jacobs, the Technical Manager of Pretoria Moot Hospital.

Finally, but not least, I acknowledge and thank the Creator of the sun, to whom this dissertation is dedicated, for empowering, strengthening and moulding my way to its successful completion thereof.

ABSTRACT

In South Africa, a significant amount of electrical energy is used for air conditioning in commercial buildings, on account of the high humidity experienced. Due to its geographical location, the levels of solar irradiation and the demand for air-conditioning of commercial buildings reach maximum levels simultaneously. The South African region daily solar radiation average varies between 4.5 and 6.5 kWh/m^2 and when compared to the United States $3.6\,kWh/m^2$ and Europe's $2.5\,kWh/m^2$, solar thermal powered cooling technologies has significant potential as this solar irradiation is also available all year around [1].

Utilizing solar energy for an air conditioning system has the advantage that the availability of solar radiation and the need for cooling reach maximum levels simultaneously and proportionally. This type of air conditioning system has an electrical energy saving benefit in light of increasing energy tariffs and the energy crisis currently facing Eskom in South Africa.

Solar-assisted Absorption Cooling systems decreases the peak electricity consumption, is less noisy and vibration free, since it does not contain a compressor and this gives a higher reliability, low maintenance and its electricity consumption is approximately four times less (21.8kW versus 5.5kW for 35kW of Cooling) than that of an electric driven chiller containing a mechanical compressor [2].

However, due to the high capital cost of solar powered air-conditioning plants, it is essential that a feasibility analysis be undertaken to indicate and establish a return on capital investment.

The main objective of the present study is to investigate and establish the feasibility of a solar-assisted air-conditioning system based on Lithium Bromide and Water ($LiBr/H_2O$) absorption chillers on a medium scale for commercial buildings in terms of energy saving and performance. This study presents the results of the experiment on a solar-assisted air-conditioning facility constructed and installed in October 2009 at Pretoria's Netcare Moot Hospital.

This study has confirmed that a payback period of 13 months can be achieved and the performance parameters of the manufacturer's specifications for a solar-assisted air conditioning system are exceeded for the South African climate.

Keywords: *Absorption Chiller, Solar-Assisted HVAC, Solar Collector Efficiency, Energy Efficiency, Feasibility Analysis*

LIST OF CONTENTS

LIST OF FIGURES

LIST OF TABLES

NOMENCLATURE

Latin Symbols

a	Contact area/Tower volume	$[m^2/m^3]$
A	Area	$[m^2]$
C_p	Specific heat capacity	[kJ/kgK]
G	Global Solar Radiation	$[W/m^2]$
G_m	Gas mass	[kg]
h	Enthalpy	[J/kg]
K	Mass transfer coefficient	$[kg/ms^2]$
L	Water rate (cooling tower)	$[kg.ms^2]$
L_m	Liquid mass	[kg]
$\dot{m}$	Mass flow rate	[kg/s]
P	Power	[kWh]
q	Energy per unit mass	[kJ/kg]
$\dot{q}$	Rate of energy per unit collector area or per unit mass	$[W/m^2$ or W/kg]
Q	Energy (heat)	[kJ]
$\dot{Q}$	Rate of energy	[W]
T	Temperature	[K or °C]
U_L	Overall heat loss coefficient for the collector	$[W/m^2K]$
V	Active cooling volume/plan area	$[m^3/m^2]$
W	Work	[kJ]

Dimensionless numbers

F_R	Collector's heat removal factor
n	Number of
R_H	Relative Humidity

Greek symbols

α	Heat loss coefficient	$[W/m^2K]$
α_{la}	Linear heat loss coefficient	$[W/m^2K]$

α_{2a}	Quadratic heat loss coefficient	[W/m^2K^2]
ΔT	Difference between two temperatures	[K or °C]
ε	Effectiveness	[-]
η	Efficiency	[-]
$\tau\alpha$	Collector transmittance absorptance product	[-]

Subscripts

0	Without heat losses
a	Air-water vapour mixture at wet bulb temperature
abs	Absorption process
aper	Aperture
avg	Average
b	Bulk water
c	Cold water
coll	Collector (solar)
elec	Electrical
gen	Generator
h	Hot water
L	Refrigerated space
m	Mean
o	Environment
pump, in	Pump input
rad	Radiation (Solar)
rev, abs	Reversible conditions for the absorption process
s	Heat source
solar	Solar
tank	Hot water storage tank
U-pipe	U-pipe collector
w	Air-water vapour mixture at bulk water temperature

LIST OF ABBREVIATIONS AND ACRONYMS

BMS	Building Management System
COP	Coefficient of Performance
CSIR	Council for Scientific and Industrial Research
CHWRT	Chilled Water Return Temperature
CHWST	Chilled Water Supply Temperature
CWRT	Cooling Water Return Temperature
CWST	Cooling Water Supply Temperature
DBSA	Development Bank of Southern Africa
DME	Department of Minerals and Energy
HVAC	Heating, Ventilation and Air Conditioning
HWRT	Hot Water Return Temperature
HWST	Hot Water Supply Temperature
IEA	International Energy Agency
ISE	Institut Solare Energiesysteme
Mtoe	Million tonnes oil equivalent
PI	Proportional Integral
PID	Proportional Integral Derivative
RAC	Refrigeration and Air Conditioning
UHI	Urban Heat Island
USA	United States of America

CHAPTER 1: INTRODUCTION

This Chapter contextualizes the study of the Solar-assisted Absorption Cooling system investigated in this thesis. The background presents the importance and need for the study followed by the Aims and Objectives, the Scope and the Thesis Layout. The Original Contribution and Publications are also presented in this Chapter.

1.1 Background

Thermal comfort is a necessity for corporate and commercial environments in South Africa. Due to the construction of multiple storey commercial and office buildings and the warm, humid South African climate, natural ventilation is not adequate to ensure thermal comfort of occupants for a conducive and productive occupational space. For this reason, most, if not all these buildings employ air conditioning systems to control indoor air circulation, humidity and temperature.

These air conditioning systems are predominantly chilled water cooling systems driven by mechanical compression plants using R134a refrigerant. These chillers have a coefficient of performance (COP) typically of between 2.5 and 3.5. However, the electricity consumption by these chillers is significantly higher than the electricity consumption of other building services. Typically building services that include lighting, electronic devices and appliances account for 57% of the electricity consumption and thermal comfort systems (Heating, Ventilation and Air Conditioning - HVAC) make up the remaining 43%. Figure 1.1 depicts the energy consumption and costs breakdown for an office building in Pretoria, South Africa.

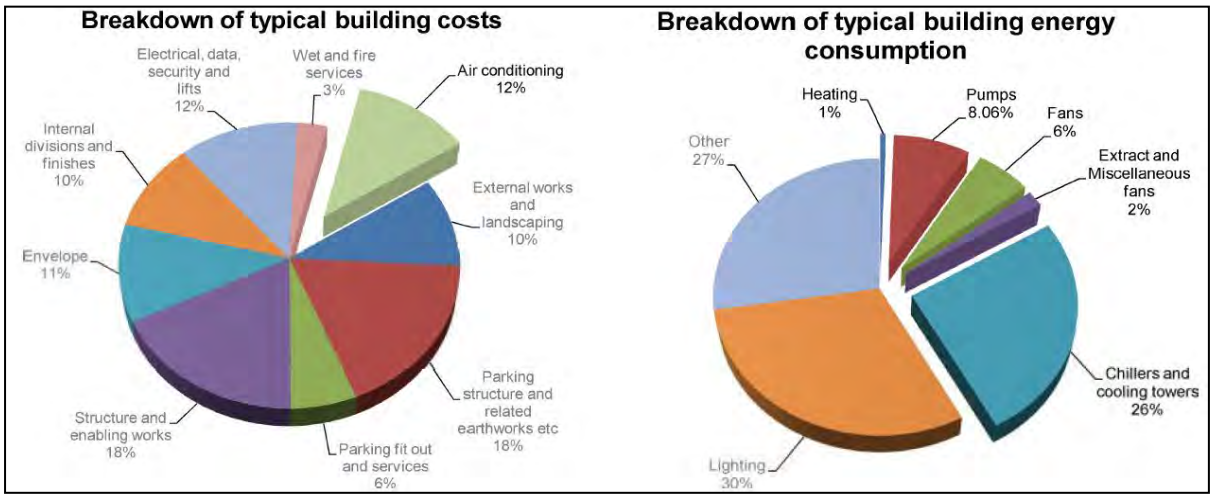

Figure 1.1 Typical buildings cost and energy costs of buildings facilities/utilities share breakdown for an office building in Pretoria, South Africa [3].

In some instances, for areas experiencing higher humidity like Durban and Cape Town, HVAC systems can account for more than 50% of the electricity usage in office buildings. Comparing the two breakdown costs presented in Figure 1.1, it can be seen that the major cost implications of HVAC systems does not occur in the 'building cost' breakdown where the capital cost of equipment and installation is represented, but in the 'energy cost' breakdown. The HVAC system consumes almost 50% of the cost of the buildings energy. The cost incurred for 'Building Costs' are fixed compared to that incurred for 'Energy Costs' that are subject to fluctuations and in light of the present energy crisis and uncertainty in the availability of electricity at all times, it is increasing steadily. Installing an HVAC system that minimizes capital cost at the expense of electrical energy consumption cost exposes the energy consumption model to possible exorbitant cost that may exceed the building cost and thus asset value of the building service.

In the later months of 2007 South Africa started experiencing widespread rolling blackouts as supply fell behind demand, threatening to destabilize the national grid. With a reserve margin estimated at 8% or below, such "load shedding" is implemented whenever generating units are taken offline for maintenance, repairs or re-fueling (in the case of nuclear units) [4].

In light of South Africa's public utility provider, Eskom's reserve margin being 10% below the required 15% reserve margin as recorded in November 2008, reducing electricity demand is unavoidable [5]. Due to South Africa's fortunate position in terms of its abundant insolation experienced all year around, absorption cooling cycles driven by thermal energy exploits the availability of this solar energy.

Absorption refrigeration systems are an alternative to vapour compression systems due to the increase of environmental problems and electricity cost. In recent years, research has been increased to improve the performance of the absorption systems [6].

Vapour Absorption Systems using water as the refrigerant and Lithium Bromide as the absorbent represent the simplest idea in absorption refrigeration technology and are assuming greater importance due to their environmentally friendly operation. The cost of these systems is dependent on whether they are single or double effect. This in turn depends on the application and the source of heat available [7].

The performance and hence viability of vapour absorption cooling cycles driven by a solar thermal energy source is dependent on factors prevailing at the installed location, i.e. humidity and insolation

available. Many absorption cycle solar thermal driven systems have been proven and installed worldwide, [8] however these types of systems have received little attention in South Africa.

The present study aims to investigate the viability of solar absorption based cooling systems driven by a solar thermal energy source for commercial and office buildings in South Africa.

1.2 Aims and Objectives

Due to the nature of air-conditioning in that it involves temperature and humidity control of an enclosed space, the challenges that arise will be different at the various geographical locations. The challenges further differ in nature when one decides to utilize solar energy available as insolation falling on the earth differs at various geographical locations.

Various technologies exist and have been in the market for the last few decades that utilize solar energy for air conditioning of enclosed spaces which proves that the scientific principle on which it operates is successful. There is a need to demonstrate that the technology is efficient and that it will ensure a significant saving of electrical power, taking into consideration the prevailing conditions at the specific geographical location. There exists a need to investigate the implementation of the Solar-assisted Air conditioning technologies in South Africa, a country situated in the Southern Hemisphere.

The aim of this study is to establish the feasibility in terms of electrical energy savings and cooling performance of an efficient solar-assisted air-conditioning system to reduce the energy consumption of commercial buildings.

To achieve this, an assessment of an absorption cooling plant that uses Lithium Bromide and water ($LiBr/H_2O$) as a working pair be completed. The objectives of this study are summarized below:

1. Actual testing of the solar-assisted HVAC system performance.

2. Assess the feasibility of implementing a medium scale Solar-Assisted Space Heating and Air Conditioning System.

3. Anticipate a 50% saving in electricity cost by running this type of system instead of a conventional compressor-refrigerant air conditioning system powered through the electricity grid.

1.3 Scope of the study

The study focused on the analysis of the parameters involved in the production of chilled water using solar thermal energy via a single effect Absorption chiller into a storage buffer tank. The study investigates the performances of the solar thermal collector system and the absorption chiller for the four seasons in the year. The capital cost, maintenance and operating cost and payback period of adopting a solar absorption cooling plant were also studied.

Included in the study is the investigation of the various parameters such as passive cooling, heat transfer, air distribution, absorption cooling, etc. involved in the design process of any cooling system in general. The full content of the study is summarized in Chapter 1.4 following.

1.4 Thesis Layout

The dissertation is set out to achieve the aims and objectives in ten chapters. Each Chapter's content is summarized below.

Chapter 1 presents the background to the study which explores the importance and need for Solar Powered Absorption Cooling systems in office buildings. Contained in this Chapter are the orientation, layout, content, scope and original contribution of the study.

Chapter 2 is a literature review and presents the feasibility analysis of Solar-assisted Absorption Cooling Systems that were installed in countries outside of South Africa. The review is done in the format of a case study.

Chapter 3 describes the various types of Solar Thermal Cooling technologies available in the international market. A snapshot of the installed Solar Thermal Cooling systems around the world is given together with a comparison of all the systems.

Chapter 4 investigates the Energy Consumption in South Africa, Energy use by sector carbon-dioxide emissions of countries around the world and the economic sectors in South Africa responsible for greenhouse gases emissions. This Chapter also covers South Africa's public utility provider, Eskom's energy crisis and the link between air conditioning and electricity usage and the renewable energy potential in South African countries.

Chapter 5 covers the energy efficient design principles resulting in reducing the internal air conditioning load, addressing absorption cooling principles, solar thermal collectors, Air Handling Units, Cooling Tower, Control System and the manner in which they are all connected.

Chapter 6 sets out the testing methodology, i.e. the testing models that were developed to achieve the aims and objectives; data acquisition and the parameters being monitored for the testing of the Absorption Cooling Plant at Pretoria's Netcare Moot Hospital.

Chapter 7 gives a description of the testing facility at the Pretoria Netcare Moot Hospital Absorption Cooling Plant.

Chapter 8 presents and discusses the results of the performance of the Absorption Cooling Plant at Pretoria's Netcare Moot Hospital.

Chapter 9 investigates the feasibility analysis of the Absorption Cooling Plant in terms of Electricity savings and technical efficiency of the Absorption Cooling Technology.

Chapter 10 summarizes the conclusion from the results obtained in Chapters 8 and 9. The recommendations for the future work are also given in this Chapter.

1.5 Original Contribution of the study

Solar-assisted absorption cooling systems using water as a refrigerant and Lithium Bromide as an absorbent is not a new technology, however it has not previously been installed and tested in South African climate and therefore there is no existing performance data for this type of air-conditioning system. This study contributes to the knowledge and feasibility data of the Absorption Cooling system using Solar-thermal heat in South Africa.

1.6 Publications

Appendix A1 contains the published peer reviewed conference paper entitled "Utilizing Solar Energy for Air Conditioning".

CHAPTER 2: LITERATURE REVIEW

This Chapter presents feasibility analyses of Solar-Assisted air conditioning systems that were carried out for countries outside of South Africa. The case studies are based on Solar-Assisted Absorption Cooling systems similar to the Cooling system investigated in this dissertation for various countries. Each case study has systems that vary in cooling capacity and spatial usage and their feasibility analyses were carried out using tariff assumptions and costs pertaining to the specific country of installation.

2.1 Introduction

The International Energy Outlook 2005 projects that world net electricity consumption will nearly double over the next two decades. The energy to run all the refrigeration machines, including air conditioning plants and heat pumps accounts for between 10% and 20% of the total worldwide electricity consumption [9]. Urbanization results in the increased need for thermal comfort. This phenomenon is discussed in more detail in Chapter 4.2. It was deduced that the increasing need for cooling can be due to the increase in the number of office buildings.

Figure 1.1 shows that HVAC consumed about 43% of typical buildings total energy consumption in Pretoria. Air conditioning consumed approximately 40% of the total electricity consumption in comparison to lighting and other electrical appliances in office buildings in Malaysia [10].

A survey conducted by the Japan Refrigeration and Air Conditioning Industry Association (JRAIA) showed that the number of air conditioners in the world are increasing rapidly, which will have an effect on the electricity consumption since worldwide production of cooling is mainly based on conventional vapour compression chillers [9]. Absorption cooling systems have been established as an energy-saving and environment friendly alternative to conventional vapour compression cooling devices [11].

2.2 History of Absorption Cooling

The discovery of refrigerants gave birth to the refrigerator, “artificial ice” and later on space cooling systems. The earliest record of artificial cooling comes from ancient Egypt when slaves were required to fan earthenware pots. This is the same idea as the earthenware milk cooler.

Water was in a shallow earthenware dish below and milk in a bottle was placed in the water and a second deeper earthenware dish was placed over it. The evaporation of the water keeps the upper cover wet which cools the milk inside. Earlier techniques and methods of cooling were more natural than artificial. Rome used to collect snow and using insulation the snow could last for a surprisingly large period of time without melting. The Romans cooled their wine and also made ice cream.

By the 19th Century various other liquids were discovered that evaporated much faster than water, e.g. alcohol. It was also discovered during that time that various gases, when compressed will condense to liquid.

Carbon dioxide was also used as a refrigerant as it is a liquid under pressure at room temperature. By opening the valve of a cylinder of carbon dioxide, it will very quickly evaporate into a gas with the cooling effect being quite dramatic. If this gas is however collected and compressed again, it will go back into a liquid and a cycle is established. This cycle is the principle of refrigeration and the role of the refrigerant in space cooling [12].

This gave birth to the mechanical compression cooling cycle which persists to the present times using predominantly R134a refrigerant. The mechanical compression cycle is efficient and reliable; however, due to the rise in electricity costs and uncertainty about its availability from present resources being utilized, alternatives to the mechanical compression cycle have been explored. These alternatives are not necessarily new inventions; on the contrary, they are inventions that have been existing for many decades that didn't receive much attention, for example the absorption cooling cycle.

The absorption cycle was invented by Ferdinand Carre when he sought to produce ice with heat input in 1846. The absorption cycle was used much in the 1920s in gas powered refrigerators/ice makers using the principle that absorbing ammonia in water causes the vapour pressure to decrease. This cycle is often viewed as chemical vapour-compression cycle with the compressor replaced by a generator, absorber and liquid pump [13].

Dutil and Rousse (2010) [14] reviewed the history of solar cooling technologies in their publication on "A review of active Solar Cooling Technologies" which is summarized in the paragraphs below.

At first glance, solar cooling is counter intuitive: how do you cool something by using a heat source, while not violating any laws of Thermodynamics. There is the simple solution of using a photovoltaic solar panel to drive a classical heat pump or a thermoelectric cooler. Alternatively, one could use the

heat to drive a thermal motor, which itself would drive the thermo-pump. If those techniques are possible, they tend to be ineffective. This is why, in most system, the functional principle is to emulate the classical heat pump evaporation-condensation cycle by replacing the compressor by a sorption cycle, which has the same function.

The cooling technologies based on this principle are quite old. In 1929, Miller [15] described several systems, which utilized silica gel and sulfur dioxide as an adsorbent/adsorbate pair. During the 1930s and 40s, Midgley, jr. [16] and co-workers, working for the Kinetic Chemical Company revolutionized the chemistry of operating fluids for refrigeration. Simultaneously, Altenkirch and Bichowsky [17] were putting forward concepts and technical solutions for open absorption systems that are still used today. Later, Berestneff [18] developed LiBr/H_2O systems for the Carrier Corporation. However, the development of cheap reliable compressors and electrical motors and the improvement in power station efficiency as the introduction of CFCs in the 1930s, sorption refrigeration became a niche technology [19].

In the 1960s, solar-powered absorption systems were considered for air-conditioning [20, 21]. The first large-scale experiment of their usage for air-conditioning can be traced to the 1970s. Indeed, in 1976, around 500 solar-powered air-conditioning systems were installed in USA, most of them were absorption systems using the LiBr/H_2O cycle [14]. Meanwhile in Japan, a solar heating and cooling system with flat-plate collectors and absorption refrigeration machine was installed [22].

In 1977, the International Energy Agency (IEA) started the Solar Heating and Cooling program. The Task 25 of this program Solar-Assisted Air Conditioning of Buildings, which ended in 2004, focused on the use of solar energy for air-conditioning of buildings. The main objective of the task was to improve conditions for the market entry of solar-assisted cooling systems [23].

Following the second oil shock in 1979, many projects on solar cooling were developed; some of them were available in the market [24]. In the 1990's, the need to curtail the usage of the ozone depleting refrigeration fluid, following the introduction of the Montreal protocol in 1988, lead to a renewal in interest for the alternative cooling technologies [25].

Solar cooling technology presents a great advantage of being well coupled with the thermal load, which attenuates the peak electricity demand driven by cooling needs in summer. As the planet warms and heat island increases, this problem will become more pressing in the future. The total energy consumption is also reduced. In southern European and Mediterranean areas, solar-assisted cooling systems can lead to primary energy savings in the range of 40–50% [26]. Today, the technology is

relatively mature, and many commercial solar cooling systems are sold. These are essentially based on three technologies: absorption, adsorption and desiccant cooling. Recently, a few systems were also developed to provide both cooling and water heating [27].

Presently the technology developments have made the absorption refrigeration cycle an economic and effective alternative to the vapour compression cooling cycle [28].

2.3 Solar Thermal Technologies Development

Solar energy is receiving much more attention in building energy systems in recent years. Solar thermal utilization should be based on integration of solar collectors into buildings [29]. The solar thermal collector component of the solar-assisted absorption cooling system is the single most expensive component of the system that serves as a generator of power. Much focus has been placed on the optimum design of the solar collector to optimize its efficiency while reducing the capital cost required. Two categories are addressed and vital with regards to the incorporation of solar collectors into building structures. The installation mode of the solar collectors is one of them. Without spoiling building facades, it is possible for solar collectors to be installed on balconies, roofs and walls. The design of the hot water systems is the other category vital to the integration of solar collectors [29]. It is best to install the hot water storage tanks in equipment rooms or in attics, such that they are separate from solar collectors [30, 31].

Typical dimensions of roof module collectors or solar roofs are about $20m^2$ in Europe and may sometimes include roof insulation and beams [32]. Hassan and Beliveau [33] designed an integrated roof solar collector that adequately addressed the ease of construction, energy efficiency, functional integration, composite behavior, reliability and economic feasibility. This lead to a collector design that combines replicability in manufacturing, quality and simplicity. The thermal performance was evaluated by three-dimensional finite element models that were developed for the integrated roof solar collector. According to the thermal performance results obtained, approximately 85% of the building space heating requirements and hot water demand were supplied by the integrated roof collectors and this is acceptable performance [33].

Matuska and Sourek [34] investigated integrating solar thermal collectors concept for water heating as a façade into the existing building stock in the Czech Republic utilizing panel and brick blocks for the construction of flats that were ready for large-scale renovation. The thermal behavior of facade collector systems compared with that of standard roof located collectors were undertaken for domestic hot water systems. Results reported that facade solar collectors should have and area larger by

approximately 30% in order to attain the required 60% solar fraction as compared with conventional solar roof collectors at a 45 degree angle to the horizontal surface [34].

Chow et al. [35] embarked on an experimental study of a centralized photovoltaic and hot water collector wall system that could be used as a water pre-heating system. The solar collectors were secured on vertical facades. The result of the thermal efficiency was about 38.9% at zero reduced temperature at the corresponding electricity conversion efficiency of 8.56%. This was done during the late summer in Hong Kong [35].

Wei et al. [36] studied balcony-integrated solar collectors. Evacuated tubular solar collectors were placed horizontally on sideboards of balconies at a height of 1.1m. The motherboards of balconies were additionally extended outwards by 0.15m in accordance to the solar collectors thickness [36]. One of the main disadvantage faced by solar collectors is aesthetic in nature as its black colour and unsightly tubes and absorber sheet corrugations are not welcomed by architects. For this reason a certain freedom in colour choice would be desirable, without sacrificing thermal performance. Using many layers of interference filters on the collector glazing produces a colored reflection. This aids in camouflaging the corrugated metal sheet, without significantly hindering the transmittance of the absorber. Schuler et al. explored the potential of quarter-wave stacks. This was accomplished by simulating their optical behavior. The required number of individual layers in the multilayer stack together with the choice of refractive indices and thin film materials were discussed. Using these parameters, combinations for efficient multilayer designs were presented [37].

Tripanagnostopoulos et al. [38] tested different outdoor models. These were constructed with black-brown, blue-brown and red brown absorbers. It was estimated that solar collectors with coloured absorbers were useful, from their experimental and theoretical results, for solar thermal applications. They provided the flexibility needed for the aesthetic reasons of architects who would not otherwise want to use black absorbers for a variety of applications that required aesthetic compatibility for the purposes of integrating solar collectors with building [38].

Renovation of buildings provides another feasible opportunity for the integration of solar collectors into buildings. Zhai [39] and Dalenback [40] reported that solar collectors might improve the building envelope e.g. when a flat roof is rebuilt to an inclined ‘solar roof’, or new space was created by adding ‘solar attic’ onto a flat-roofed building. The research and development related to solar cooling systems is centered more often on solar absorption cooling systems presently. More than ten solar cooling demonstration projects have been installed following the installation of the first solar powered absorption cooling system in Shenzhen in 1987 [29].

During 1995-2000, a large scale solar absorption air conditioning system driven by evacuated tubular solar collectors, for the Ninth Five-year research project, was installed in Rushan, the province of Shandong. [41] The cooling capacity of the system is rated at 100kW, with average cooling Coefficient of Performance (COP) of 0.57 [41]. Another solar absorption air conditioning system with 100kW cooling capacity driven by flat-plate solar collectors was commissioned in Jiangmen, province of Guangdong. The average cooling Coefficient of Performance (COP) was 0.4 calculated from experimental results [42].

During 2001-2005, for the Tenth Five-year research project, the two popular solar absorption cooling systems of Tianpu and Beiyuan were all built in Beijing. This contributed greatly to the concept of the green Olympics in 2008. A 200kW solar absorption cooling system constructed for the Tianpu demonstration project, assisted by a ground source heat pump with the cooling capacity of 391kW [43]. Chilled water produced by the solar cooling system was stored in the cold storage water tank of 1200m^2 capacity, in this system. Constructed underground with the intention of reducing thermal loss, was the large water tank. More importantly, it had the ability of fulfilling seasonal energy storage needs. During the spring season, the solar cooling system produced chilled water which could be stored potentially for use in the summer period. Maintaining the contents of the cold storage water tank at the preset temperature meant that the ground source heat pump had to be switched on when the water temperature rose higher than $18\,^{\circ}C$ and as required between 22:00 and 07:00 to reap the benefit of low priced electricity. It was concluded that the cooling output could reach 266kW with a thermal Coefficient of Performance of 0.8. The solar Coefficient of Performance was between 0.2-0.3. The solar collecting efficiency averaged more than 40%.

At present, the largest solar cooling system constructed in China is the demonstration project at Beiyuan. This was commissioned in 2005 [44]. This system employed heat pipe evacuated tube solar collectors with the totaling an area of 665m^2. Solar collectors of this type have the highest thermal efficiency and frost resistance and this is vital as the solar cooling system's energy is derived from the thermal energy collected from the collectors. It also works efficiently at high operating temperatures as the operating temperatures in summer is between $80\,^{\circ}C$ - $95\,^{\circ}C$. A single effect LiBr absorption chiller was chosen to supply cooling for the building area of 3000m^2. A COP of 0.7 was achieved when the hot water temperature was between $83\,^{\circ}C$ and $88\,^{\circ}C$, this calculated to a cooling capacity of 360kW. An electric boiler was used as an auxiliary heat source maintained the hot water thermal requirement for high efficiency cycles of the chiller. A hot water storage tank with a volume of 40m^3 was installed to collect and store heat from the solar collectors and electric boilers. An additional water tank with a holding capacity of 30m^3 capacity was employed to store chilled water produced by

the chiller. It was concluded from the experiments that when the atmospheric or outside temperature was about 30.3 °C , the average solar collecting efficiency and Coefficient of Performance of the chiller were 0.42 and 0.75 respectively. The average indoor air temperature was 23.8 °C .

The case studies of three Absorption cooling systems from countries outside of South Africa will be presented as a showcase of their economic viability.

2.4 Case Study 1: Solar Absorption Cooling system in Malaysia (2009)

Haw et al, [10] performed an overview of solar-assisted air conditioning systems in small office buildings in Malaysia. Their investigation provided a technical overview and economic feasibility of a solar-assisted air conditioning system under Malaysian climatic conditions. The study was not confined to a specific installed system, but was sized for a generic case should one consider using a solar-assisted Absorption Cooling System. The sizing of the evacuated solar collector tubes was designed for a BROAD chiller. BROAD chillers are a brand of chillers manufactured in China. The following calculation was performed to determine the number of chillers needed. According to the study performed by Haw et al, [10], the required collector area per cooling capacity is defined by the following three parameters:

- Incident solar radiation for Malaysia (G) = 800W/m^2 or 0.8kW/m^2
- Solar collector efficiency (η_{coll}) = 0.7 or 70%
- Chiller COP = 0.7 or 70% (Using BROAD Chiller = 23kW)

The following equation was used to determine the collector area needed for the Malaysian climate in South East Asia in the Northern Hemisphere:

$$A = \frac{1}{G \times \eta_{coll} \times COP} \quad \text{..... (Equation 2.1)}$$

Where:

A Area (m^2)

G Incident Solar Radiation (kW/m^2)

η_{coll} Solar Collector Efficiency (%)

COP Coefficient of Performance [-]

Using Equation 2.1 and the parameters above gives the following:

$$A = \frac{1}{G \times \eta_{coll} \times COP} = \frac{1}{0.800 \times 0.7 \times 0.7} = \frac{1}{0.392} = 2.55 m^2 \text{ per kW}$$

For a 23kW absorption chiller, the required area for the solar collectors using the Figure calculated above is given below:

Coverage area of evacuated tubes = 23 kW $\times$ 2.55 m^2/kW
= 58.65 m^2

For evacuated tubes that have an area of 0.1 m^2 each, the number of tubes required is calculated below:

$$\textbf{Number of evacuated tubes needed} = \frac{58.65 m^2}{0.1 m^2} = 587$$

If each set has 30 evacuated tubes, the number of sets needed is 20. Similarly, to power 35kW of cooling, 20 sets of evacuated tubes are required for the daily average solar radiation of between 4.21kWh/m^2 to 5.56kWh/m^2.

The economic feasibility of this solar-assisted air conditioning system is deducted from the payback period using the 2009 electricity tariff in Malaysia and the cost of the solar-assisted air conditioning system. The assumptions for the payback period calculation are given below:

- 2009 Electricity tariff rate in Malaysia is USD 0.13 per kWh
- For 23kW or 6.6RT (Refrigeration Tons) hot water driven 'BROAD' absorption chiller, the COP is 0.7
- Assume the operation of air conditioning in small office buildings is 10 hours per day
- Cost of Solar-Assisted air conditioning system based on 23kW 'BROAD' absorption chiller and evacuated tubes is USD 62 857.14.

Based on the four assumptions above the chiller is running at 16.1 kW (0.7×23kW). The cooling energy cost is calculated below:

Cooling Energy Cost = 16.1kW $\times$ USD 0.13 per kWh $\times$ 10 hours per day = **USD 20.93 per kWh/day**

Therefore the payback period is given as follows for a capital cost of USD 62 857.14:

$$\textbf{Payback period} = \frac{\text{USD } 62857.14}{\text{USD } 20.97} = 2997.5\,\text{days} = 8.21\,\text{years}$$

The lifespan of the major components of the solar-assisted air conditioning system like the evacuated tubes, solar collector, absorption chiller is generally approximately 20 years. This indicates significant savings in electricity cost after the eighth year. There will also be significant CO_2 emission reductions as this air conditioning system uses green technology as a result of its environmentally friendly working fluids Lithium Bromide and Water ($LiBr/H_2O$) and is powered by hot water from solar energy. For a tropical country like Malaysia with an abundance of annual average daily solar irradiation of 5.56kWh/m^2, solar-assisted air conditioning system application is ideal. This evaluation was done by Haw et al, for Malaysia in 2009 [10].

2.5 Case Study 2: Solar Absorption Cooling System in Australia (2011)

The State Government of Victoria produced a case study on the solar-assisted cooling project done by the Echuca Regional Health for the public hospital in Echuca, about two and half hour's drive north of Melbourne, partially subsidized by "Sustainability Victoria" [45]. The system uses 102 vacuum tube collectors that cover 300m^2 to power a 500kW cooling capacity 'BROAD' chiller. The daily solar radiation average is 12MJ/m^2 per day. The large arrays of 1600 evacuated tubes are mounted on the roof of the hospital's maintenance and engineering building [46]. The project capital cost was AUD 2 191 000 (Australian Dollar) with a savings of AUD 60 000 per annum. This project received a subsidy which covered 20% of its capital cost. This would realize a payback period of 12-14 years based on 2011 Australian electricity tariffs; however this will be considerably shortened, should the projected tariffs be used instead [47].

2.6 Case Study 3: Solar Absorption Cooling System in Brazil (2010)

In Brazil the energy demand for refrigeration and air-conditioning correspond to approximately 15 % (134 TWh/year) of the total country energy use. Around 48% of energy is consumed in commercial and public buildings due to air conditioners, usually by driving electrical vapour compression chillers [48].

The object of the case study is the intended auditorium at the UNESP University in Guaratingueta, which is likely to be equipped with a solar cooling system. The solar radiation in Guaratingueta lies around 5.5 kWh/m² in between. Guaratingueta lies between Sao Paulo and Rio de Janeiro in the Brazilian Megalopolis. Before the economic feasibility can be calculated the acquisition and operation cost must be investigated. Below are actual cost tables (Tables 2.1 and 2.2) for the applicable solar-assisted air-conditioning system and Split Air conditioning system [48].

Table 2.1: Acquisition and specific costs per kW cooling capacity for two different system combinations [48].

ACQUISITION COST [R$]			SPECIFIC COST [R$ per KW cooling capacity]	
Component	A: complete solar cooling "kit"	B: individual comp.	A:	B:
Flate Plate collectors, 80 m² Bosch Bruderus Logasol SKN 3.0	37.234 (13.790 €)	37.234 (13.790 €)	1.064	1.064
SolarNext chilli ® Cooling Kit WFC35, incl.: 1 x Yazaki WFC-SC10 Absorption chiller 1 x wet cooling tower with auto accessories filling and emptying, and fan speed control 1 x hot water pump 1 x cooling water pump 1 x chilli ® System Controller HC incl. Temperature Sensors 1 x cold storage 2000 l without insulation 1 set of sensors f. Chilled water storage 1 x pump f. cold distribution with accessories 1 x hot water storage 2000 l with insulation 1 set of sensors f. hot water storage 2 x changeover valve with actuator	126.700 (46.926 €)	18.225 (6.750 €) estimated price for all these comp. except: chiller, cooling tower and controller	3.620	
1 x pump f. solar collector curcit	945 (350 €)	945 (350 €)		
4 x fan coil unit	10.268 (3840 €)	10.268 (3840 €)	293	293
Yazaki WFC-SC10 35 kW Absorption Chiller		43.501 (16.700 €)		1.242
wet cooling-tower F-32 Refrigeracao International		7.370 (2.729 €)		211
SolarNext chilli ® System Controller H		5.624 (2.083 €)		
4 x Split Air-conditioner back-up* Electrolux SPLIT SE 30 F (30.000 BTU / 8,8 kW)	16.000 (5.926 €)	16.000 (5.926 €)	457 (169 €/KW)	457 (169 €/KW)
TOTAL	191.147 (70.772 €)	139.167 (52.178 €)	5.461 (2.022 €/KW)	3.976 (1473 €/KW)

Table 2.2: Comparison of electricity consumption and operation costs of a solar-assisted air conditioning system and electrically driven compression vapour split air conditioning system. [48]

ELECTRICITY CONSUMPTION & OPERATION COST		
Component	solar-assisted air-conditioning system	conventional split air-conditioning system
4 x water pumps	360 W	
wet cooling-tower fan	280 W	
Yazaki WFC-SC10 35 kW Absorption Chiller	210 W	
4 x fan coil units	480 W	
4 x Split Air-conditioner Electrolux SPLIT SE 30 F (30.000 BTU / 8,8 kW)**		13.600 W
TOTAL	1.330 W	13.600 W
1 Month (30 days x 9 h)	359 kWh	3.672 kWh
9 Months	3232 kWh	33.048 kWh
TOTAL 10 Months operating (1 year) *	with 1 Month split-air conditioning back-up 6.904 kWh	36.720 kWh
Operation Cost (1 year) by 0,38 R$/kWh (Guaratingueta Edp Bandeirante Energia)	2.624 R$	13.954 R$
Operation Cost (1 year) by 0,598 R$/kWh (Minas Gerais -Cemig)	4.106 R$	21.959 R$

The next two Figures 2.1 and 2.2 shows the different acquisition and operation costs for a solar-assisted air conditioning system against a split air conditioning unit system in two countries, namely Guaratingueta and Minas Gerais. Besides the shown cost development due to the specific electricity cost in Guaratingueta, it has presented the cost gradient through a higher electric energy price, which exists for example in Minas Gerais, where, as well, very good solar irradiance occurs.

There are no interest rates on the investment capital or maintenance cost considered, as well, no intended possible public subsidies and electricity cost elevation. If there is an interest rate of only 1.5 % per year of the investment cost of 191.147 R$ the payback-time would be 5 years longer. This means a payback period of around 21 years, thus the system would not be profitable during the system's lifespan. The usual interest rate of such a credit in Brazil is around 8.5 % per year. Hence it is essential to become profitable with a very low interest rate, lower than 1.5 % per year.

In Brazil, as yet there is no subsidy or tax relief for those who exploit renewable energy. However, the Brazilian government just discussed a law (Lei 630/03) [48] which proposes financial support. In Germany there are several solar thermal energy incentives. For example the Reconstruction Loan Corporation (KfW) pays 30% of the solar cooling system investment, if the collector array is bigger than 40 m² [48].

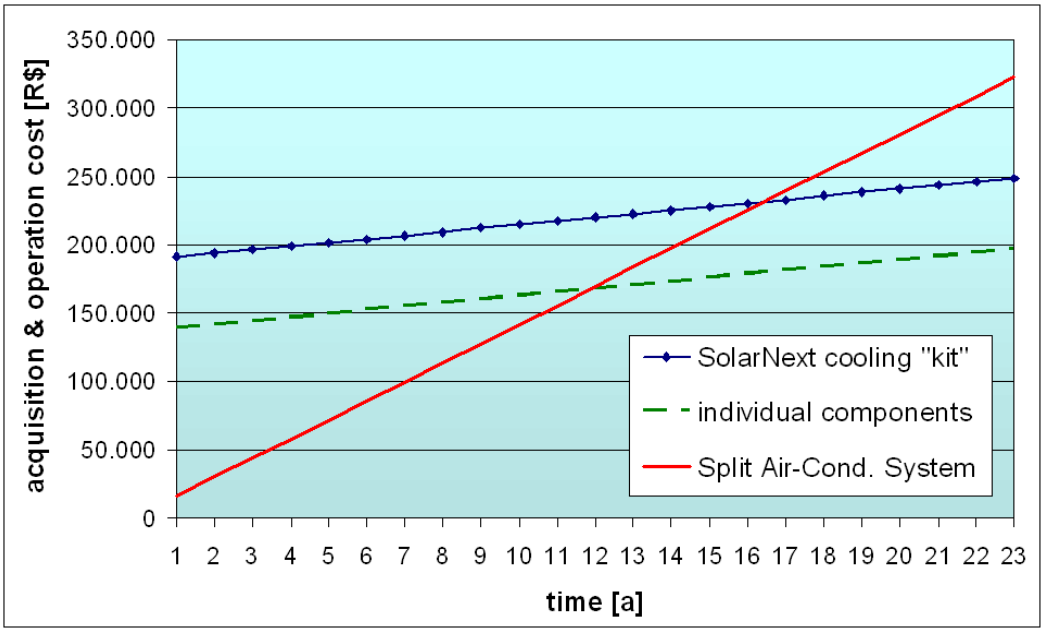

Figure 2.1 Acquisition and operation cost of solar-assisted air-conditioning system and conventional split air-conditioning system in Guaratingueta [48].

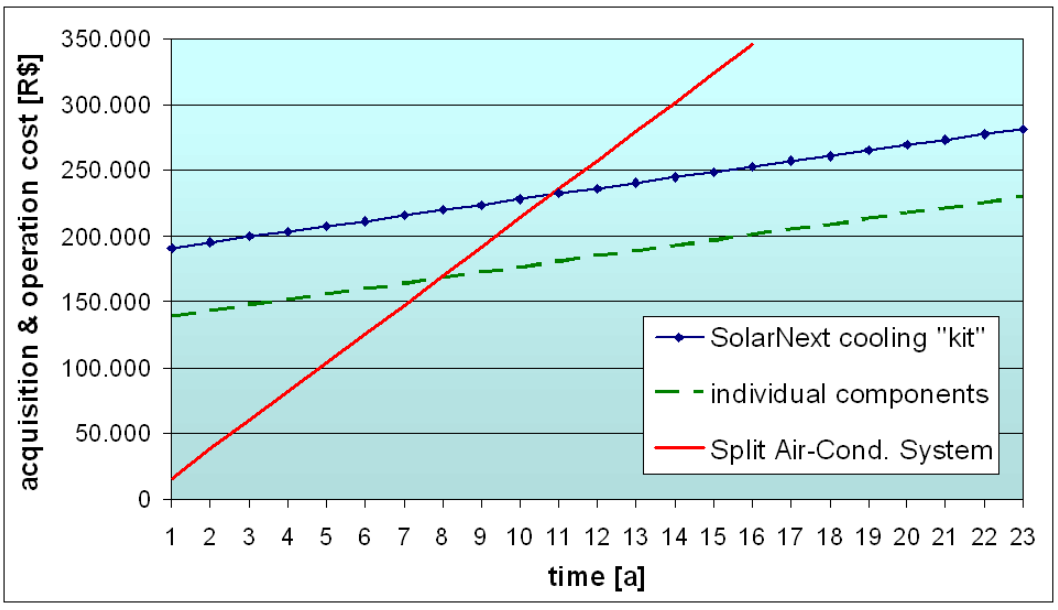

Figure 2.2 Acquisition and operation cost of solar-assisted air-conditioning system and conventional split air-conditioning system in Minas Gerais [48].

Note: Operation costs are calculated with an electric price of 0.60 R$/kWh which is the price in the Brazilian State of Minas Gerais by CEMIG (companhia energetica de Minas Gerais) in Figure 2.1 and 2.2 graphs.

An important definition to evaluate the economic feasibility is the meaning of "critical operation time", which is understood as the payback period of the capital cost of using a solar assisted air conditioning system. If the solar cooling system within the lifetime (here 20 years) will be longer in operation than the critical operation time, the high cost of acquisition pays off.

CHAPTER 3: SOLAR THERMAL COOLING TECHNOLOGIES

This Chapter presents a description of the various solar cooling technologies available in the market today. The comparison of the Coefficient of Performance (COP) of the solar cooling technologies concludes the Chapter.

3.1 Types of Solar Thermal Cooling Technologies

The vapour absorption cycle uses two fluids and some quantity of heat input, rather than the electrical input as in the more familiar vapour compression cycle to achieve air conditioning. The vapour compression and absorption air conditioning cycles both achieve the removal of heat via evaporation of a refrigerant at a low pressure and reject heat through the condensation of the refrigerant at a higher pressure. The method employed to create the pressure difference and to circulate the refrigerant is the primary difference between the two cycles.

This cycle is interesting as it uses a renewable source of energy to drive the cooling process. Due to the nature of the solar resource as a renewable source of energy, it can be used for its thermal energy and for its solar radiation to produce electric power. Thus there are three broad categories of Solar Cooling Technologies based on the manner in which solar energy is utilized. Solar Electrical Cooling Technologies utilize the solar radiation for electricity by suitable conversion technologies, Solar Thermal Cooling uses the thermal energy from the solar radiation and the third category uses a combination of Solar Thermal and Electrical energy.

The use of 'solar to electrical power' cooling systems works on the principle of providing electricity from conversion of solar radiation to electricity via the photovoltaic cell storing electrical energy in a battery which is used to energize conventional mechanical compression cycle chillers. The combined solar thermal and electrical cycle systems can be of various types and are hybrid systems that use stored electricity captured from solar energy to minimize or eliminate the use of electrical energy from the grid for their operation. The solar thermal cooling technologies are classified according to their cycle operation, i.e. open, closed and thermomechanical as illustrated in Figure 3.1.

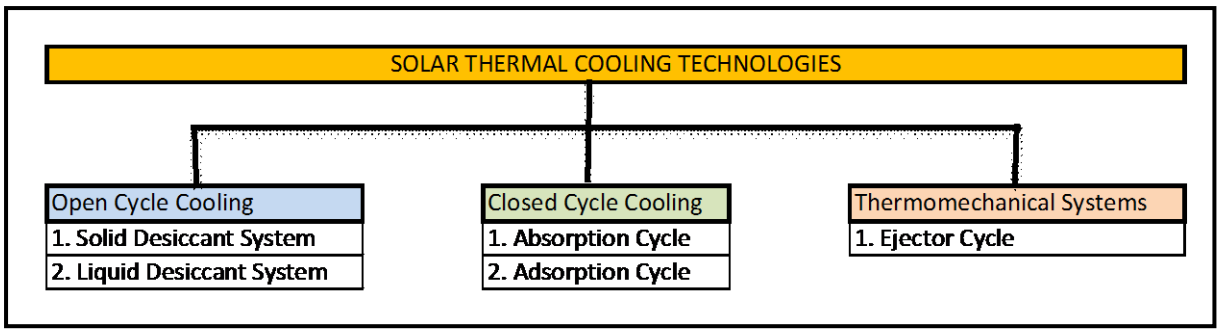

Figure 3.1: Solar thermal cooling technologies

The solar thermal cooling systems incorporate different setups and cycles that can be classified into 3 main groups, the Open Cycle, which uses the Liquid and Solid Desiccant systems, the Closed Cycle which is the Absorption and Adsorption cycle and the Thermomechanical System which uses the basic principle of the Ejector cycle.

The Ejector cycle is not a cooling solution that is available off the shelf. The Absorption, Adsorption, solid and liquid desiccant systems existing around the world in 2006 are represented in Figure 3.2. In 2006, much of the Solar Thermal Cooling market is dominated by the Absorption cooling system followed by the Adsorption Cooling Cycle and the Desiccant Cooling (DEC) liquid and solid systems are in the minority as can be seen in Figure 3.2. However, in Figure 3.3, which shows the solar driven chillers market share in 2008, the Adsorption Cooling systems are in the minority with the Desiccant Cooling (DEC) systems taking the second largest portion of the market share.

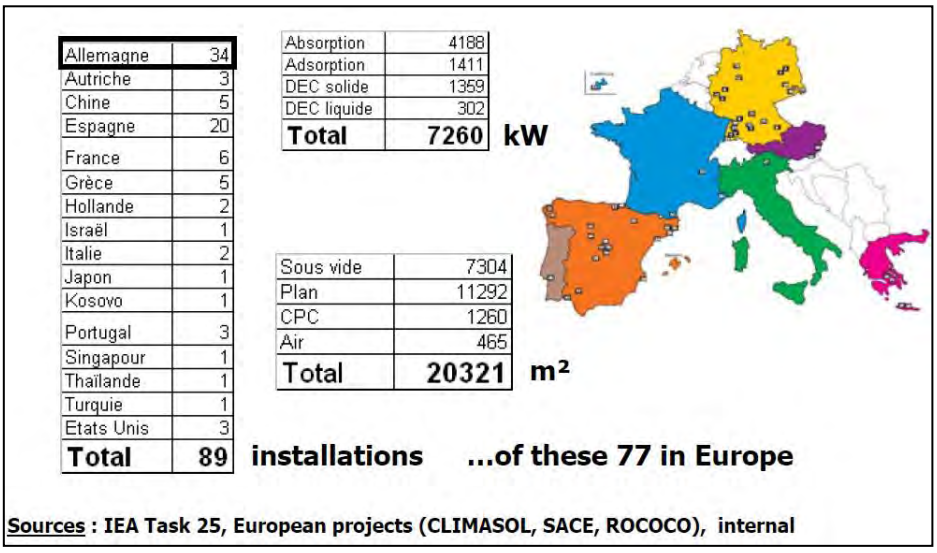

Figure 3.2: Solar Thermal Cooling Installations around the world in 2006 [8].

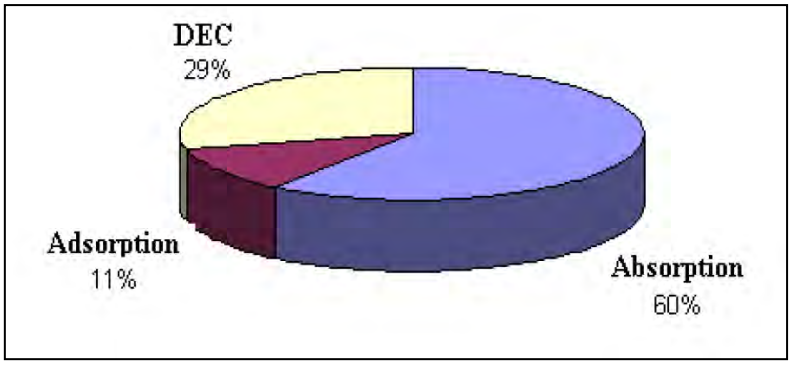

Figure 3.3: Solar Thermal driven chillers share in 2008 [8].

3.2 Closed Cycle Cooling

Closed loop cycles produce chilled water in thermally driven chillers for which any type of distribution system can be employed to circulate the cold between working fluids. These chillers are called absorption and adsorption chillers, with absorption chillers being the more popular option. A thermal compression of the refrigerant is achieved by using a liquid sorbent/solution and a heat source, thus replacing the electric power consumption of a mechanical compressor.

3.2.1 Absorption Cooling

The principle of operation of this type of cooling is explained in detail in Chapters 5 and 7 that follow. The main components of an absorption chiller are the generator, condenser, absorber and evaporator as shown in Figure 3.4.

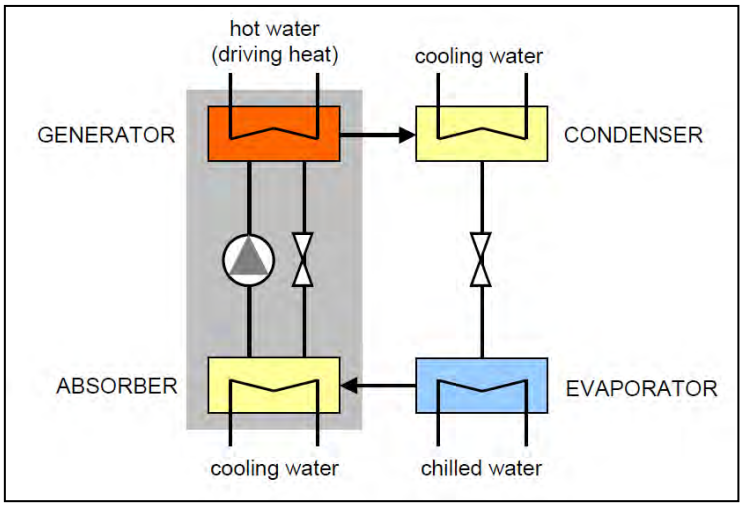

Figure 3.4: Main components of an absorption chiller [49].

The cooling effect is achieved by the evaporation of the refrigerant, such as water in the evaporator at a very low pressure. The vaporized refrigerant is absorbed in the absorber, thereby diluting the liquid sorbent, such as Lithium Bromide solution, ammonia or Lithium Chloride. The solution is pumped to the generator where the solution is regenerated by the application of driving heat (such as hot water). The refrigerant leaves the solution and condenses on the condenser by the circulation of cooling water and is circulated back to the evaporator through the expansion valve.

This type of cooling uses two working liquid pairs that have an affinity toward each other such as water and Lithium Bromide (H_2O/LiBr), water and Lithium Chloride (H_2O/LiCl) and water and ammonia (H_2O/ NH_3). The most popular chillers used for space cooling are the chillers that use the H_2O/LiBr working pair whereas the H_2O/NH_3 working pair is used mainly for refrigeration. The process of absorption cooling will be covered in detail in Chapter 4 and Chapter 6. The cycles can employ double effect refrigeration stages to achieve greater COPs.

There are many different manufacturers of solar absorption chillers and their market captured out of 280 installations is represented in Figure 3.5.

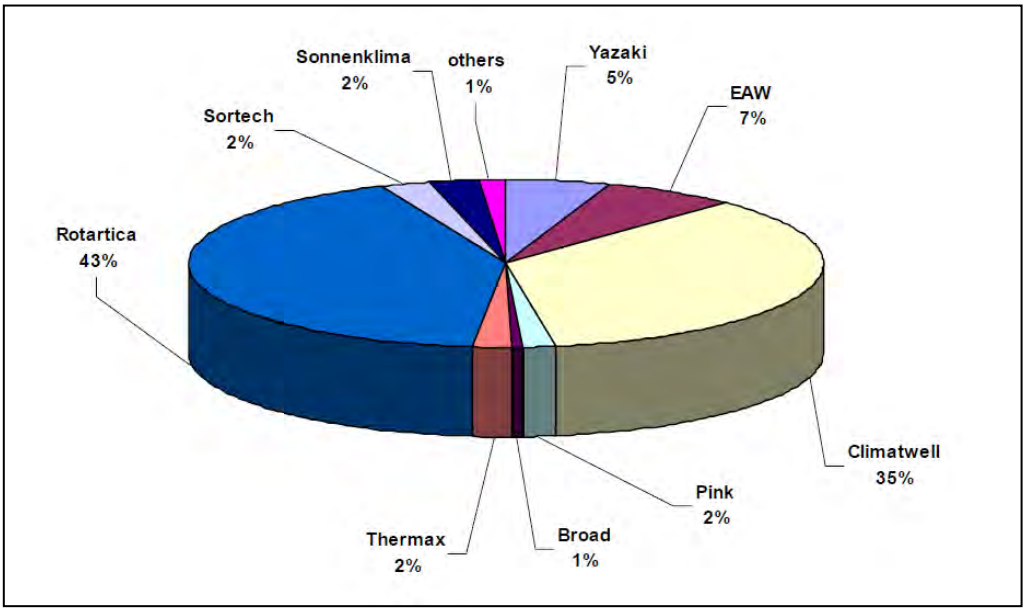

Figure 3.5: Absorption chiller brand market share out of 280 installations, 2008 [8].

3.2.2 Adsorption Cooling

In the adsorption chiller, instead of liquid sorbents, a solid sorbent is employed and water is used as a refrigerant. The adsorption process incorporates two sorbent compartments indicated by 1 and 2 in Figure 3.6, one of which is the evaporator and the other the condenser. While the sorbent, typically silica gel, is regenerated in the first compartment using an external heat source, typically hot water, the sorbent in the second compartment adsorbs the water vapour entering from the evaporator. Cooling water circulated in compartment 2 ensures a continuous adsorption. The water in the evaporator is changed into a gas phase causing the cooling effect.

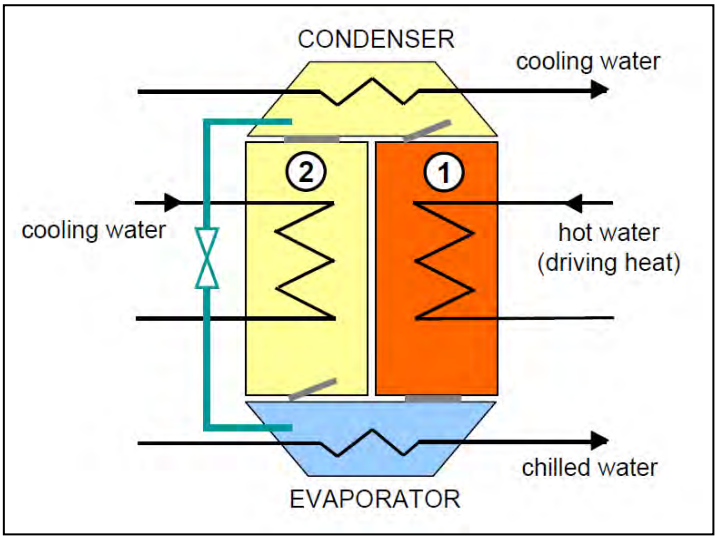

Figure 3.6: Adsorption Cycle [49]

The driving temperatures required for adsorption chillers are usually around 80 °C , with an acceptable temperature as low as 60 °C , however their typical COPs are lower than that of absorption chillers, and that being 0.6. The major commercial manufacturers of these chillers are Japanese manufacturers, Nishyodo (70kW to 500kW) and Maekawa (50kW to 350kW),

3.3 Open Cycle Cooling: Desiccant Cooling Systems

This type of cooling involves the direct cooling/treatment of ambient air. Desiccant Cooling Systems use water as a refrigerant in direct contact with air. The cycle is a thermally driven process that involves the combination of evaporative cooling with air dehumidification by a desiccant which is a hygroscopic material. The refrigerant after providing the cooling effect is discarded from the system and replaced with new refrigerant, hence the term open cycle. This type of system uses silica gel or Lithium Chloride as sorption materials on a rotating wheel.

Warm, humid ambient air enters the slowly rotating desiccant wheel and is dehumidified by the adsorption of water as depicted in process 1-2 in Figure 3.7. This air then passes through a heat recovery wheel where the air is precooled (2-3). The air is then conditioned to a desired temperature and humidity between process 4-5 and 3-4 respectively. The return air or air removed from the rooms is humidified close to saturation point (6-7) for maximum cooling potential to enable an effective heat recovery (7-8). The desiccant wheel is finally regenerated by the application of external heat (50 °C to 70 °C) to allow continuous operation of the dehumidification process. This system can also be modified for space heating modes.

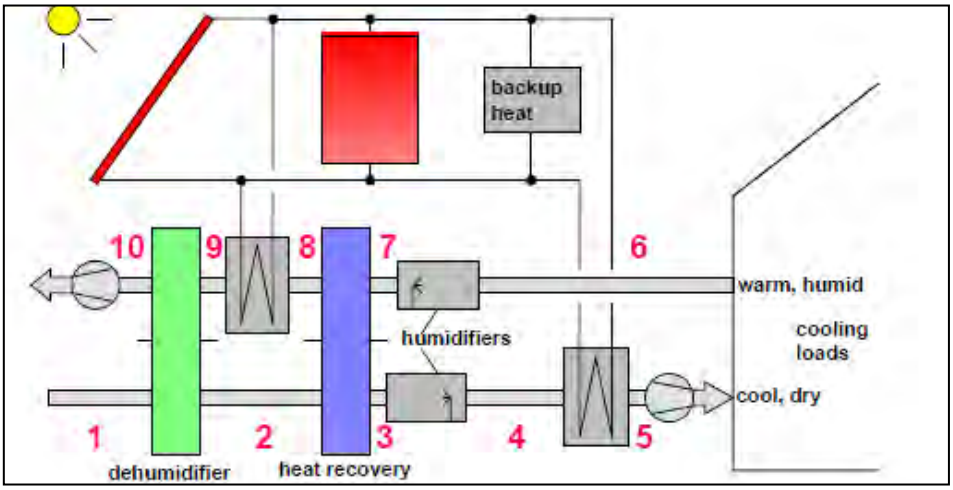

Figure 3.7: Solid Desiccant Cooling [49].

Liquid desiccant cooling systems, utilize water/lithium chloride solution as sorption materials to dehumidify the air. This type of system shows several advantages over solid desiccant cooling systems as they achieve a higher air dehumidification at the same driving temperature and will be better suited to areas that have high humidity.

3.4 Thermomechanical Cooling: The Ejector Cycle

The ejector cycle works on the principle illustrated in Figure 3.8. This system uses a generator powered by low grade heat, evaporator condenser, expansion device, and ejector and circulating pump. Low grade heat (Q_b) at around 80 °C is used to evaporate high pressure liquid refrigerant into vapour (process 1-2) which enters the ejector and is referred to as the primary fluid and accelerates through the nozzle.

The reduction in pressure that results induces vapour from the evaporator at point 3, known as the secondary fluid. The primary and secondary fluids mix and enter the diffuser section where the flow decelerates and pressure recovery occurs. The mixed fluid then rejects heat to the surroundings (Q_c) upon being condensed. Some of the fluid flowing out of the condenser at point 5 is pumped to the boiler for the completion of the cycle whereas the rest of the liquid is expanded through the expansion device. This then enters the evaporator at point 6 as a mixture of liquid and vapour. Evaporation occurs producing a cooling effect (Q_e) and the resulting vapour is then drawn into the ejector at point 3. The refrigerant which is the secondary fluid mixes with the primary fluid in the ejector and is compressed in the diffuser section before entering the condenser at point 4. The cycle is then repeated.

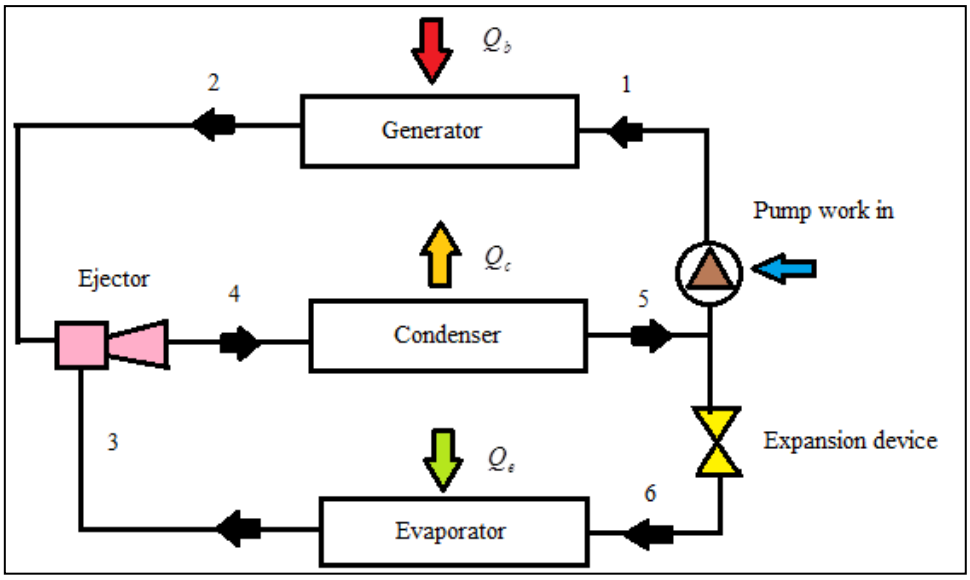

Figure 3.8: Ejector cooling cycle

Due to the low COP (0.2-0.3) of such a system, it is not commercially available off the shelf and requires a sufficient availability of low grade heat.

3.5 Comparison of Solar Thermal Cooling systems

The cooling technologies that use solar thermal energy each has its advantages and disadvantages based on the materials being used and the type of cycle employed. The Absorption cycle using the H_2O/LiBr working pair is the most successful on the commercial market due to its high thermal COP in comparison to the other technologies as seen in Figure 3.9. The thermal COP is the ratio of the cooling capacity of the system to the heating power delivered to the system by solar collectors directly or indirectly through storage vessels.

The heat rejection medium temperature usually gives a good indication of what the COP of the thermal driven system is and this can be seen in Figure 3.10. The higher the heat rejection medium temperature, which is the cooling water, the lower the COP of the system represented in Figure 3.9.

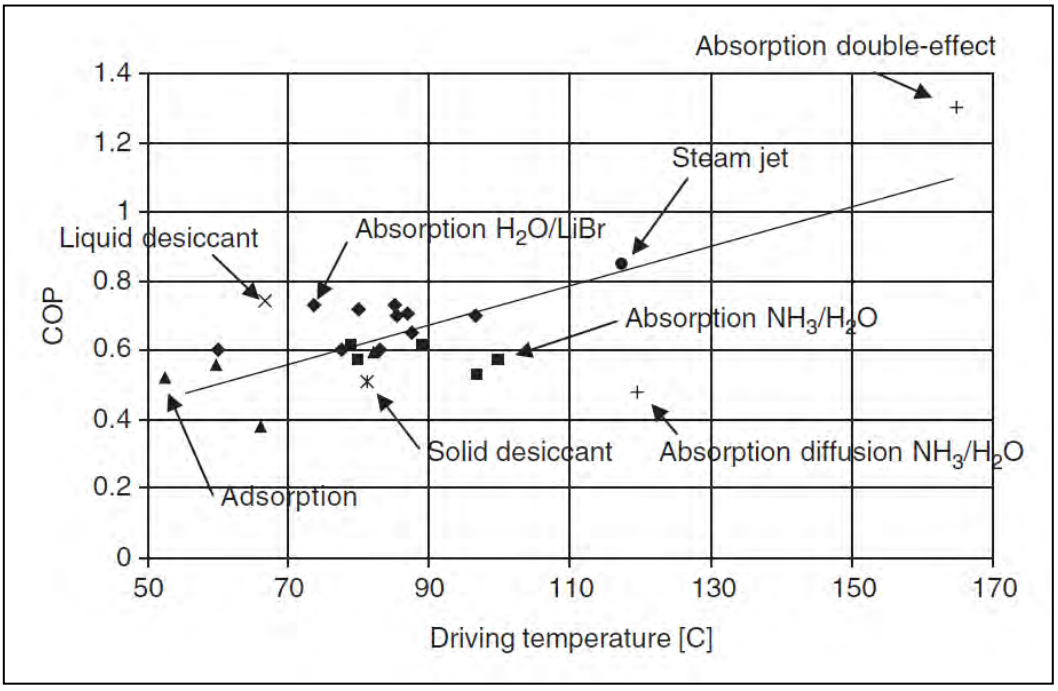

Figure 3.9: COP as a result of heating medium temperature [50].

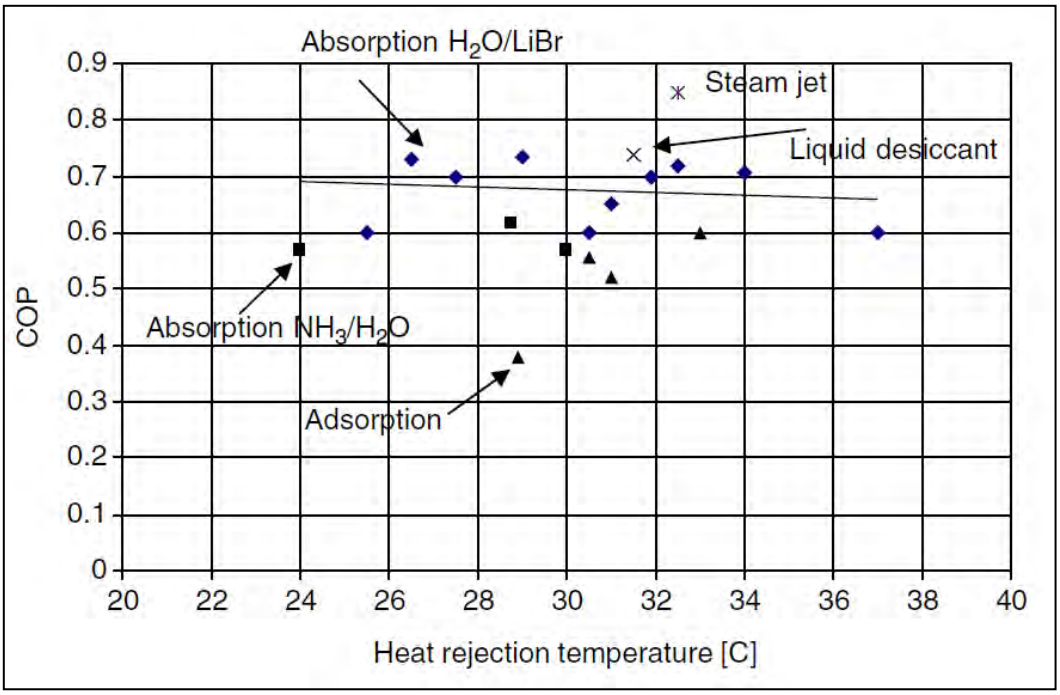

Figure 3.10: COP as a result of heat rejection medium temperature [50].

One of the disadvantages of solar thermal cooling technologies is the high capital cost involved compared to mechanical vapour compression cooling technologies using the R134a refrigerant. The high capital cost is due to the cost of the solar collector array needed to capture the thermal energy that drives the absorption cooling cycle. An indication of the influence of the collector area needed to the capital cost can be seen in Figure 3.11.

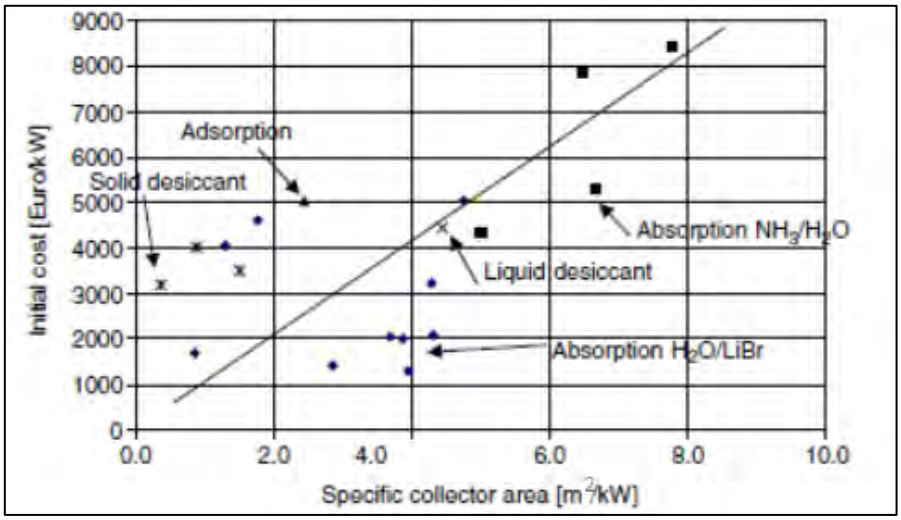

Figure 3.11: Initial system cost as a function of the specific collector area [50].

Water and Lithium Bromide absorption chillers have a relatively average initial cost compared to other solar thermal powered cooling cycles. The collector area needed for optimum operation of chillers depends on the solar insolation received at the location that it is installed. The thermal coefficient of performance of solar thermal based cooling cycles can be seen in Figure 3.12.

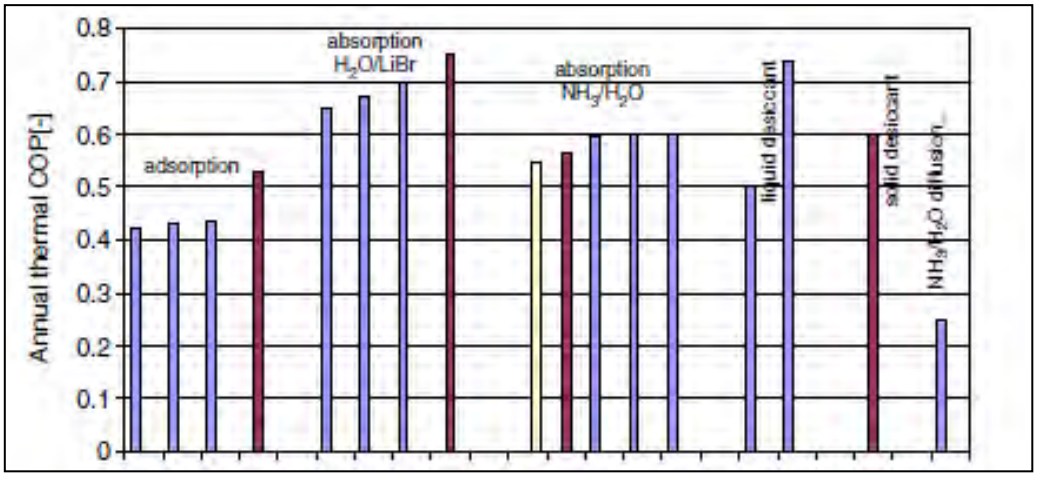

Figure 3.12: Annual thermal performance for the evaluated projects [50].

Although South Africa presently has one of the cheapest electricity costs in the world, solar thermal driven cooling cycles has not received much attention. However, due to the present energy crisis experienced by South Africa's public utility provider, Eskom, these technologies are being considered. Chapter 4 investigates the energy usage in South Africa. Owing to the nature of solar energy, these technologies need to be proven in South Africa and hence the focus of the present study.

CHAPTER 4: ENERGY IN SOUTH AFRICA

This Chapter gives the energy use in South Africa for the past years for primary energy supply and energy consumption per Gross Domestic Product (GDP). A snapshot of the energy use per sector is given together with the CO_2 emissions and the overview of South Africa's Electricity Supply Industry. The relationship between air conditioning and electricity usage is investigated and the potential for renewable energy in South Africa is given.

4.1 Energy Consumption in South Africa

South Africa has three groups of electricity generators, i.e. the national public electricity utility, Eskom, the municipal generators and the Auto-generators. The Auto-generators are industries which generate electricity for their own use and these include the pulp mills, sugar refineries, Sasol, Mossgas and metallurgical industries [51]. The country's total primary energy supply can be seen in Figure 4.1.

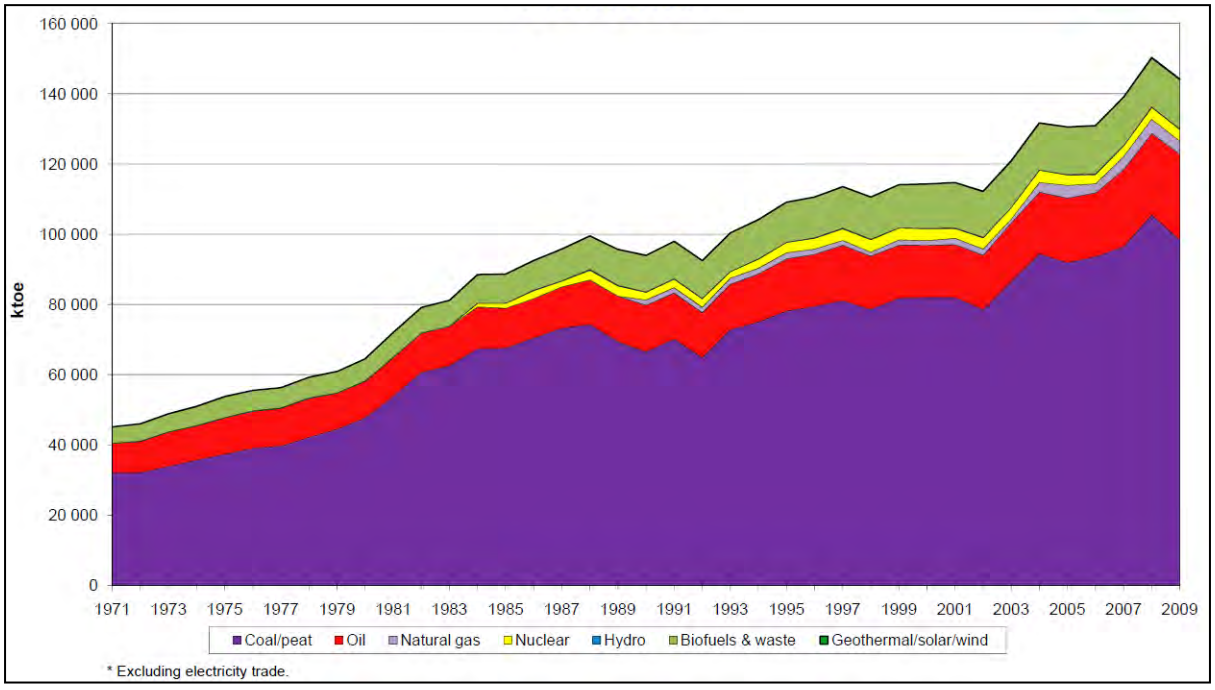

Figure 4.1: Total Primary Energy Supply in South Africa [52]

It can be seen that South Africa relies heavily on coal, oil and biofuels and waste for its energy, of which coal, biofuels and waste is mainly used for energy production. This can be seen in Figure 4.2. A significant portion used for electricity generation as depicted in Figure 4.3.

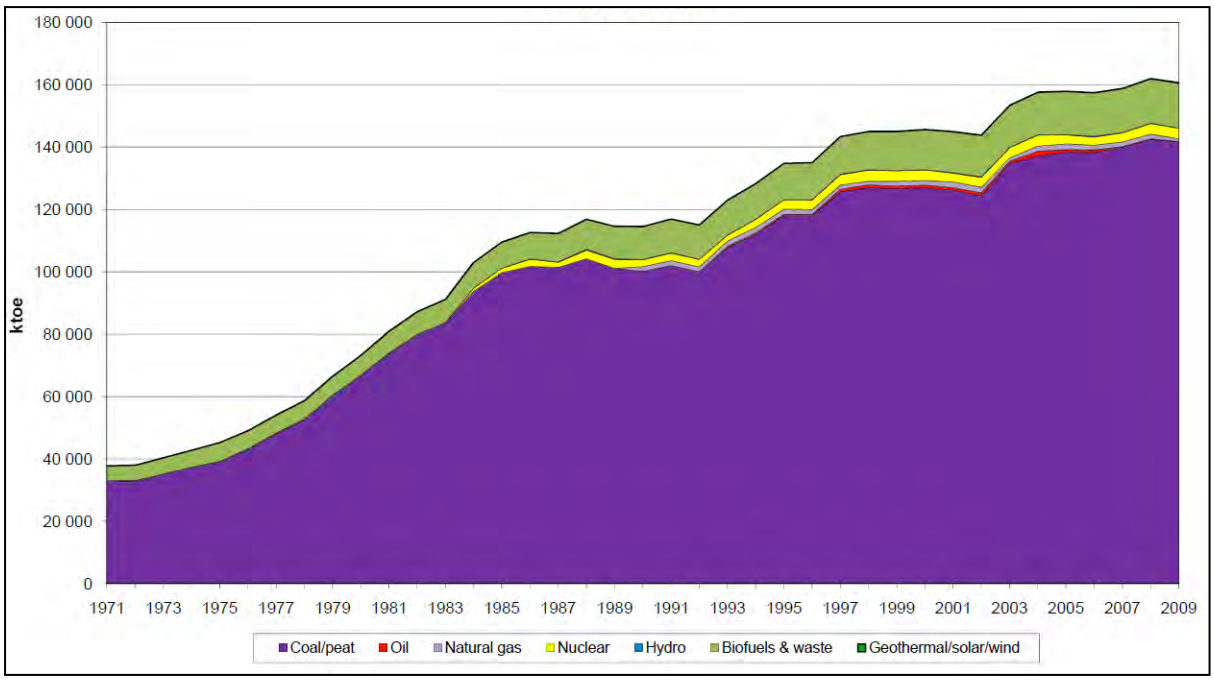

Figure 4.2: Energy Production in South Africa [52]

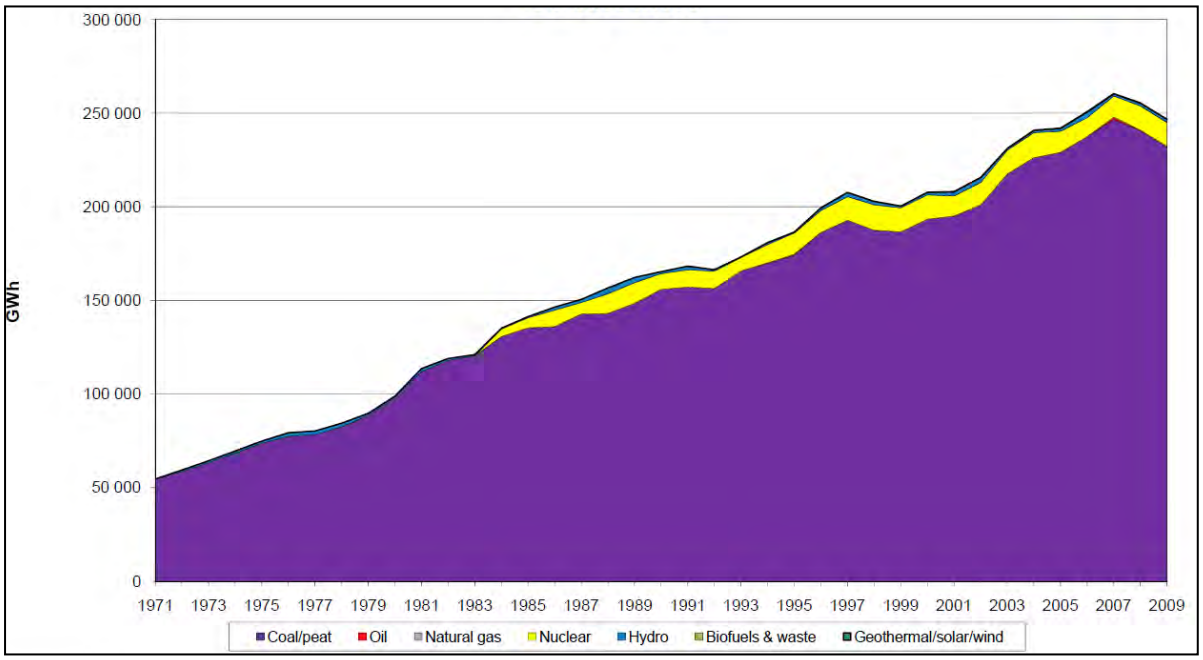

Figure 4.3: Electricity generation by fuel in South Africa [52]

The Gross Domestic Product (GDP) of South Africa had the 16th largest energy consumption in the year 2001. Figure 4.4 shows their GDP in relation to energy consumed in comparison with other countries in the world. One of the reasons for this is due to their nature of activities that dominate their economy. Mining, minerals processing, metal smelting and synthetic fuel production are

intensive users of energy. Figure 4.5 and Figure 4.6 show the final energy use by sector and final energy use by carrier respectively.

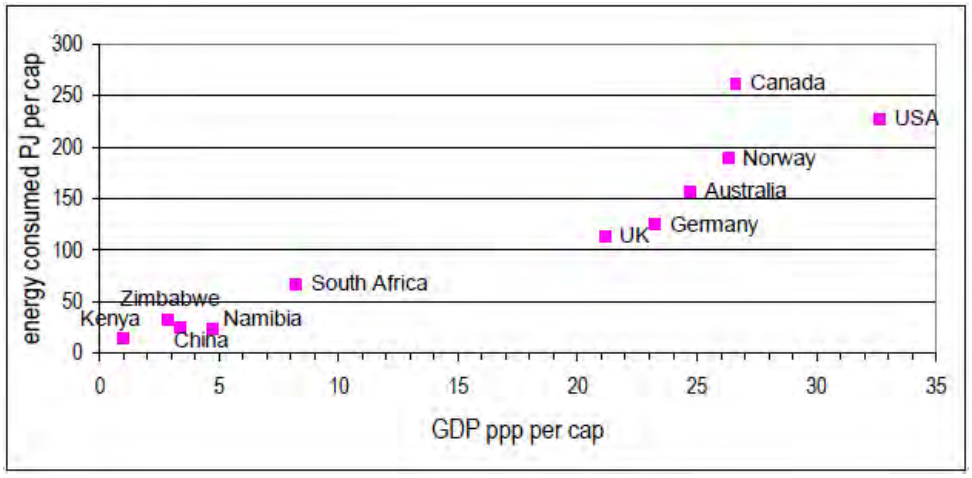

Figure 4.4: Energy Consumption per GDP per capita (2000) [53]

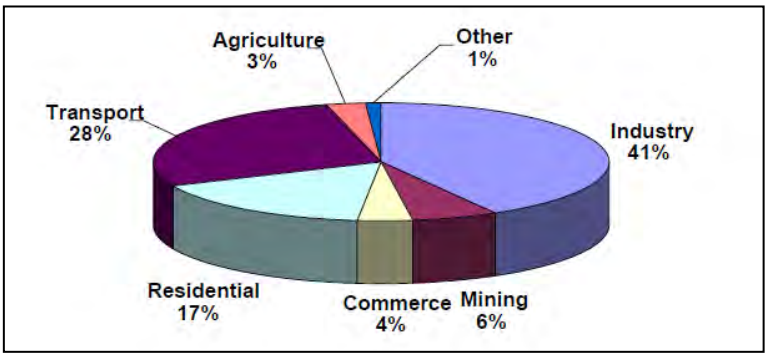

Figure 4.5: Energy Use by Sector, year 2000 [53]

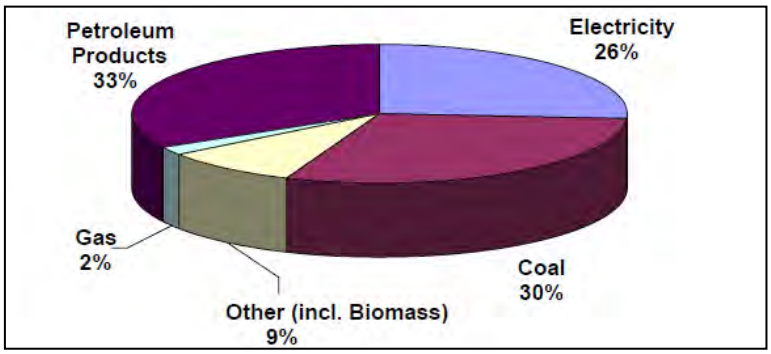

Figure 4.6: Energy use by carrier, year 2000 [53]

Another reason for the high energy intensity is that there are instances where South Africa is wasteful in their use of energy. There was a lack of awareness during this time of energy efficiency, especially in the emission of greenhouse gases.

In the year 1999, South Africa relied almost completely on fossil fuels as a primary source of energy, i.e. 90%, with coal making up 75% of this Figure. South Africa is one of the main contributors to carbon dioxide emissions, which is the main greenhouse gas linked to climate change due to their combustion of coal to produce electricity. Figure 4.7 shows their ranking of CO_2 emissions amongst the countries of the world in 1999. Their emissions per capita is close to half that of the United States of America, whereas their economic development is ranked "two worlds" behind the USA.

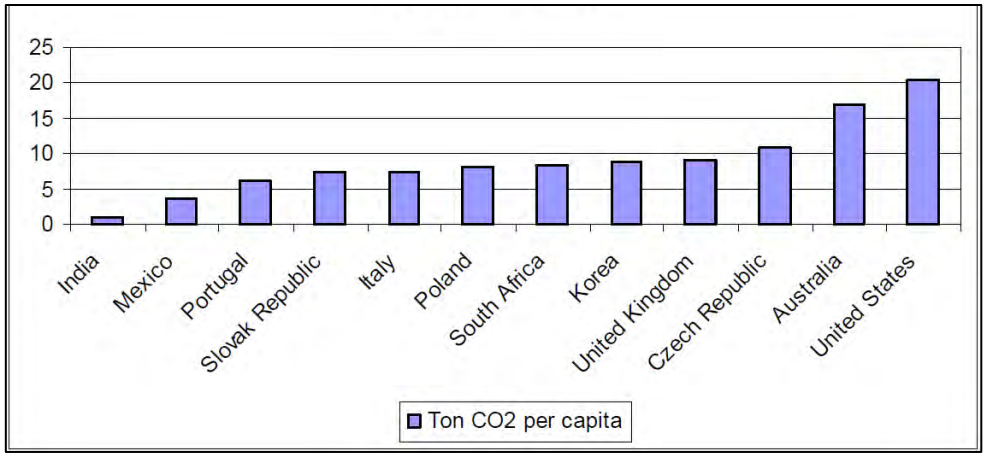

Figure 4.7: Carbon dioxide emissions per capita (IEA 2001) [54].

The economic sectors responsible for greenhouse gas emissions in South Africa can be seen in Figure 4.8.

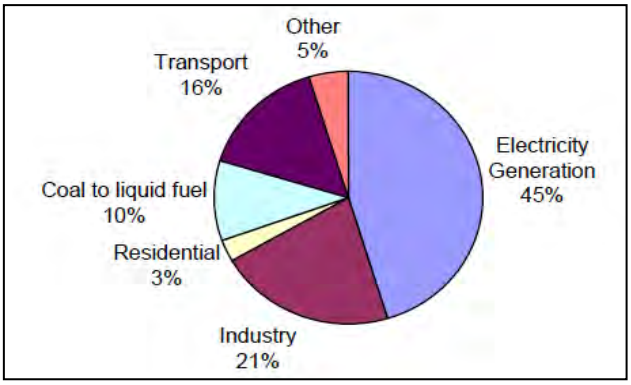

Figure 4.8: Economic sectors responsible for greenhouse gas emissions in 2000 [51].

The "Energy Outlook for South Africa: 2002" [15] document released by the Eskom Energy Research Institute showss that there was a high growth in electricity demand during the 1960s and 1970s, where it was above 8%, in some years, followed by a drop in growth of demand to about 2% in the 1990s.

Due to the past large demands for electricity, Eskom had built large coal power stations which allowed them to have surplus capacity until 2008. Unfortunately Eskom had not built additional capacity to cope with the electricity demand increases after 2008 and the electricity consumers in the country that relied on energy from Eskom had to suffer periodic load shedding.

South Africa's operating power stations providing electricity to the country cannot cope with the present demand as the installed electricity infrastructure has reached its full capacity. Planning should have occurred such that additional capacity was installed timeously to meet the power demand of a booming economy. Figure 4.9 and Table 4.1 shows Eskom's installed and operating power stations and the projected demand respectively.

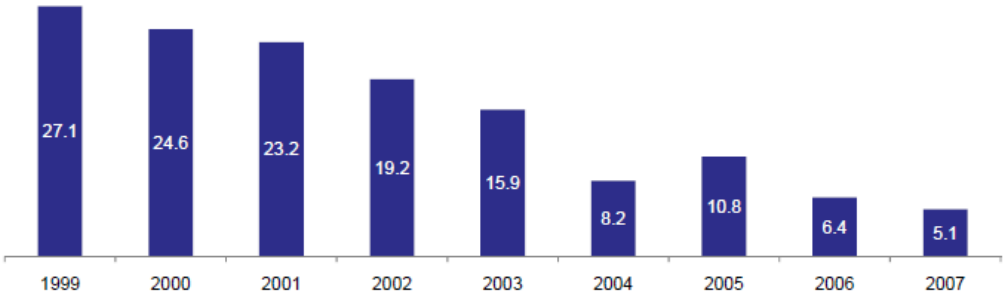

	1999	2000	2001	2002	2003	2004	2005	2006	2007
Reserve Margin	**27.1**	**24.6**	**23.2**	**19.2**	**15.9**	**8.2**	**10.8**	**6.4**	**5.1**
Capacity added (MW)	900	300	300	0	0	0	195	377	1 684
UCLF (%)	2.4	2.1	2.0	3.0	4.1	3.1	4.1	4.3	5.0
Load Factor (%)	**61**	**60.5**	**60**	**62.5**	**66.5**	**69.0**	**70.0**	**72.5**	**74.0**

Source: Eskom

Figure 4.9: Eskom's Electricity capacity [55]

Table 4.1: Projected growth of electricity demand [55]

Revised Reserve Margin
(factoring in Risk Adjusted Supply/Demand Options with Eskom Build)

	Year	Annual Peak Demand (Megawatts)	Eskom Generation Available	Reserve Margin	Supply/Demand Options other than Eskom Build*	Reserve Margin (with Other Options)
		(MW)	(MW)	(%)	(MW)	%
Projected (Demand Growth @ 4%)	2008	37 974	39 604	4.3%	571	5.8%
	2009	39 492	41 518	5.1%	2 930	12.5%
	2010	41 072	41 968	2.2%	5 670	16.0%
	2011	42 715	42 253	-1.1%	6 790	14.8%
	2012	44 424	43 053	-3.1%	8 540	16.1%
	2013	46 201	46 119	-0.2%	9 590	20.6%
	2014	48 049	49 185	2.4%	10 150	23.5%
	2015	49 971	51 585	3.2%	11 270	25.8%
	2016	51 969	53 185	2.3%	11 270	24.0%
	2017	54 048	54 185	0.3%	11 270	21.1%

Source: Eskom

Eskom has plans to build more power stations; however the era of cheap electricity is over in South Africa due to limited coal reserves, awareness of global warming and energy efficiency and conservation in light of a global energy crisis.

This was the "eye opener" together with the awakening of the country to the news of global warming that caused the government to realize that it needed to review the manner in which energy was utilized by the country. The growth of electricity demand can be stabilized or decelerated through improved efficiency in electrical usage, energy conservation and the use of renewable or alternate sources of energy to generate electricity for the power grid.

4.2 Air conditioning electricity usage

Air Conditioning accounts for a significant portion of the electricity consumption in urbanized countries. There are certain developed countries like the USA that face the challenge of urban heat island that affects metropolitan areas. The urban heat island (UHI) was first investigated and described by Luke Howard in the 1810s. This phenomenon is identified where the temperature difference between the metropolitan area and the surrounding rural areas is usually larger at night than during the day and is more noticeable in weak winds. The main cause of this UHI is the modification of the land surface by urban development. Urban development involves the building of structures such

as offices and commercial buildings, shopping malls and facilities that utilize construction materials which effectively retain heat. This phenomenon can be seen in Figure 4.10.

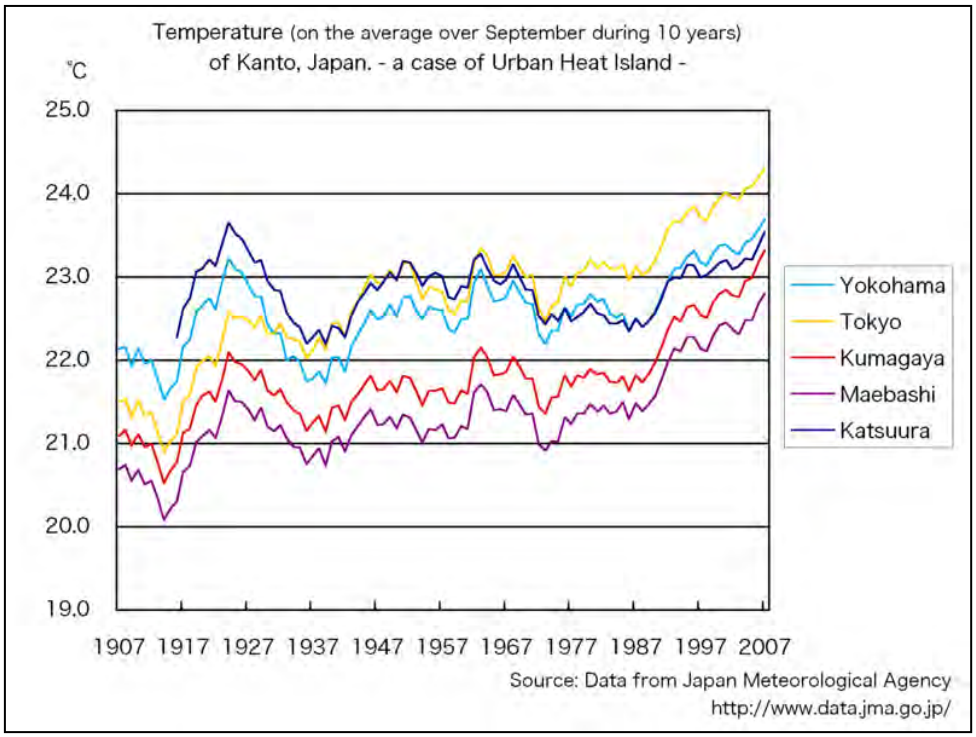

Figure 4.10 Urban Heat Island phenomenon observed for a century [56]

The UHI phenomenon has many impacts on wind patterns, developments of clouds and fog, the humidity and rates of precipitation and even has the potential to influence the health and welfare of urban residents. Urbanization results in greater energy usage and for this reason the energy consumption of developed nations are much greater than that of emerging economies as can be seen in Figure 4.11.

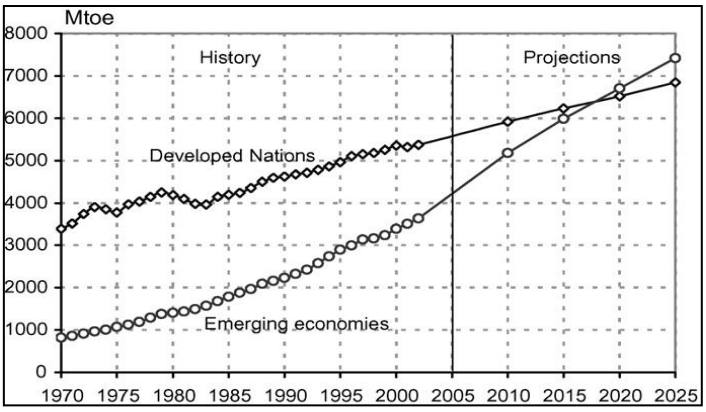

Figure 4.11: World Energy Use by region [57].

Energy use by nations with emerging economies (Southeast Asia, Middle East, South America and Africa) will grow at an average annual rate of 3.2% and will exceed, by 2020 that for the developed countries (North America, Western Europe, Japan, Australia, New Zealand) at an average growing rate of 1.1% [54].

The UHI effect also has a consequence on energy usage as the need for air conditioning increases as buildings use materials that retain heat. The sale of Refrigeration and Air Conditioning (RAC) units is depicted in Figure 4.12 while Figure 4.13 shows the resulting increase in installed electric capacity.

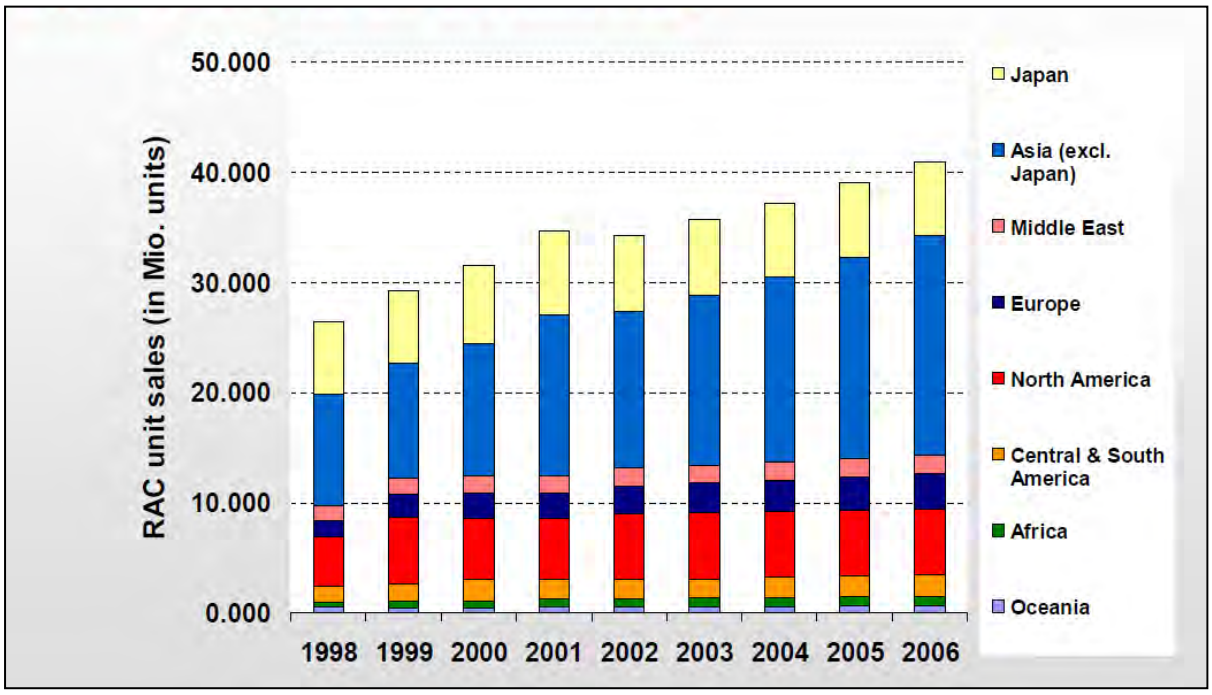

Figure 4.12: Sale of Refrigeration and Air Conditioning (RAC) units [58].

Commercial and office buildings require electricity for lighting, heating, cooling, extraction fans, pumps, etc. In most developed countries HVAC (Heating, Ventilation and Air Conditioning) is one of the most significant energy consumers of these buildings as can be seen in Figure 1.1 in Chapter 1.

From Figure 1.1 and together with the fact that urbanization results in the need for greater amounts of energy, there is a directly proportional relationship between the need for cooling and the electricity consumed as the use of air conditioning systems consume significantly greater amounts of electricity in commercial and office buildings.

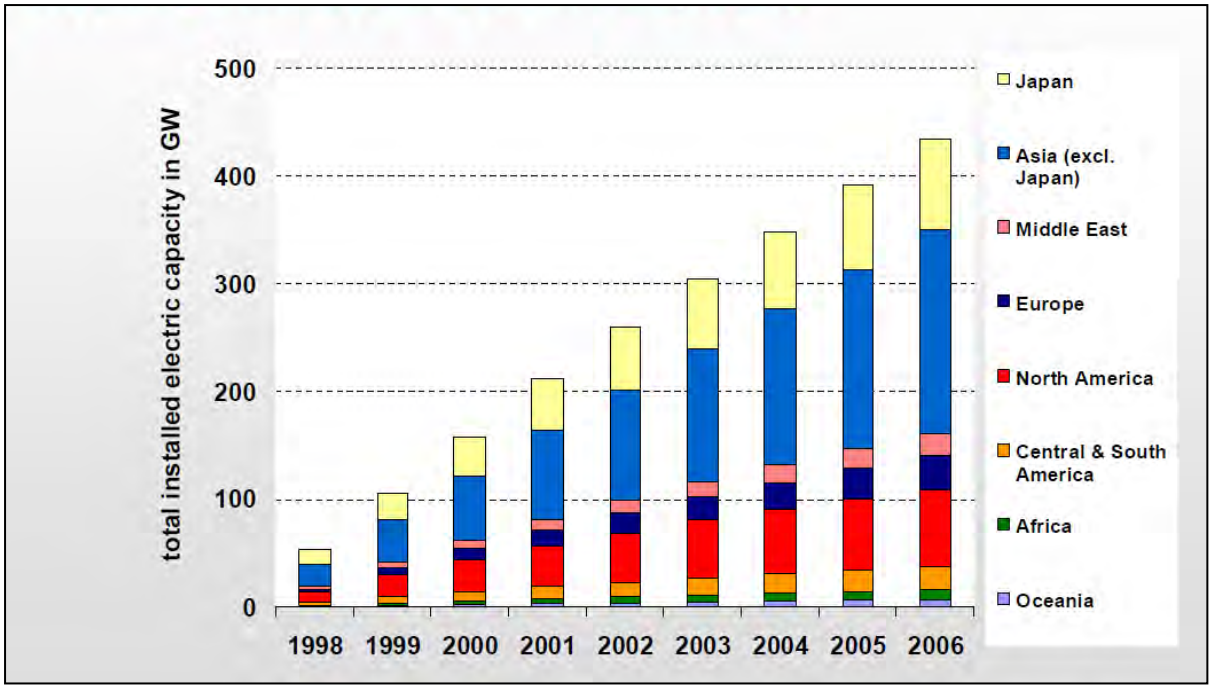

Figure 4.13: Installed electric capacity in various regions [58].

4.3 Renewable Energy Potential in South Africa

Two centuries ago, the Industrial Age was birthed due to the energy-rich hydrocarbon found in coal which replaced wood as a primary fuel source. This energy stored in coal provided the power needed by investors and industrialists to power machinery, process steel and propel steamships. The world's need for energy continued to increase and a hundred years ago, petroleum and natural gas was used as principal fuels. Atomic energy was used about 50 years ago when scientists trapped uranium to fuel nuclear reactors.

However, the definition of non-renewable indicates to us that the supply of these resources will be exhausted, sooner than later. This will mean no power, which will mean that our convenient, modern way of life will terminate. The technological crash will lead to stagnation in technological progress of this generation and those that will come after, to the primitive ages. However not all life will come to an end. The earth and its ecosystem will go on living efficiently – if human impact on them is not taken into consideration. Thus it can be confidently said that other forms of energy do exist – and like our discovery of non-renewable energy resources required infrastructure to release, capture and convert the energy into a form usable for our machinery, etc., so will renewable sources of energy require infrastructure to capture/convert this energy.

The source of the ecosystem's energy is the sun, which is the source of heat and light sustaining life on earth. The earth's surface receives insolation of 10^8 kWh daily, which represents a thousand times any oil reserve on earth. This makes solar energy a readily and abundantly available source of energy that needs only to be captured and/or converted. This insolation, however, is not equally distributed over the earth's surface, thus certain areas receive more intense and longer periods of sunshine hours than others.

The South African region daily solar radiation average varies between 4.5 and 6.5kWh/m^2 and when compared to the United States 3.6kWh/m^2 and Europe's 2.5kWh/m^2 the opportunity of the application of solar energy as a renewable resource is abundant [59]. Refer to Figure 4.14 to view the solar radiation distribution over South Africa.

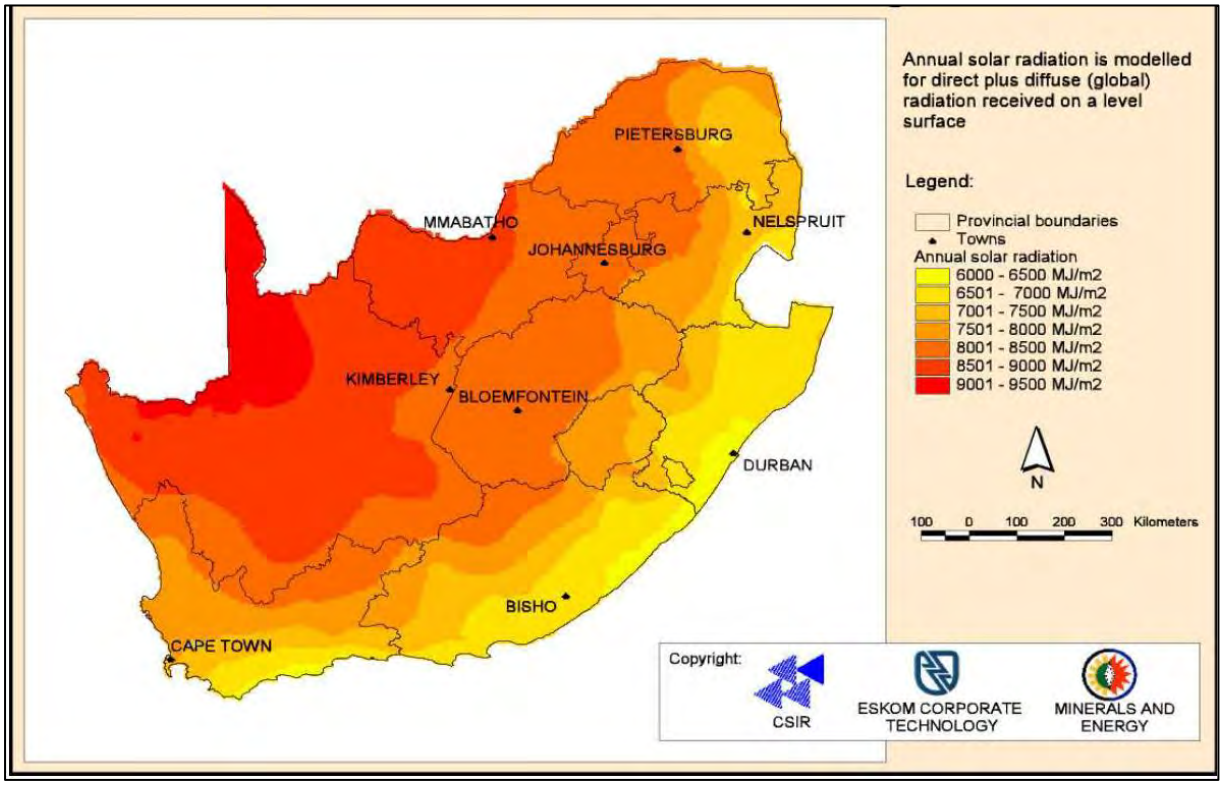

Figure 4.14: Annual direct and diffuse Solar Radiation for South African provinces [54].

The advantage with having abundant solar energy adequate for use in renewable energy technologies is that it can be used for thermal energy and to generate electricity. This project utilizes the solar thermal energy as a generator for an air conditioning cycle.

CHAPTER 5: ENERGY EFFICIENT ABSORPTION COOLING SYSTEM DESIGN

This Chapter explores the design principles of the components of the Solar-assisted absorption cooling system, such as the Absorption Chiller, Solar Water Heater and Storage tank, air handling unit and air distribution system, Cooling Tower and the control system. It also includes passive cooling design for buildings and concludes with the overall components connections.

5.1 Passive Cooling

Passive Cooling Techniques will seek to minimise the cooling load of the building. Passive cooling techniques are numerous; however it narrows down when one considers a building that has already been constructed.

Architectural methods of passive cooling are in this case limited or omitted, thus the focus will be on non-architectural methods of passive cooling. There are two ways in which passive cooling is achieved.

The first is by keeping heat from entering a building and the second is to prevent the cooler air from escaping the building due to a thermal gradient between the air inside of the building and air outside the building. Solar shading prevents heat from entering the building and this can be achieved using solar window screens.

Solar window screens deflect the sun's heat and glare before it hits the windows, significantly reducing the heat gain in the building by radiation. When the sun’s rays strike the glass, it is too late to control heat gain. When the direct radiation from the sun hits the floor or furniture or any other object within a building, anything from 20% to 80% of that energy is absorbed depending on the texture and colour of the surface. Refer to Table 5.1.

When interior design and decor is done, thought should be given to colour, texture and materials of furnishing with the intention of reducing solar heat gain into the space to be cooled.

Insulation is a means of reducing heat transfer by conduction, convection or radiation. Factors that affect the type and amount of insulation to be used for a building are the climate, ease of installation, durability (resistance to degradation from compression, moisture, decomposition, etc.), ease of

replacement at end of life, cost effectiveness, toxicity, flammability, environmental impact and sustainability. These factors would be examined when consideration is given to reducing the cooling load of a building by insulation installation.

Table 5.1: Solar and Temperature Absorption indices for various surface colours [60].

Surface	**Solar Radiation Absorption [-]**	**Low Temperature Radiation (25 °C) Emission and Absorption [-]**
Polished Aluminium	0.15	0.06
White	0.14	0.97
Yellow	0.30	0.95
Cream	0.25	0.95
Light Gray, Green Blue	0.50	0.87
Med.Gray, Green Blue	0.75	0.95
Dark Gray, Green Blue	0.95	0.95
Black	0.97	0.96

Other methods of passive cooling will not be discussed in detail here as the building that we are intending to cool with the absorption system prototype already constructed.

5.2 Absorption Chiller

In the vapour compression cycle (refer to Figure 5.1 and Figure 5.2), a mechanical compressor creates the pressure difference necessary to circulate the refrigerant. The absorption cycle employs a secondary fluid or absorbent to circulate the refrigerant.

When a liquid evaporates, it absorbs heat. This is the principle on which all air conditioning is based. When a liquid condenses, it cools. The heat given up when a liquid condenses is called the latent heat of condensation. The absorbed heat is called the latent heat of evaporation.

The next principle in air conditioning is that the boiling point of a liquid is related to pressure. When a given body of water becomes hotter, the more it wants to become a gas, however the higher the pressure of the water, the more it wants to condense into a liquid.

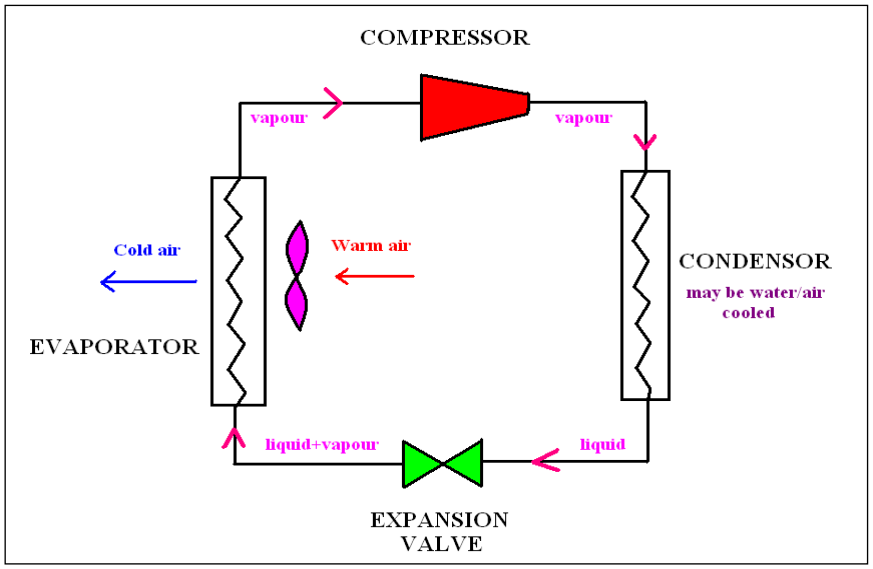

Figure 5.1: Single Stage Mechanical Vapour Compression Refrigeration

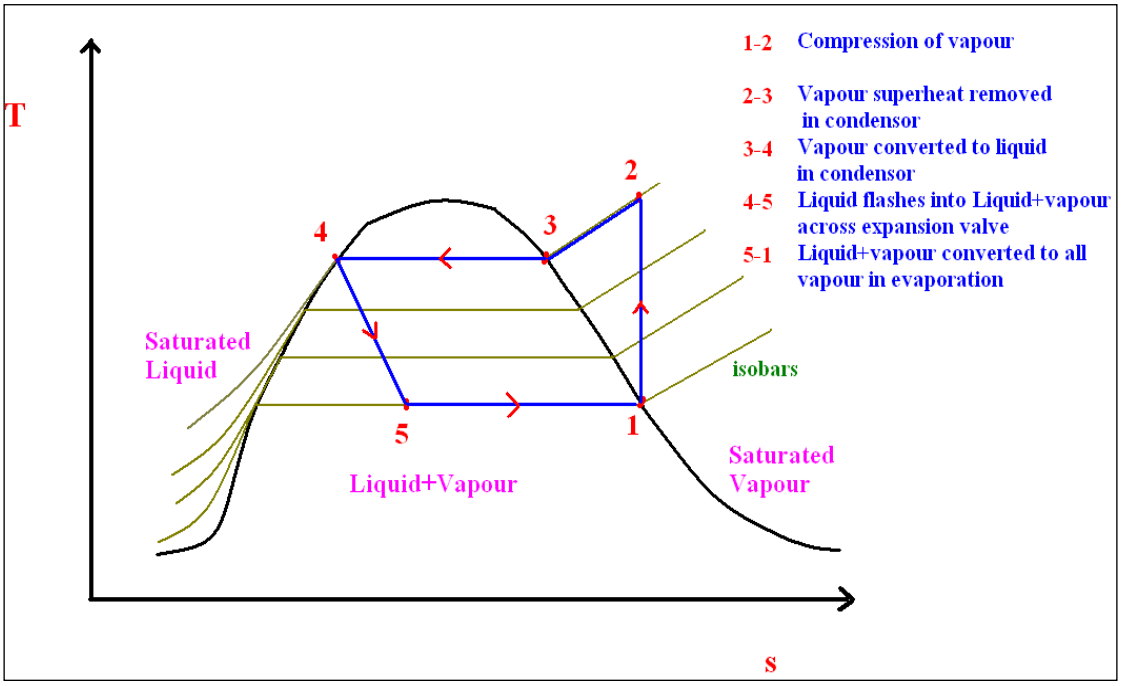

Figure 5.2: Temperature-Entropy Diagram of mechanical vapour compression cycle.

Absorption cooling uses the affinity of some pairs of chemicals to dissolve in one another. Some examples are Lithium bromide and water (which will be used in this project), water and ammonia, and so on. The two factors governing this affinity are temperature and the concentration of the solution.

Figure 5.3 illustrates the main components of the Single-effect absorption refrigeration cycle. High-pressure liquid refrigerant (2) from the condenser passes into the evaporator (4) through an expansion valve (3) that reduces the pressure of the refrigerant to the low pressure existing in the evaporator.

The liquid refrigerant (3) vaporizes in the evaporator by absorbing heat from the material being cooled and the resulting low-pressure vapour (4) passes to the absorber, where it is absorbed by the strong solution coming from the generator (8) through an expansion valve (10), and forms the weak solution (5). The weak solution (5) is pumped to the generator pressure (7), and the refrigerant in it is boiled off in the generator. The remaining solution (8) flows back to the absorber and, thus, completes the cycle [61].

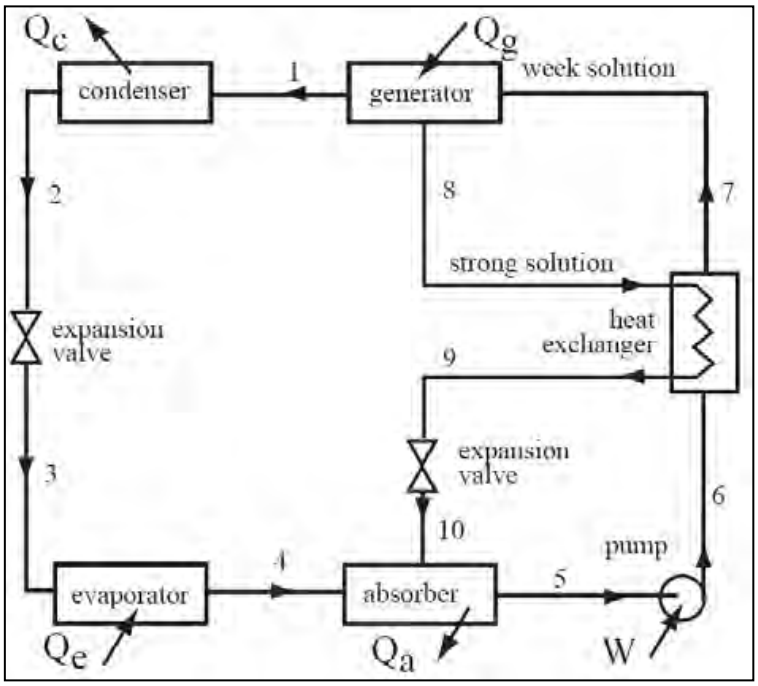

Figure 5.3: Single-effect absorption refrigeration cycle [61].

The temperature requirements to drive the cycle (Q_g) fall into the low-to-moderate temperature range and this can be achieved by utilizing solar thermal energy, and significant potential for electricity savings exist. The process occurs in two vessels or shells that are maintained at two different pressure levels for a successful absorption cooling cycle to result. These pressures are illustrated independently from Figure 5.3 in a Pressure-Temperature graph in Figure 5.4 (i.e. the numbers do not correspond). The upper shell, maintaining a higher pressure contains the generator and condenser and the lower shell, maintained almost in a vacuum, contains the absorber and evaporator which enables the boiling point of water to be decreased significantly. The heat supplied in the generator section is added to a solution of LiBr/H_2O. This heat causes the refrigerant (water or H_2O) to be boiled out of the solution in a distillation process.

The water vapour that results passes into the condenser section where a cooling medium is used to condense the vapour back to a liquid state. The water then flows down into the evaporator section

where it passes over the heat exchanger containing the fluid to be cooled. By maintaining a very low pressure in the absorber-evaporator shell, the water boils at a very low temperature [62].

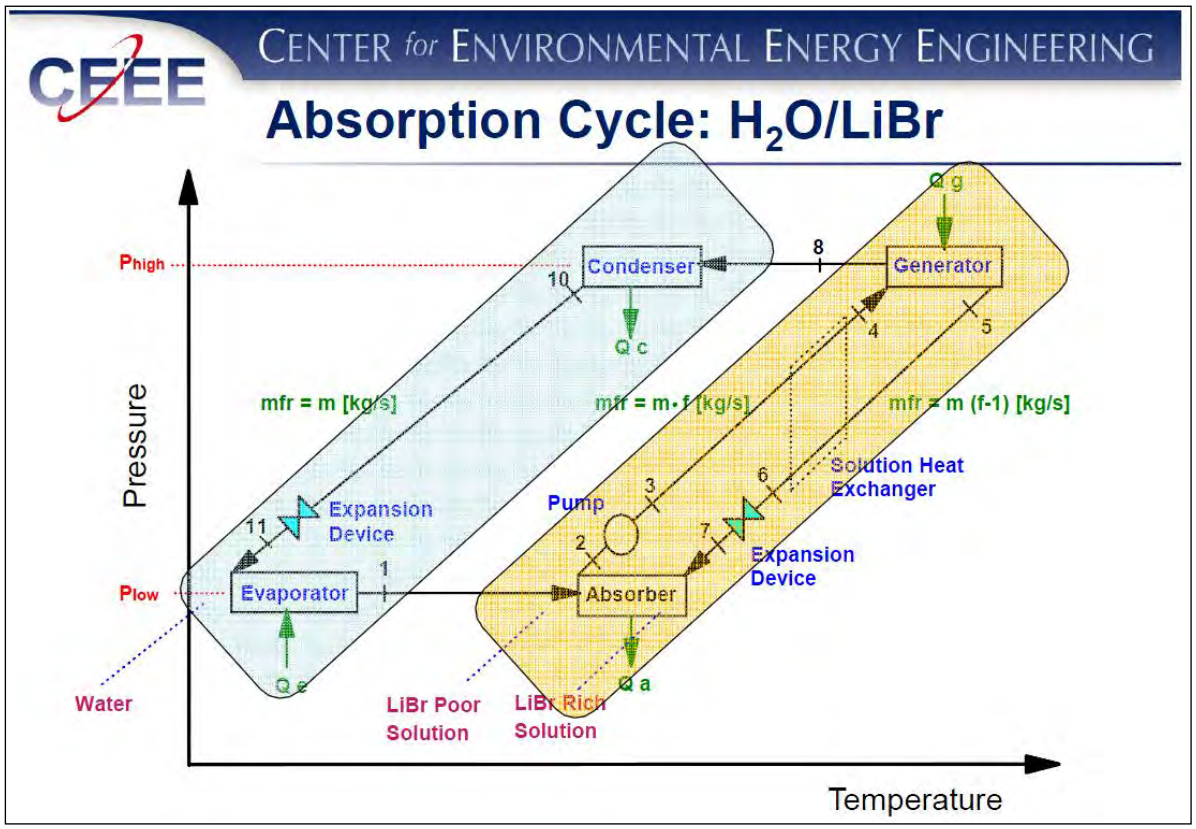

Figure 5.4: Diagram of Pressure versus Temperature for the absorption cycle [63].

The difference between the vapour absorption air conditioning and vapour compression air conditioning is that the former uses thermal energy as work input and the latter uses compressor energy as work input. The success and coefficient of performance of the cycle that brings about air conditioning centres around heat transfer. Actually, the reason that there is a need for air conditioning is because of heat transfer. Heat is a form of energy and energy is a force of nature. Energy cannot be created nor destroyed, but is transferred [64].

Heat exchangers facilitate this heat transfer in the chiller. Heat exchangers are classified according to flow arrangement and type of construction. The simplest heat exchanger is one for which hot and cold fluids move in the same or opposite directions in a concentric tube (or double pipe) construction. In the parallel flow arrangement, the hot and cold fluids enter at the same end, flow in the same direction and leave at the same end. In the counterflow arrangement, the fluids enter at opposite ends, flow in opposite directions and leave at opposite ends. Fluids may also move in cross flow (perpendicular to

each other) and are found in finned and unfinned tubular heat exchangers. Another configuration is the shell and tube heat exchangers.

Heat transfer (or heat) is thermal energy in transit due to a spatial temperature difference. There are three modes of heat transfer that exist, namely conduction, convection and radiation. Conduction is the transfer of energy from the more energetic to the less energetic particles of a substance due to interactions between the particles.

In conduction, these molecular interactions occur when both bodies are in contact or through a continuous mass. Convection heat transfer has two mechanisms, energy transfer due to random molecular motion (diffusion) and transfer of energy by the macroscopic motion of the fluid. This type of motion in the presence of a temperature gradient contributes to heat transfer. Convection is classified according to the nature of the flow. Forced convection is caused by external means such as a fan, pump or atmospheric winds. Natural convection is where flow is induced by buoyancy forces, which are due to density differences caused by temperature variations in the liquid.

Thermal Radiation is energy emitted by matter that is at a nonzero temperature. Regardless of the forms of matter, the emission may be attributed to the changes in the electron configurations of the constituent atoms or molecules. The energy of the radiation field is transported by electromagnetic waves (or alternatively photons). While the transfer of energy by conduction or convection requires the presence of a material medium, radiation does not. Radiation occurs most efficiently in a vacuum. The radiation concept is relevant to the solar water heating and passive cooling designs [65].

Heat exchangers will be designed with the concepts of conduction and convection. The nature of heat exchangers is that their conduction of heat dramatically decreases if the heat exchanger is not regularly maintained. This directly affects the COP of the chiller. Another important aspect in air conditioning is the refrigerant. The refrigerant is the heart of any cooling system as it is the agent by which heat is extracted from the environment to be cooled.

Choosing a refrigerant for an air conditioning system is of environmental concern due to global warming potential of most refrigerants like the R134a (which is the most commonly used refrigerant today). The Pretoria Moot Hospital Absorption Cooling plant uses water as a refrigerant and Lithium Bromide as an absorbent. These are just a few of the design concepts that come into play when designing a chiller for an air conditioning system.

5.3 Solar Water Heater and Storage Tank

This section of the system deals with collecting the heat, transporting the heat and storing the heat. The solar water heater is a thermal collector and it is usually connected to an insulated storage tank. Many designs exist for the various applications, e.g. for swimming pools, for geysers, etc. Newer designs are focussed on improving selective coatings for absorbers using sputter technology, optimising the heat transfer from the absorber to the tubes through improved welding or soldering techniques (ultrasonic or plasma welding) reducing glazing reflection losses through antireflective layers.

Thermal collectors are classified according to the calorific losses between radiation absorbers and their surroundings. Below is a Table of the collector types and their front Heat Transfer Coefficient, (U_f).

Table 5.2: Classification of Collectors by U_f value [66].

Collector type	**Heat resistance between absorber and exterior in direction of incident irradiance**	**Front Heat Transfer Coefficient (U_f)**
Uncovered Swimming pool absorber	Direct radiative and convective heat exchange with environment	Greater than 20
Flat Plate collector with uncoated black absorber	Standing air layer between absorber and transparent cover	5 to 6
Selectively coated flat plate collector	Standing air layer with reduced radiative exchange	3 to 3.5
Selectively coated vacuum tube collector	Reduced convective and radiative heat exchange between absorber and transparent cover	1 to 1.5

The glass evacuated-tube solar collector is the type that is proposed to be utilized in this project to achieve the hot water temperature required by the generator. There are two types of evacuated tube solar collector, one is the heat pipe and the other is the U-tube solar collector. The Heat Pipe solar collector consists of a closed glass tube, inside which is a metal absorber sheet with a heat pipe in the middle, containing the heat transfer fluid. The space between the outer glass tube and the inner absorber tube contains almost no air, i.e. it is evacuated/ in a vacuum which makes heat loss much slower and enabling water to heat up to higher temperatures.

The difference between these collectors is that in the U-tube or U-pipe heat collectors, the heat energy transfer to the water or working fluid is through solar radiation when passing through the entire length of the collector, whereas the water or working fluid is separately contained at the top of the collector in the heat pipe collector and is heated by removing the latent heat through condensation of the water vapour (thus heat exchange) that rose to the top of the heat pipe which was formed when it was heated by the solar radiation. The U-pipe and heat-pipe configuration can be seen in Figure 5.5 and Figure 5.6 respectively.

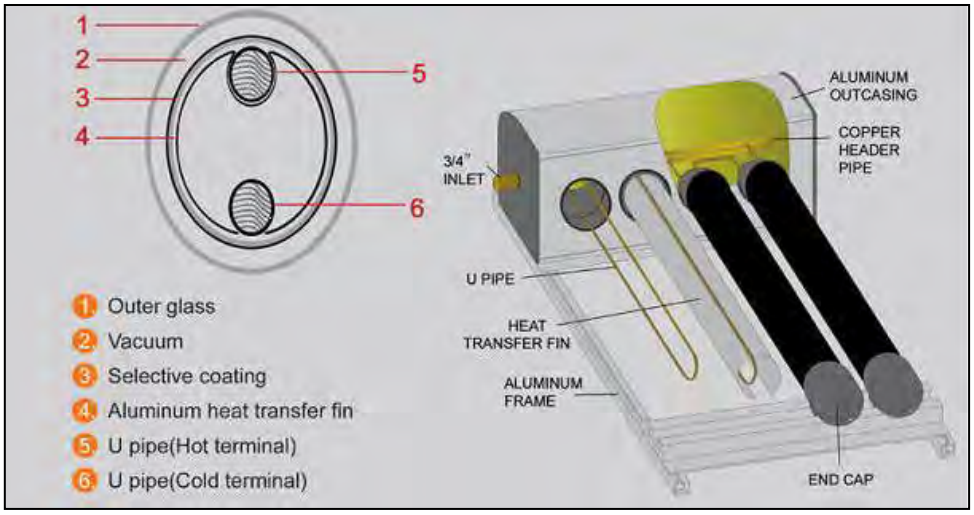

Figure 5.5: Schematic of U-pipe collector [54].

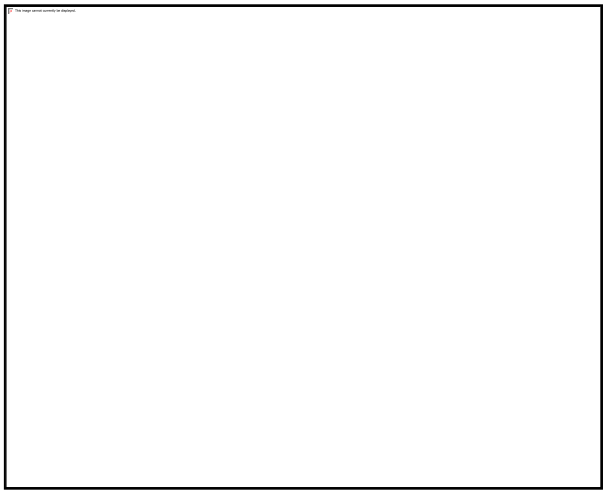

Figure 5.6: Schematic of Heat-pipe collector tube [67].

Glazed or evacuated collectors are described by the following equation:

$$\dot{q}_{coll} = F_R(\tau\alpha)G - F_R U_L \Delta T \quad \text{..... (Equation 5.1)}$$

Where:

$\dot{q}_{coll}$	energy collected per unit collector area per unit time (W/m^2)
F_R	Collector's heat removal factor [-]
τ	Transmittance of the cover [-]
α	Shortwave absorptivity of the absorber [-]
G	global incident solar radiation on the collector (W/m^2)
U_L	Overall heat loss coefficient for the collector (W/m^2K)
ΔT	Temperature differential between the working fluid entering the collectors and outside (K)

Efficiency of the Solar Water Heater is vital to achieve the water temperature required by the generator. Thus, the type of collector used needs to be efficient and capable of reaching the temperature required. Figure 5.7 presents various solar water heater efficiencies

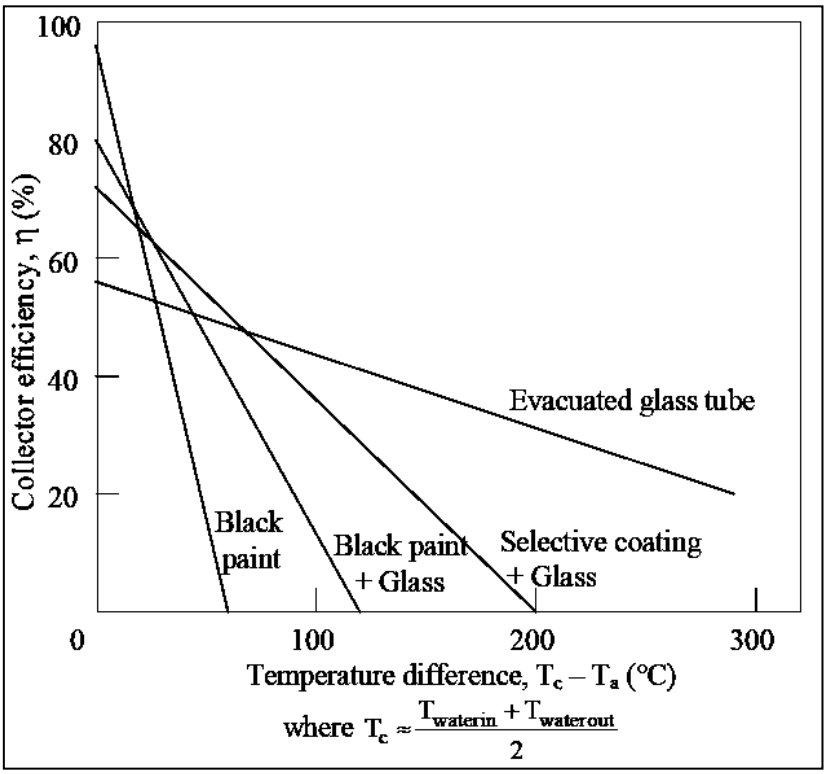

Figure 5.7: Typical solar water heater efficiencies [68].

The factors that come into play in the design and selection of components are the overheating, expansion relief, corrosion, air bubbles pressure, automatic air relief and gas loaded heat pipe temperature control. A control system would be compulsory to ensure that all these factors are taken care of. A maintenance plan should also be drawn up to ensure that the system is operating at its maximum. The type of system arrangement needs to be chosen based on parameters to be determined when the space to be cooled by the air conditioning system is secured.

5.4 Air Handling Unit and Air Distribution System

The air handling unit is the last stage of heat exchange where the heat energy from the air of the space to be conditioned is removed. It contains the fan and its motor, the evaporator together with the inlet and outlet pipes for the chilled water going through the evaporator and the air ducts (supply and return) and the damper for the fresh air intake (refer to Figure 5.8). The air distribution system is connected to the air handling unit and serves to deliver conditioned air and return air to be conditioned to/from the space.

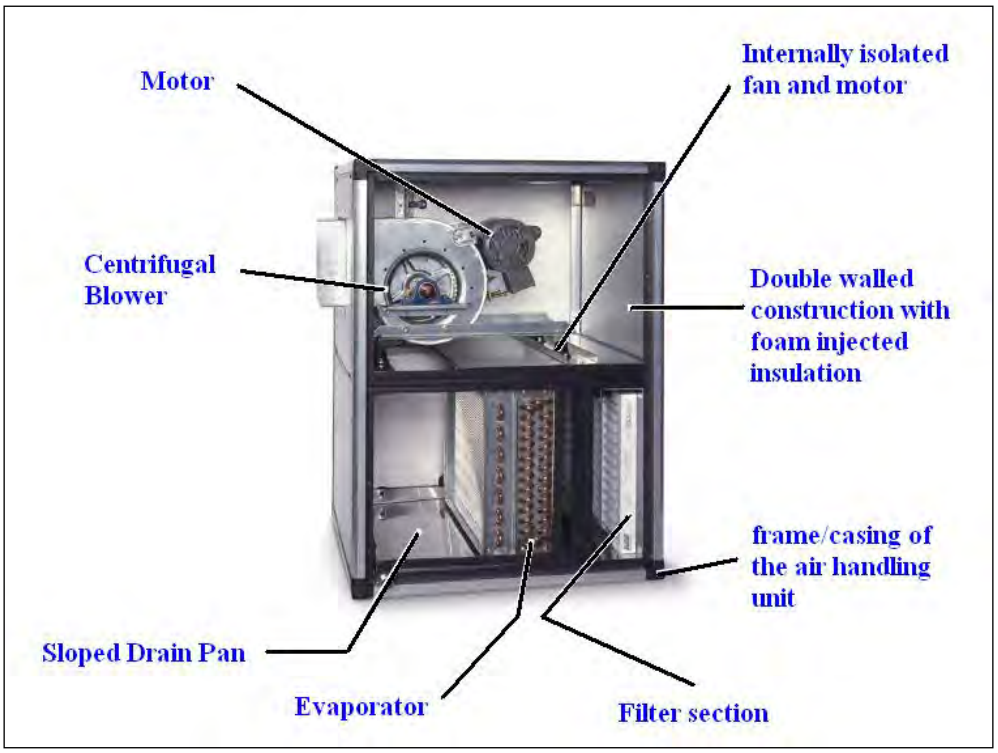

Figure 5.8: Typical air handling unit components [69].

Several design parameters exist that influence the efficiency of an air handling unit (AHU). Two major AHU design choices need to be mentioned for the interest of this project: reducing the pressure

drop and incorporating the most efficient fan 'system'. These design factors are additional to the efficiency of heat exchange between the evaporator and air to be cooled.

Reducing the AHU pressure drop will include lowering the surface velocity which necessitates larger area coils and filter elements and larger AHU housings than conventionally used. Another way to reduce the pressure drop will be to consider filter loading and Variable Frequency Drives (VFDs). In ventilation systems for large buildings, variable-frequency motors on fans save energy by allowing the volume of air moved to match the system demand. Other factors that reduce the AHU pressure will be addressed in the design stage of this project.

Incorporating the most efficient fan design will include choosing the correct fan type and its drive mechanism, motor efficiency and sound power requirements. Attenuators are used to reduce a fan's noise output, but it increases the pressure drop of the AHU. These devices can negate the energy savings from face velocity reductions. Economizer should be used to save energy in both cooling and heating modes of the AHU when the mixing of return air and fresh air is permitted [70].

When designing this system, the concept of 'chaotic air' behaviour needs to be addressed and avoided as this behaviour increases power consumption – which means it requires more energy. The term 'chaotic air' is used to describe the disorganised behaviour of air flow in a ventilated room. The effects of chaotic air flow are instability and sensitivity in temperature and performance reduction in the air conditioning system makes it undesirable.

The term 'chaotic air' is often associated with the term 'butterfly effect' which is a metaphor that encapsulates the concept of sensitive dependence on initial conditions in chaos theory; namely that small differences in the initial condition of a dynamical system may produce large variations in the long term behaviour of the system [71].

Explanation of such behaviour may be sought through analysis of a chaotic mathematical model, or through analytical techniques. The approach to detect chaos in a given system is to investigate numerical results.

5.5 Cooling Tower

Cooling towers provide a means of removing low grade heat from cooling water. Its function is similar to the function of a motor vehicle's radiator. Hot water from the heat exchangers is sent to the

cooling towers. The cooled water exits the cooling tower and is sent back to the heat exchangers and/other components so that these components can continuously be cooled.

In the absorption chiller of this HVAC system, the cooling towers play a vital role in the condenser and absorption heat exchangers. It can be stated that the efficiency of the chiller depends on the efficiency on the cooling towers. Cooling towers fall into two categories according to their configuration: natural draft cooling towers and mechanical draft cooling towers. Natural draft cooling towers employ large concrete chimneys to introduce air through the water and are used for flow rates exceeding 45000m^3/h.

These types of cooling towers are used for utility power stations. Mechanical draft cooling towers are used more often than natural draft cooling towers. They utilize large fans to force air through circulated water. The water falls downward over surfaces which help increase the contact time between the water and air. This maximises heat transfer (loss from water to air) between the two.

The cooling tower theory is that heat is transferred from water droplets passing through the cooling towers to the surrounding air by the transfer of sensible and latent heat. This movement of heat can be modelled with a relation known as the Merkel Equation: [72]

$$\frac{KaV}{L} = \int_{T_c}^{T_h} \frac{dT_b}{h_w - h_a} \quad \text{..... (Equation 5.2)}$$

Where:

$\frac{KaV}{L}$ Tower characteristics [-]

K mass transfer coefficient ($kg\ water/ms^2$)

a contact area/tower volume (m^{-1})

V active cooling volume/plan area (m)

L water rate (kg/ms^2)

T_h Hot water temperature (°C)

T_c Cold water temperature (°C)

T_b Bulk water temperature (°C)

h_w Enthalpy of air-water vapour mixture at bulk water temperature (J / kg dry air)

h_a Enthalpy of air-water vapour mixture at wet bulb temperature (J / kg dry air)

In cooling tower design, charts are typically used to evaluate $\frac{KaV}{L}$, although they can be calculated. These charts can be found in the Cooling Tower Institute Blue Book [73], to estimate $\frac{KaV}{L}$ for given design conditions. Three key points are important to note in cooling tower design: a change in wet bulb temperature (due to atmospheric conditions) will not change the tower characteristics $\frac{KaV}{L}$; a change in the cooling range will not change $\frac{KaV}{L}$; however a change in the $\frac{L_m}{G_m}$ ratio (discussed below) will change $\frac{KaV}{L}$.

Thermodynamics dictates that the heat removed from the water should equal the heat absorbed by the surroundings/ambient air:

$$L_m(T_h - T_c) = G_m(h_2 - h_1) \quad \text{(Equation 5.3)}$$

When rearranged gives

$$\frac{L_m}{G_m} = \frac{h_2 - h_1}{T_h - T_c} \quad \text{(Equation 5.4)}$$

Where:

$\frac{L_m}{G_m}$ Liquid to gas mass flow ratio (kg/kg);

T_h Hot water temperature ($°C$)

T_c Cold water temperature ($°C$)

h_2 Enthalpy of air water vapour mixture at exhaust wet bulb temperature ($J/kg dry air$)

h_1 Enthalpy of air-water vapour mixture at inlet wet bulb temperature (J/kg dry air)

The engineer defines the cooling water flow rate, inlet and outlet water temperatures for the tower and then designs the tower to be able to meet these criteria on a "worst case scenario" which is during the hottest months. The required tower size will be a function of the cooling range, approach to wet bulb temperature, mass flow rate of water, wet bulb temperature, air velocity through tower or individual tower cell and the tower height.

The components of a typical cooling tower will be the frame and casing; fill material, cold water basin, drift eliminators, air inlet, louvers, nozzles and fans. Refer to Figure 5.9 for the cooling tower arrangement.

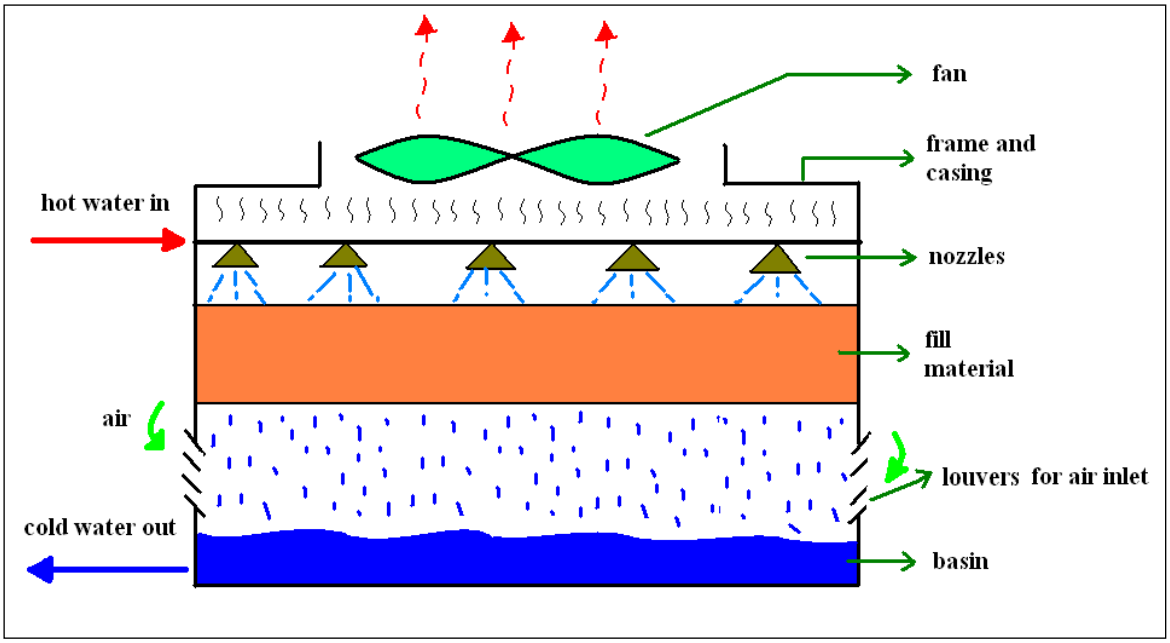

Figure 5.9: Cooling tower arrangement

Not indicated in the Figure 5.9 is the make-up water for the losses that will occur in the process of cooling in the cooling towers. Water losses include evaporation, drift (water entrained in discharge vapour), and blowdown (water released to discharge solids) [72].

The losses in the cooling tower are expressed as follows:

Drift losses = 0.1% and 0.2% of water supply……..…….… (Equation 5.5)

Evaporation Loss (in m^3/hr) = 0.00085*water flow rate (in m^3/hr) * ($T_1 - T_2$)…….... (Equation 5.6)

$$\text{Blow down Loss} = \frac{\text{Evaporation Loss}}{\text{Cycles} - 1} \quad \text{…….……} \text{ (Equation 5.7)}$$

Where cycles = the ratio of solids in the circulating water to the solids in the makeup water.

Total Losses = Drift Losses + Evaporation Losses + Blow down Losses……..……. (Equation 5.8)

The make-up water is provided by a fixed source that is readily available to cover up for the total water losses calculated above. Wood or plastic is commonly used as fill to facilitate heat transfer. This fill maximizes water and air contact. Fill material used is of the splash and film type.

In splash fill, water is designed to fall over successive rows of horizontal splash bars, causing further breaking into smaller droplets as well as wetting the fill surface. The plastic type fill facilitates better heat transfer than the wood splash fill. The film fill is made up of plastic surfaces that are spaced closely over which water spreads – this allows a thin film of water to be in contact with air. The film fill may be honeycombed, flat or corrugated. The fill type is more efficient than the splash type and provides the same heat transfer in a smaller volume.

The water basin at the sump of the cooling tower collects the cooled water which flows/falls from the tower fill sections. This basin usually connects to the cold water discharge. The use of drift eliminators in the air stream are employed to capture water droplets. Air inlets introduce air into the tower by means of louvers. This allows the equalization of air flow into the fill and this assists in retaining the water in the cooling tower. Nozzles provide a means for the hot water (water to be cooled) to be distributed over the fill. Fans are used to induce draft and aid the cooling down of the water.

Even though a percentage of the water is evaporated into the air, the impurities are re-circulated into the system. Concentration of the dissolved solids increases rapidly, and will reach unacceptable levels, if not controlled. This may lead to scaling, corrosion and sludge accumulations which reduces heat transfer efficiencies. Thus it becomes necessary that chemical treatment be implemented and bleeding off a small amount of the circulating water so that the system can be topped up with fresh water. The growth of algae and other microorganisms calls for the use of biocides.

Cooling towers will be designed to be as energy efficient as possible as the core objective of this project is to utilize the minimum amount of grid power.

5.6 Control System

Electronic controls ensure that operations run sequentially for the optimum efficiency of the air conditioning process and the safety of pressurized vessels, pumps, fans, motors, etc. Each component that has a process within itself has a control system. This will imply that many control systems will

exist in this solar-assisted HVAC system, and the question of efficiency arises if these control system are not integrated correctly. Some of the systems controls are the chiller controls, the renewable energy controls (i.e. the solar collector and storage tanks setup), the cooling towers controls and the air handling unit controls.

Control systems have microprocessors (PI controllers and PID controllers), sensors (temperature, humidity, air velocity, pressure), actuators (electronic chilled water/cooling valves, dampers) which all work together in an environment where a sequence of inputs, processing and outputs are coordinated by the microprocessors, the inputs are fed into them from the sensors and the commands are outputs going to the actuators.

Typical controls for a chiller (i.e. >10kW) features the safety cut outs, overrides, capacity control, indications and general start up and operational checks such as diagnostics, recall of alarm and alert messages, etc. The safety cut outs will include, (for a LiBr/H_2O chiller) the absorbent pump motor overload, low chilled water temperature, low cooling water temperature, generator high temperature, generator high pressure, chilled water flow, cooling water flow, chilled water pump interlock, high solution concentration. Overrides will include solution concentration control and capacity control will monitor leaving chilled water and the chilled water reset. Some of the indications will be the chiller operating status, dilution cycle, power-on, pre-alarm alert, alarm, safety shutdown messages, elapsed time/hours of operation, remote/local and standby mode.

5.7 Components Connections

The construction of the project will be measured against the project design and building models developed. The physical connection between them will be as shown in Figure 5.10 below.

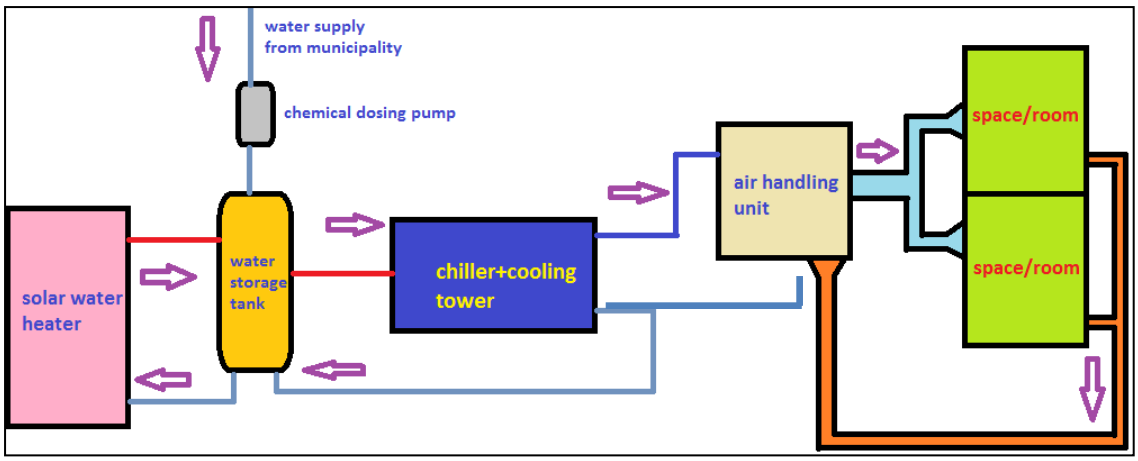

Figure 5.10: Indication of physical connection between components designed in the HVAC system

The objectives of the physical layout would have been designed to minimise material usage, thus keeping cost to a minimum, ensuring that maintenance can be carried out on every system component with ease in terms of access and space to work. Also, consideration will be given to the environment that the components in the system will be placed under to ensure that their operation and longevity will not be compromised.

CHAPTER 6: TESTING METHODOLOGY

The aims and objectives of the present study need to be fulfilled and hence due to this being an experimental study, it is vital that an approach or methodology be established to satisfy the objectives set out in Chapter 1. The solar-assisted HVAC plant installed at the Pretoria Moot Hospital consists of multicomponent parts working together and thus a technical functionality test needs to be undertaken. Once it is established that all these components function correctly both independently and together, the air conditioning efficiency and solar collector efficiency need to be investigated in order to draw conclusions on the technical feasibility of such a plant.

6.1 Testing Models Development

6.1.1 Functionality Test Model

This testing will occur in four parts. They are testing of the individual components or sections that make up the system, acquiring test certificates for selected equipment, testing of component integration after the installation of the working fluids and testing of all electronic controls, i.e. sequential running, safety and maintenance controls.

These tests of functionality for individual components are performed on the fans, motors, valves, pumps, chilled water control/actuator, heat exchangers, water storage tanks, solar water heater, switches, thermostats, thermometers and other sensors.

Apart from testing equipment selected and manufactured for the system, factory testing will have already been done on mechanical equipment such as pumps, motors, fans that were selected and purchased for the system. In this instance, certificates of the tests performed and passed have been acquired. Nameplates attached to the equipment have been captured during the design phase of the project.

Tests for leakages on the air distribution system and water leakages in the chilled water lines have been carried out before putting in the working fluids. When the working fluids are installed, testing of the components integration should also be done. Testing of the features of the electronic control system is the final test in the functionality testing phase. It will as far as possible test all the features for general functionality – the sequential, start and stop commands for the fans, chiller, etc., the safety controls and, where possible, the maintenance indicators, such as dirty filters has been carried out. Procedures for the functionality testing of each component in the system have been established

during the design of the system's components. The outcomes of the functionality testing are indicated in Table 6.1.

Table 6.1: Functionality Test Model

Required design outcome/output	Procedures/actions to achieve output
1. System must be electrically safe and wired according to relevant standards.	Have electrical wiring installed by a qualified electrician and have the installation certified as required by legislation.
2. System must be mechanically safe and implement precautions to reduce risk of hazards.	Pumps, motors, valves, piping, storage vessels, chiller, fans, ducting will be installed only if certified according to standards and full system should be inspected by a competent person.
3. No air leaks, refrigerant or LiBr leakages to be present in the system.	Pressure testing of the system will occur before installation of working fluids will commence.
4. All safety features in the control system for critical equipment must be fully functional to avoid accidents should the system malfunction or its behaviour become uncontrolled.	Control system (sensors, software/commands, and controllers) needs to be tested for functionality on the electronic safety features.
5. System should integrally be given at least one successful test run to ensure that other testing will be striving toward obtaining valid results.	Procedures for a complete test run should be developed and standards should be developed for the expectation of a 'successful run' for the integrated system.

6.1.2 Air Conditioning Test Model

The absorption chiller will be the focus of attention when calculating the air conditioning efficiency. The performance efficiency of the HVAC system is called the coefficient of performance and is calculated according to Equation 6.1. [74]

$$COP_{abs} = \frac{output}{input} = \frac{Q_L}{Q_{gen} + W_{pump,in}} \cong \frac{Q_L}{Q_{gen}} \quad \text{(Equation 6.1)}$$

Where:

Q_L the energy of the refrigerated space

$W_{pump,in}$ the work input (from the pump, as there is no compressor work involved)

Q_{gen} the energy contribution from the generator (which is the solar water heater)

The maximum COP that an absorption system can have is determined by assuming totally reversible conditions, which yields Equation 6.2.

$$COP_{rev,abs} = \left(1 - \frac{T_o}{T_s}\right)\left(\frac{T_L}{T_o - T_L}\right) \quad \text{(Equation 6.2)}$$

Where:

T_o temperature of environment

T_L temperature of refrigerated space

T_s temperature of heat source

The absorption chiller, however, has many components and the COP of the chiller depends on all of these components and thus their efficiency also needs to be looked at. The testing outcomes for the air conditioning efficiency are presented in Table 6.2.

Table 6.2: Air Conditioning Test Model

Required design outcome/output	**Procedures/actions to achieve output**
1. Coefficient of Performance (COP) for air conditioning should be calculated and compared to the usually accepted COP of between 0.6-0.75 for 'water fired, single effect, $LiBr/H_2O$ absorption' chillers.	Derive formulae and procedures for calculation and account should be made in the instance of COP outside of the accepted range.
2. Set air conditioning efficiency expectations/targets.	These expectations should be in line with the solar-assisted absorption cooling plant design parameter.
3. Investigate the trends of the cooling tower and generator.	Present the Cooling tower and generator data and account for their performances.

6.1.3 Solar Collector Efficiency Test Model

The amount of solar energy per unit area per unit time that strikes the earth's surface is termed insolation. To determine what is called the solar constant, one would make measurements normal to the sun's rays in outer space and this will give a fixed amount of solar radiation. However the energy that we receive here on earth is totally different from the solar constant. Figure 6.1 below shows the amount of solar energy, as a percentage reaching the earth.

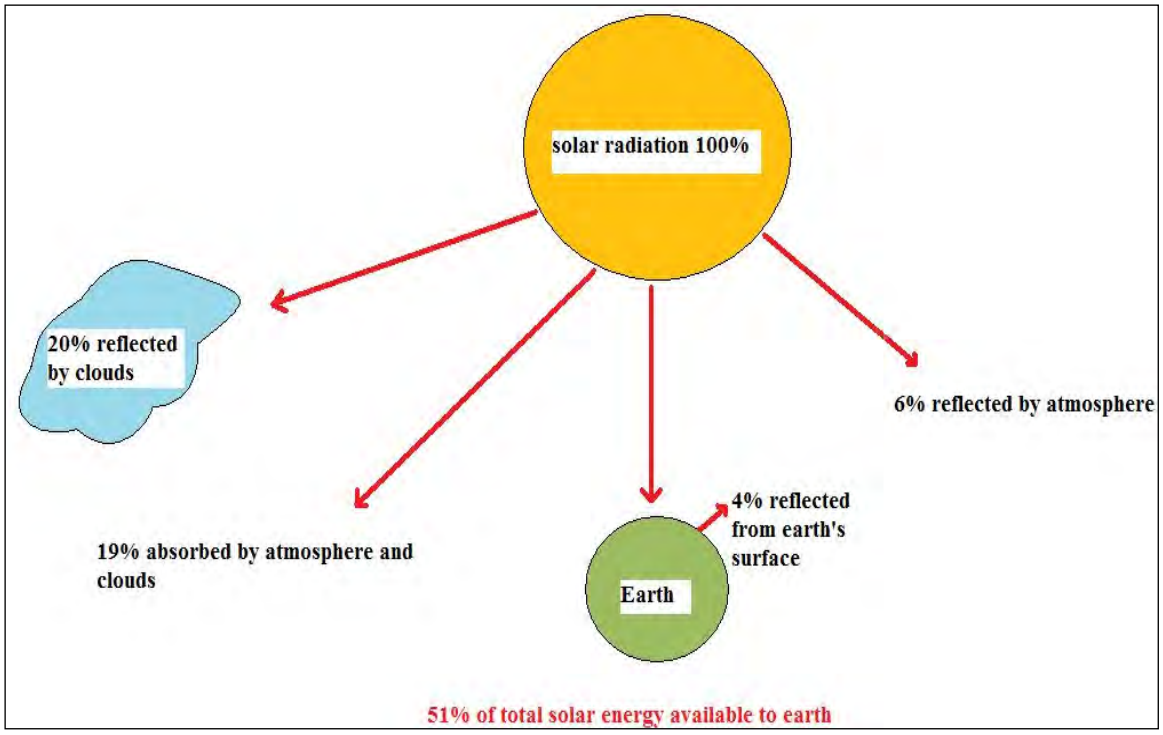

Figure 6.1: Solar radiation available to the earth

It is therefore vital to test the efficiency of the solar collector that will be used to heat water for the generator section of the chiller. On the same level of importance is the conformance of the solar collector system (which is a solar water heater) to the existing standards as laid down by the Government of South Africa in the South African Bureau of Standards (SABS).

In South Africa, the standards that need to be complied with for Solar Water Heaters/ collectors is the SANS 1307:2009 (South African National Standards). The purpose of this standard is to promote energy efficiency, reduce the risk as perceived by the purchaser, end-user or regulator and to establish

norms for safety and performance. The expected outcomes of the efficiency tests of the solar collector are contained in Table 6.3.

Table 6.3: Solar collector Test Model

Required design outcome/output	Procedures/actions to achieve output
1. The solar thermal collector will be tested for its overall efficiency.	Procedures developed to calculate this.
2. The storage tank's heat loss, i.e. the effectiveness of its insulation, will be determined to ensure maximum efficiency.	Procedures developed to test/model its heat loss to the environment.
3. Calculate overall solar water heating system efficiency.	Procedures developed to calculate this.

6.2 Data Acquisition

The Pretoria Moot Hospital was the first site in South Africa to install an absorption cooling plant driven by solar thermal collectors. The plant's system components were installed with many data logging devices at various monitoring points to be viewed and retrieved via a Building Management System (BMS).

The intention of the installation contractor, Voltas Technologies, was to collect data that will be used to study the performance of the plant for the climate of Pretoria in South Africa. The BMS was a system programmed through PlantVisorPro as depicted in Figure 6.2 and the absorption cooling plant system schematic can be seen in Figure 6.3.

Figure 6.2: BMS System Computer programmed through PlantVisorPro software

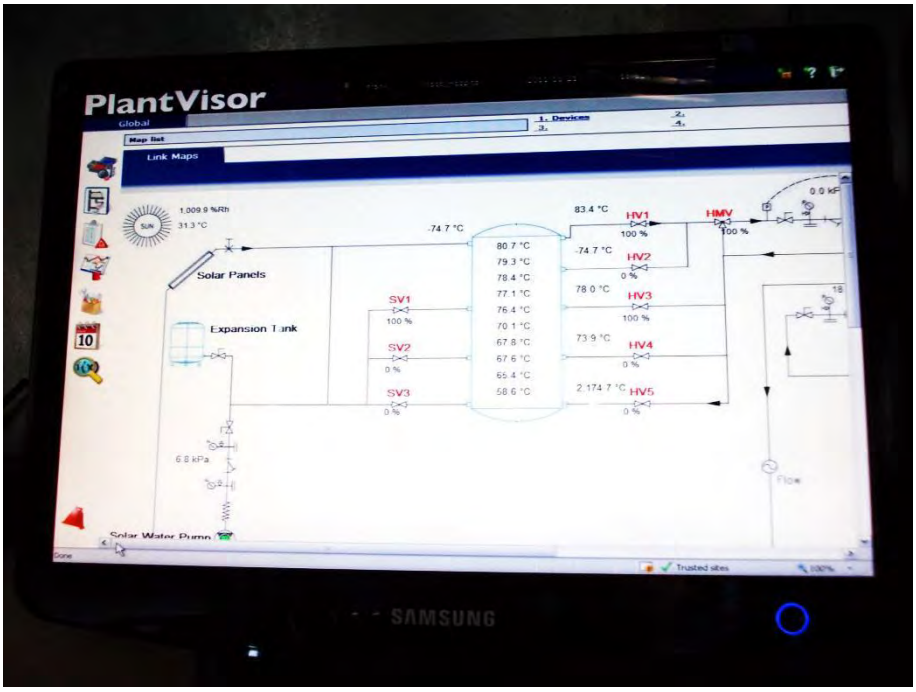

Figure 6.3: Absorption Cooling System overall schematic on the BMS

The solar irradiation data was logged separately on another data logging system onto a memory card that could be downloaded for analysis. The panel in which the memory card was contained is seen in Figure 6.4.

Figure 6.4: Solar irradiation data was logged and stored for retrieval on a memory card in this panel

6.3 Parameters being monitored

The PlantVisorPro logged parameters for the absorption chiller and cooling tower, the hot water storage tank and the power analyzer, whereas a separate system logged the solar irradiation. The probe measuring the solar irradiation can be seen in Figure 6.5.

Figure 6.5: Weather sensor measuring the global solar irradiation received

The parameters that were logged for the various components can be seen in Table 6.4.

Table 6.4: Parameters that were logged by the BMS

Component	Parameter	Description
Absorption Chiller	CHWRT	Chilled Water Return Temperature
	CHWST	Chilled Water Supply Temperature
	C_start	Chiller Start
	C_stop	Chiller Stop
	Flow rate	Chilled water flow rate
	HWST	Hot Water Supply Temperature
	HWRT	Hot Water Return Temperature
Cooling Tower	CWRT	Cooling Water Return Temperature
	CWST	Cooling Water Supply Temperature
Hot Water Storage Tank	T1-T10	Temperature 1 to Temperature 10 (along the height of the hot water tank)
	ΔT_solar	Difference between the temperature of the water in the hot water storage tank and the temperature of the hot water in the solar collectors.

	Solar Temp	Temperature of water in the solar collectors
	Solar Water flow	Flow of water in the solar collectors
	Solar Water Return Temperature	Temperature of water entering the solar collectors
	T11-T16	Temperature 11 to Temperature 15 along the height exiting the storage tank to the chiller and T16 entering the Hot water storage tank from the solar collectors.
Atmospheric Conditions	Tamb	Ambient Temperature
	R_H amb	Ambient relative humidity
Power Analyzer	P_avg	Average power
	P	Power
	P_act	Active power
	P_{avg} app	Average Apparent Power
	T_elec	Electric Chiller Chilled water supply temperature

The solar valves and heat medium valves can be seen in Figure 6.6. The solar valves controlled the flow of water from the hot water storage tank to the solar thermal collectors whereas the heat medium valves controlled the flow of water from the hot water storage tank to the absorption chiller's generator. The temperature probes on a section of the hot water storage tanks can be seen in Figure 6.7.

Figure 6.6: Solar Valve (SV) [left] and Heat Medium Valve (HV) [right]

Figure 6.7: Temperature probes on a section of the absorption cooling system

CHAPTER 7: THE PRETORIA MOOT HOSPITAL ABSORPTION PLANT

This Chapter provides an overall description of Netcare's Pretoria Moot Hospital Heating, Ventilation and Air Conditioning (HVAC) plant that controls the temperature and humidity in the hospital's reception area, foyer, trauma unit and operating theatres. It includes the description of the components of the plant and the control logic that is executed. The Chapter concludes by comparing the plants specifications to that of the "Design and Building Models" that were stipulated in the research proposal where the initial intention was to design and build a prototype Solar-Assisted Absorption Cooling Plant.

7.1 General Description of Absorption Cooling Plant

The Pretoria Moot Hospital HVAC plant is in the province of Gauteng, 1400 metres above sea level. The original installation, completed and commissioned in October 2007, consists of a chiller driven by mechanical compression, delivering a maximum cooling capacity of 48.11kW. This chiller is designed for outdoor installation and is positioned on the roof of the Netcare Moot Hospital.

The chiller's condenser is air cooled and the chilled water produced at 7 °C is sent to a cold buffer tank. Refer to Table 7.1 below for specifications of the chiller.

Table 7.1 Specifications of compressor driven chiller at Moot Hospital HVAC plant

Item	Specification
Model	Aqua CIAT 300Z Series LDH
Cooling Capacity	48.11kW
Entering Chilled Water Temperature	12 °C
Leaving Chilled Water Temperature	7 °C
Chilled Water flow rate in litres per second	3.6 l/s
Refrigerant type	R-410A
Design Ambient Temperature	35 °C

The buffer tank holding the chilled water is well insulated to ensure that there is negligible heat gain into the chilled water until it is required by the air handling unit.

Refer to Figure 7.1 and Figure 7.2 for pictures of the chiller and buffer tank respectively.

Figure 7.1: Mechanical Compression Chiller at the Moot Hospital Plant

Figure 7.2: Chilled water buffer tank to which chilled water is sent from the chiller

Chilled water is circulated between the heat exchanger of an air handling unit and the buffer tanks via four pumps as the cooling demand fluctuates. Refer to Figure 7.3 and 7.4 for pictures of the pumps.

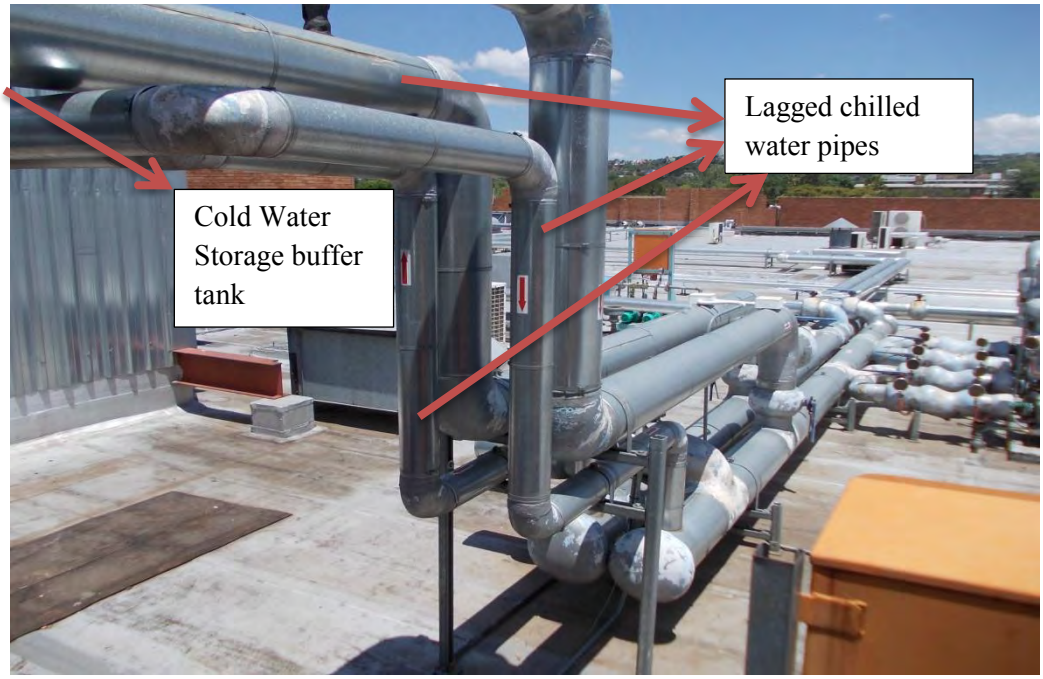

Figure 7.3 Lagged Chilled Water Pipes leading from buffer tank (top left) to pumps

Figure 7.4 Pumps circulating chilled water between the buffer tank and air handler

The air handling unit or air handler, which is the last desired heat exchange between the return air from the conditioned spaces and the chilled water closed circuit, filters the return air and rejects the

heat contained in it to the chilled water which is sent back into the buffer tank. Specifications of the air handling unit are contained in Table 7.2 below.

Table 7.2 Specifications of the air handling unit

Item	Specification
Model	TAD0608BH
Cool air flow	2.9m^3/s
Air Coil Entering (dry bulb temperature)	20.3 °C
Air Coil Entering (wet bulb temperature)	14.6 °C
Air Coil Leaving (dry bulb temperature)	8.7 °C
Air Coil Leaving (wet bulb temperature)	8.6 °C
Total Cooling	48.11kW
Sensible Cooling	33.97kW
Chilled Water Flow	1.57 l/s
Chilled Water on/off	6/13.3 °C
Water Pressure drop	22.8kPa
Air Pressure Drop	240Pa
Coil Face Velocity	1.93m/s
Number of Coils	1
Coil FPI	10fpi
Coil rows	8
Coil Fin Material	Blue Fin
Coil Casing material	Stainless Steel
Drain pan	Stainless Steel
Electric Heater	15kW

Included in the air handling unit are 3 heaters which total 15kW heating capacity and a steam humidifier which delivers 10kg/h an 11kW variable speed drive motor to drive a centrifugal supply air fan of double inlet, double width impeller. Due to the fact that the conditioned spaces include the trauma unit and operating theatres, the air handling unit comprises of 3 types of air filters. This is the primary, secondary and HEPA filters. Refer to Table 7.3 for their specifications. Refer to Figure 7.5 for pictures of the air handling unit.

Table 7.3: Specifications of filters in Air Handling Unit

Type of filter	Specification
Primary filters	G4 plate consisting of chemical fibre Resistance: initial = 55Pa, final = 250Pa
Secondary filters	F6 bag filter consisting of chemical fibre Resistance: initial = 55Pa, final = 250Pa
HEPA filters	F9 mini pleat consisting of glass fibre Resistance: initial = 135Pa, final = 600Pa

Figure 7.5: Air handling unit

The air handler outputs filtered conditioned air returned from the space to be conditioned via galvanised metal air ducts through diffusers at constant air flow to the conditioned space. The various sections of the air handling unit is pictured is Figures 7.6, 7.7, 7.8, 7.9 and Figure 7.10. The supply and return air ducts can be seen in Figure 7.11.

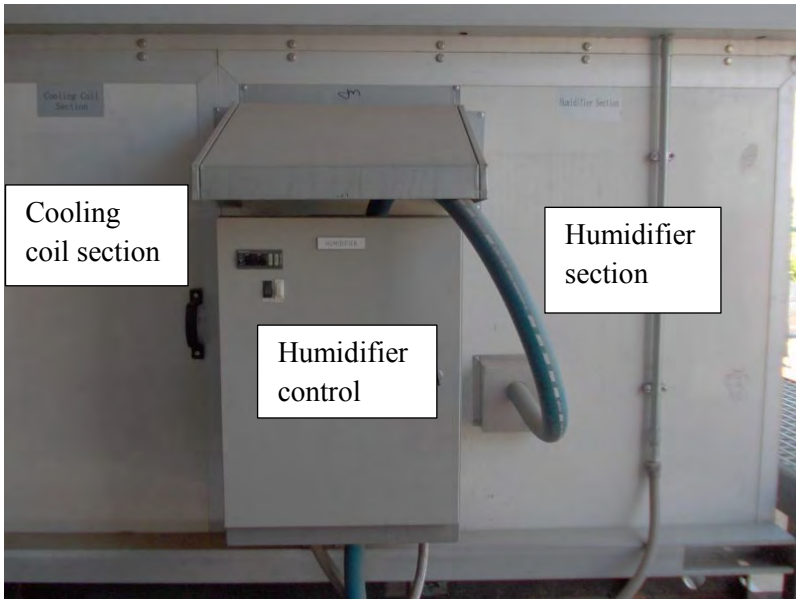

Figure 7.6: Steam humidifier and cooling coil sections of the air handling unit

Pretoria has a lower humidity than other areas in South Africa such as Durban and Cape Town, therefore it is necessary to humidify the air to maintain thermal comfort levels and thus a steam humidifier is used to achieve this as shown in Figure 7.6.

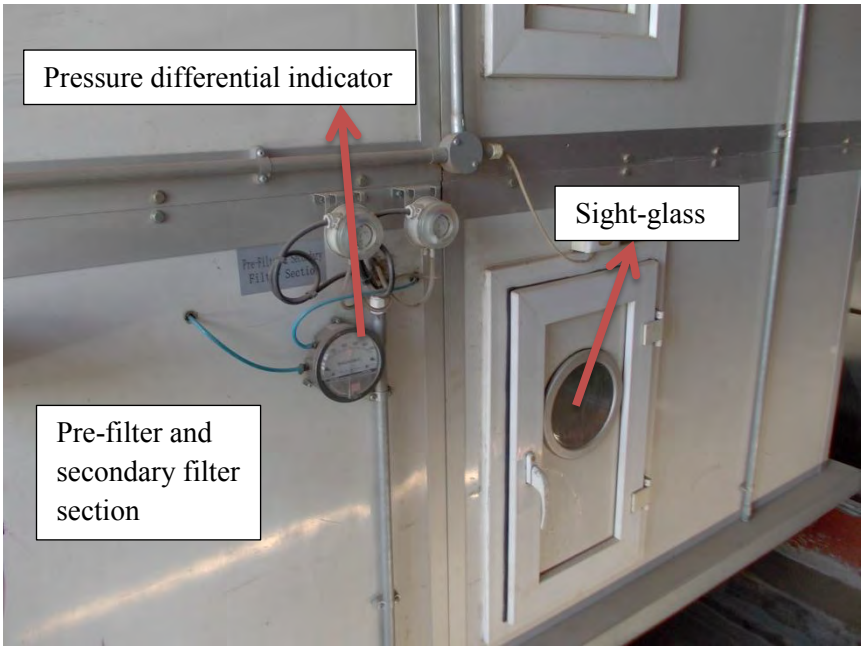

Figure 7.7: Prefilter and secondary filter sections showing pressure differential indicator

The filters section have pressure differential indicators (Magnehelics) that indicate when the filters are dirty and thus serve as a maintenance indicator as seen in Figures 7.7 and 7.8.

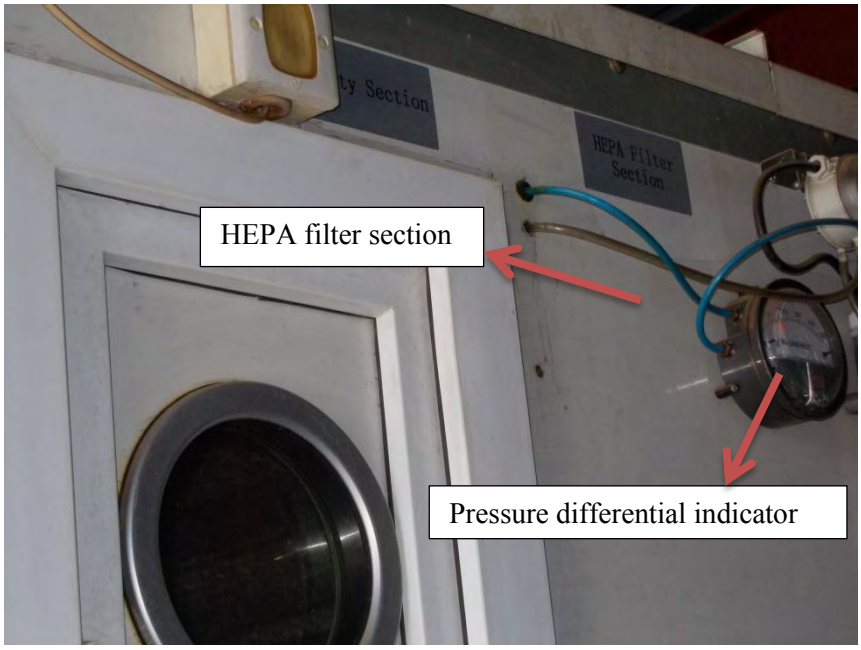

Figure 7.8: HEPA filter section with pressure differential indicator for maintenance

Temperatures sometimes go below thermal comfort in winter and heating is required and therefore the air handling unit has an electric heater section as shown in Figure 7.9.

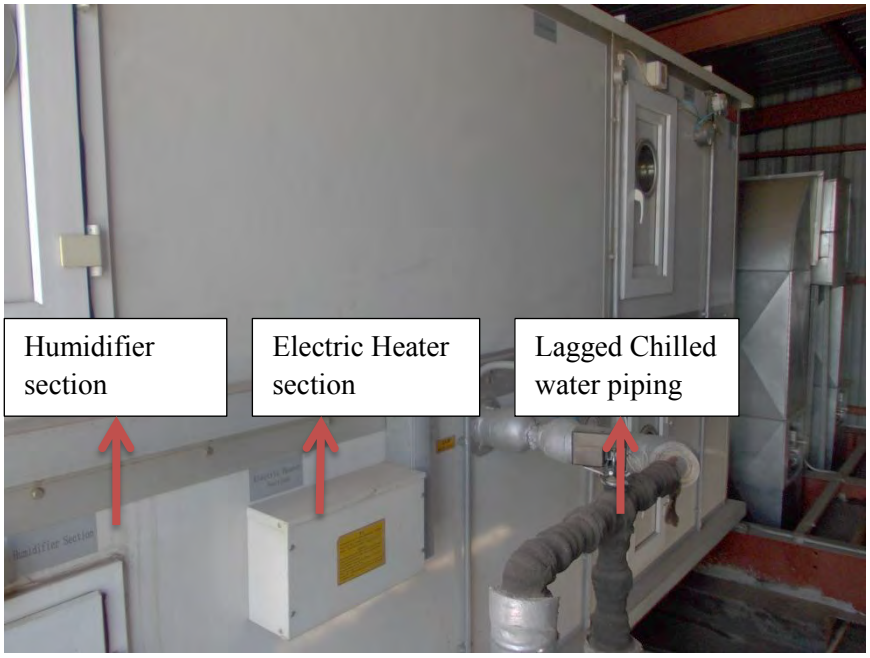

Figure 7.9: Humidifier, electric heater section, lagged chilled water piping and section of duct

The blower and diffuser, with the sound attenuation are shown in Figure 7.10. The air handling and distribution is a closed loop system, not introducing fresh air into its loop, the supply and return air ducting is shown in Figure 7.11.

Figure 7.10: Blower, diffuser and sound attenuator section

Figure 7.11: Supply and return air ducting

The air handling unit does not incorporate fresh air into the conditioned air delivered to the space, but a separate ventilation system isolated from the HVAC plant introduces fresh air into the refrigerated space. Fresh air volume delivered to all conditioned spaces is at a 0.52m^3/s.

The conditioned spaces are the Hospital's Trauma Unit, Operating Theatres and the Reception area and Foyer. The Foyer, Trauma Unit and Reception areas setpoint is at 22 °C, whereas the Operating Theatres setpoint is at 10 °C. The temperature operating range of the Trauma, Reception Area and Foyer areas is at 17 °C to 22 °C at humidity of 40% to 60%. The Reception and foyer areas air is filtered by Primary and Secondary filters, whereas the Trauma and Operating Theatres air is filtered through the HEPA filters.

In October 2009, assistance was provided to the plant by the installation of a solar powered absorption plant of 35kW cooling capacity based on water (H_2O) as the refrigerant and Lithium Bromide (LiBr) as the absorbent. The system was installed to reduce the demand on the electrically powered compressor driven chiller during the daylight hours by using solar energy to remove the solar heat gain of the conditioned spaces, thus saving on power during the peak period.

The absorption cooling plant is powered by 52 solar water collectors of which 40 are U-pipe evacuated tube collectors and 12 are heat pipe evacuated tube collectors. These collectors circulate water to a hot water buffer tank which then supplies the generator of the absorption chiller. The chiller produces chilled water at 7 °C to the cold buffer tank that supplies the air handling unit of the plant.

The focus of this project is on the feasibility analysis of the absorption cooling plant and hence the testing of the Absorption plant for performance and energy saving will be executed, thus the details of the Absorption cooling installation will be covered elaborately in this Chapter.

7.2 Solar Thermal Collectors and Hot Water Storage Tanks

The "renewable energy" applications of the system are the solar thermal collectors supported by the hot water buffer tank. There are two types of solar collectors used in the Pretoria Moot Hospital Plant.

Due to the fact that this plant was the first solar powered absorption cooling plant installed in South Africa, the intention of installing heat-pipe and U-pipe collectors was to test the effectiveness of two types of solar collectors. The operation was short lived due to complexities experienced in integrating the two systems and the cost to incorporate controllers and sensors to monitor for efficiency calculations, therefore the efficiency was never carried out. The U-pipe solar evacuated tube collector can be seen in Figure 7.12.

Figure 7.12: U-pipe Solar Collectors on the roof of Netcare's Moot Hospital in Pretoria

The specifications of the U-pipe Solar collectors can be found in Table 7.4.

Table 7.4 Specification of U-pipe solar collectors

Item	**Specification**
Model	HUJ-16/2.1
Aperture Area	1.8m^2
Maximum Temperature	120 °C
Rated Pressure	0.6MPa
Frame Material	6063T5
Dimensions of vacuum tube	Diameter of 58mm and length of 2100mm
Length, width and height	2278mm×1636mm×134mm

The Heat pipe solar collector was the second type that was used and it can be seen in Figure 7.13.

Figure 7.13: Heat pipe Solar Collectors on the roof of Netcare's Moot Hospital in Pretoria

The specifications of the Heat Pipe Solar Collector are found in Table 7.5 below.

Table 7.5: Specification of heat-pipe solar collectors

Item	**Specification**
Model	HRJ-12/1.8
Aperture Area	$1.1m^2$
Maximum Temperature	120 °C
Rated Pressure	0.6MPa
Frame Material	6063T5
Dimensions of vacuum tube	Diameter of 58mm and length of 1800mm
Length, width and height	1978mm×1200mm×134mm

The U-pipe made of copper, is in a Borosilicate 3.3 tube that is under a vacuum degree of 5×10^{-4} Pa transferring irradiation to an aluminium fin covered in a AIN-SS/AIN-CU film layer with an absorptance of 94% to 96%.

The collectors are installed facing North at an inclination of 30 degrees from the horizontal surface of the roof of the Netcare's Pretoria Moot Hospital. For most installations (especially important in flat plate solar collectors) in the Southern hemisphere will face the North and tilt at an angle equal to the latitude of the location in which the plant is installed. The correlation of these collectors were given to

Voltas Technologies by the German Fraunhofer Research Institute in Stuttgart and can be seen in Equation 7.1 for U-pipe solar collector and Equation 7.3 for heat pipe solar collector.

Correlation used for the U-pipe Solar Water Heaters is given by Equation 7.1

$$\dot{Q}_{solar} = n_{U-pipe} \times A_{aper}\left[\eta_0 \times G - \alpha_{1a}\left(\frac{T_1 + T_2}{2} - T_o\right) - \alpha_{2a}\left(\frac{T_1 + T_2}{2} - T_o\right)^2\right] \ldots\ldots\ldots \text{(Equation 7.1)}$$

Where:

$\dot{Q}_{solar}$ Heat Energy transferred to the solar water heaters (referred to as "collectors") (W)

n_{U-pipe} Number of U-pipe Solar Water heaters [-]

A_{aper} Aperture area of Solar Water Heater = $1.764 m^2$

η_0 Efficiency of collector without heat losses, this implies the efficiency when the mean Collector fluid temperature is equal to the ambient temperature = 0.779

G Global irradiance on the collector area (W/m^2)

α_{1a}, α_{2a} Coefficients of heat loss of the collector = $2.103 W/m^2K$, $0.0107 W/m^2K^2$

T_1 Temperature of water entering into the collectors (K)

T_2 Temperature of water exiting the collectors (K)

T_o Ambient Temperature of the environment outside the collectors (K)

Equation 7.1 can be simplified to give Equation 7.2 below:

$$\dot{Q}_{solar} = n_{U-pipe} \times A_{aper}\left[\eta_0 \times G - \alpha_{1a}(T_m - T_o) - \alpha_{2a}(T_m - T_o)^2\right] \ldots\ldots\ldots\ldots\ldots\ldots \text{(Equation 7.2)}$$

Where $T_m = \frac{T_1 + T_2}{2}$ is the mean temperature of the collector fluid.

The same correlation can be used for heat-pipe solar water collectors as their tubes have the same orientation towards the incoming irradiance. However for a difference of 5K between the mean collector fluid and ambient temperature, the correlation will simplify to Equation 7.3

$$\dot{Q}_{solar} = n_{U-pipe} \times A_{aper}\left[\eta_0 \times G - \alpha_{1a}(T_m - T_o)\right] \ldots\ldots\ldots\ldots\ldots\ldots\ldots\ldots\ldots\ldots \text{(Equation 7.3)}$$

The working fluid is water which is circulated through the solar collectors to an insulated heat storage/buffer tank from which it is released to the generator of the absorption chiller via a controlled process. The buffer tanks can be seen in Figure 7.14.

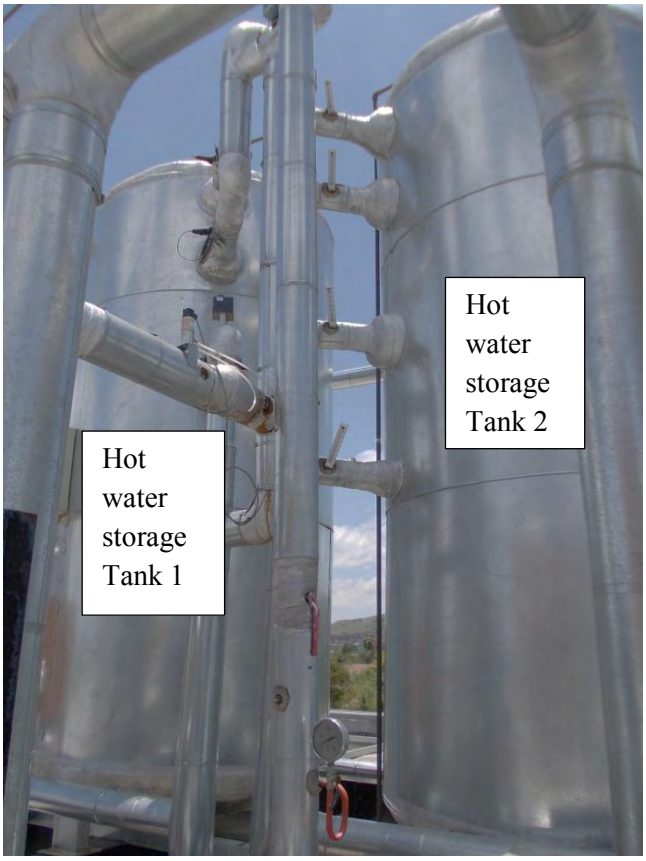

Figure 7.14: Two 6000l hot water buffer tanks

The intention of two hot water storage tanks was that the extra tank will be used to experimentally investigate the use of phase change materials as an opportunity for heat storage so that the chiller could run even with the absence of solar irradiation on the collectors. However this investigation into the use of phase change materials was not done due to lack of funds. The design of the 6000l hot water buffer/storage tank was such that it was to be stratified using metal plates or disks.

The 1.31m diameter steel tank with a height of 3m (excluding the dome height) exhibited the stratification of water, a phenomenon present in stagnant water to prevent mixing or turbulence. The colder the water is, the higher is its density and due to the low thermal conductivity of water, it tends to remain in separate layers. There were three metal plate disks placed into the tank, the top two plates have holes through the centre and the bottom plate is just a grid intended to facilitate improvements in the heat storage of the tank by the use of material with heat storing capacities. Refer to Figure 7.15 for a view inside the tank.

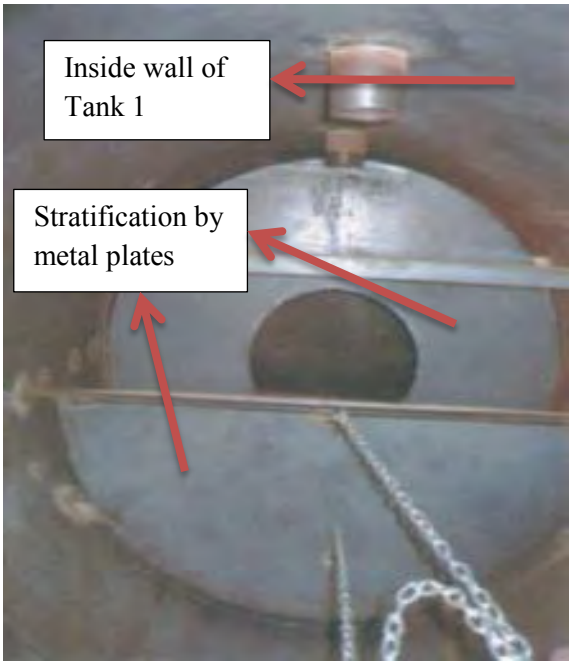

Figure 7.15: View inside the Steel Hot Water Buffer/Storage Tank taken during installation
(Picture taken from Voltas Technologies files at their office in Midrand, Gauteng, South Africa)

The hot water stored in the hot water buffer/storage tank remains in the tank until it has reached the temperature required by the generator of the chiller. The purpose of stratification in the tank allows this temperature to be reached sooner by some portion of the water in the storage/buffer tank, than waiting for the working fluid in the entire tank to reach the required temperature for the generator of the absorption chiller.

7.3 Aroace Yazaki Absorption chiller

Once the required temperature for the generator of the Yazaki Absorption chiller is reached in a particular section of the hot water storage tank, it is transferred to the 35kW Aroace Yazaki Single effect Absorption chiller. A picture of the chiller is shown in Figure 7.16.

Absorption cooling uses the affinity of some pairs of chemicals to dissolve in one another. Some examples are Lithium bromide and water (which will be used in this project), water and ammonia, and so on. The two factors governing this affinity are temperature and the concentration of the solution. The absorption chiller set up is shown in Figure 7.17.

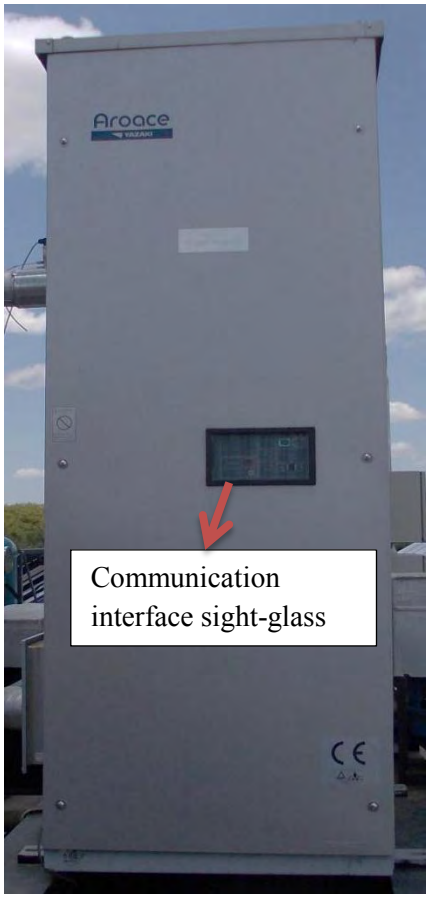

Figure 7.16: 35kW Absorption Chiller on the roof of Netcare's Moot Hospital in Pretoria

The process occurs in two vessels or shells. The upper shell contains the generator and condenser and the lower shell, the absorber and evaporator. The process begins when hot water heated by the solar collectors is passed through the generator of the chiller and the solution pump begins pumping a solution of $LiBr/H_2O$ (diluted). This heat circulating in the generator causes the refrigerant (water) to be boiled out of the solution in a distillation process.

The hot water vapour (refrigerant vapour) that results passes into the condenser section over coils circulating cold water and is condensed to a liquid state. The cooled refrigerant water then flows down into the evaporator section where it passes over the evaporator circulating the water to be cooled, thus producing chilled water. Due to a low pressure being maintained in the absorber-evaporator shell, the refrigerant water boils off the evaporator coil at a very low temperature.

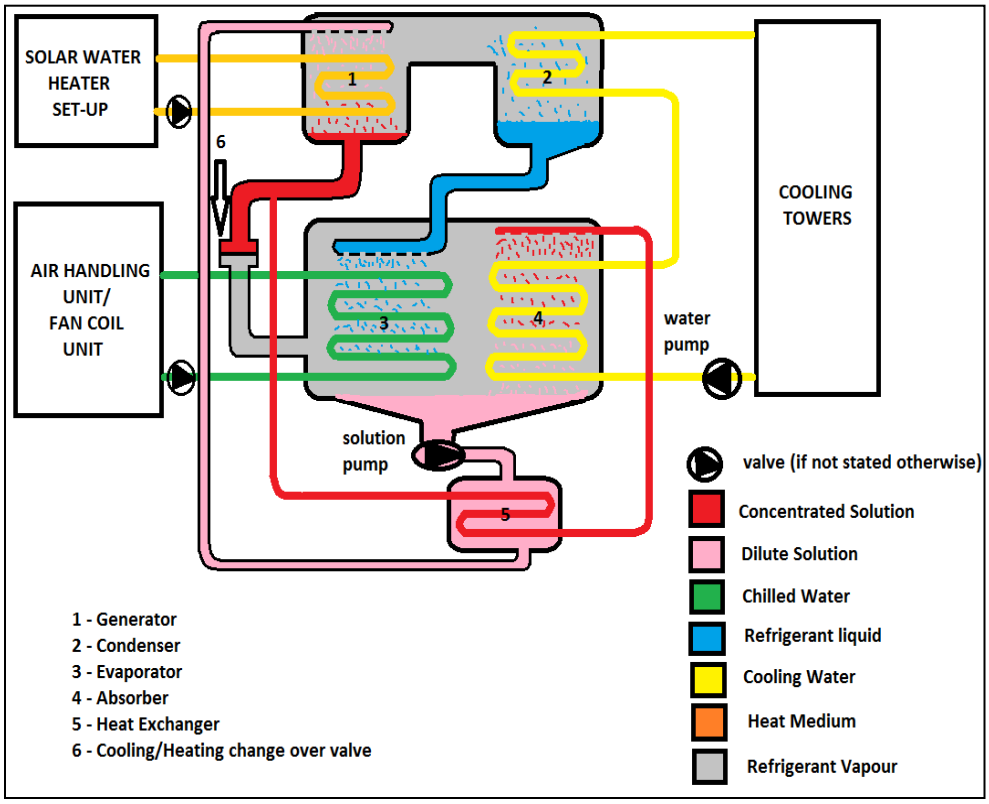

Figure 7.17: Components of chiller and its relation to other HVAC plant components

Water vapour refrigerant is then absorbed by the concentrated LiBr that passed from the generator (where the refrigerant was first separated from the solution), through the heat exchanger and over the cooling water where was cooled. This absorption process is as a result of the affinity of LiBr towards water; the resulting dilute solution is then ready to be pumped back to the generator where the cycle is repeated.

The difference between the vapour absorption air conditioning and vapour compression air conditioning is that the work input is different in that the former uses thermal energy as work input and the latter uses compressor energy as work input.

This chiller also has the ability to provide heating through a heating cycle. Refer back to Figure 7.17. The LiBr/H_2O solution is pumped to the generator by the solution pump where it is heated to boiling point by the circulating heat medium. Water vapour (refrigerant) is released from solution and flows to the condenser. The cooling tower is however not operational and the hot water vapour condenses on the coil of the evaporator. The heat of condensation is transferred and the circulating chilled/hot water increases in temperature to be sent to the air handling unit for heating purposes.

Due to partial separation of the LiBr and H_2O solution occurring in the generator, an increase in the concentration of the LiBr solution occurs. The changeover valve is open as the cooling towers are not functional, allowing the concentrated LiBr into the base of the evaporator shell and is diluted as it absorbs the condensed hot refrigerant liquid. The process is then repeated. Specifications for the chiller can be found in Table 7.6.

Table 7.6: Specifications of Aroace Yazaki Absorption chiller using LiBr/H_2O

Item	**WFC-SH10**
Chilled Water: Cooling Capacity	35 kW
Hot Water: Heating Capacity	48.6 kW
Chilled Water: Temperature Inlet (Cooling)	12.5 °C
Chilled Water: Temperature Outlet (Cooling)	7 °C
Hot Water: Temperature Inlet (Heating)	47.4 °C
Hot Water: Temperature Outlet (Heating)	55 °C
Chilled/Hot Water: Evaporator Pressure Loss	56.1 kPa
Chilled/Hot Water: Maximum Operating Pressure	588 kPa
Chilled/Hot Water: Flow Rate	1.53 l/s
Chilled/Hot Water: Water Retention Volume in litres	17 l
Cooling Water: Heat Rejection	85.5 kW
Cooling Water: Temperature Inlet	31 °C
Cooling Water: Temperature Outlet	35 °C
Cooling Water: Absorber/Condenser Pressure Loss	85.3 kPa
Cooling Water: Coil fouling factor	0.086 M^2hr°K/kW
Cooling Water: Maximum Operating Pressure	588 kPa
Cooling Water: Flow Rate	66 l/s
Cooling Water: Water Retention Volume	66 l
Heat Medium: Heat Input	50.2 kW
Heat Medium: Temperature Inlet	88 °C
Heat Medium: Temperature Outlet	83 °C
Heat Medium: Temperature Range	70 °C - 95 °C
Heat Medium: Generator Pressure Loss	90.4 kPa
Heat Medium: Maximum Operating Pressure	588 kPa
Heat Medium: Flow Rate	2.4 l/s
Heat Medium: Water Retention Volume	20.8 l

...continued	
Electrical Power Supply	400 3 Phase 50Hz
Electrical Consumption	210 W
Electrical Current	0.43 A
Control Cooling	On/Off
Control Heating	On/Off
Width	760 mm
Depth	970 mm
Height (includes fixing plate)	1920 mm
Dry Weight	500 kg
Operating Weight	604 kg
Acoustics: Noise Level	46 dB(A)
Piping Diameter: Chilled/Hot Water	40 mm
Piping Diameter: Cooling Water	50 mm
Piping Diameter: Heat Medium	40 mm

The cooling performance, de-rating factor for reduced heat medium flow, heating performance and noise performance can be seen in Figures 7.18 to 7.23.

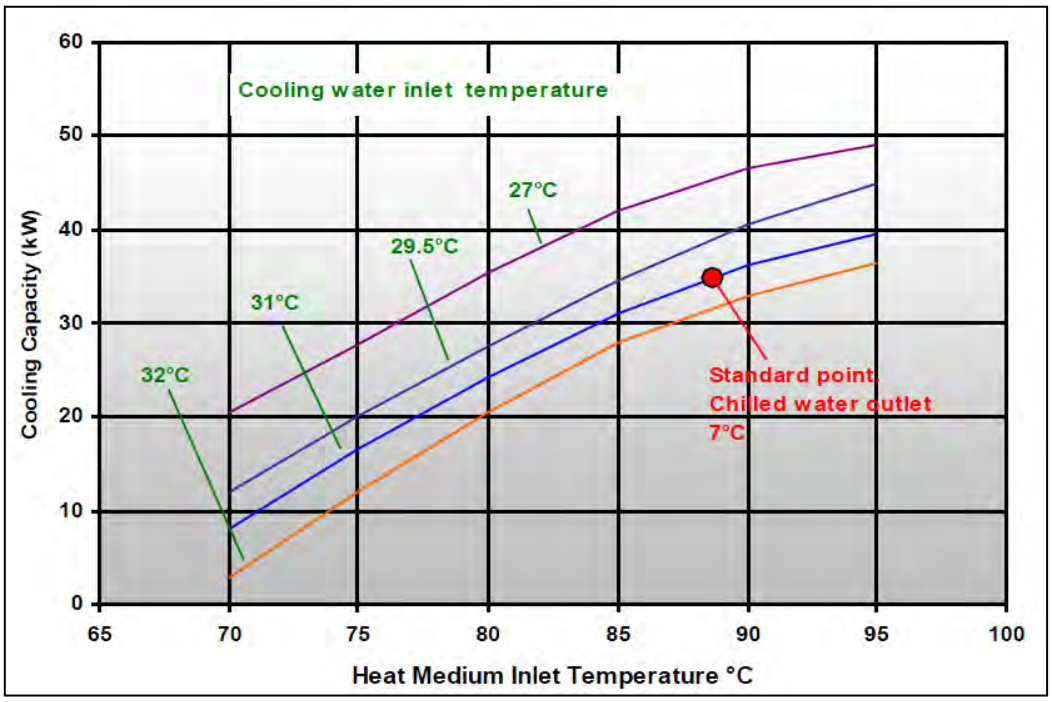

Figure 7.18: Specification - typical Cooling Performance for heat medium operational range [75]

The cooling capacity is the highest at the lowest cooling water inlet temperatures as seen in Figure 7.18 and the heat medium input is higher for lower cooling water inlet temperatures at the same heat medium inlet temperatures.

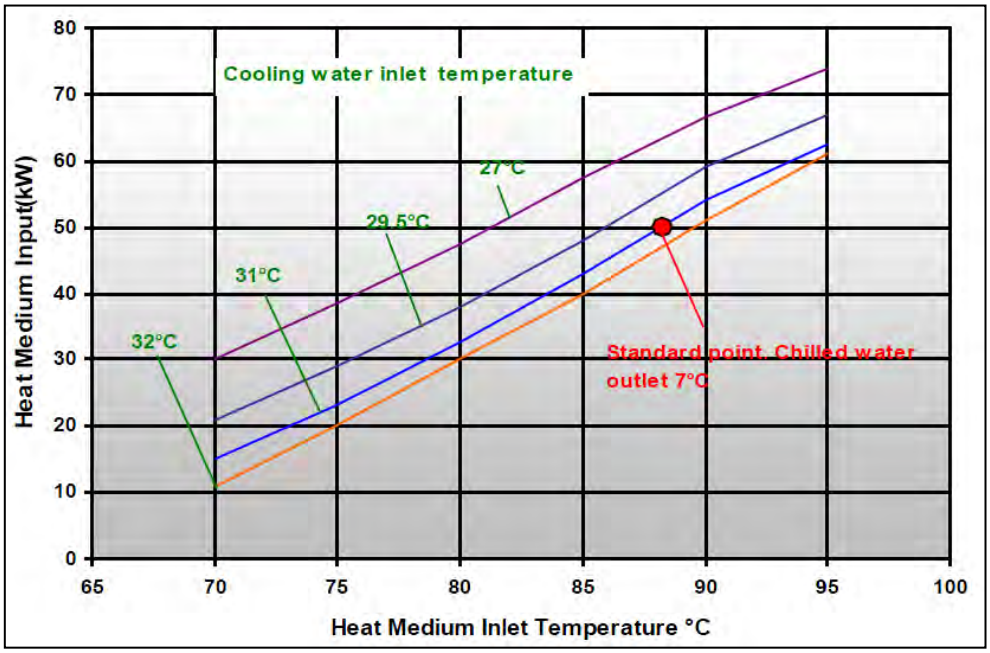

Figure 7.19: Specification – Cooling Performance corresponding typical heat energy input [75]

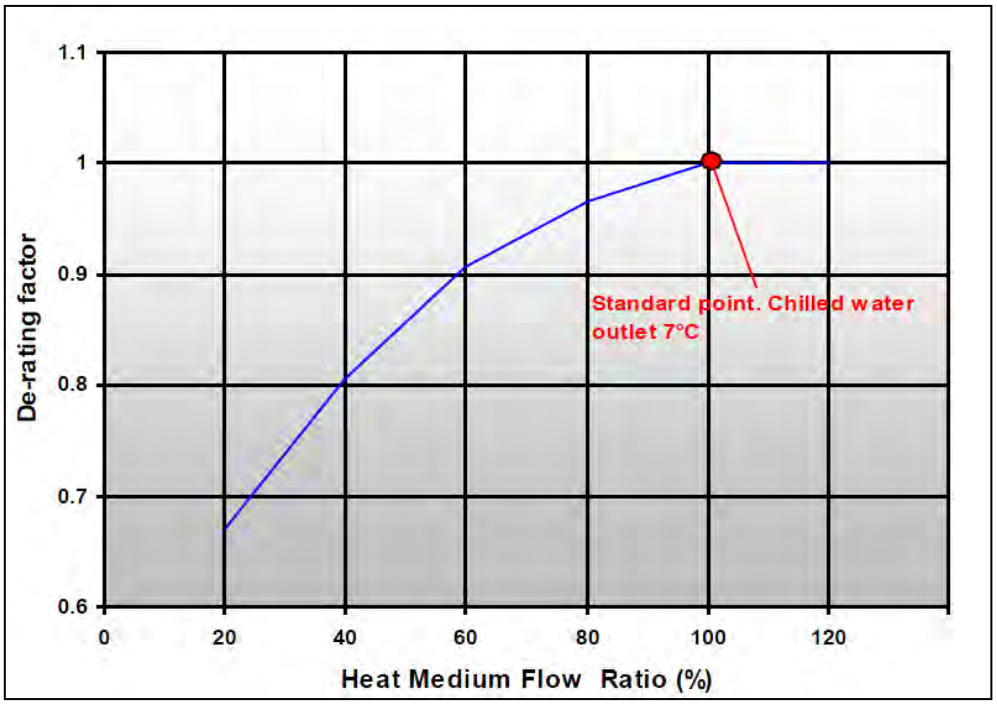

Figure 7.20: Specification - De-rating factor for reduced heat medium flow (typical) [75]

As the heat medium flow ratio percentage is decreased, the rated performances decrease exponentially as can be seen in Figure 7.20 and 7.21 shows the heating capacity to be 50kW at around 88 °C as a standard point of operation.

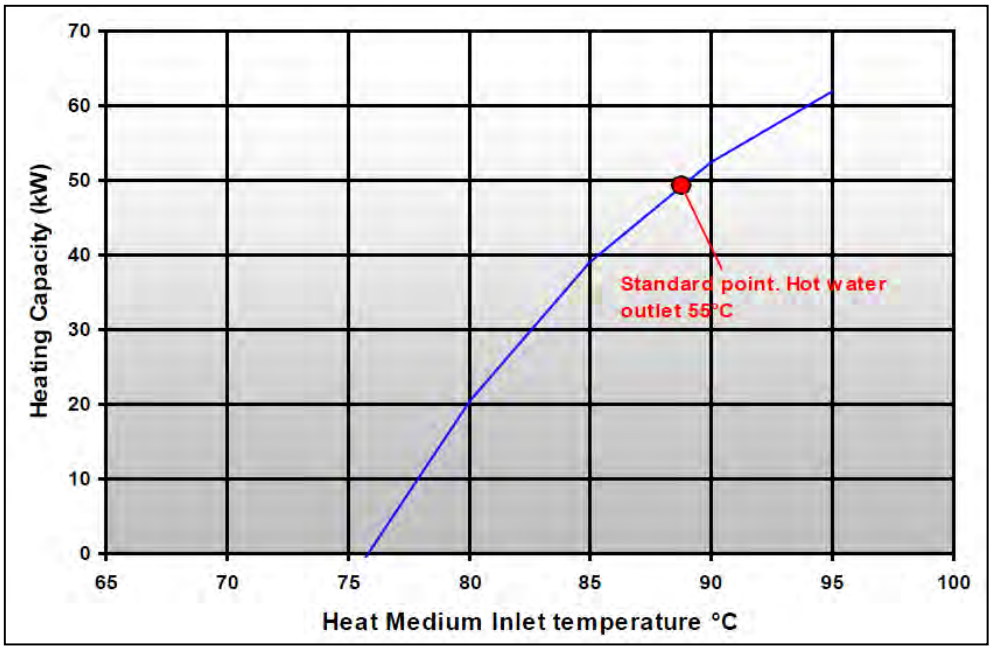

Figure 7.21: Specification – typical Heating Performance [75]

The heating capacity of the chiller reaches a maximum of approximately 60kW for a maximum generator inlet temperature of 95 °C .

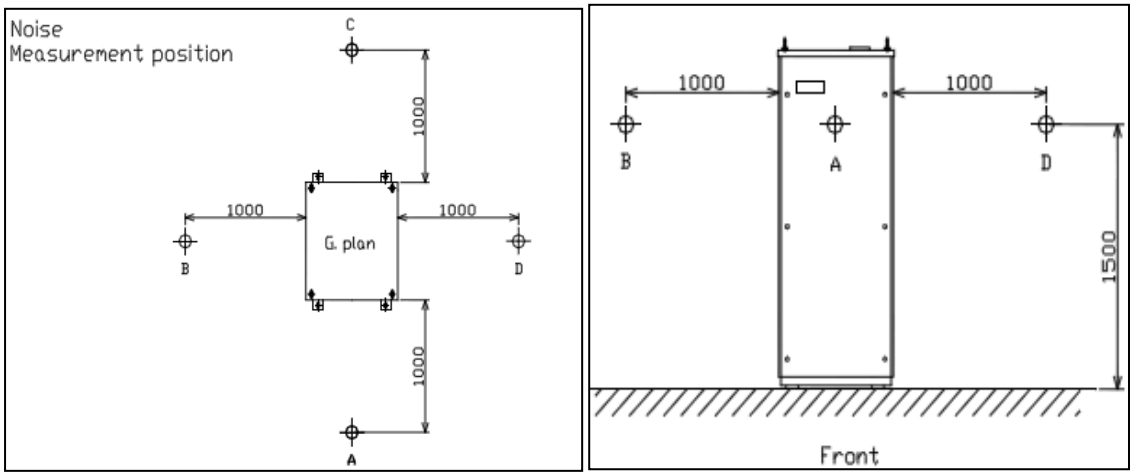

Figure 7.22: Positions around the chiller at which sound was measured [75]

Normal conversation is at 60dB to 70dB and when this is compared to the noise emitted in the chart contained in Figure 7.23 at positions measured in Figure 7.22, the chiller is less noisy at 40dB. This means that a normal conversation could be held around this chiller without difficulty of being heard.

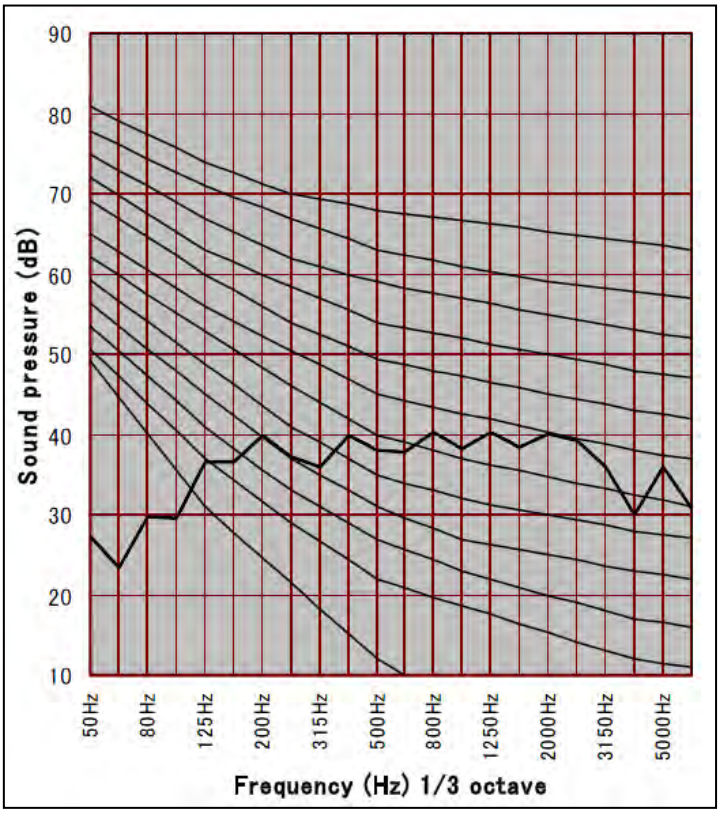

Figure 7.23: Noise measurement positions depicted on top and NC curves above [75]

7.4 King Sun Cooling Tower

During the cooling cycle of the chiller, the cooling tower is the cold reservoir to which the heat is rejected from the hot concentrated LiBr and the hot H_2O vapour refrigerant. The cooling tower used in this plant is from King Sun of type KST N50. The cooling tower casing is made of Fibre Reinforced Plastic (FRP) which has high structural strength and is able to withstand wind velocity. The construction allows for minimal amount of water in the bowl shaped basin and shields for drawing in air for cooling the water.

The absorption chiller investigated in this study is water cooled, whereas the electric chiller is air cooled. Refer to Figure 7.24.

Figure 7.24: Cooling Tower (in front)

Water is sprayed down through pressurized nozzles and flows through the fill where the water is cooled to almost the wet bulb temperature. The fan is engaged when the water reached a certain temperature. Refer to Figure 5.9 for the schematic on the working principle of the cooling tower.

7.5 Control Logic of the HVAC system

The control logic will describe the production of chilled water at 7 °C by the Yazaki absorption chiller which has the priority over the mechanical compressor driven chiller from 7:00 to 17:00 provided that it is able to deliver cooling. This will be possible only if the solar water collectors can deliver water at a temperature of 85 °C to the hot water storage tank. The mechanical compressor driven chiller has two stages of compression. The control logic for the chillers operations can be seen in Figure 7.25.

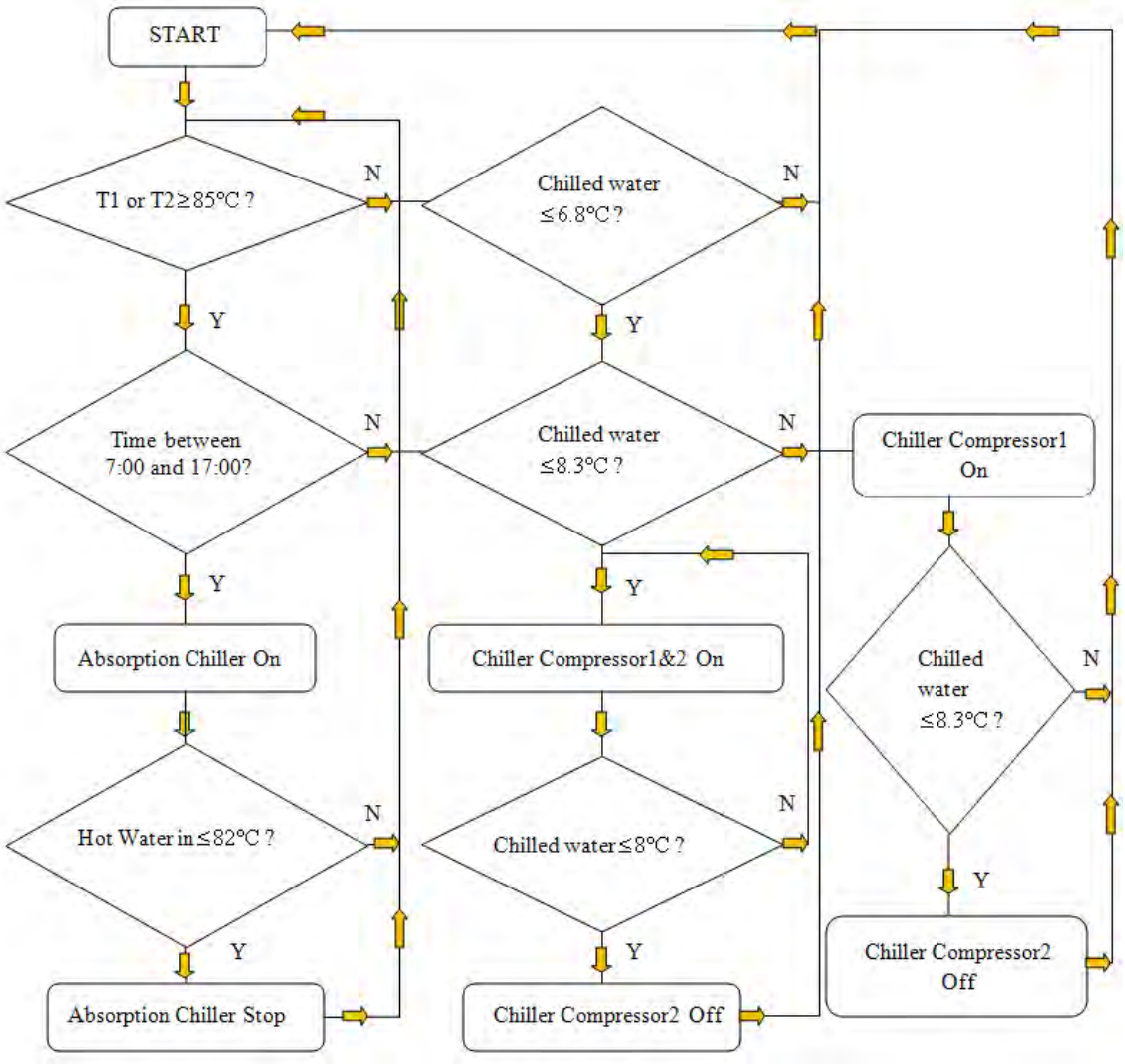

Figure 7.25: Control logic for sequence of the Chillers

The schematic of the hot water tank can be seen in Figure 7.26.

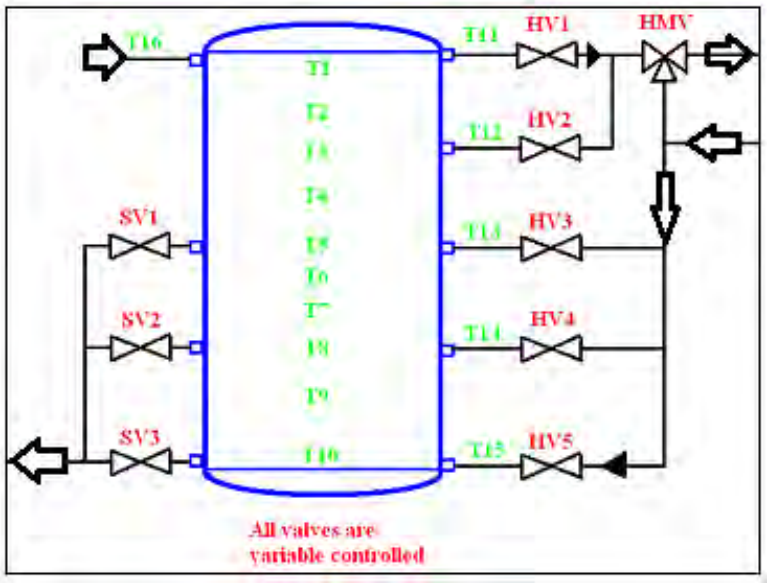

Figure 7.26 Schematic of the Hot Water buffer/storage tank

Where:

T1 to T10	Temperature 1 to Temperature 10 of the water along the height of the tank
T11 to T15	Temperature 11 to Temperature 15 of the water leaving to the chiller through the valves HV1 to HV5 respectively.
T16	Temperature of water returning from the solar water collectors.
SV1 to SV3	Two way variably controlled valves that release water from the Hot Water Tank to the Solar Water Collectors termed Solar Valves 1, 2 and 3.
HMV	Three way variably controlled valve (Heat Medium Valve) that provides the connection of supply to the generator of the chiller.
HV1 and HV2	Two way variably controlled valves (Heat Valve 1 and 2) that are connected to a three way valve that is the direct supply path to the generator of the absorption chiller.
HV3 to HV5	Two way variably controlled valves (Heat Valve 3, 4 and 5) that form the return path for hot water from the generator, but can also be the supply to the generator through the HMV.

The control logic of the Hot Water tank to the Solar Water collectors can be seen in Figure 7.27.

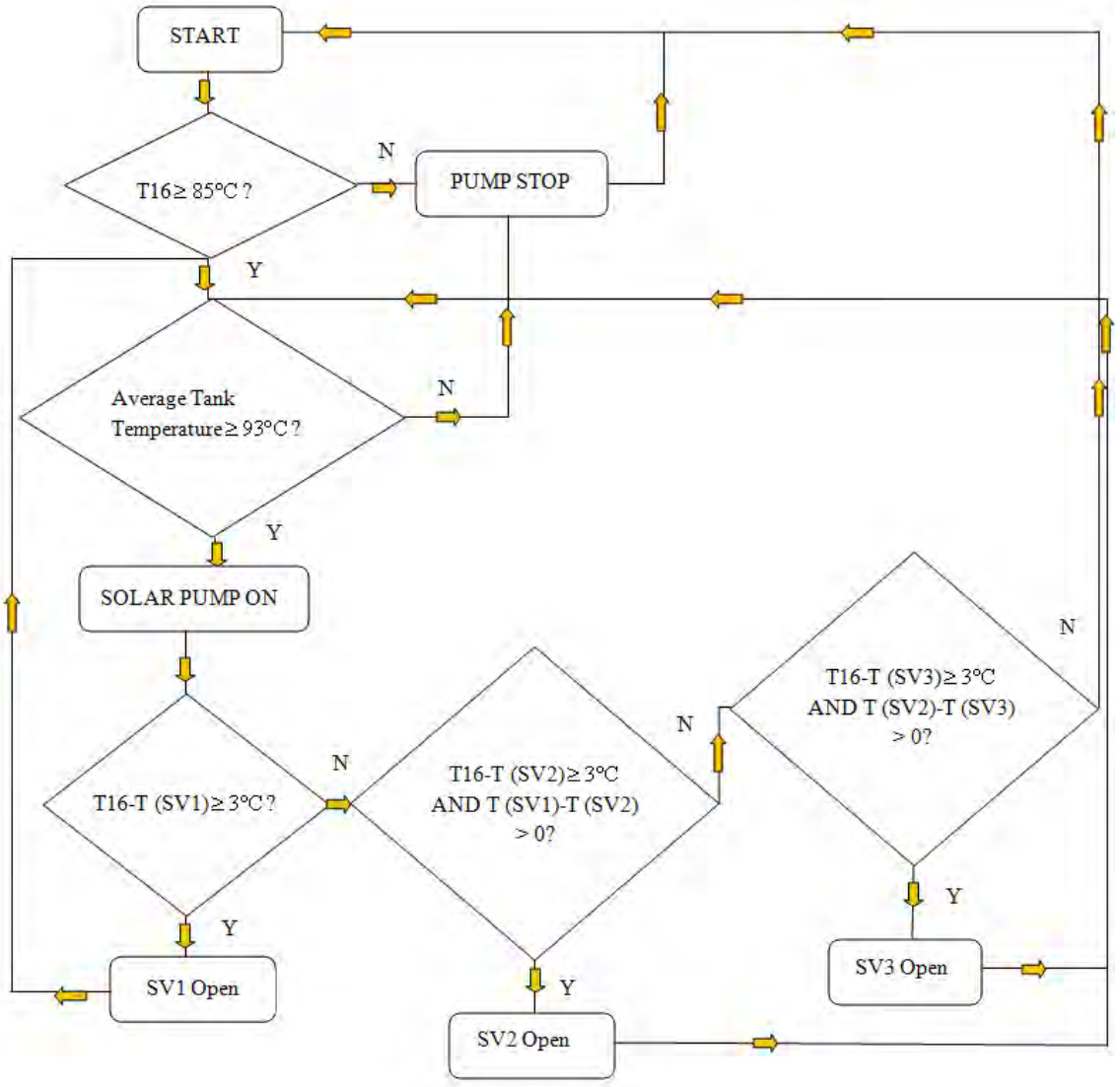

Figure 7.27: Control logic of the hot water from storage/buffer tank to solar water collectors

The T (SV1), T (SV2) and T (SV3) are the temperatures of the water present at that point in the pipes.

The control logic of the Hot water tank to the generator section of the chiller can be seen in Figure 7.28.

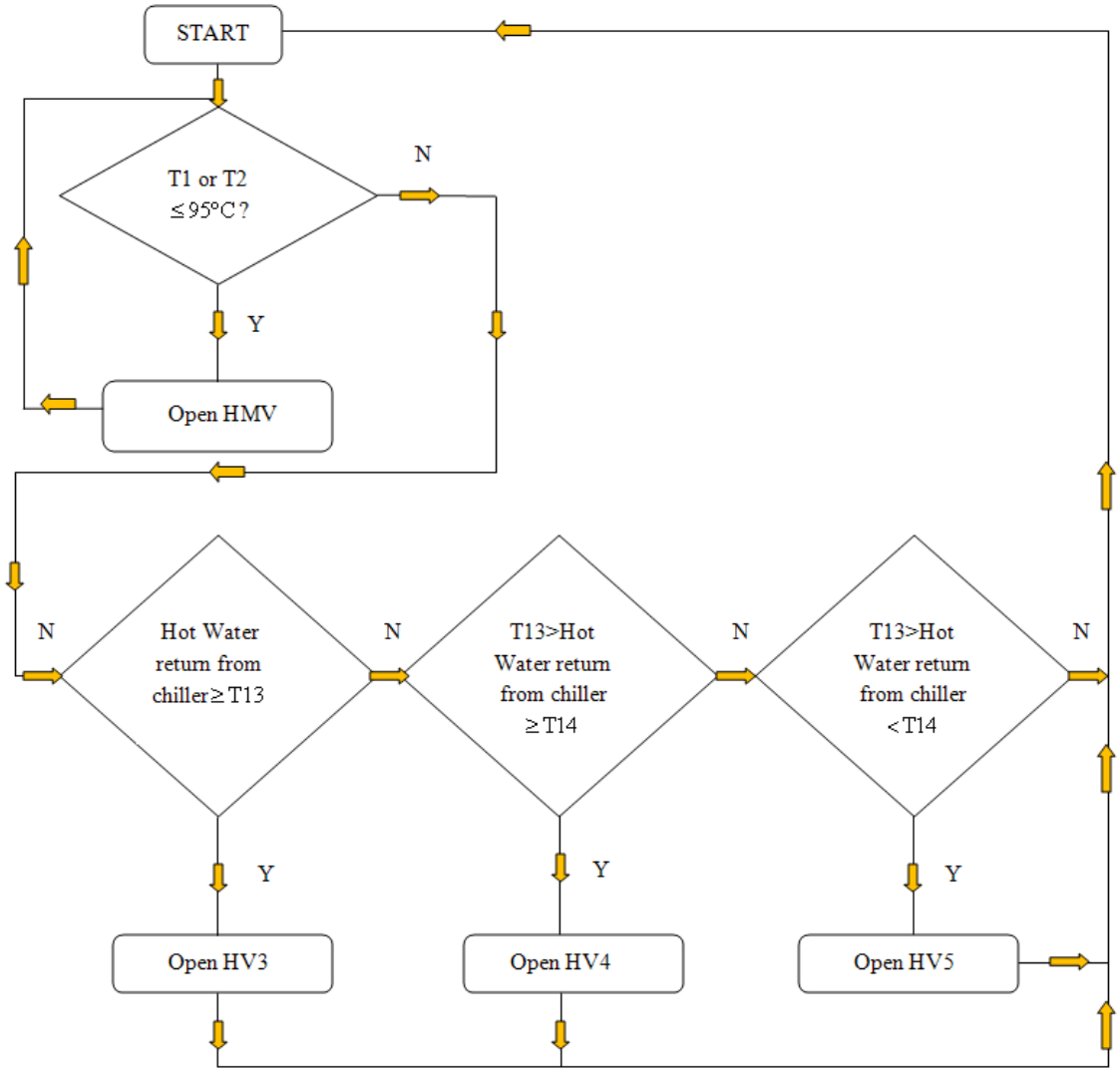

Figure 7.28: Control logic of the hot water from buffer/storage tank to chiller

The evaporative cooling tower which is operational in the cooling cycle of the chiller has a three way valve connection (V10) to the chiller. This is used to bypass the cooling tower if the cooling water supply to the cooling tower is less than 28 °C .

The control logic of the chiller can be seen in Figure 7.29.

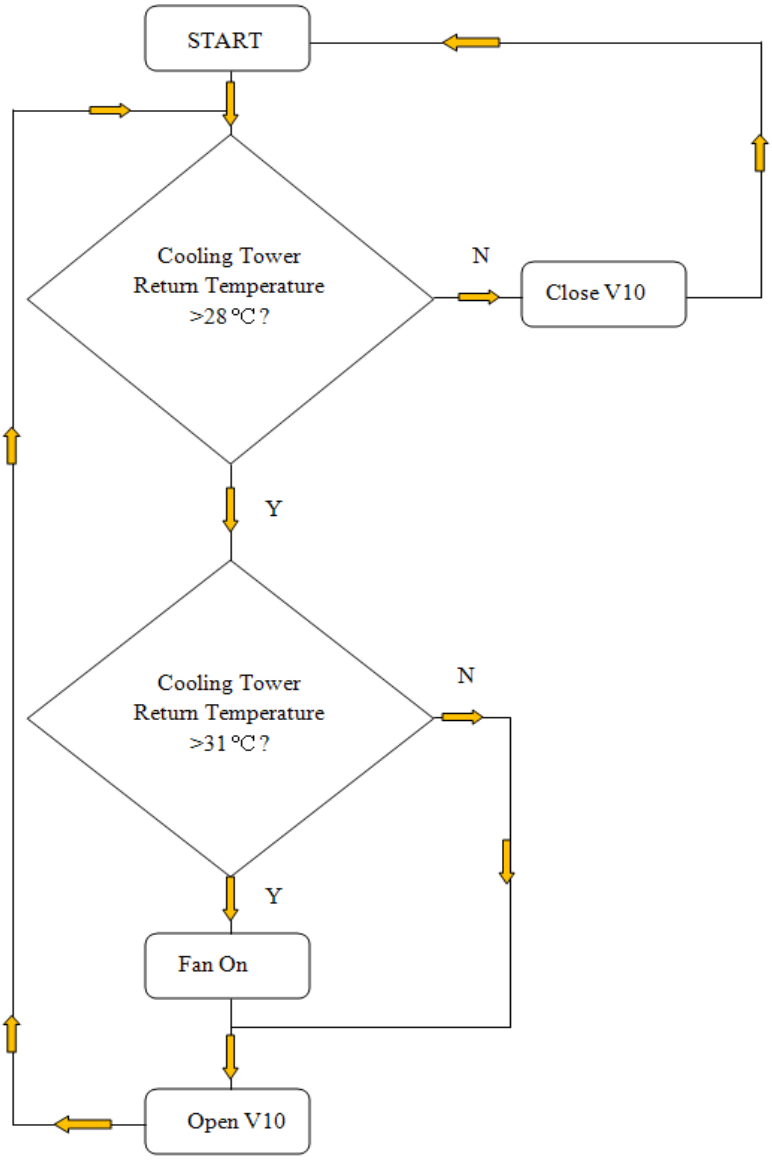

Figure 7.29: Control logic of the cooling tower.

The control logic for the various components discussed in this Chapter will need to be recalled in the next Chapter where the Testing of the plant will be discussed.

Refer to Appendix B for the layout drawings of the plant.

7.6 Compliance to Project Design and Building models

The initial intention of the project was to design and construct a Solar-Assisted Space Heating and Cooling and ultimately perform the feasibility analysis on it. The testing models presented in Chapter 6 were based on the design and building models for a solar-assisted absorption cooling plant. Thus, a comparison of the Pretoria Moot Hospital plant to the design and building models is carried out for the testing models to be executed accordingly. The models are presented in Tables 7.7 to 7.11.

Table 7.7: Outdoor Design Conditions for HVAC system

Location	**Proposed: EThekwini, UKZN (Howard College)**	**Actual: Pretoria Netcare Moot Hospital**
Altitude above sea level	As sea level	1400m above sea level
Longitude/Latitude	29°52′09.34″S / 30°58′38.29″E	25°42′48.05″S / 28°13′05.37″E
Summer ambient design temperature	31 °C dry bulb	32 °C dry bulb
Summer relative humidity	26 °C wet bulb	21 °C wet bulb

Table 7.8: Control of temperature and moisture content (humidity) model

Required design outcome/output	**Component(s) designed to satisfy output**	**Actual: Pretoria Netcare Moot Hospital**
1. Control of temperature should be within 0.5 °C of the setpoint input of the thermostat	Chiller and heat exchanger in air handler (evaporator)	Control of temperature is within 3 °C of the setpoint temperature.
2. Humidity should be within the ASHRAE Standards of thermal comfort which is 50%.	Chiller and heat exchanger in air handler (evaporator)	Humidity is maintained between 40% and 60%. These are also acceptable levels of comfort.
3. Control of temperature and humidity should be such that condensation will not occur in the space to be	Electronic Controllers and chiller unit	No condensation occurs in any of the conditioned spaces at Moot Hospital.

conditioned.		
4. The system will operate within space temperature limits and thus should be designed to output air conditioning between two threshold temperature setpoints.	Electronic Controllers and chiller unit	System operating limits for the Reception, Foyer and Trauma Unit is between 17 °C and 21 °C . For operating theatres, temperatures should not exceed 10 °C or go below 7 °C .

Table 7.9: The air quality and circulation control model

Required design outcome/output	**Component(s) designed to satisfy output**	**Actual: Pretoria Netcare Moot Hospital**
1. Air distribution configuration should be chosen such that air conditioned air reaches all the rooms to be conditioned.	Duct supply configuration	Duct configuration employs a combination such that convenience is guaranteed and less material is used.
2. Duct air temperature gain or losses should be minimised between the air handler and the supply outlets and between the return register and the air handler.	Insulation on all ducted air lines (supply and return)	Supply and Return air ducting is insulated with fibreglass.
3. Ensure balanced supply and return air flows to maintain neutral pressure in the conditioned space.	Fan blowing air from the air handling unit	Both the supply and return of conditioned air and isolated ventilation system is balanced. The ventilation system uses door grilles and louvers to maintain a neutral pressure in the conditioned space.
4. Ensure that conditioned air is clean with respect to dust particles	Filters (primary and secondary) should be installed and always fit for purpose.	Primary plate filters and secondary bag filters using chemical fibres are used in the foyer, reception areas, whereas HEPA filters using glass fibres are used in the Trauma Unit and Operating Theatres.

Table 7.10: The renewable energy model

Required design outcome/output	**Component(s) designed to satisfy output**	**Actual: Pretoria Netcare Moot Hospital**
1. Solar Water Heater should be chosen such that the temperature required by the chiller's generator is achieved or an economic plan should be made to reach this temperature if this temperature cannot be achieved.	Solar water heater and storage tank	The range of temperatures required by the generator section of the chiller is 70 °C to 95 °C . Both the U-pipe and Heat pipe solar collectors can reach the temperatures as their maximum temperature reach are both at 120 °C .
2. Passive cooling design should reduce the calculated cooling load measured without energy saving components by 10%.	Passive cooling design	In Operating Theatres where temperatures required are about 10 degrees colder than in the other conditioned spaces, the roof is made of a concrete slab of 350mm thickness and a vinyl made of key plaster, 5mm thick insulates the walls. The windows are glazed.
3. Photovoltaic technology with battery storage should be designed to provide power to the control circuitry and gauge displays. Integration with main grid power should also be done to ensure that there is fairly constant current flowing to these circuits.	Photovoltaic cells and batteries with control system and filtering for the current/voltage.	Not Applicable in this plant. There is no power produced via photovoltaic cells.

Table 7.11: Control system model

Required design outcome/output	Component(s) designed to satisfy output	Actual: Pretoria Netcare Moot Hospital
1. Control system should provide safety features for the chiller, solar collector, storage tanks, pumps and pipes under pressure.	Safety checks and warning indications with automatic action for cases that may give rise to hazardous or potentially hazardous situations.	When temperature of hot water coming in to the generator exceeds 90 °C , the chiller shuts off.
2. HVAC system should respond to thermostat temperature setting changes to 0.5 °C accuracy.	Chilled water temperature control	Tolerance is within 3 °C of setpoint.
3. HVAC system should deliver thermostat setting temperature within a maximum time period allowed (which will be stipulated in the design of the chiller) under design conditions stated in Table 7.7.	Chilled water capacity and chilled water control valve (reduce hunting)	It should be noted that the temperature output is constant and heat gain response is via the chilled water valve fluctuating the chilled water flow. This chilled water valve on the air handler was not included on the BMS and thus it was not possible to draw a conclusion on this.
4. Control system should ensure correct sequence of operations and integrate efficiently the processes in the Solar-Assisted HVAC system.	Sequential optimization of algorithm.	Logic is such that there is a central cold buffer tank into which the absorption and mechanical compressor chillers input chilled water. Absorption chiller deals with cooling demand until 35kW, then mechanical compression driven chiller makes up the rest of the demand.
5. Ensure that humidity is monitored and controlled to 50% as stipulated in	Chilled water temperature control	Steam Humidifiers are used to maintain humidity between 40% and 60%.

Table 7.7.		
6. Ensure optimal air circulation/ diffusion, i.e. no drafts and no dead spots.	Design for speed of fans in air handling units to ensure no chaotic air behaviour.	This was not done, however a constant air volume is required in the Operating Theatres Conditioned Space.
7. Incorporate maintenance indicators on equipment like air filters, bearings, heat exchangers, etc so that the system works efficiently all the time.	Maintenance module checks to be incorporated.	The air Handling Unit has Magnehelics to indicate when maintenance of filters will be required. Grease nipples are included on the fan motor plumber block (Bearings on Shafts).

The chiller and its controls will be discussed. The functions of the Yazaki Water fired chiller depends on the in-built microprocessor and the associated controls and devices.

CHAPTER 8: PERFORMANCE DATA

This Chapter presents the performance of the Absorption chiller based HVAC plant installed at Pretoria's Netcare Moot Hospital. The performance of the solar-assisted absorption cooling plant tested here will be presented according to the testing models discussed in Chapter 6 of this study.

8.1 Functionality Testing

The functionality test model developed for the corresponding compliance was executed during the commissioning of the plant.

Table 8.1: Functionality Test Model

Required design outcome/output	**Procedures/actions to achieve output**	**Actual: Pretoria Netcare Moot Hospital HVAC Plant**
1. System must be electrically safe and wired according to relevant standards.	Have electrical wiring installed by a qualified electrician and have the installation certified as required by legislation.	The installation of the plant was carried out by Luft Technik, a sister company of Voltas Technologies.
2. System must be mechanically safe and implement precautions to reduce risk of hazards.	Pumps, motors, valves, piping, storage vessels, chiller, fans, ducting will be installed only if certified according to standards and full system should be inspected by a competent person.	The installation of the plant was done by a sister company of Voltas Technologies.
3. No air leaks, refrigerant or LiBr leakages to be present in the system.	Pressure testing of the system will occur before installation of working fluids will commence.	Refer to inspection certificate of the Absorption chiller in Appendix C1.
4. All safety features in the control system for critical equipment must be fully functional to avoid accidents should the system malfunction or its behaviour become	Control system (sensors, software/commands, and controllers) needs to be tested for functionality on the electronic safety features.	Absorption plant was successfully commissioned and has been in operation since October 2009.

uncontrolled.		
5. System should integrally be given at least one successful test run to ensure that other testing will be striving toward obtaining valid results.	Procedures for a complete test run should be developed and standards should be developed for the expectation of a 'successful run' for the integrated system.	Absorption plant was successfully commissioned and has been in operation since October 2009.

The commissioning data and certificate are given in Appendix C.

8.2 Air-Conditioning Efficiency Performance

The air conditioning efficiency performance investigated is done in three parts as stipulated below and according to Table 6.2: Air Conditioning Test Model of Chapter 6:

- The chiller efficiency in accordance with its design specification which requires the COP to be about 0.7.
- The cooling water and generator temperatures should also be investigated and the factors affecting their performance.
- The design target of the air conditioning system is to produce chilled water at 7 °C to a cold storage buffer tank.

Therefore this section will present the performance of the chiller to meet these conditions together with the varying cooling water and the generator temperatures. The specific design requirement of the control system to produce chilled water at 7 °C to a cold storage buffer tank will also be presented. Due to the fact that the solar-assisted absorption cooling system performance relies on solar energy which varies according to season to produce chilled water, the parameters listed above will be investigated for the spring, autumn, summer and winter season.

The design specifications for the chiller as depicted in Figures 7.20, 7.21 and 7.22 in the last Chapter states that the chiller produces 35kW of cooling (chilled water at 7 °C) for 50kW of heat medium input (which is at 88 °C) for a cooling water inlet temperature of 31 °C as depicted in Figure 8.1. The targets that will be set for the performance of the chiller will be derived from Figure 7.20 and Figure 7.21 and is represented in Table 8.2.

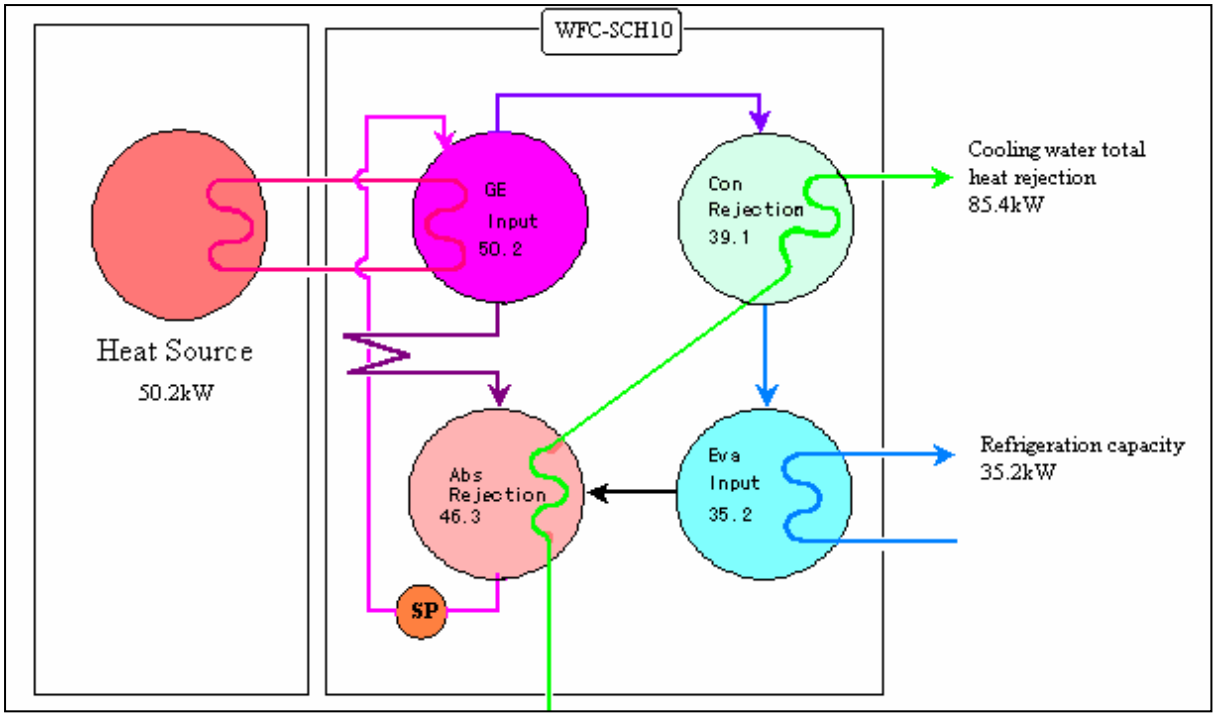

Figure 8.1 Heat Balance for the WFC-SC/SH 10 Cooling cycle [75].

Table 8.2: Performance of the chiller according to design specifications

Cooling Water Inlet Temperature (°C)	Cooling Capacity (kW)	Heat Medium Inlet Temperature (°C)	Heat Medium input power (kW)	COP
27	49	95	74	1.510
	46	90	66	0.697
	42	85	58	0.724
	35	80	48	0.729
29.5	45	95	66	0.681
	41	90	59	0.695
	35	85	48	0.729
	28	80	38	0.737
31	40	95	63	0.635
	36	90	55	0.655
	32	85	44	0.727
	25	80	33	0.756
32	36	95	61	0.590
	33	90	51	0.647
	28	85	40	0.700
	20	80	30	0.667

The design specifications of the chiller represented in Table 8.2 is depicted in the graph below in Figure 8.2.

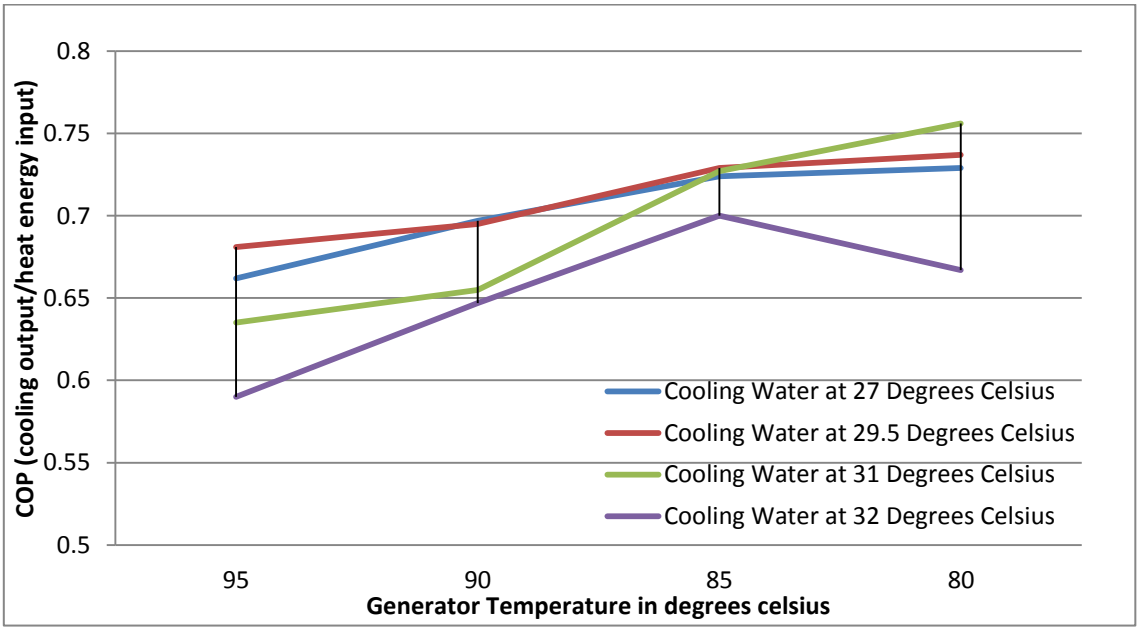

Figure 8.2: COP of the absorption chiller at various cooling water temperatures

The graph depicts the COP of the system to lie between 0.6 and 0.75 for cooling water temperature between 27 °C and 32 °C at generator temperatures between 80 °C and 95 °C .

The operation of the chiller is shown in Figure 8.3 in terms of its heat and mass flow and pressure. The numbers shown in Figure 8.3 into and out of the various components of the chiller (Evaporator – E, Absorber – A, Generator – G and Condenser – C), represent mass flow, enthalpy, entropy and temperature readings that have been taken. The condenser and generator are in a shell where the pressure is higher than that of the shell where the Absorber and Evaporator are maintained.

The Generator receives hot water from the Hot water storage tank being heated by the solar thermal collectors and is represented by the numbers 11 and 12. The heat Q_G brought in from the solar collectors at 11 liberates the water from the dilute $LiBr/H_2O$ coming in at 4 and releases it as a vapour to the Condenser where the cooling water circulating from the Cooling Towers at 15 and 16 remove the heat Q_C from the vapour causing it to condense to a liquid.

This liquid is then throttled down to a lower pressure from 8 to 9 to boil off at the Evaporator at 9 by the removal of heat Q_E from the chilled water circulating between the cold water storage buffer tank

at 17 and 18. This vapour then is combined with the concentrated LiBr/H_2O solution from 6 by its affinity to LiBr (absorption process) and condensed due to the heat removed Q_A from it via the cooling water circulating from the cooling water at the absorber. The Heat exchanger is used as an intermediate stage to cool to concentrated solution coming from the generator by the dilute solution running through it.

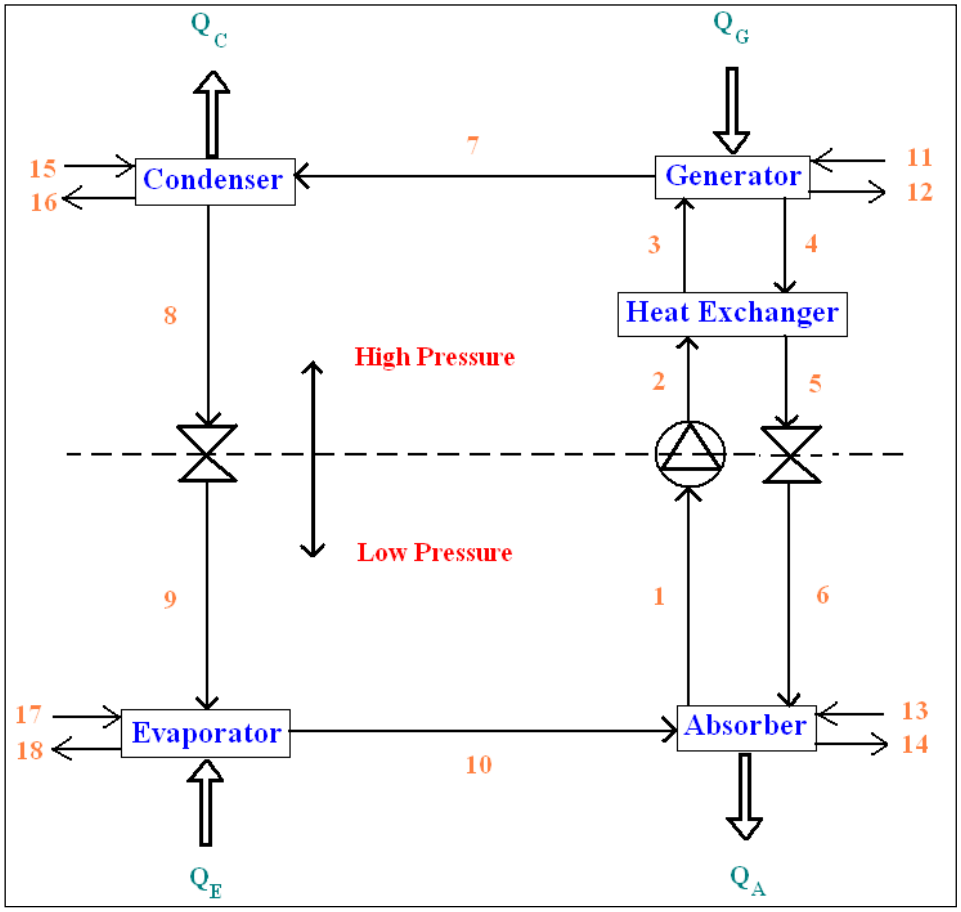

Figure 8.3: Schematic used for the description of the mass, enthalpy, entropy and temperature readings and heat flow

The air conditioning efficiency will calculate the coefficient of performance of the absorption process for different generator heat inputs and cooling tower inputs according to the following Equation 8.1:

$$COP_{abs} = \frac{Cooling Output}{Heat Input} = \frac{\dot{Q}_L}{\dot{Q}_G} = \frac{\dot{m}_{17} C_{p\_water} (T_{17} - T_{18})}{\dot{m}_{11} C_{p\_water} (T_{11} - T_{12})} \quad \text{..... (Equation 8.1)}$$

Where:

$\dot{Q}_L$	Energy from the air conditioned space which is the heat energy removed from the chilled water (kW)
$\dot{Q}_G$	Heat energy input from the generator (kW)
$\dot{m}_{11}, \dot{m}_{17}$	Mass flow of water according to Figure 8.3 in kg/s.
C_{p_water}	Specific heat of water at constant pressure (kJ/kgK)
T_{11}, T_{12}	Temperature of mass flow according to Figure 8.3 (K)

The COP for the absorption process as calculated from Equation 8.1 for the various seasons were superimposed and is shown in Figure 8.4 {COP versus time of day for the four different seasons of the year. The data used to draw the graphs in Figure 8.4 is taken for the following dates for the Spring, Summer, Autumn and Winter seasons.

- Spring (2nd September 2010)
- Summer (1st December 2010)
- Autumn (1st March 2011)
- Winter (1st June 2011)

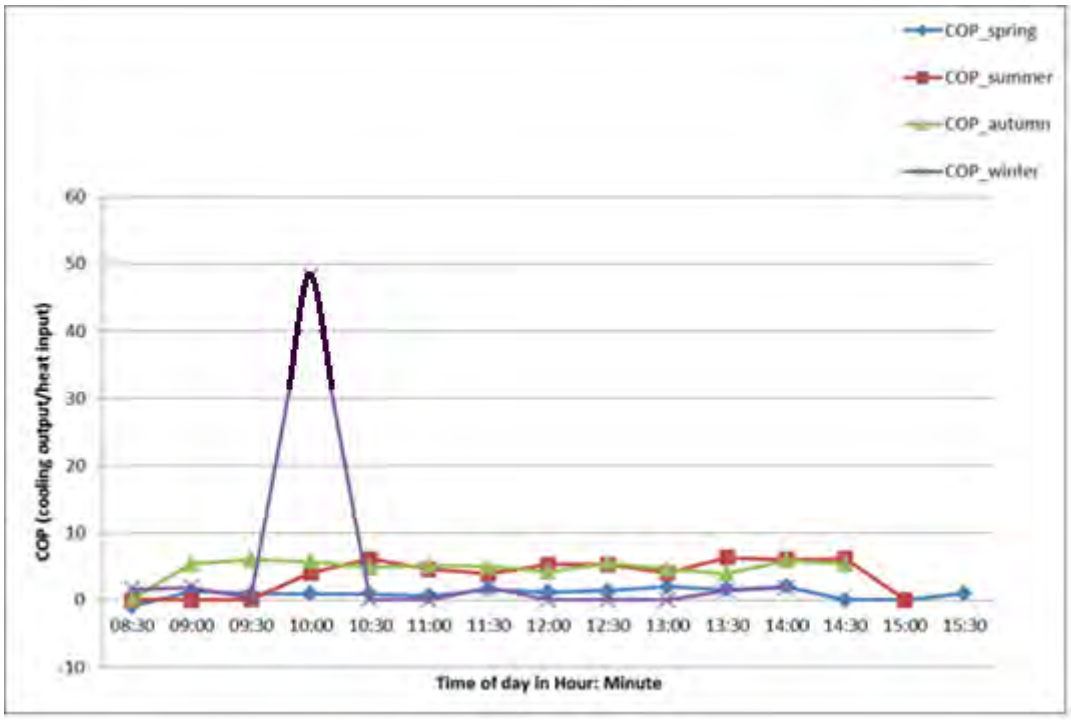

Figure 8.4: COP for the absorption chiller in Pretoria (South Africa)

The COP for the process is above 0, but mostly lying in the region of between 0 and 5. Some points on the graph lie on zero and this is due to the flow rate of the chilled water or hot water feed from the generator being zero or stopped according to the control logic of the absorption process.

It can be seen that one point lies totally out of the range for the winter season COP trend, this was due to the 'leaving chilled water' temperature being below the required 7 °C by 1 °C . There was a 3.6 °C difference between the chilled water return and leaving temperatures at flow rates of chilled water being 15 l/s and a hot water flow rate of 0.7 l/s giving a COP of 48. The process control logic immediately slowed down the absorption cooling process by increasing the hot water feed flow rate to 6 l/s as can be seen in the point following the COP point of 48.

The first important parameter to observe when looking at the COP is the numerator of the Equation 8.1 which is the chilled water leaving and return temperatures and their flow rates. The chilled water leaving and returning temperatures together with their flow rates can be seen in the Figures 8.5, 8.6 , 8.7 and 8.8 for the Spring, Summer, Autumn and Winter seasons respectively.

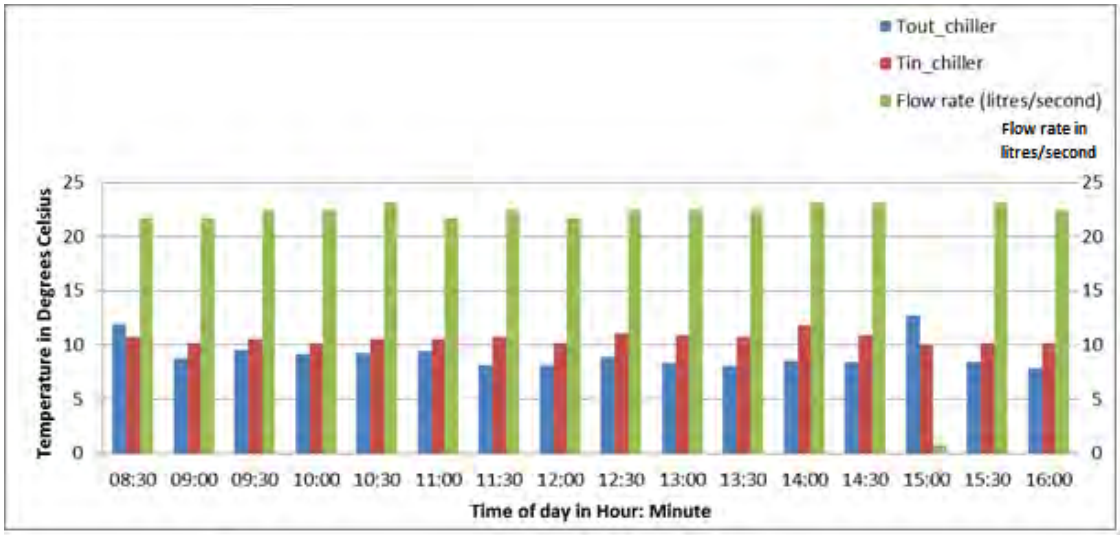

Figure 8.5: Chilled Water supply and return temperatures for the 2nd of September 2010

The flow rate of the chilled water fluctuates according to the control logic of the absorption process. The flow rate is adjusted primarily to maintain the leaving chilled water temperature at 7 °C and secondarily by the cooling demand of the building which can be roughly estimated to the energy in the difference of the supply and of the return temperature of the chilled water. However, it cannot be an instantaneous measure as the chilled water sent to the air handling unit is not directly from the chiller, but is sent to a cold storage buffer tank as the intermediate storage.

It can be seen from Figure 8.5 and comparing with Figure 8.6 that the flow rate of the chilled water for the spring season is averaging around 22 l/s, whereas for the summer season it averages about 30 l/s.

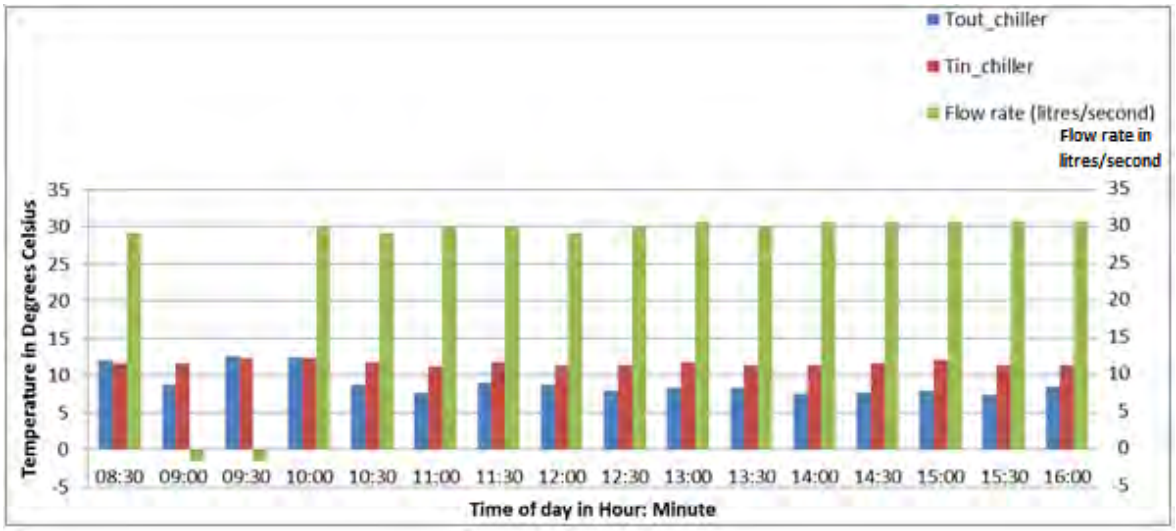

Figure 8.6: Chilled Water supply and return temperatures for the 1st December 2010

If the comparison is taken further to include Figure 8.7 and Figure 8.8 for the Autumn period an average flow rate of 32 l/s is recorded and 15 l/s is seen for the Winter season. The comparison of the flow rates can be seen in Table 8.3.

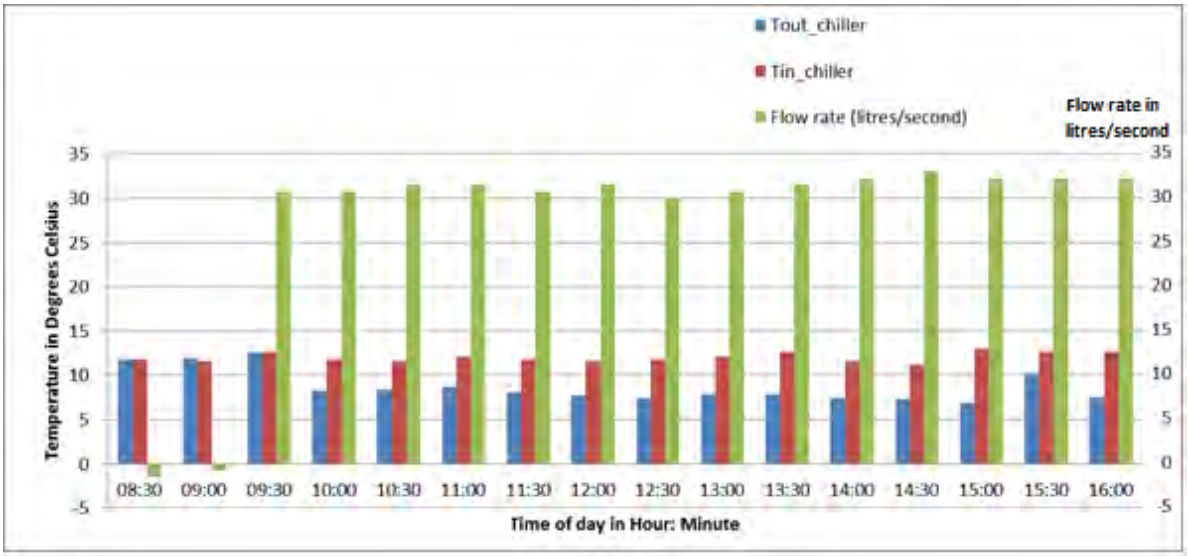

Figure 8.7: Chilled Water supply and return temperatures for the 1st March 2011

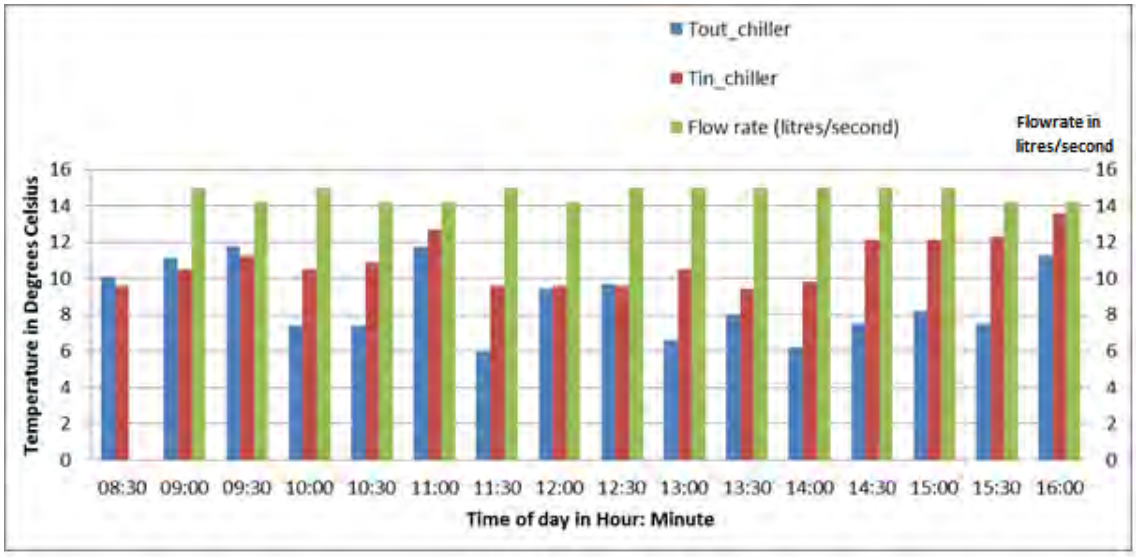

Figure 8.8: Chilled Water supply and return temperatures for the 1st June 2011

The chilled water flow rate is a parameter adjusted by the air conditioning control system to match the building's cooling demand. It can be seen that the higher building heat loads are experienced in the Summer and Autumn seasons with Spring being the average and Winter being the smallest Building heat loads experienced.

Table 8.3: Seasonal comparison of chilled water flow rate

Season	**Spring**	**Summer**	**Autumn**	**Winter**
Chilled water flow rate (l/s)	22	30	32	15

The building heat loads fluctuate according to building occupancy (internal heat loads) and solar heat load. The solar radiation for the Spring, Summer, Autumn and Winter can be seen in Figure 8.9. The solar irradiation values impacts not just on the building heat load, but it also play a vital role in the absorption process by providing the thermal energy required for the process via solar collectors. The Solar Noon defined as the time when the Sun is at the zenith (directly above) for these dates can be seen in Appendix D.

The Generator of the absorption chiller provides the chiller with hot water stored in a hot water storage tank circulated through solar thermal collectors. The generator temperatures and their water flow rates can be seen in Figures 8.10, 8.11, 8.12 and 8.13 for the Spring, Summer, Autumn and Winter seasons respectively.

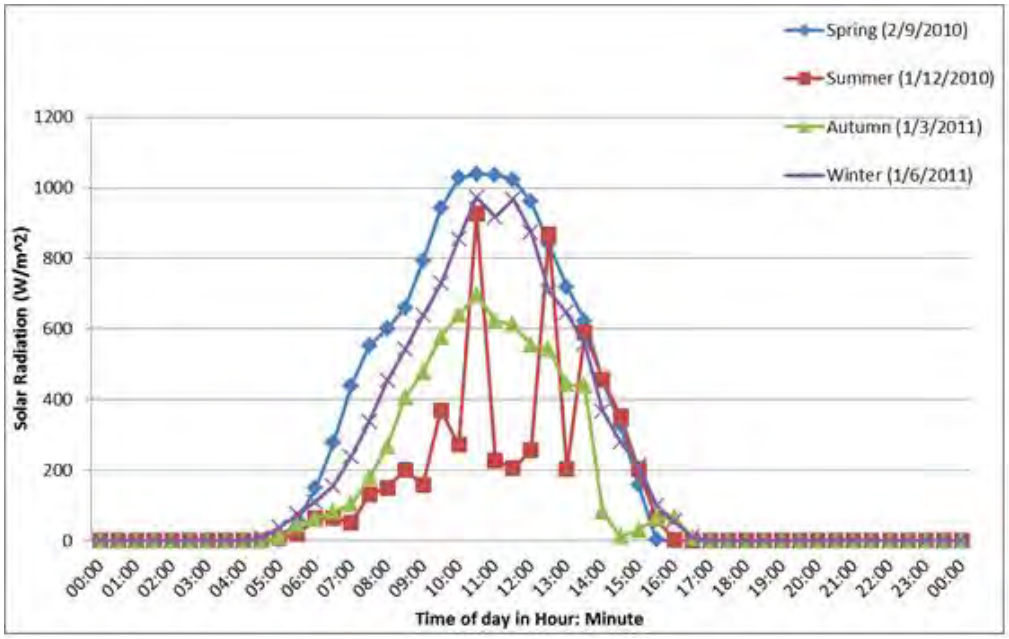

Figure 8.9: Solar irradiation values for the four seasons

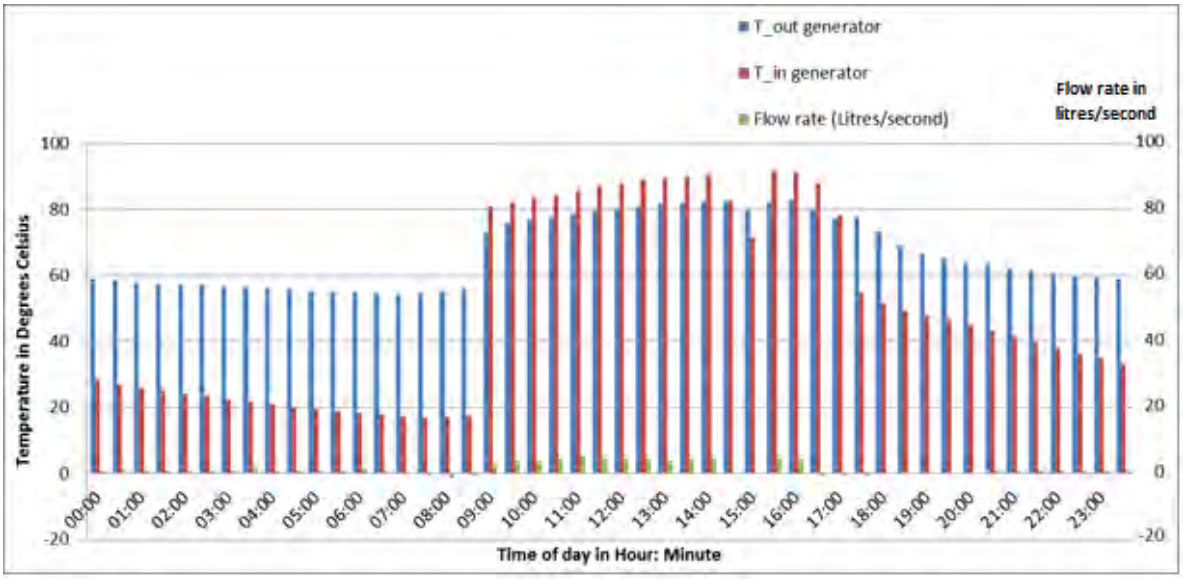

Figure 8.10: Hot water Generator Temperatures for 2nd September 2010

One of the factors that can be considered as a disadvantage in the solar-assisted absorption cooling process is the intermittent solar energy received. The generator of the chiller needs to be supplied with at least 80 °C to a maximum of 95 °C of hot water constantly in order for the absorption process to function. The intermittent solar radiation caused by cloud cover can result in the control system shutting off and starting up the heat medium pump in order to ensure that the temperature requirements of the process is met. To reduce this from occurring, the employment of a hot water storage tank allows a constant flow of hot water between 80 °C and 95 °C to a certain extent. The

effects of the intermittent solar radiation are counteracted as can be seen in the Figures 8.10, 8.11, 8.12 and 8.13.

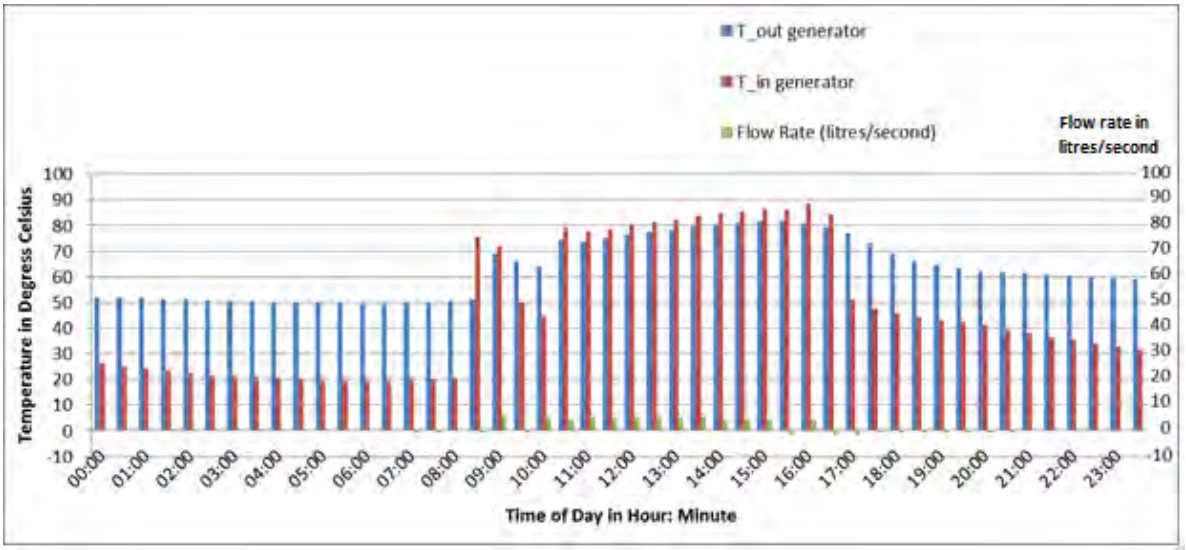

Figure 8.11: Hot water Generator Temperatures for 1st December 2010

The most intermittent solar radiation can be seen for the summer season. This intermittent behaviour can be seen in the hot water generator temperatures (Tin_generator) between 9am and 10:30am, however, this behaviour is not seen further into the day as the hot water storage tank contained water with the required temperature for the absorption process.

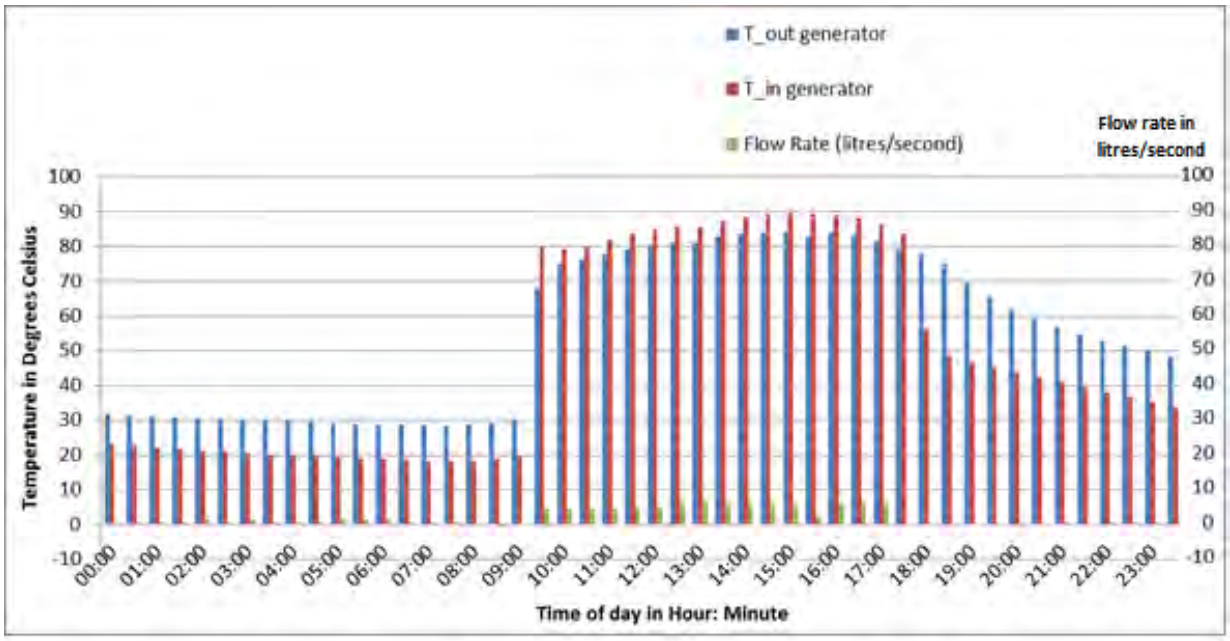

Figure 8.12: Hot water Generator Temperatures for 1st March 2011

The drop in solar radiation for winter at around 11:00 (Figure 8.9) can be seen from the generator inlet temperature (Tin_generator) in Figure 8.13. The hot water temperature had dropped to 80 °C at 11:30 and stayed that way until 12:00 when the temperature then further dropped. The effects of the intermittent solar radiation experienced at 11:00 is seen around 12:30 due to the hot water storage tank overall temperature being decreased by the circulation of water from the solar collectors not being heated at 11:00 as much as they were at 10:30. This shows the ripple effect that intermittent solar radiation can cause. It is clearly seen for the winter season due to the loss of heat from the hot water storage tank to the surroundings as the winter atmospheric temperatures are much lower than that for the other seasons.

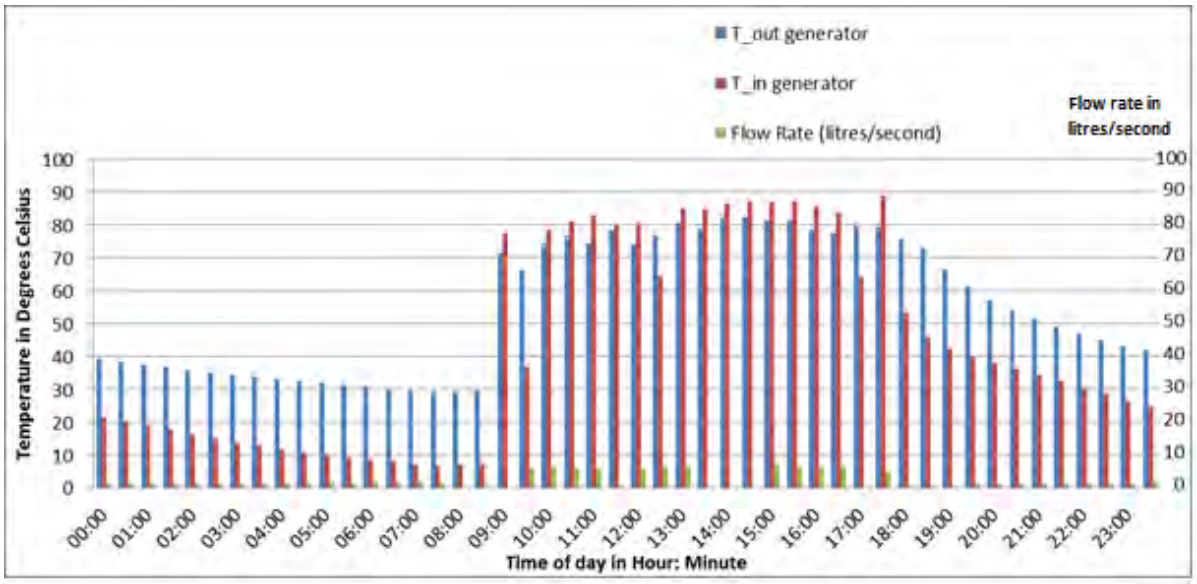

Figure 8.13: Hot water Generator Temperatures for 1st June 2011

It can be observed from Figure 8.4 that the most steady trend of COP values is held by the autumn season and the varying trend is held by the summer season (with the exception of the outlying winter COP point which was explained. This is due to the properties of air at the different seasons. The Autumn season air is less humid than the summer season air. The air being dryer (denser) has more potential to remove the heat from the cooling water via evaporation. The cooling water temperatures play a vital role in the absorption process.

The cooling water supply and return temperatures together with their flow rates for the various seasons can be seen in Figures 8.14, 8.15, 8.16 and 8.17. It can be seen from Figure 8.14 that the cooling water (T_in Cooling Tower) generally determines the flow rate of cooling water. It can be seen that the cooling water flow rate increases with the increase of the temperature of the cooling water.

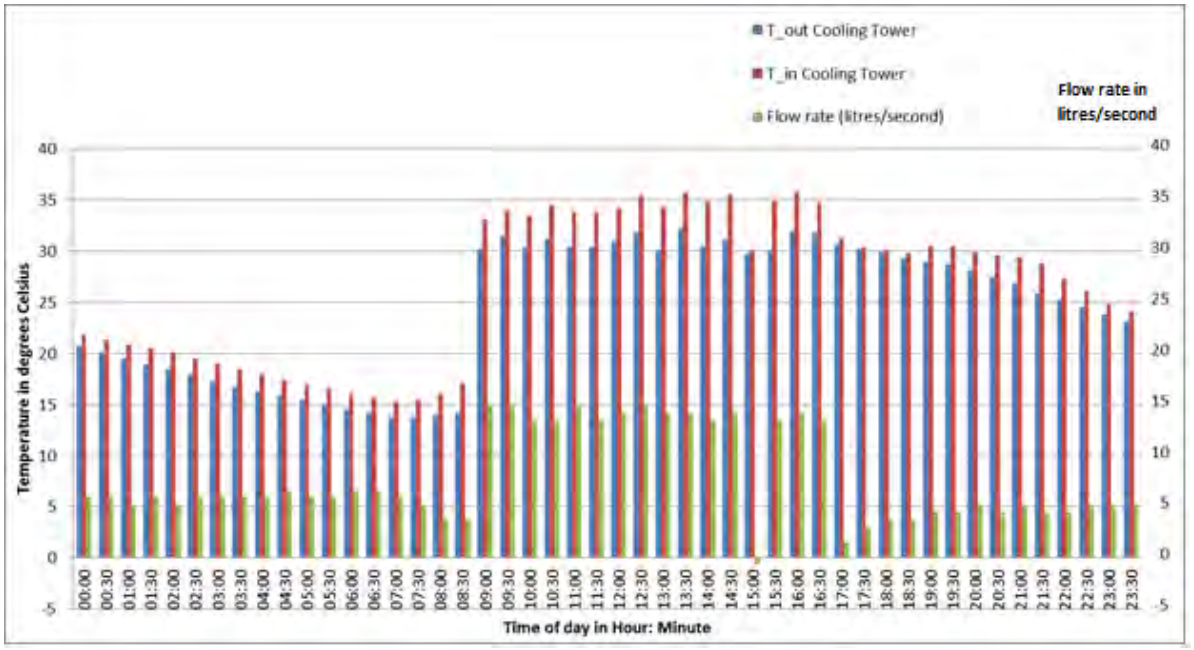

Figure 8.14: Cooling Water Temperatures for the 2nd September 2010

Comparing the data points in Figure 8.14 and Figure 8.15, it can be seen that to maintain the cooling water outlet (T_out Cooling Tower) below 30 °C when the cooling water is coming in at approximately 35 °C on average, the flow rate required in the spring season is higher at about 14 l/s whereas for the summer season the average flow rate is below 10 l/s. This indicates that the spring season is more humid than the summer season in Pretoria.

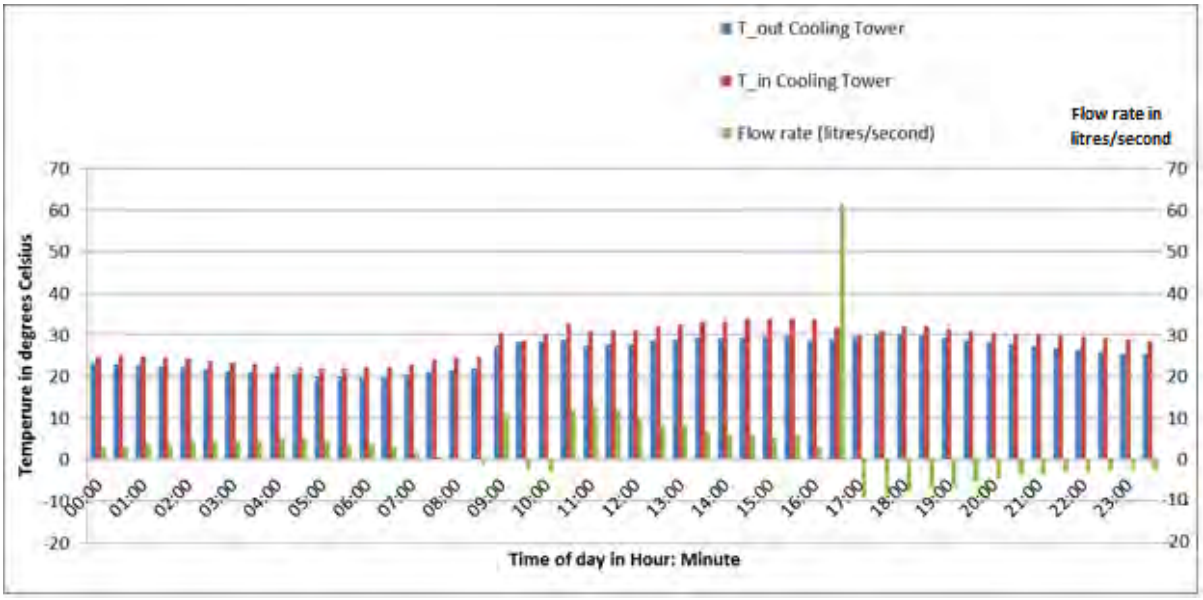

Figure 8.15: Cooling Water Temperatures for the 1st December 2010

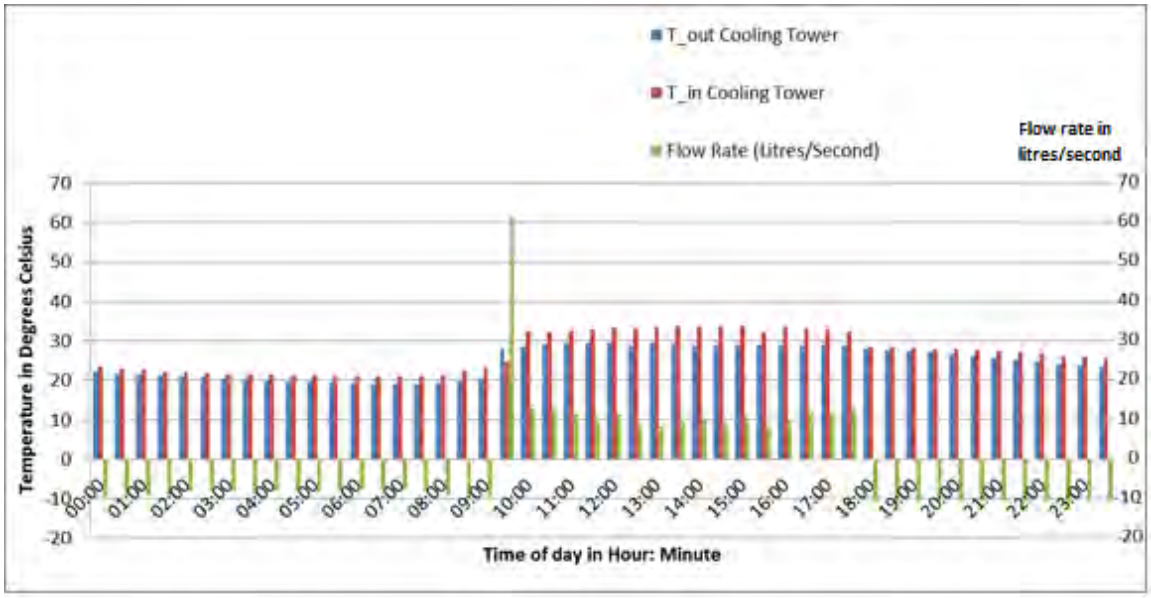

Figure 8.16: Cooling Water Temperatures for the 1st March 2011

The Cooling tower pump is off for a long duration (about 1 hour) as the atmospheric temperatures during winter are quite low and thus the cooling water heat loss to the air is greater.

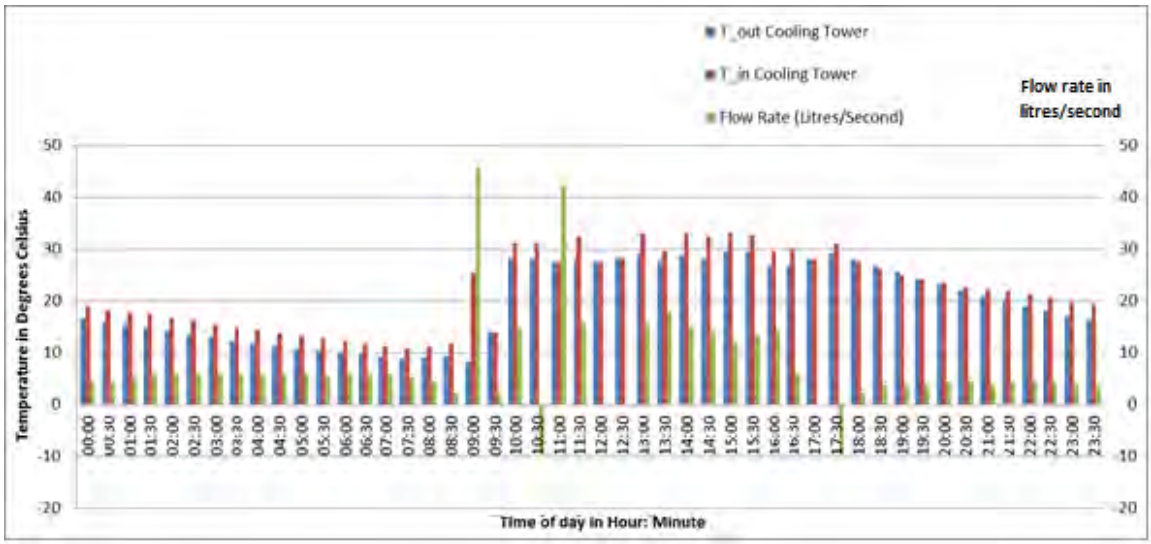

Figure 8.17: Cooling Water Temperatures for the 1st June 2011

The roles played by the cooling water, generator and evaporator have been observed in determining the COP of the absorption process. The amounts of energy given up or removed from the system in order for the process to function correctly can be seen in Figures 8.18, 8.19, 8.20 and 8.21. The energy given up in the generator, removed by the cooling towers and the refrigeration capacity of the evaporators is calculated according to the Equations 8.2, 8.3 and 8.4 from the diagram shown in Figure 8.3 as follows.

$$\dot{Q}_G = \dot{m}_{11} C_{p\_water} (T_{11} - T_{12}) \quad \text{(Equation 8.2)}$$

Where:

$\dot{Q}_G$	Heat energy for the generator (kW)
$\dot{m}_{11}$	Mass flow rate of hot water into the generator of the chiller (kg/s)
C_{p_water}	Specific heat capacity of water (KJ/kgK)
T_{11}	Temperature of water entering the generator (K)
T_{12}	Temperature of water exiting the generator (K)

The energy removed by the cooling water is calculated according to Equation 8.3:

$$\dot{Q}_C = \dot{m}_{15} C_{p\_water} (T_{16} - T_{15}) \quad \text{(Equation 8.3)}$$

Where:

$\dot{Q}_C$	Heat energy of the cooling water (kW)
$\dot{m}_{15}$	Mass flow rate of cooling water into the chiller (kg/s)
C_{p_water}	Specific heat capacity of water (kJ/kgK)
T_{16}	Temperature of water entering the cooling tower (K)
T_{15}	Temperature of water exiting the cooling tower (K)

The refrigeration capacity of the chiller can be calculated according to Equation 8.4 below:

$$\dot{Q}_E = \dot{m}_{17} C_{p\_water} (T_{18} - T_{17}) \quad \text{(Equation 8.4)}$$

Where:

$\dot{Q}_E$	Heat energy of the chilled water (kW)
$\dot{m}_{17}$	Mass flow rate of chilled water into the chiller (kg/s)
C_{p_water}	Specific heat capacity of water (kJ/kgK)
T_{18}	Temperature of water entering the chiller (K)
T_{17}	Temperature of water exiting the chiller (K)

The graphs of the energy balance follows for each season of the year. The times of day that have no data points are when the chilled water pump is switched off. Measurements could not be recorded for these points.

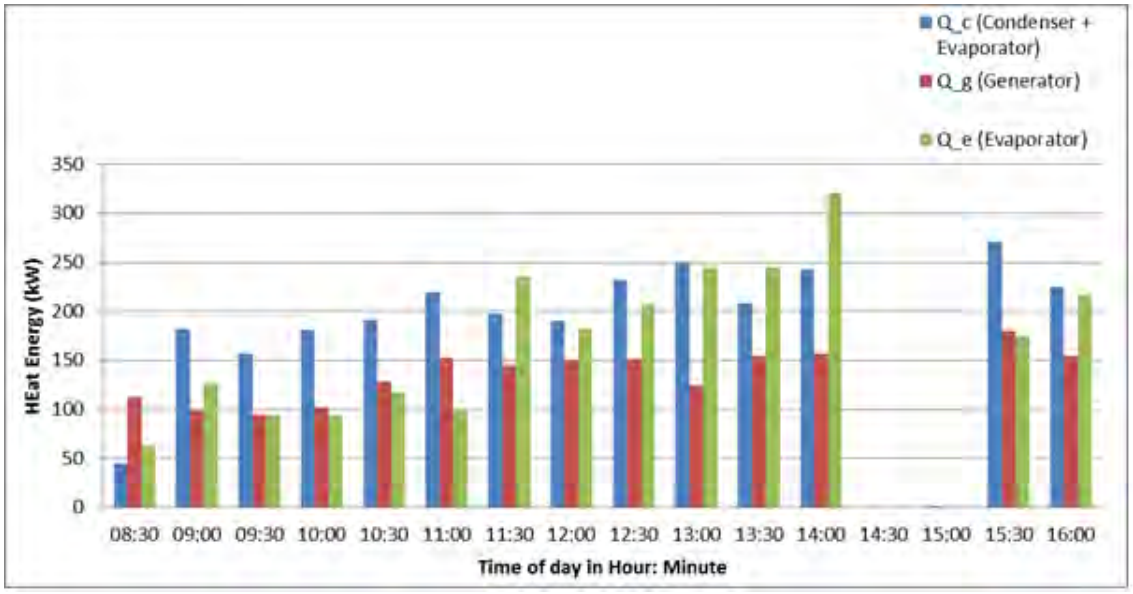

Figure 8.18: Heat Balance for the Chiller's Absorption process (Spring)

According to the COP of the absorption process as depicted in Figure 8.1, the refrigeration capacity should be 70% of the heat source and the heat rejected to the cooling water should be greater than the heat source.

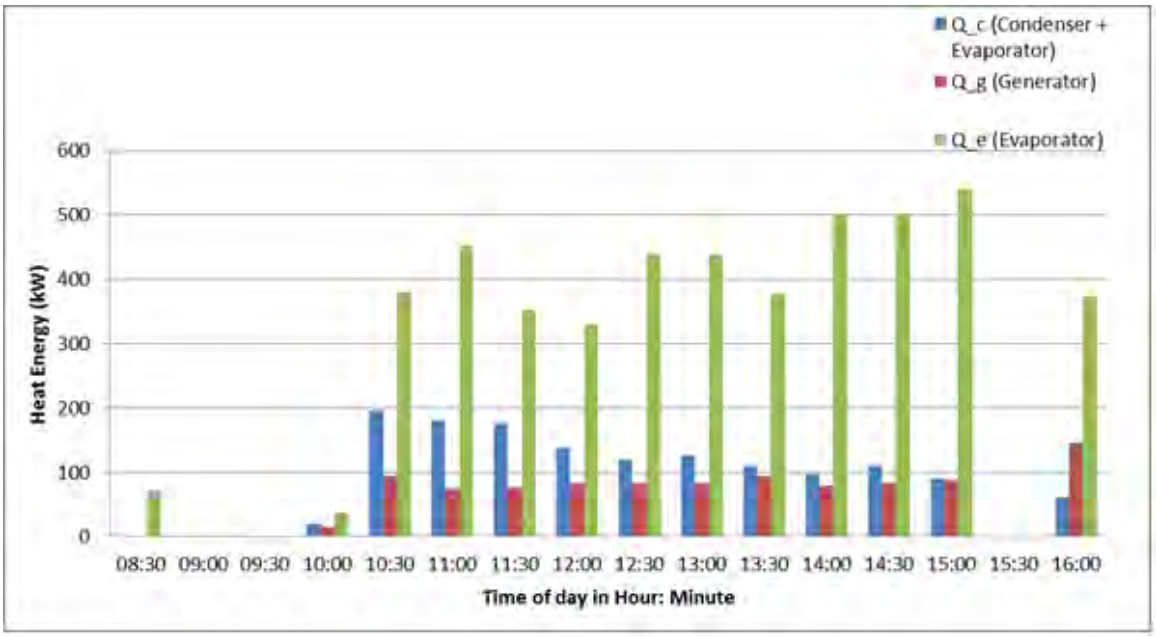

Figure 8.19: Heat Balance for the Chiller's Absorption process (Summer)

It can be seen that this pattern is not shown in the graphs for most of the seasons, especially for Autumn, where the heat energy rejected to the cooling water is less than half that of the refrigeration capacity. This is due to the air being less humid in the Autumn period and thus not requiring much flow rate for ensuring that the water is being cooled according to the desired temperature for the cycle to continue.

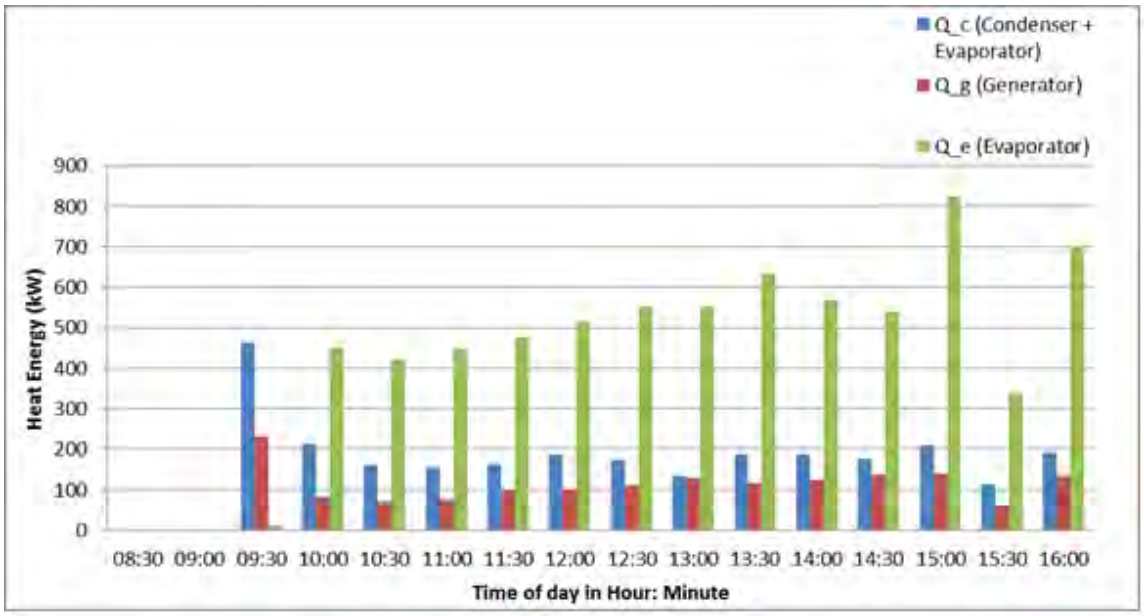

Figure 8.20: Heat Balance for the Chiller's Absorption process (Autumn)

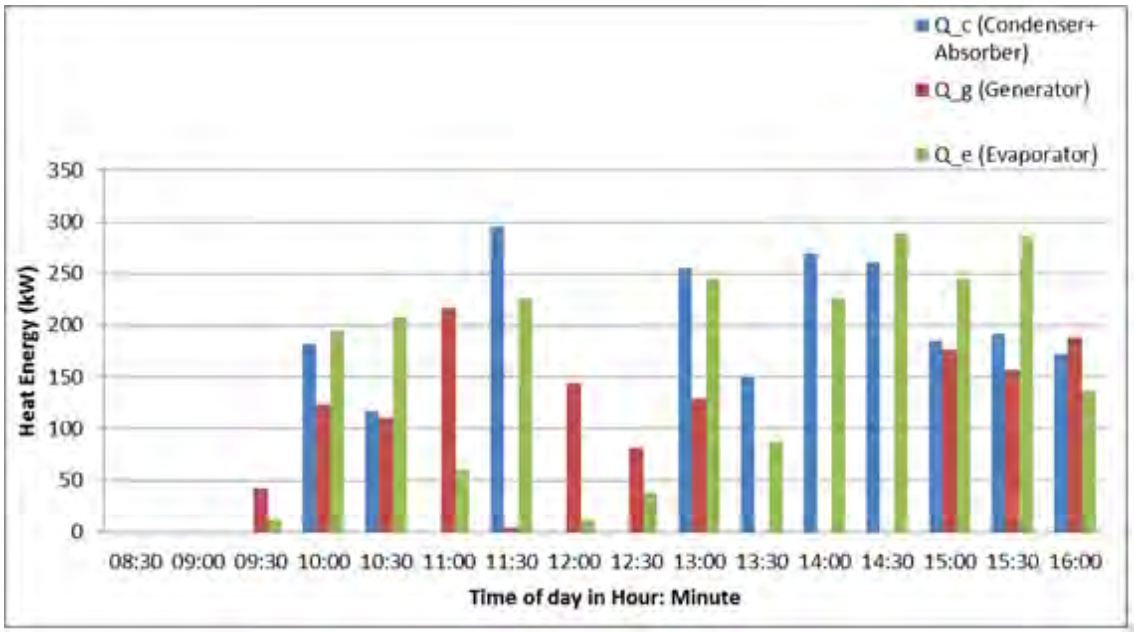

Figure 8.21: Heat Balance for the Chiller's Absorption process (Winter)

The relationship between the Generator inlet temperature and the COP of the absorption process can be seen in Figure 8.22, taken on the 13th August 2010 during about 3 hours from the Solar Noon for that day which occurred at 12:12. Refer to Appendix D.

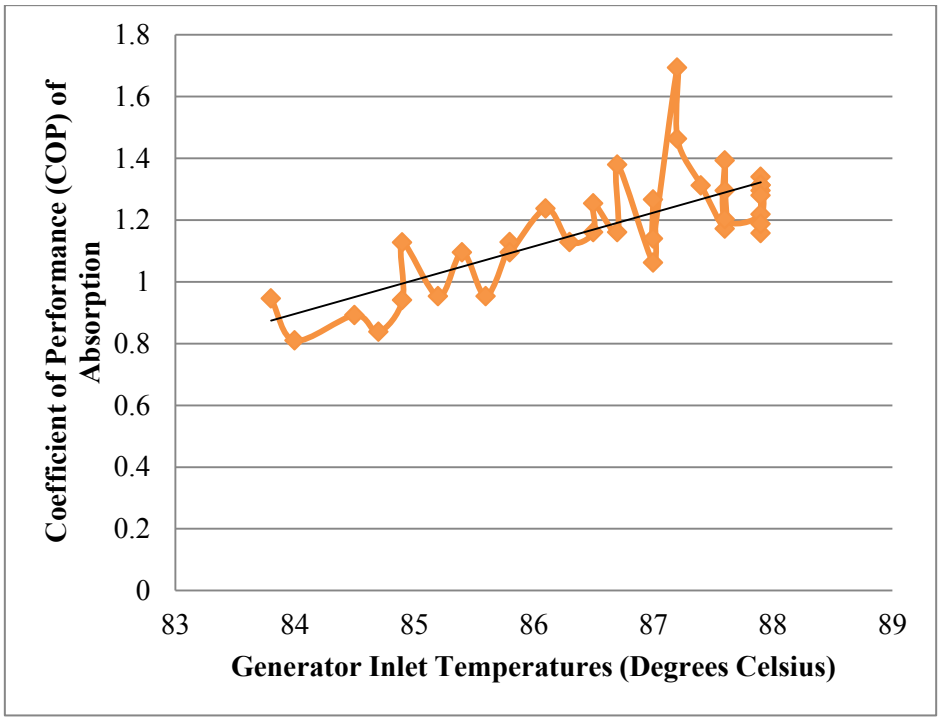

Figure 8.22: COP of absorption for varying generator temperatures

The increase in COP of the absorption process seems to gradually increase, however with many fluctuations from around 0.8 to over 1. This change can be due to the cooling water inlet temperature fluctuations.

The corresponding heat rejected to the cooling water for the COP of absorption established above will be plotted to account for its fluctuating COP in the mid-operating range of the generator inlet temperatures (83 °C to 88 °C). Refer to Figure 8.23.

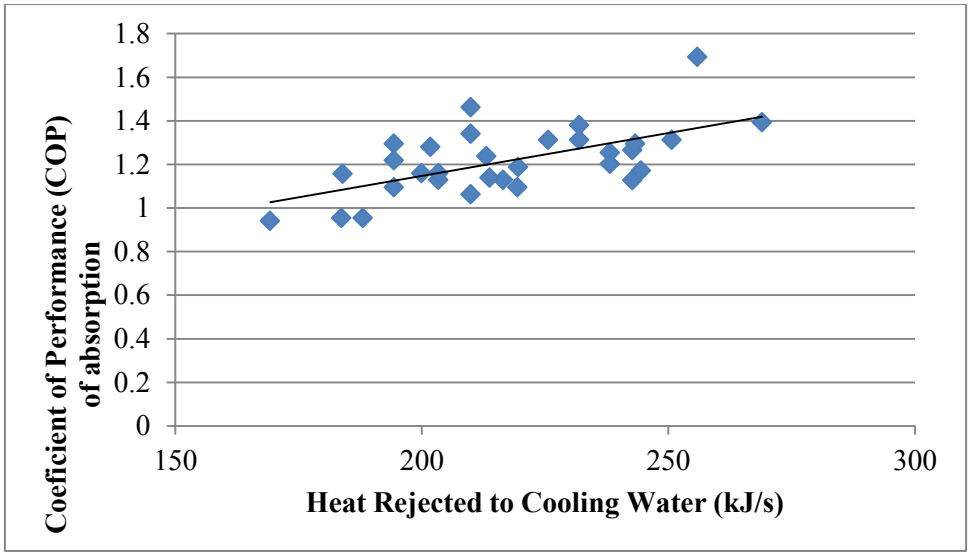

Figure 8.23: COP of absorption for various amounts of heat rejected to the cooling water

The graph shows that an increase in COP is directly proportional to the heat rejected which means that the greater the heat rejected, the more efficient is the absorption cycle. The fluctuations in heat rejections can be attributed to the cooling water inlet temperature which rejects heat at the cooling towers based on two methods through evaporative cooling, i.e. via a variable speed pump which squeezes the cooling water through high pressure nozzles so that it falls over the fill material and is cooled and through a variable speed fan which aids the cooling process. The cooling tower pump engages when the cooling water to the cooling tower is greater than 28 °C and the fan engages when the cooling water to it is greater than 31 °C . Refer to Figure 8.24 for the Cooling water inlet temperatures to the chiller.

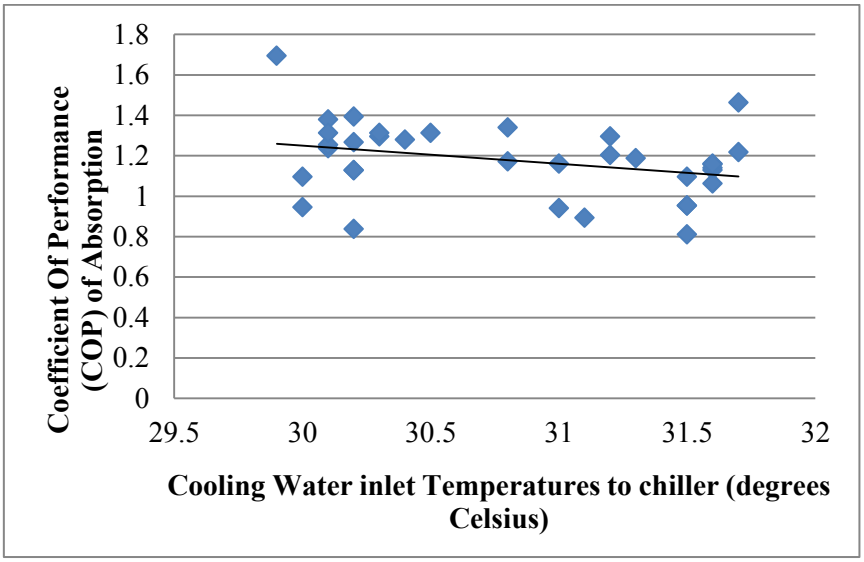

Figure 8.24: COP of Absorption for various Cooling Water inlet temperatures

From Figure 8.24 it can be seen that there is an inverse relationship indicating that the COP of the absorption process decreases with an increase in the cooling water inlet temperatures to the chiller.

The maximum COP of the absorption process which is $COP_{rev,abs}$ calculates the theoretical absorption assuming totally reversible conditions. It is calculated according to Equation 6.2.

This maximum COP will be calculated for the Operating Theatres setpoint of $10\,°C$ and the operating temperature limits of $17\,°C$ and $22\,°C$ for the Trauma unit, Reception and Foyer areas of the Moot Hospital. The three conditions are that the ambient temperature is at $25\,°C$ with the normal operating Generator inlet temperature of $88\,°C$, the extreme ambient temperature which is the outdoor design dry bulb temperature of $32\,°C$ with Generator inlets at $88\,°C$ and $95\,°C$. Refer to Figure 8.25.

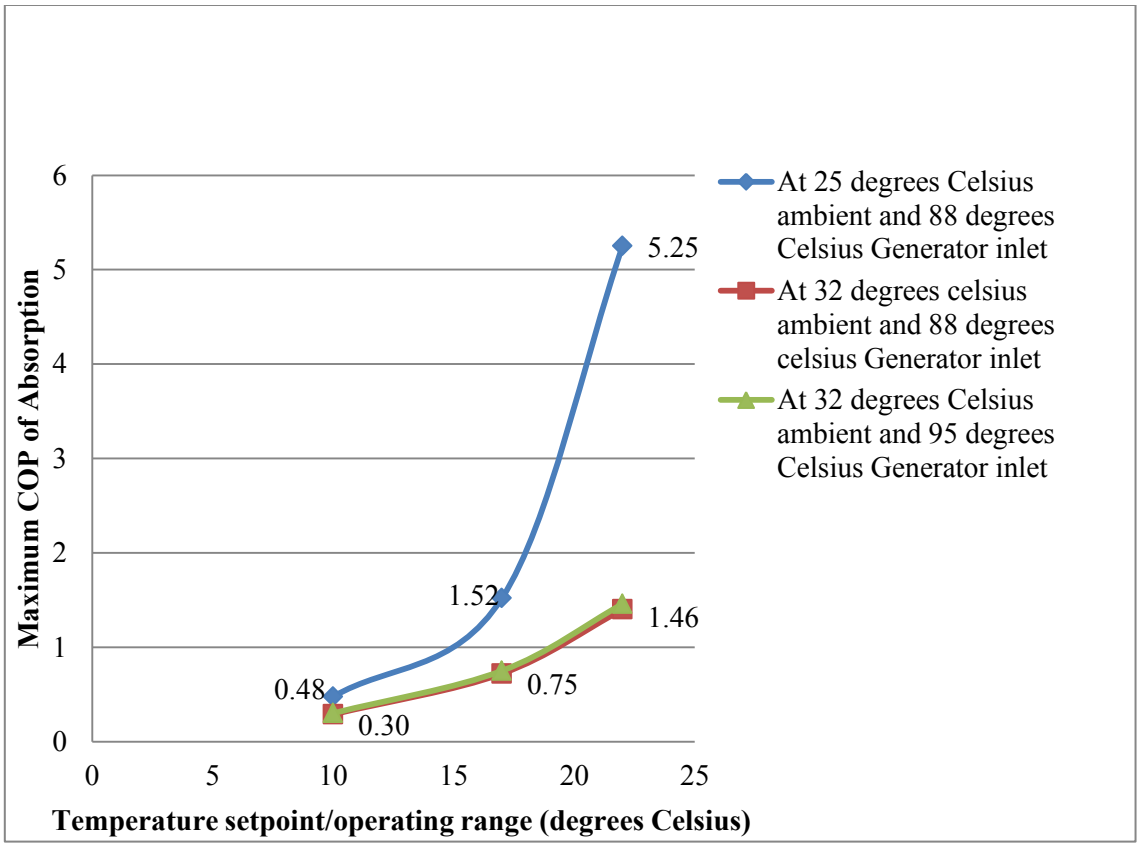

Figure 8.25: Maximum COP of Absorption for temperature set-points/operating limit

It can be seen from Figure 8.25 that the maximum or theoretical COP of absorption that can be reached for the output setpoint of the Operating Theatres is 0.3 and for the Foyer, Reception and Trauma Unit is 1.46 for the system's maximum design temperature operating at maximum generator heat input.

The coefficient of performance of the single effect LiBr Absorption Air conditioning involves calculating the ratio of the Cooling output to the total power input. Figure 8.25 depicts the theoretical COP of the absorption process taking into account the thermal and electrical energy inputs. Figure 8.26 shows the Electrical Energy COP of the process according to the Equation 8.5 below:

$$COP_{elec} = \frac{\text{Cooling output}}{\text{Electrical input}} = \frac{\dot{Q}_E}{P_{elec}} \quad \text{(Equation 8.5)}$$

Where:

COP_{elec}	Coefficient of Performance based on Electrical energy input [-]
$\dot{Q}_E$	Cooling in the Evaporator (kW)
P_{elec}	Electrical energy (kW)

The graph shows an increase in the Electrical COP with increasing Cooling Capacity outputs.

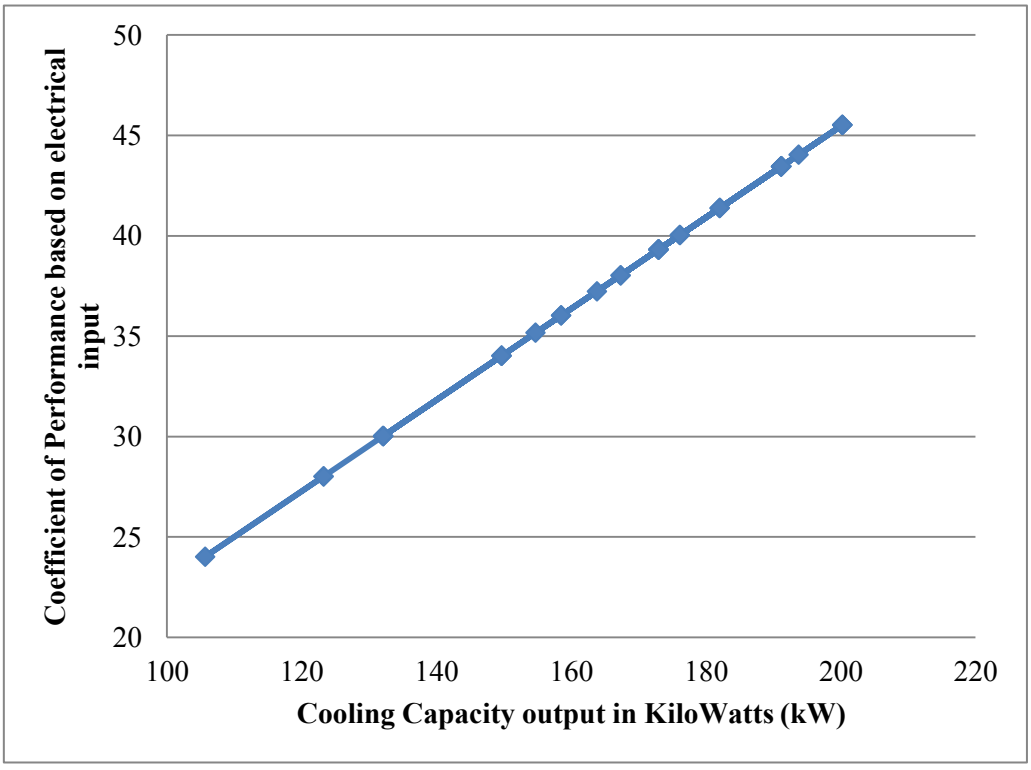

Figure 8.26: Electrical Energy COP for varying cooling capacities

8.3 Solar Collector Efficiency Performance

The solar collector and tank efficiency performance will be done to achieve three objectives as stipulated in Table 6.3 of Chapter 6 for the Spring, Summer, Autumn and Winter seasons. The three objectives are as follows:

- Calculate the efficiency of the solar collector array
- Calculate the effectiveness of the hot water storage tank insulation
- Calculate the overall solar water heating system efficiency

The four seasons dates that are used for this analysis is the same as used for the investigation of the air conditioning efficiency performance in Section 8.2. The efficiency of the collector array will be calculated according to the Equation 8.6 below:

$$\eta_{coll} = \frac{\dot{Q}_{solar}}{A_{coll} \times G} \quad \text{..... (Equation 8.6)}$$

Where:

η_{coll}	Efficiency of the collector array [-]
$\dot{Q}_{solar}$	Heat Energy transferred to the collector array (W)
A_{coll}	Total aperture area of the collector array (m^2)
G	Global irradiance on the collector area (W/m^2)

$\dot{Q}_{solar}$ will be calculated from Equation 7.1 in Chapter 7 and the A_{coll} will need to include the Heat pipe and the U-pipe aperture areas and the total area is calculated below:

$$A_{coll} = n_{U-pipe} \times A_{aper\_U-pipe} + n_{Heat-pipe} \times A_{aper\_Heat-pipe} \text{..... (Equation 8.7)}$$

The number of U-pipe solar collectors in the array is 40 and of the Heat pipe is 12. Their aperture areas are given in Table 7.4 for the U-pipe, which is $1.8m^2$ and in Table 7.5 for the Heat pipe which is $1.1m^2$. The total area then is $85.2m^2$. To calculate the efficiency of the collector array, the heat transferred to the collector array $\dot{Q}_{solar}$ needs to be calculated. The heat transferred to the collector for the solar irradiation for the four seasons are shown in Figures 8.27, 8.28, 8.29 and 8.30.

The incident solar energy on the collector area have been superimposed on the heat absorbed or transferred to the solar collector array to show their relationship. It can be seen from Figure 8.27 that the energy absorbed into the collectors is directly proportional to the incident solar energy experienced.

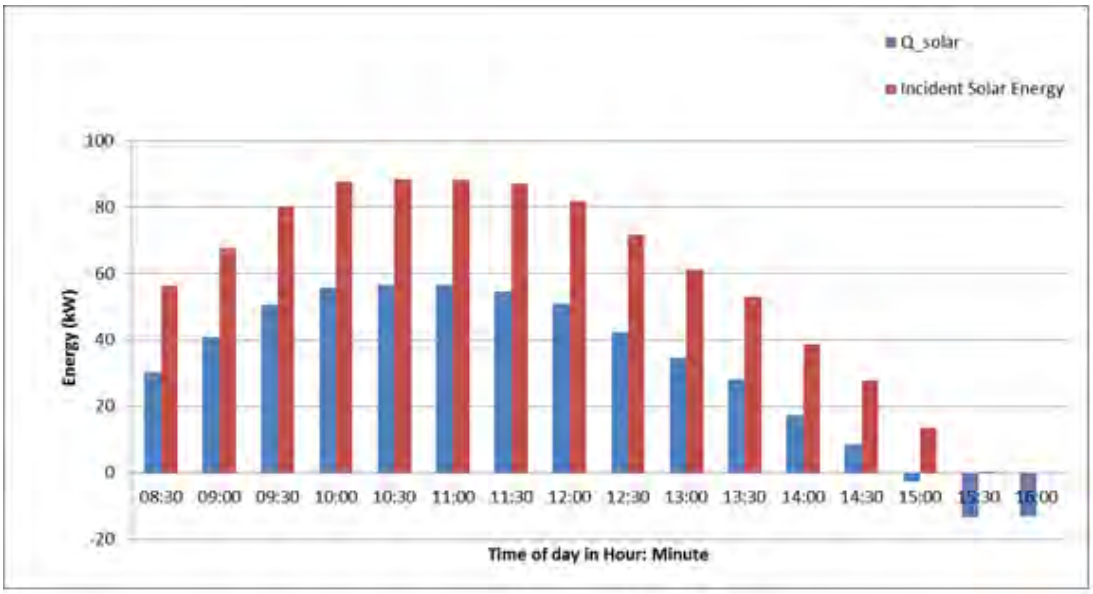

Figure 8.27: Incident Solar Energy and Heat transferred to the collector (Spring)

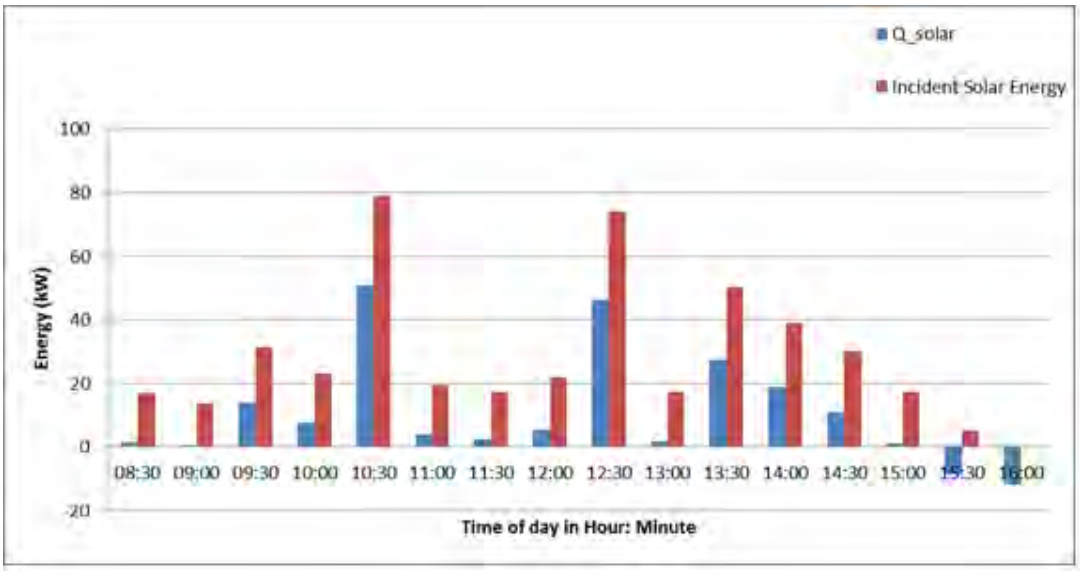

Figure 8.28: Incident Solar Energy and Heat transferred to the collector (Summer)

It can be seen that the increase or decrease in incident solar radiation on the collectors causes an immediate response on the absorption of energy into the collectors. It can be seen that when the incident solar radiation drops significantly, there is a dramatic decrease in the energy absorbed. This

pattern is noticed in each graph toward the end of the day where the energy absorption turns into an energy loss, due to natural convection of the heat into the environment which is influenced by the ambient temperature. Figure 8.31 shows the ambient temperature for the four seasons.

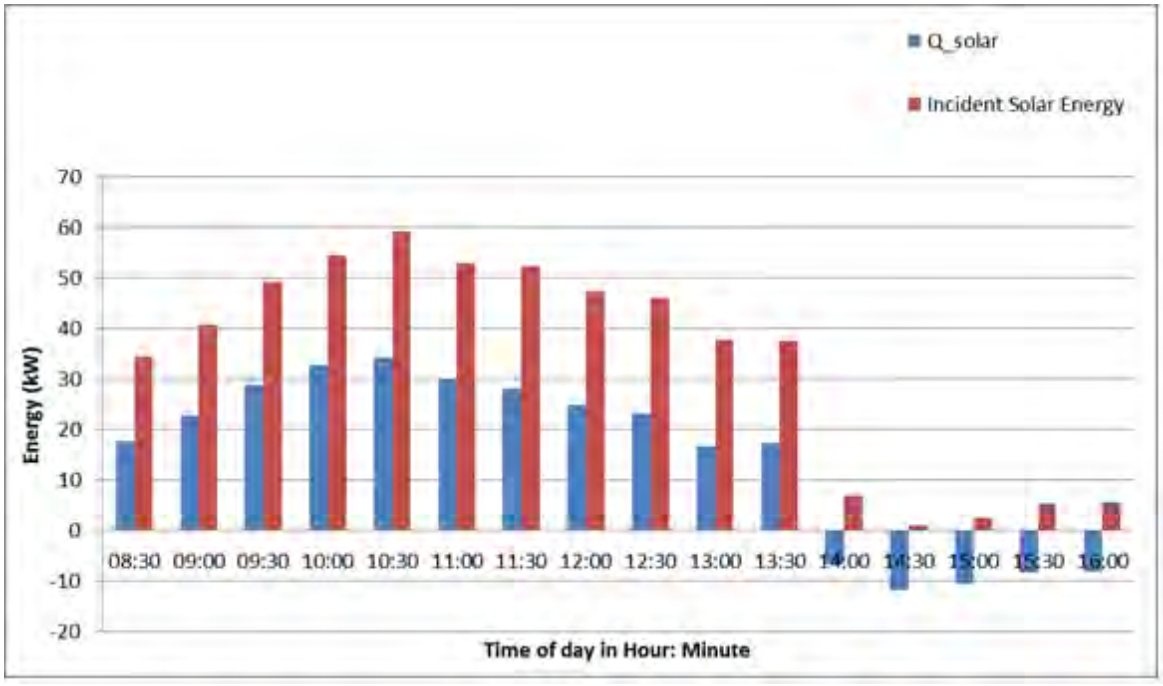

Figure 8.29: Incident Solar Energy and Heat transferred to the collector (Autumn)

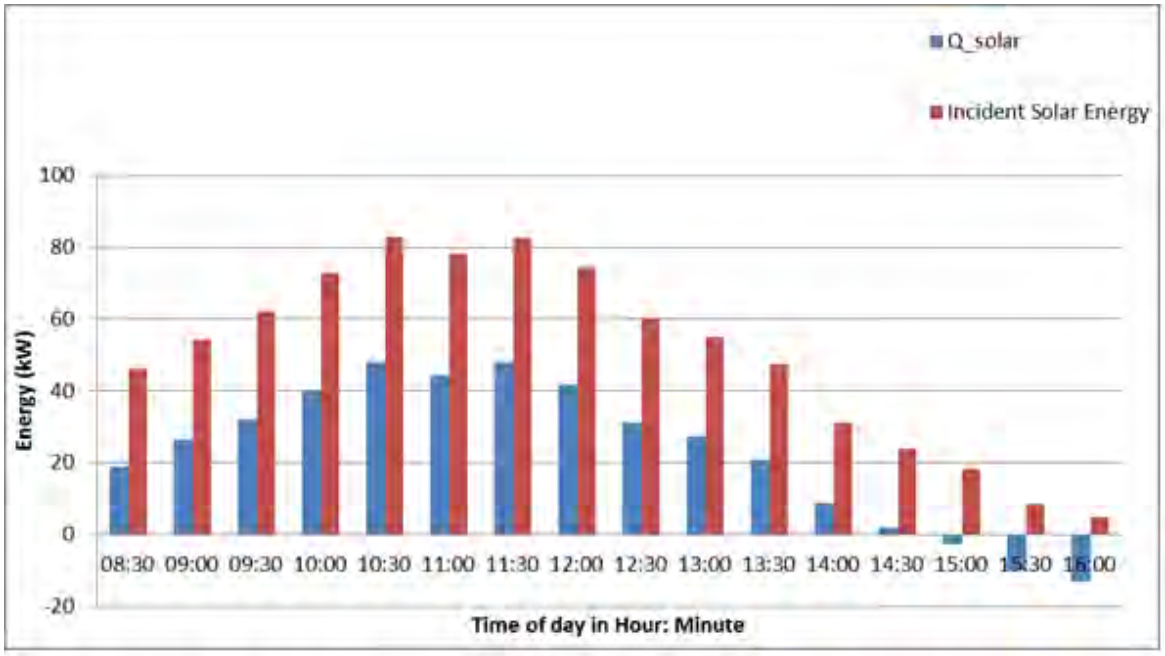

Figure 8.30: Incident Solar Energy and Heat transferred to the collector (Winter)

Figure 8.30 indicates a heat loss of the collector even though incident solar radiation energy is present toward 15:00; this is due to the colder temperatures that are experienced in the winter season towards the afternoon as compared to the other seasons shown in Figure 8.31.

The humidity and ambient conditions can be seen in Appendix E. The weather data presented in Appendix E is recorded as an average for the Pretoria, however the data presented in the graph in Figure 8.31 is specific to the Pretoria Moot Hospital site.

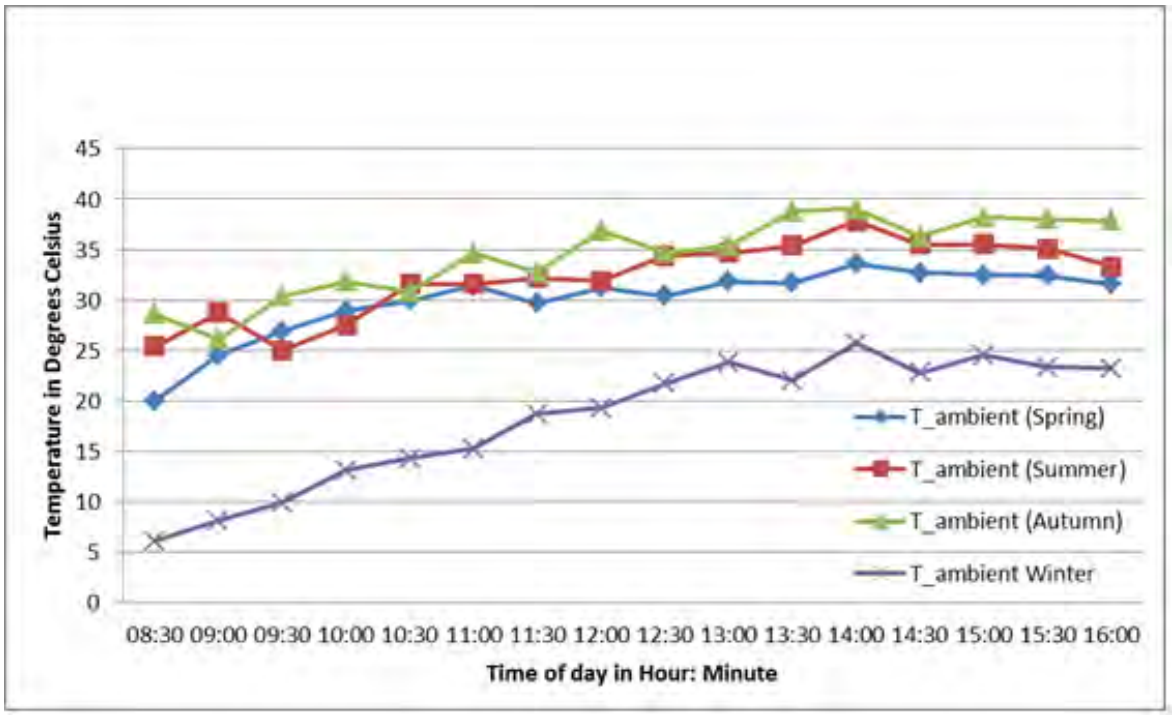

Figure 8.31: Ambient Temperature for the four seasons

The efficiency of the solar collectors according to Equation 8.4 is the solar energy absorbed by the collectors over their incident solar energy. Their efficiency can be seen in Figure 8.32. For the time period between 08:30 and 13:30, the efficiency predominantly lies in the region of 0.5 to 0.65.

The solar collectors play a vital role in capturing solar energy, however, the hot water storage tank is also a major component in the cycle as it stores the energy captured by the solar collectors until such time it reaches the desired temperature to be used in the generator of the chiller. The hot water storage tank provides a certain measure of protection against the intermittent behaviour of incident solar radiation which if used directly will result in many interruptions of the cycle in a day.

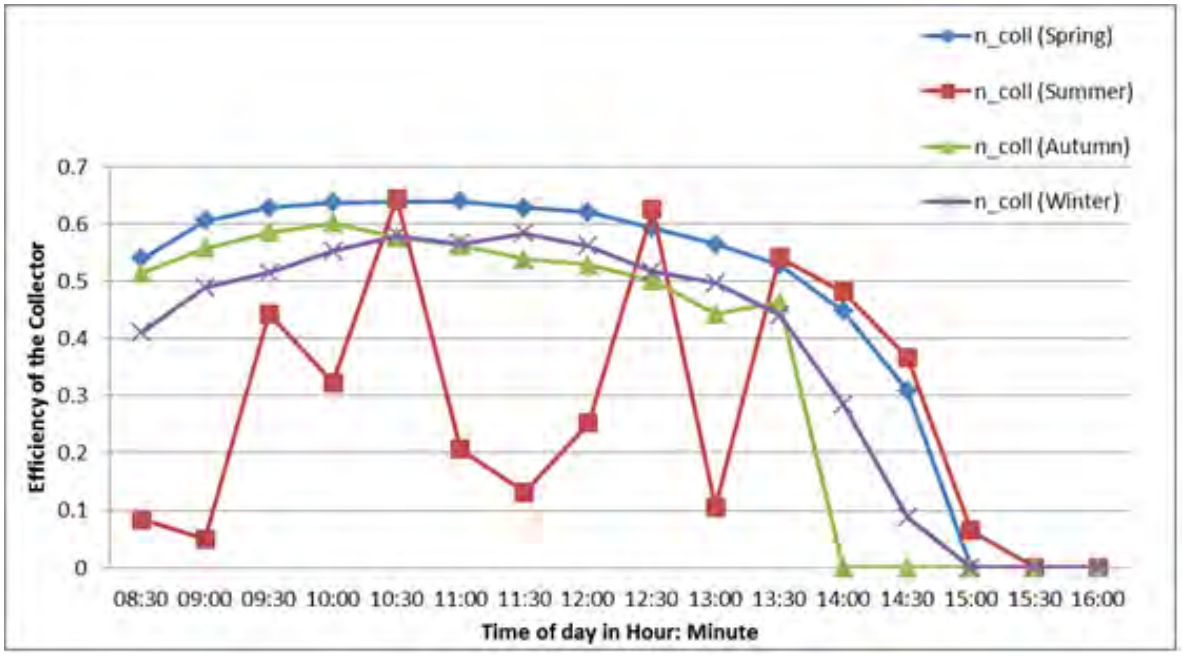

Figure 8.32: Solar Collector Efficiency for the four seasons

The solar hot water storage tank was constructed such that it is stratified into 3 sections to heat one of the three sections of the 6000l hot water tank at a time to the required temperature of the generator which is in the range of 80 °C to 95 °C .

Each layer within the tank has about 3 temperature sensors and the rest of the temperature sensors are alongside the heat medium valves that allow hot water to circulate between the chiller and the Hot water storage tank and the solar valves that allow water to circulate between the solar collectors and the Hot water storage tanks. The full schematic of the Hot water storage tank is contained in Appendix B and in Chapter 7, Figure 7.27.

Insulation of the Hot water storage tank is therefore critical and the heat losses from the Hot water storage tank will defer according to the temperature difference between the water within the Hot water storage tank and the outside ambient temperature as this will determine the rate of natural convection. The tank temperatures can be seen in Figures 8.33, 8.34, 8.35 and 8.36 for the four seasons.

The temperatures viewed in the Figures 8.33 to Figure 8.36 can be viewed in conjunction with the data contained in Appendix D for the solar noon temperatures and in Appendix E for the ambient temperatures and humidity.

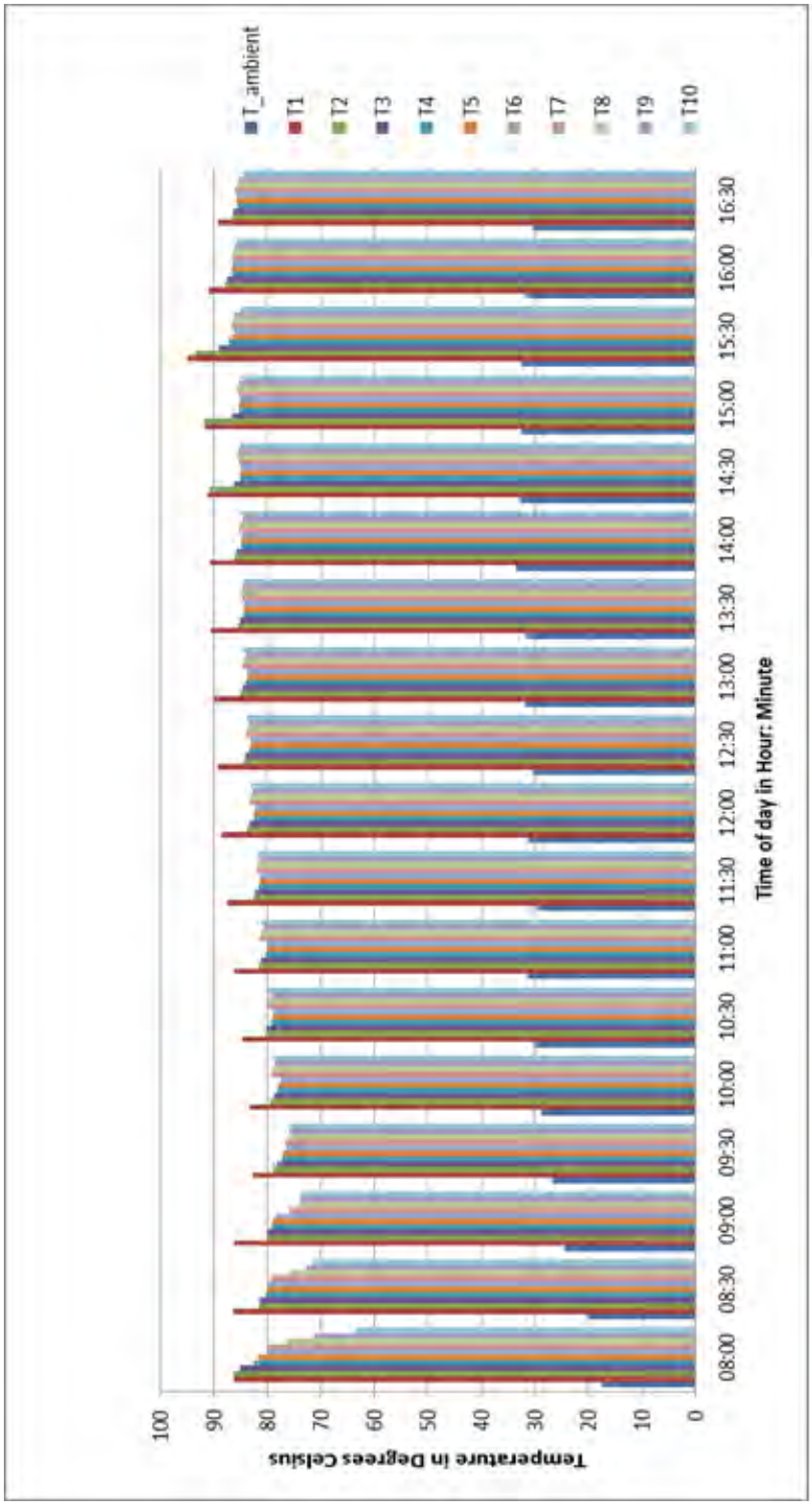

Figure 8.33: Hot water tank temperatures for Spring

It can be seen from Figure 8.33 that the Tank temperature T1 which is the topmost layer of the first section in the Hot water storage tank heats up first to the temperature required by the generator and the control logic then switches over to allow the other sections to heat up to over 80 °C . The

temperature difference of about 30 °C between the tank's topmost and bottommost sections (T1 and 10) are reduced to an approximate ΔT of 5 °C in two hours.

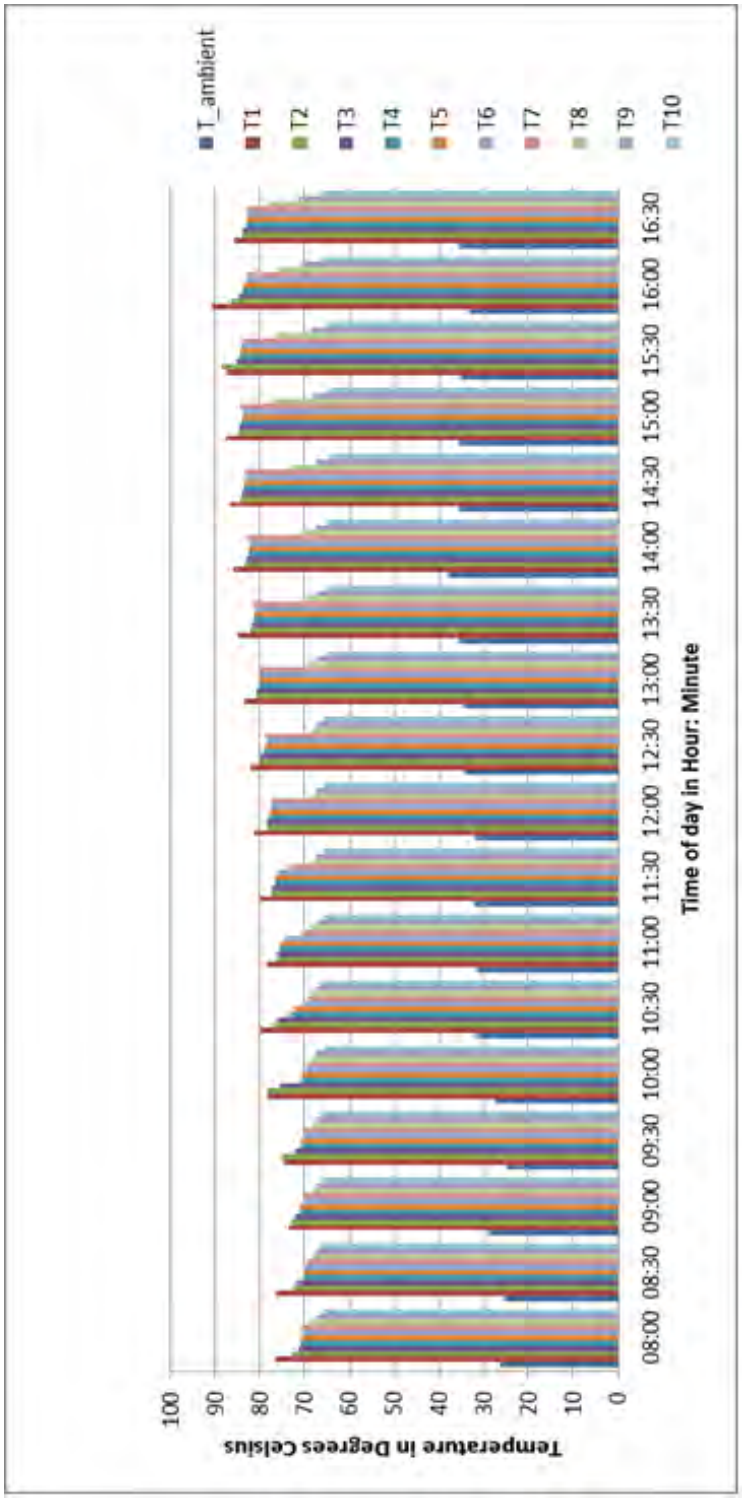

Figure 8.34: Hot water tank temperatures for Summer

The summer season solar radiation was intermittent for the day chosen, i.e. 1st December 2010. The effect of the intermittent solar radiation can be seen by comparing the temperatures reached by the topmost section of the tank in Figures 8.33 and 8.34. The solar loads would have also been much higher for summer, as the ambient temperatures for Summer reached a maximum of about 38 °C compared to Spring's 33 °C and this would mean that the use of heat for the chiller would have been at a higher rate, thus not allowing the hot water tank temperature at T1 reach over 90 °C.

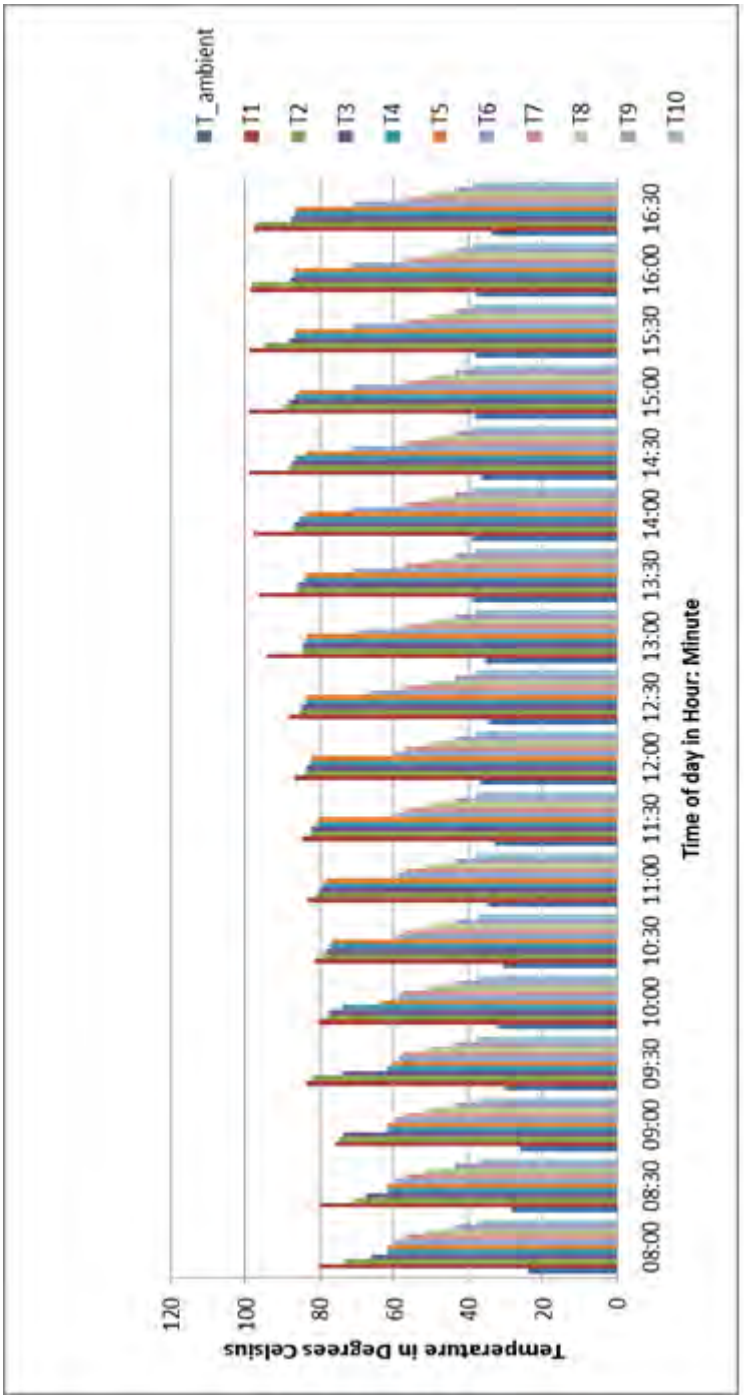

Figure 8.35: Hot water tank temperatures for Autumn

The temperatures of the Hot water tank, especially the topmost region reached a maximum of 100 °C and for most of the afternoon stayed at about 90 °C. Observing the ambient temperatures for the day, it can be seen that the temperatures are quite high and reaching a maximum of 39 °C, it would be expected that the external building heat load would be large and this would result in the limiting of T1 to below 90 °C. The humidity for the Autumn season is much lower in Pretoria than for its Summer season and hence the building load is lower allowing the hot water storage tank to retain the heat instead of it being used in the generator at the rate of the summer season usage.

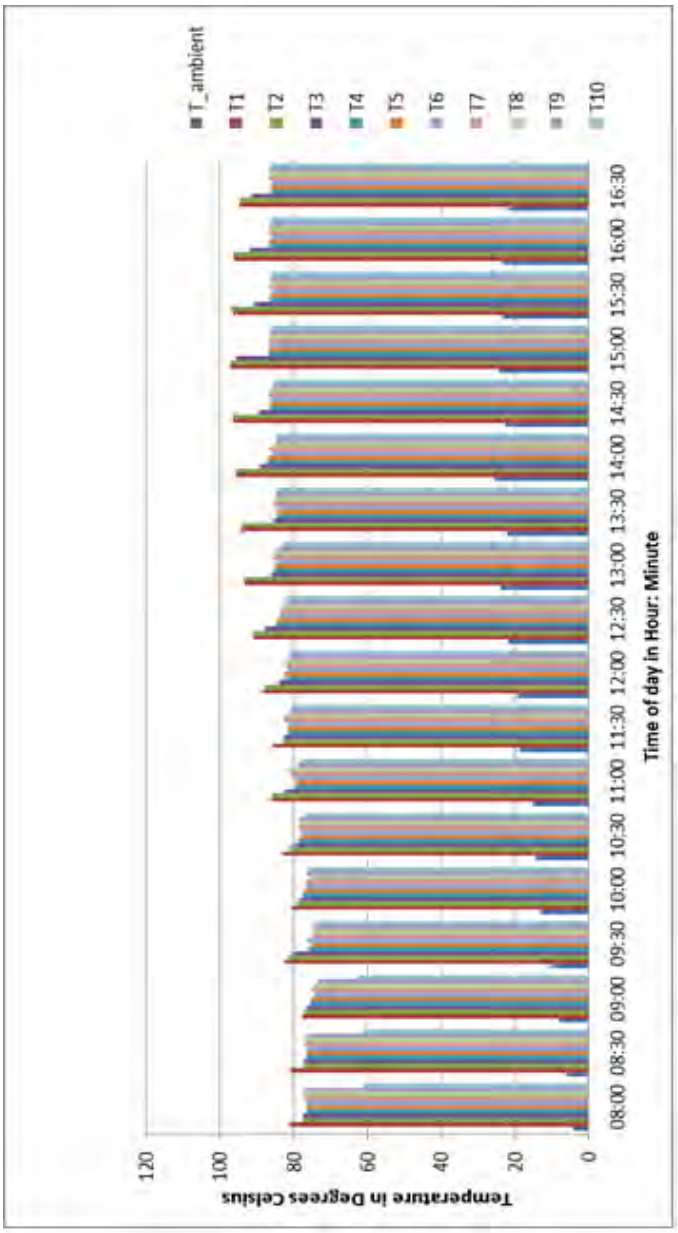

Figure 8.36: Hot water tank temperatures for Winter

The major difference with Figure 8.36 and Figures 8.33, 8.34 and 8.35 is that the ambient temperatures are significantly lower. The tank temperatures are mostly constant throughout the day; however it is limited due to heat loss to the environment to about 95 °C in the topmost section, T1. The solar radiation seems to be in line with the other seasons with the peak being around 1100W/m^2.

The solar collectors are the evacuated tube type and are therefore quite well insulated from heat loss to the environment and the collector array efficiency gave us a range of mostly about 0.5 to 0.65 according to Figure 8.32. Comparing the collector temperature with the Hot water tank's top section of T3 is a good test to observe the time taken for the top section of the tank to heat up to the Collector temperature. The ambient temperature plays an important role in this difference as it will give an indication of the heat load of the building and the potential of heat loss to the environment. The relationship between the ambient temperature and the ΔT between the solar collector temperature and the hot water tank top section temperature (Tsolar – T3) is given is Figures 8.37, 8.38, 8.39 and 8.40 for the four seasons.

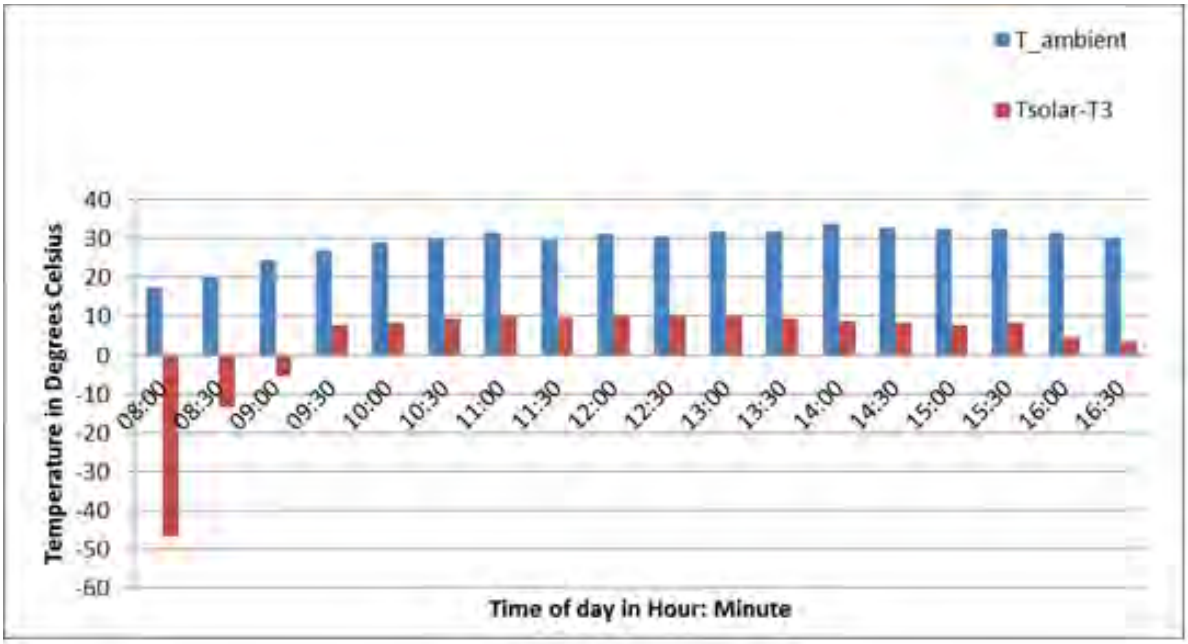

Figure 8.37: Solar Collector and Hot water Tank Temperature difference (Spring)

From Figure 8.37 it can be seen that the ΔT between the Solar collector and the top section of the Hot water storage tank decreases with the increase in the ambient temperature. It is interesting to note that at 8:00 to about 9:00, the tank temperature was larger than the solar collector temperature. This is due to the time required for the solar radiation to heat up the water (about 2000litres) to the solar collector temperature. The temperature difference is approximately 10 °C throughout the 2nd of September 2010.

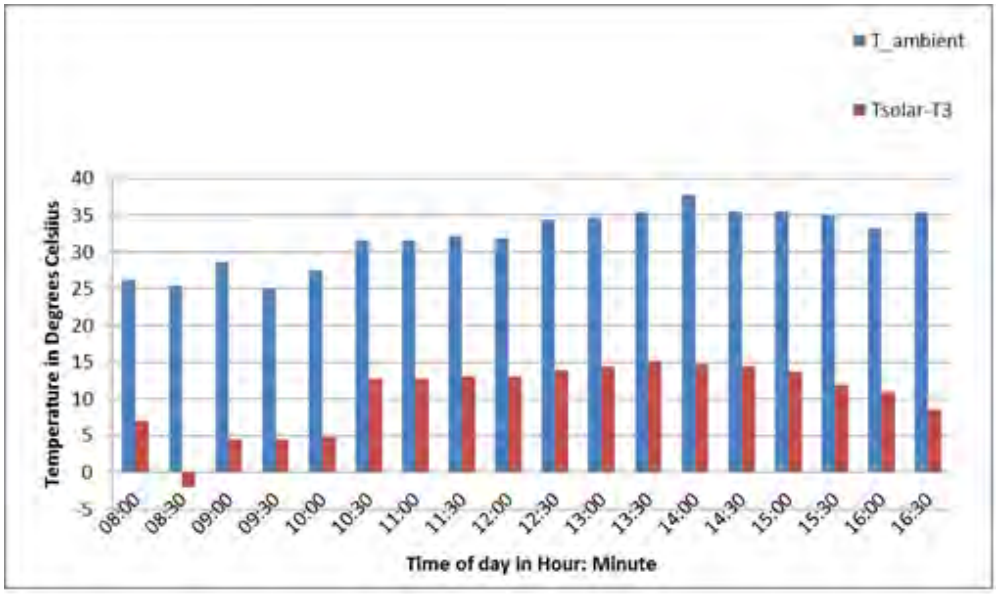

Figure 8.38: Solar Collector and Hot water Tank Temperature difference (Summer)

The ΔT of (Tsolar –T3) is positive at 08:00 as opposed to the ΔT seen in Figure 8.37, meaning that the Solar temperature is already higher than the top section of the hot water tank temperature. This can be accounted to the fact that a higher ambient temperature (T_ambient) by 10 °C is experienced at 08:00 for Summer. This will mean that the heat loss to the environment will be smaller from the Hot water storage tank and the solar collector allowing the collector temperature to be heated up much faster than for Spring in Figure 8.37.

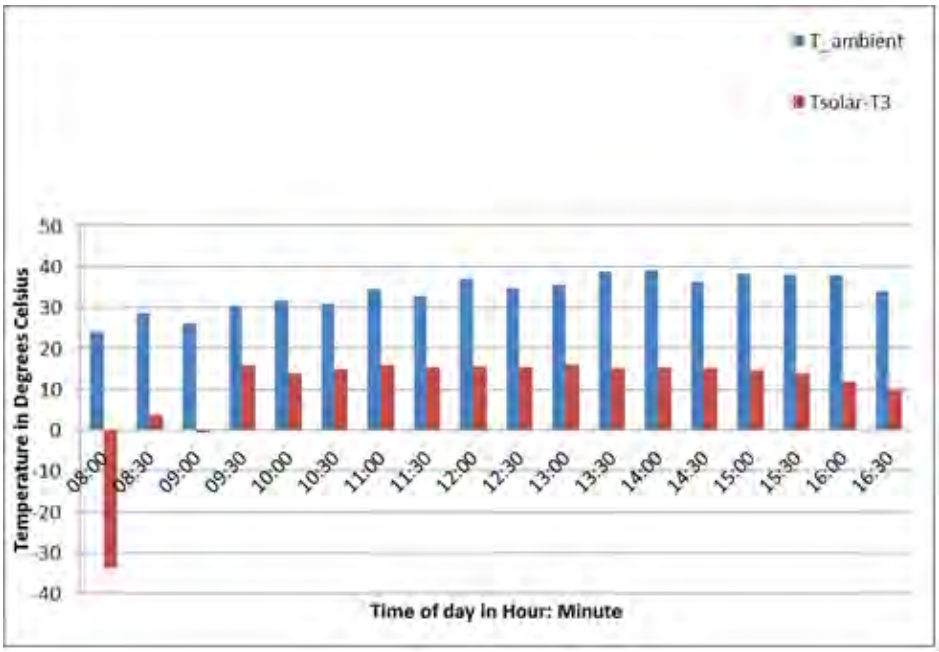

Figure 8.39: Solar Collector and Hot water Tank Temperature difference (Autumn)

Comparing Figure 8.39 with Figure 8.38, the difference can be seen at 08:00, even though the ambient temperature is about the same at 26 °C . It is observed that the Solar Temperature is lower than the Hot water storage tank temperature T3 in Autumn, whereas, in Summer, even though the same temperature ambient temperature prevails, the Solar temperature is higher than T3. This could be due to the solar radiation being higher for that time in Summer than in Autumn, but according to Figure 8.9 in Section 8.2, the solar radiation values for 08:00 to 09:00 is higher in Autumn than in Summer. The humidity, however, is much larger in Summer than in Autumn, which means that the air is less dense in Summer. Even though the temperature of the air is about the same as the Summer for the Autumn, the enthalpy of the air is lower in Autumn, due to the air in Autumn being more dense and therefore the potential for heat loss to the ambient air is greater in Autumn.

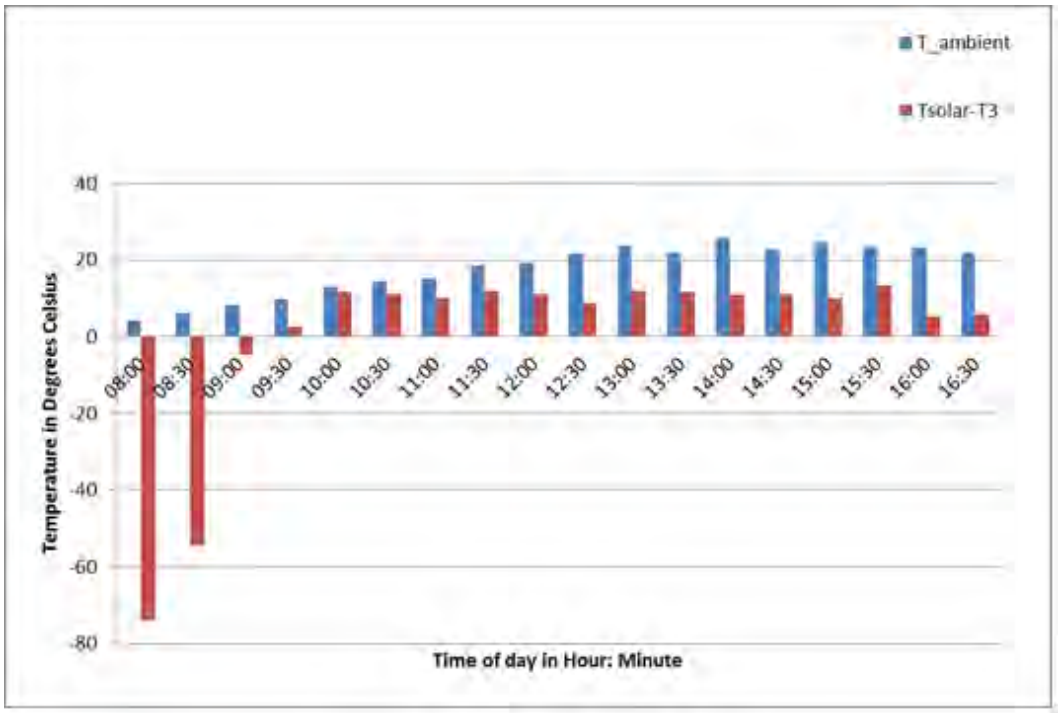

Figure 8.40: Solar Collector and Hot water Tank Temperature difference (Winter)

The ΔT of (Tsolar – T3) is higher for a longer period of time in Winter as seen in Figure 8.40. This is due to heat loss to the environment being much larger and thus taking the solar collector temperatures much longer to heat up to the tank temperatures. It is possible for the water in the solar collectors to freeze, and thus an antifreeze agent is used to prevent this.

Due to the solar collector temperatures being much larger for most of the day than the hot water tank temperatures, as seen in Figures 8.36 to 8.40, it is imperative that the rate at which heat is lost to the environment from the Hot water storage tank be investigated. The focus of the heat loss will be from

the top section of the tank. The heat loss will be calculated for the time period of 18:00 to 4:00 for the four seasons according to the Equation 8.8 below:

$$q_{loss} = q_{@18:00} - q_{@4:00} \quad \text{(Equation 8.8)}$$

Where:

q_{loss} Heat loss (kJ/kg) of the Hot water storage tank top section – Section 1 (about 2000l)

$q_{@18:00}$ Heat energy (kJ/kg) of Hot water at Section 1 of Hot water storage tank at 18:00

$q_{@4:00}$ Heat energy (kJ/kg) of Hot water at Section 1 of Hot water storage tank at 04:00

Equation 8.8 can be written as the following seen in Equation 8.9

$$q_{loss} = C_{P\_water}(T3_{@18:00} - T3_{@4:00}) \quad \text{(Equation 8.9)}$$

Where:

C_{P_water} Specific Heat capacity of water (kJ/kgK)

$T3_{@18:00}$ Temperature at 18:00 of Hot water at Section 1 of Hot water storage tank (K)

$T3_{@4:00}$ Temperature at 4:00 of Hot water at Section 1 of Hot water storage tank (K)

The duration over which the heat loss is calculated is 10hours, thus the rate of heat loss can be calculated according to the Equation 8.10 below:

$$\dot{q}_{loss} = \frac{q_{loss}}{36000} \quad \text{(Equation 8.10)}$$

Where:

$\dot{q}_{loss}$ Rate of heat loss (W/kg)

The heat loss and their rates were calculated for the four seasons and can be seen in Table 8.4.

Table 8.4: Heat Loss from Hot water storage tank

Season	Spring	Summer	Autumn	Winter
Heat loss (q_{loss}) [kJ/kg]	6.7248	14.2902	9.6669	17.2323
Rate of heat loss ($\dot{q}_{loss}$) [W/kg]	0.1868	0.39695	0.268525	0.478675

The average rate of heat loss is 0.33 W/kg. Winter has the highest heat loss followed by Summer, Autumn and then Spring. The results for Summer were corrupted due to the Heat Medium pump running throughout the night circulating the hot water, therefore it showed the second highest heat loss rate.

The role of the hot water storage tank is vital in ensuring a constant supply of thermal energy to the chiller for its operations as solar radiation is intermittent and the water's thermal response to the intermittent radiation is almost immediate. This was observed over the investigation of the incident solar radiation and the absorbed solar radiation in Figures 8.27, 8.28, 8.29 and 8.30. The intermittent solar irradiation received is cause by cloud cover. The effectiveness of the hot water storage tank in the absorption cooling plant can be seen in the investigation of the following three energy flows:

- Energy of solar radiation incident on the solar thermal collectors ($\dot{Q}_{rad}$)
- Energy of solar radiation absorbed by the solar thermal collectors ($\dot{Q}_{solar}$)
- Energy used by the generator of the chiller ($\dot{Q}_{G}$)

$\dot{Q}_{solar}$ will be calculated using Equation 7.1 and $\dot{Q}_{G}$ will be calculated using Equation 8.2, $\dot{Q}_{rad}$ is calculated according to Equation 8.11 below:

$$\dot{Q}_{rad} = G \times A_{aper\_total} \quad \text{(Equation 8.11)}$$

Where:

G Global solar radiation (W/m^2)

A_{aper_total} Total aperture area of the collectors = $85.2m^2$

The energy flows above will be observed for the four seasons in Figures 8.41, 8.42, 8.43 and 8.44. The energy flowing to the generator of the chiller is shown only if the chiller is running. When the

chiller is switched off, a value of zero is registered for $\dot{Q}_G$. The chiller is run from 08:00 to 17:00 and switched off according to the cooling demand.

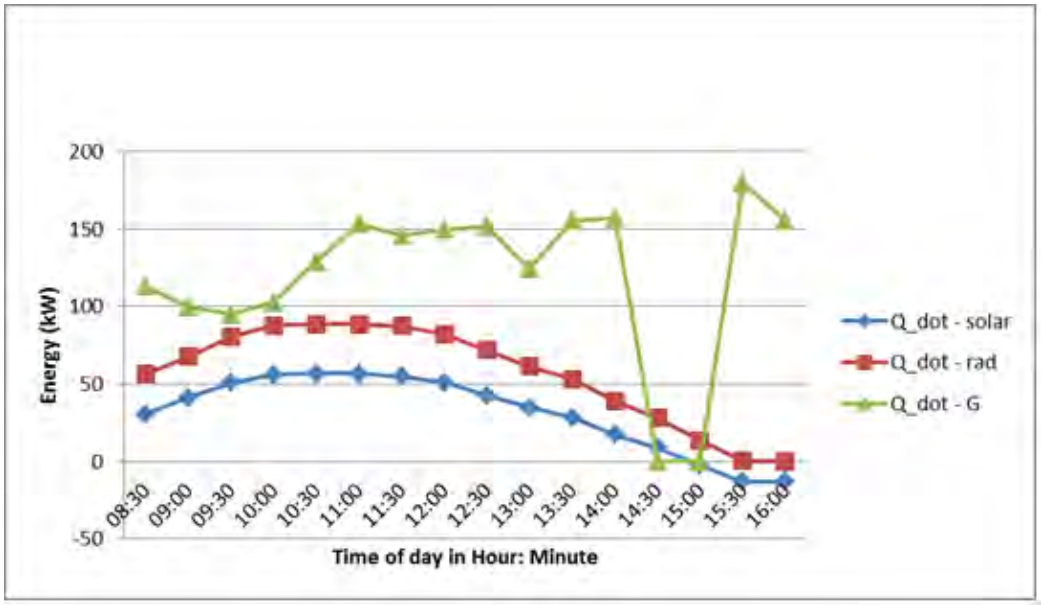

Figure 8.41: Energy Flows for the Spring season

It can be seen from Figure 8.41 that the energy used by the generator is almost twice and in some instances more than twice that of the solar radiation incident or absorbed by the solar thermal collectors. Figure 8.42 demonstrates the effectiveness of the Hot water storage tank in that the operation of the chiller is smooth from 10:30 to 13:30 delivering around 80kW to the generator even though the incident and absorbed solar radiation is fluctuating between 20kW and 80kW.

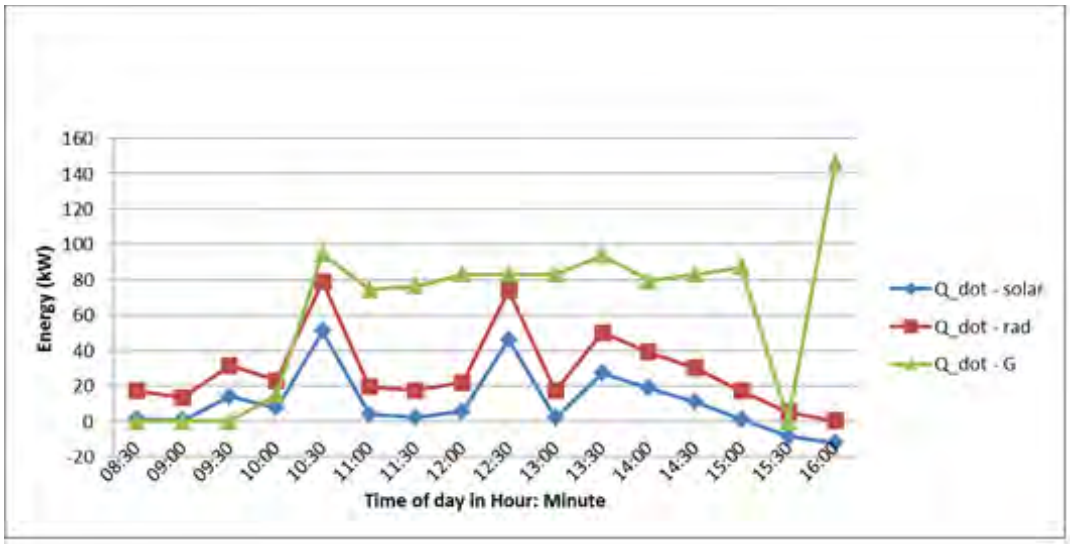

Figure 8.42: Energy Flows for the Summer season

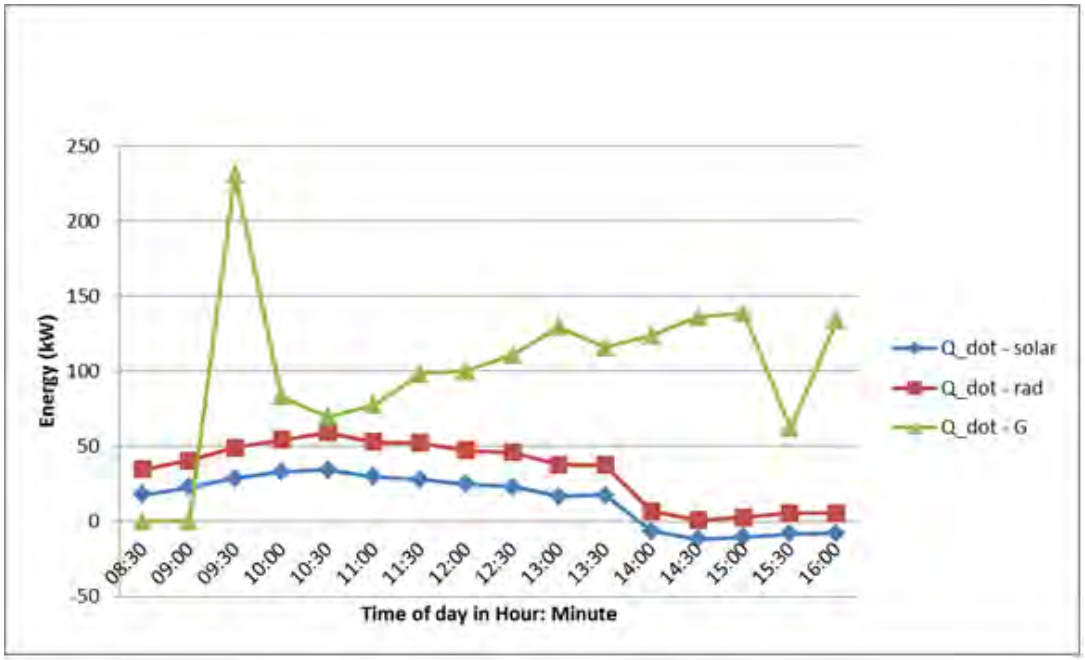

Figure 8.43: Energy Flows for the Autumn season

Figure 8.43 and 8.44 demonstrates that the chiller can be operational even if there is a lack of solar radiation incident as seen from 14:00 onwards. The Hot water storage tank effectively stores more than twice the amount of solar thermal energy incident on the collectors most of the time.

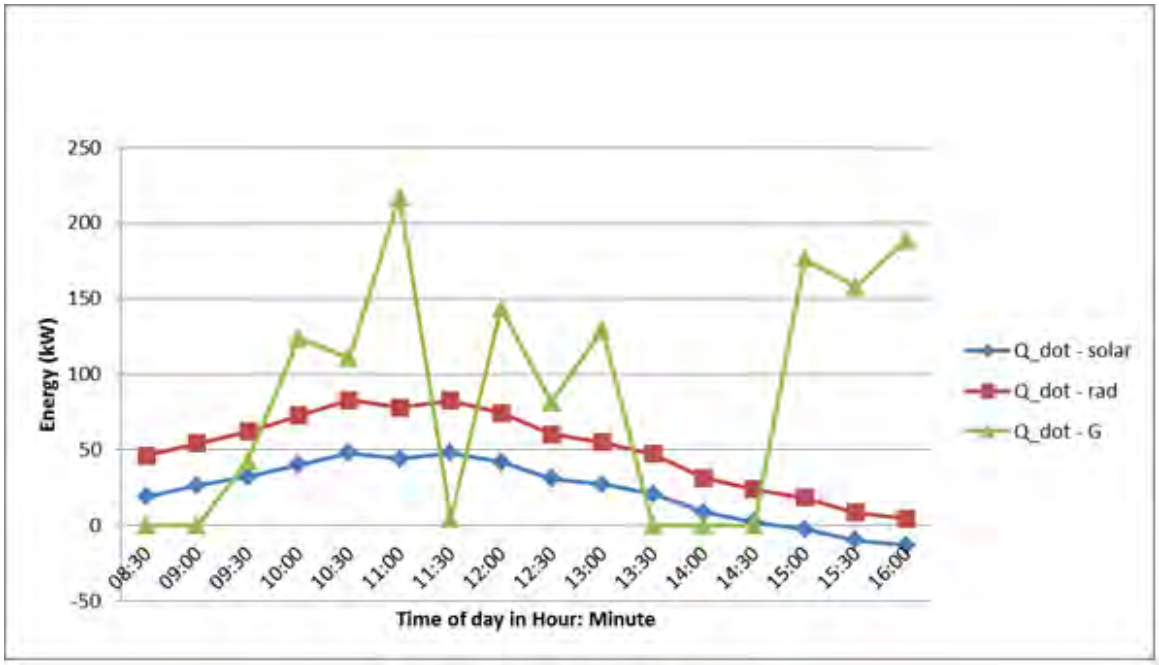

Figure 8.44: Energy Flows for the Winter season

The effectiveness of the hot water storage tank can be seen by the calculation given in Equation 8.12:

$$\varepsilon_{tank} = \frac{\dot{Q}_G}{\dot{Q}_{rad}} \quad \text{..... (Equation 8.12)}$$

Where:

ε_{tank} Effectiveness of the tank [-]

$\dot{Q}_G$ Energy used by the generator of the chiller (kW)

$\dot{Q}_{rad}$ Energy of solar radiation incident on the solar thermal collectors (kW)

The trend of the effectiveness of the Hot water storage tank for the four seasons can be seen in Figure 8.45. The Hot water storage tank can deliver more than five times of the quantity of energy incident from solar radiation.

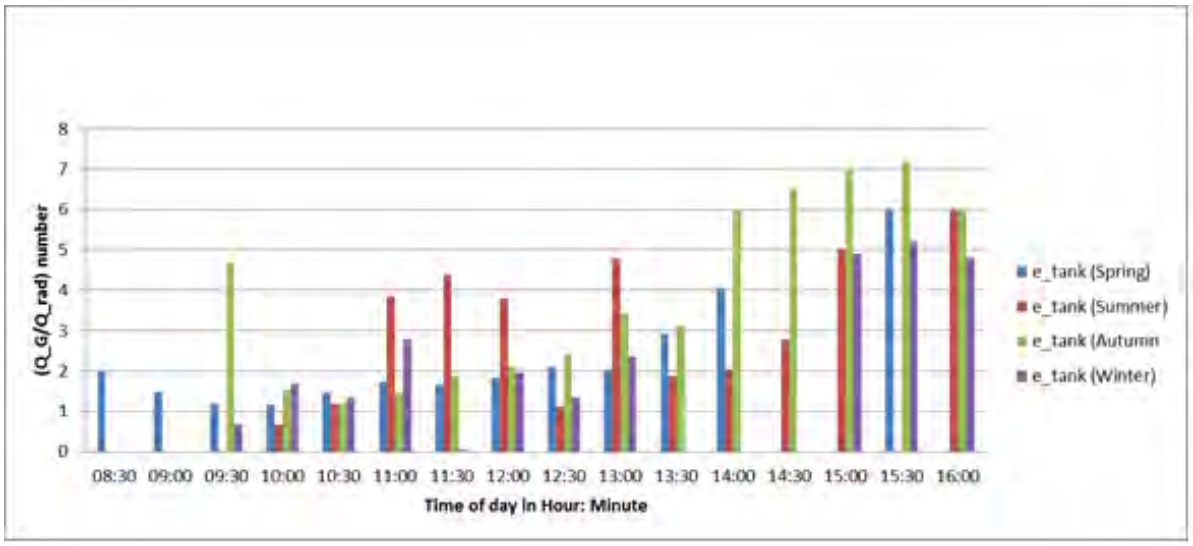

Figure 8.45: Effectiveness of the Hot water Storage tank

The Air conditioning and Solar Collector Efficiency have been investigated and their results have been discussed. The Feasibility analysis will contain the summary of the investigation.

CHAPTER 9: FEASIBILITY ANALYSIS

This Chapter presents the feasibility analysis of the study of the Solar- assisted Absorption Cooling system at Pretoria's Netcare Moot Hospital in terms of the air conditioning efficiency for the South African Climate and the return on investment for the system.

9.1 Feasibility Analysis Model

Due to South Africa having one of the lowest electricity cost in the world [76], the payback period is longer than in other countries; however this will soon change as electricity tariffs become higher due to the current energy crisis prevailing with Eskom. Refer below to Table 9.1 for cost evaluation model.

Table 9.1: Cost Evaluation Model (towards a return on investment analysis)

Required output	**Procedures/actions to achieve output**
1. State approximate capital and installation cost of the solar-assisted absorption cooling plant being tested.	Calculate capital cost of the entire system and its installation and cost of tests and relevant certificates for the system.
2. State capital and installation cost for an R134a compressor driven chiller type HVAC system of about the same cooling capacity as the absorption chiller system.	State capital and installation cost of the electric chiller that can deliver approximately the same cooling capacity as the electric chiller used at Pretoria's Netcare Moot Hospital.
3. State and compare maintenance and running costs of both absorption and compressor driven HVAC systems.	Investigate existing systems and draw up a cost analysis for both system types- compressor and absorption driven.
4. Comparison of costs for the absorption chiller HVAC system and the R134a compressor driven chiller HVAC system.	Compare costs calculated in the second and third outputs in this model.
5. Calculate a return on investment for the absorption chiller HVAC systems (including capital and/or installation costs).	Ascertain electricity tariffs and calculate a return on investment.

The model in Table 9.1 gives the approach to the cost evaluation; however, the feasibility analysis will also include the air conditioning efficiency performance for the South African Climate.

9.2 Air Conditioning Efficiency

The Coefficient of Performance of the absorption process was fully investigated in Chapter 8.2 of this study for all seasons of the year in Pretoria, South Africa for a solar-assisted absorption cooling system of 35kW cooling capacity installed at Pretoria's Netcare Moot Hospital. The system employed a single effect, LiBr/H_2O Yazaki Chiller using hot water from solar thermal energy captured by 52 evacuated tube collectors.

Figure 8.4 shows the COP of the absorption cooling process to be above the COP of 0.7 calculated from the data given in the specification sheet of the Yazaki chiller. The factors determining and affecting the COP were also investigated. These factors include the chilled water supply and return temperatures, together with their flow rates. The difference between the specified flow rates and the actual flow rates are shown in Table 9.2 and this is the reason for the high COP achieved.

Table 9.2: Difference between specified and actual flow rates of chilled water

Season	Spring	Summer	Autumn	Winter
Specified flow rate of chilled water (l/s)	1.53	1.53	1.53	1.53
Actual flow rate of chilled water (l/s)	22	30	32	15

The next important factor investigated was the solar radiation which generated the heat medium temperatures which are also observed together with the flow rates. The solar collectors capturing the solar radiation and the Hot water tank storing the solar radiation were also investigated in Chapter 8.3. Another factor that was vital for the success of the absorption process was the cooling water supply and return temperatures which was also presented with their flow rates. The absorption cycle depends on rejection of heat to the cooling towers. The heat balance for the chiller was done and the cooling output was found to be much larger than the cooling output given for the heat balance in the Yazaki specification sheet.

The relationship between the COP of the absorption process and the generator inlet temperatures was investigated on the scale of heat rejected to the cooling water. This showed a relationship of direct proportion. The COP of absorption was also found to be adversely affected by the increase in cooling water inlet temperatures. The maximum or theoretical COP of the absorption process was shown for various conditions of ambient and generator inlet temperatures for the rated flow rates given in the Yazaki Specification sheet. The electrical COP was given as well to demonstrate that almost no electrical energy is required to produce the cooling effect. The actual performance of the absorption

chiller for South African climate comfortably satisfied the manufacturer's specifications and thus it is feasible in terms of air conditioning (technology) efficiency for this climate.

9.3 Capital Cost

The capital cost of the Solar-assisted absorption cooling plant that was installed at the Pretoria Netcare Moot Hospital to share the daytime cooling load (produce chilled water at 7 °C to a cold storage buffer tank) can be seen in Table 9.3.

Table 9.3: Capital Cost of Solar-assisted absorption cooling plant

Component	**Quantity**	**Cost (excluding V.A.T)**
Chiller	1	R 196 396.27
Solar Collectors	40 U-pipe and 12 Heat pipe	R 275 693.60
Hot Water Storage Tanks	2	R 234 000.00
Open Circuit Cooling Towers with Water Treatment	1	R 80 000.00
PlantVisor Pro (controllers, sensors, visual display panels, hardware and software)	1 system	R 115 000.00
Miscellaneous (expansion tank, piping, pumps, variable speed drives, framework for components)	Various	R 180 000.00
TOTAL (excluding V.A.T)	N/A	R1 137 353.87
GRAND TOTAL (including VAT)	N/A	R1 296 583.41

Just one of the two hot water storage tanks was used to store the solar thermal energy captured by the solar collectors. The installation costs are included in the price of the equipment listed in Table 9.3. The cost of AquaCIAT2 electric chiller (LDH) series, which is air cooled, delivering a cooling capacity of 48kW = R 120 000.00.

The cost of the solar-assisted absorption cooling system is therefore about 10.8 times more than that of the electric chiller.

9.4 Maintenance Cost

The maintenance activities of the absorption chiller involve maintaining the vacuum inside the heat exchanger shells and removing the non-condensable gases. There are no moving parts except a 0.5kW

pump used to circulate the fluid. The functions of the Yazaki absorption chiller depend on the in-built microprocessor and the associated controls and devices. The maintenance can be done by a technician and the pump used to remove the air from the system can be bought as a once off item.

The annual maintenance costs required for the electric chiller consists of the service cost of R 5036.96 and a running maintenance cost of R 6 255.41 according to the HVAC plant manager of Pretoria Moot Hospital.

9.5 Operating Cost

The operational cost of the chillers refers to the cost of the power used to run them to produce the cooling required. The operation of the Yazaki absorption chiller was from 08:00 to 17:00 and the cost to produce this cooling was calculated based on tariffs for the year 2010/2011 used for Pretoria's Netcare Moot Hospital. The cooling delivered by the Yazaki Absorption chiller during its operation was then used to calculate the power the AquaCIAT Electric chiller will require in Electrical energy (kWhs) to produce the same cooling. This can be seen in Figure 9.1 below.

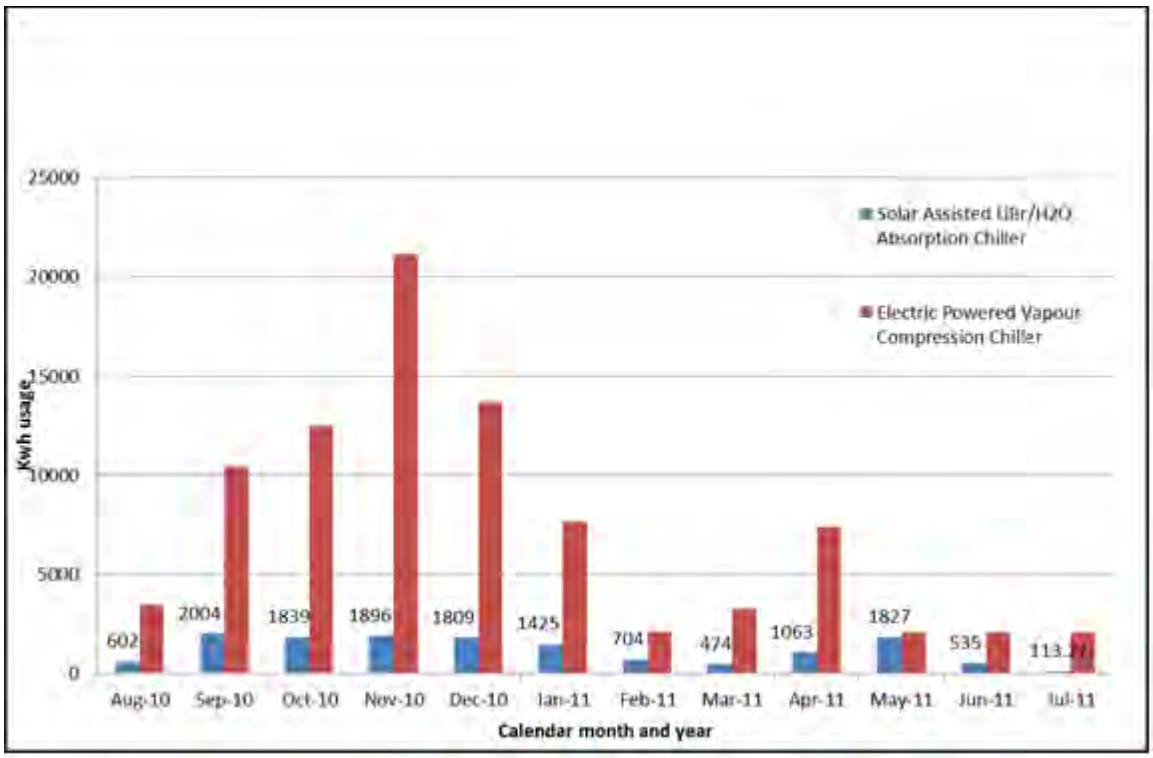

Figure 9.1: Comparison of electrical energy usage of the absorption and electric chiller

The kWh usage for the chillers shown in Figure 9.1 was then used to calculate the operational of the chillers and they are compared in Figure 9.2.

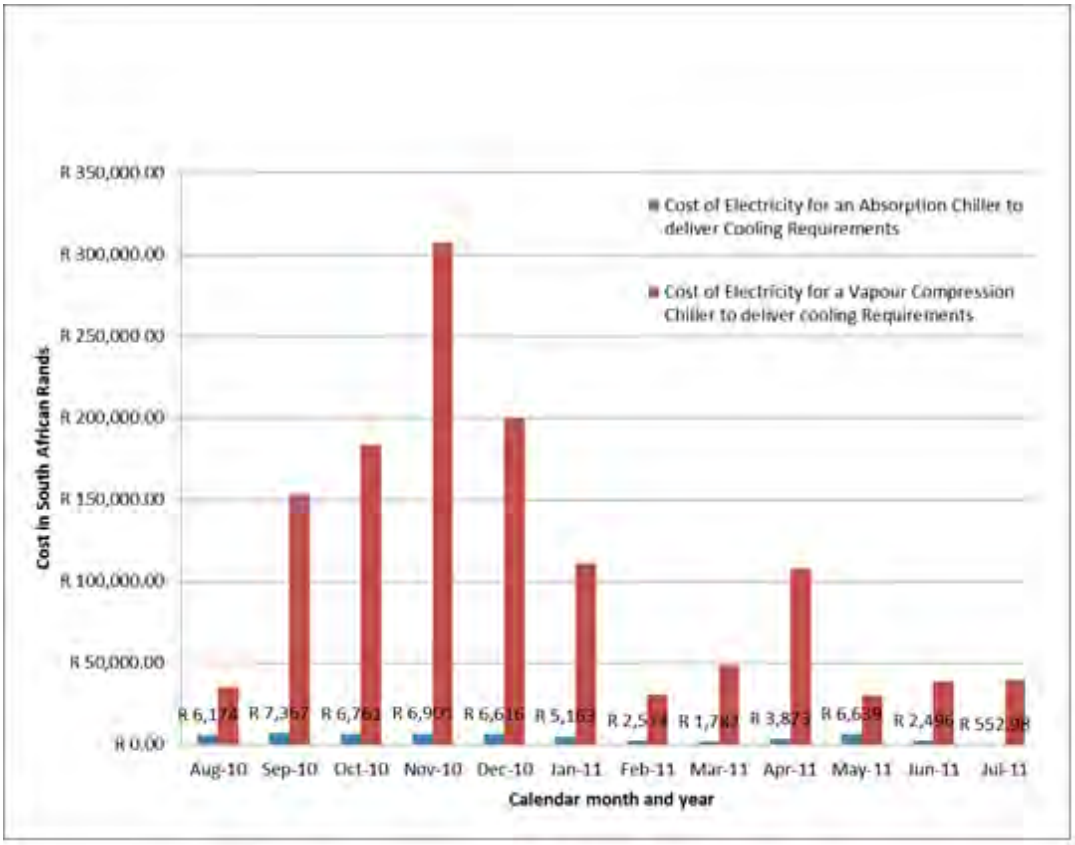

Figure 9.2: Comparison of cost of electricity used by the absorption and electric chiller

The difference between the costs of electricity to operate the chillers is significantly large with the absorption chiller being much cheaper to operate than the electric chiller in term of the cost of electricity. Their percentage differences in the cost are shown in Figure 9.3. The data represented in Figure 9.3 takes into account the running of the electric chiller at night according to the control logic in Chapter 7.5.

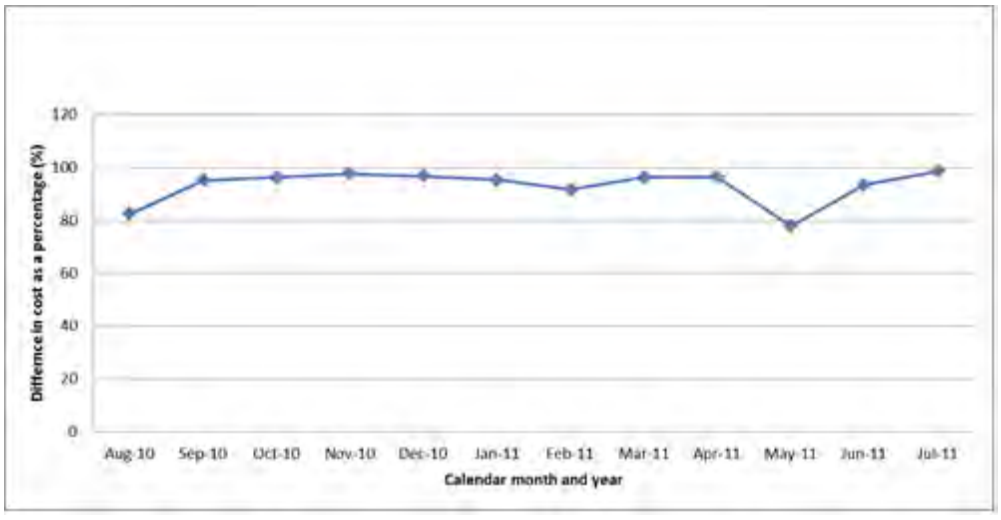

Figure 9.3: Difference in operational cost of the absorption and electric chiller

The difference in the electricity cost is a savings and is between 80% to 100%. A full comparison of cost will be done in the next section where the return on investment is calculated.

9.6 Return on Investment

The Capital, Maintenance and Operational costs of the Absorption and Electric chiller will be compared before a simple return on investment calculation will be done to determine economic feasibility. Table 9.4 shows the comparison of these three costs.

Table 9.4: Cost comparison between Absorption and Electric chiller

Type of chiller	Capital Cost	Maintenance Cost (per annum)	Operational Cost (per annum)
Absorption	R 1 296 583.41	R0	R 56 904.06
Electric	R 120 000.00	R 11 292.37	R 1 246 805.98

The return on investment will be recognized in the savings of the electrical energy costs to operate the chillers. The operational cost of the Electric chiller is significantly higher than the absorption chiller operational cost. The Table 9.5 following shows the cost savings per annum. The electricity tariffs are increased by 25% per annum and the maintenance cost at 7% per annum.

Table 9.5: Cost savings per annum

	Year 1 (operational cost)	Year 1 (maintenance cost)	Year 2 (operational cost)	Year 2 (maintenance cost)
Absorption	R 56 904.06	R0	R 71 130.08	R0
Electric	R 1 246 805.98	R 11 292.37	R 1 608 423.97	R 12 082.84
Savings	R 1 189 901.92	R 11 292.37	R 1 537 293.89	R 12 082.84

It can be seen from Table 9.5 that a payback of just over a year (13 months) can be achievable.

CHAPTER 10: CONCLUSION AND RECOMMENDATIONS

10.1 Feasibility Analysis Evaluation

The feasibility analysis of this study set out to investigate the air conditioning efficiency of a solar-assisted absorption cooling system and the economic feasibility in terms of its payback period. The COP of the absorption process was specified to be between 0.55 and 0.75; however, according to Figure 8.4 in Chapter 8, the COP calculated exceeded the specification, by increasing the flow rate of the chilled water and cooling water. The various factors that affected the COP was also investigated including the chilled water, cooling water and hot water supply and return temperatures and flow rates. It was found that in terms of air conditioning efficiency, the solar-assisted absorption cooling process using $LiBr/H_2O$ is feasible as it had performed above the manufacturer's (Yazaki) specification. The economic feasibility in Chapter 9 showed a payback period of 13 months which is attractive. Chapter 7 provided all the technical details and control operation of the plant.

10.2 Relation to Aims and Objectives

The aims and objectives of this study stated in Chapter 1 have been achieved. Actual testing was done on a solar-assisted absorption cooling plant at Pretoria's Netcare Moot Hospital. The feasibility has been assessed in Chapter 9 and summarized in Chapter 10.1. With a payback period of 13 months and performance parameters that exceed the expectations of the specification, this type of cooling system is more economical than the Electric chiller based on vapour compression. The savings of between 80 and 100% monthly on energy has also exceeded the targeted aim of at least 50%. This study has confirmed by experimental analysis that the Solar-assisted Absorption Cooling system is feasible in terms of air conditioning performance and cost for South Africa.

10.3 Recommendations

It has been observed that the chiller cycle operation, even though based on the parameters such as the heat medium inlet temperature programmed into the controller, it is over-ridden by the time schedule to operate between 08:00 and 17:00. This operation constraint should be released to realize greater energy savings. It has also been observed that the sections in the middle and bottom end of the stratified Hot water storage tank are often not used to supply the chiller. It could be that the solar water collectors and storage tank capacities have been oversized for the chiller's cooling capacity as most of the thermal heat in the water does not get utilized. It is recommended that a more accurate study be undertaken to correctly size the solar water collectors and hot water storage tank.

REFERENCES

[1] Joseph J.S., Inambao F.L., "*Utilizing Solar Energy for Air Conditioning*", Botswana Institution of Engineers 12th Biennial Conference, 5th September 2011, pp 272-276.

[2] Fulloy L., "*Study of a Solar Cooling Plant using Absorption Chiller*", September 2010, Institut National des Sciences Appliquées de Lyon (INSA de Lyon), pp .

[3] Bekker B., Carew P., "*Reducing Energy Consumption by Designing for Chiller Efficiency*", CLIMA 2010 - 10th REHVA World Congress on Sustainable Energy Use in Building, Antalya, Turkey, May 2010.

[4] http://en.wikipedia.org/wiki/Eskom#cite_note-4, (accessed 20/10/2012).

[5] Department of Minerals and Energy (DME) Republic of South Africa, "*Assessment Study of the Energy Efficiency Accord*", Final Report, November 2008.

[6] Shahata A.I., Aboelazm M.M., Elsafty A.F., "*Energy and Exergy Analysis for single and parallel flow double effect Water-Lithium Bromide Vapour Absorption Systems*", International Journal Of Science And Technology, Volume 2, No. 2, February 2012, ISSN 2224-3577.

[7] Saravanan R., Maiya M., "*Thermodynamic comparison of water based working fluid Combinations for a vapour absorption refrigeration system*", Applied Thermal Engineering, 1998.

[8] Nunez T., "*Design – State of the Art, SOLATERM Expert Mission*", Fraunhofer Institut Solare Energiesysteme (ISE), December 2008.

[9] Trygg L, Amiri S, "*European perspective on absorption cooling in a combined heat and power system – A case study of energy utility and industries in Sweden*", Elsevier, Applied Energy 84 (2007), pp 1320.

[10] Haw L. C, Sopian K, Sulaiman Y, "*An overview of Solar-Assisted Air-Conditioning System Application in Small Office Buildings in Malaysia*", Proceedings of the 4th IASME/WSEAS International Conference on Energy & Environment (EE'09), 2009, pp 244.

[11] Papaefthimiou V. D., Karampinos D. C., Rogdakis E.D., "*A detailed analysis of water-vapour absorption in LiBr/H_2O solution on a cooled horizontal tube*", Journal of Applied Thermal Engineering 26 (2006), pp 2095.

[12] Hunkin T., "*The Secret Life of the Refrigerator*", in the Television series "The Secret Life of Machines", directed by Andrew Snell (1988).

[13] Erickson, D. "*The Absorption Process*", Energy Concepts Company, viewed at www.energy-concepts.com, (accessed 17/12/2012).

[14] Dutil Y. and Rousse D. "*A review of active Solar Cooling Technologies*", Proceedings of 3rd International Conference, PALENC 2010, October 2010.

[15] Miller, E.B., *The Development of Silica Gel, Refrigerating Engineering*—The American Society of Refrigerating Engineers, 1929.

[16] Midgley, Thomas, jr., US Pat. 1 833 847 and Midgley, Thomas, jr. (1934) US Pat 1 968 049, 1931.

[17] Bichowsky, Francis, US Pat. 1 992 177, Bichowsky, Francis, US Pat. 2 083 002 and 2 090 466, Bichowsky, Francis 1938 US Pat. 2 108 248, Bichowsky, F. R., Kelley, G. A., "*Concentrated Solutions in Air- Conditioning*", *I&EC*, 27(8), 1935, 1937, 1935, pp. 879 – 882.

[18] Berestneff. Alexis, US Pat.s 2 550 665 and 2 565 943, 1951.

[19] Zigler F., *Recent developments and future prospects of Sorption heat pump systems*. International Journal of Thermals 38, 1999, pp. 191–208.

[20] Kapur, J.C., *A report on the utilization of solar energy for refrigeration and air conditioning application*. Sol Energy 4, 1960, pp. 39–47.

[21] Farber, E.A., Flanigan, F.M., Lopez, L, Polifka, R.W., Operation and performance of the University of Florida solar air-conditioning system. Sol Energy 10, 1966, pp. 91–95.

[22] Nakahara N, Miyakawa Y, Yamamoto M., *Experimental study on house cooling and heating with solar energy using flat plate collector.* Sol Energy 19, 1977, pp. 657–662.

[23] Henning, H.-M., Albers J., Decision scheme for the selection of the appropriate technology using solar thermal air-conditioning, guideline document, *IEA solar heating and cooling, task 25—solar-assisted air conditioning of buildings*, http://www.iea-shc-task25.org/english/hps6/pdf/Solar-Air-Conditioning-Decision-Scheme.pdf., 2004.

[24] Lamp, P., Ziegler, F., *European research on solar-assisted air conditioning*. International Journal of Refrigeration 21, 1998, pp. 89–99.

[25] Stephan K, Krauss R., *Regulated CFCs and their alternatives*. In: Meunier F, editor. Proceedings: Solid Refrigeration Symposium. Paris: Ministere de la Recherche et de l'Espace, 1992, pp. 32–43.

[26] Balaras, A. et al., *Solar air conditioning in Europe—an overview*, Renewable and Sustainable Energy Reviews, 11, 2007, pp. 299–314.

[27] Alghoul, M.A., Sulaiman, M.Y., Azmi, B.Z., Abd. Wahab, M., *Advances on multi-purpose solar adsorption systems for domestic refrigeration and water heating*, Applied Thermal Engineering 27, 2007 pp. 813–822.

[28] De Lucas A., Donate M., Molero C., Villasenor J., Rodriguez J. F., "*Performance evaluation and simulation of a new absorbent for an absorption refrigeration system*", International Journal of Refrigeration 27 (2004), pp. 324 - 330.

[29] Wang, R.Z., Zhai, X. Q., "*Development of solar thermal technologies in China*", Energy 35 (2010), pp. 4407 - 4416.

[30] Ruicheng Z., "*Development, direction and countermeasure for the utilization of solar*

buildings", Construction Science and Technology 2006, 23: pp. 54 - 58.

[31] Jishou Z., "*Technic approach and development strategy of solar buildings*", Solar Energy 2004, 04: pp. 22 - 23.

[32] Voss K.., "*Solar Energy in building renovation-results and experience of international demonstration buildings*", Energy and Buildings 2000:3(3): pp. 291 - 302.

[33] Hassan M. M., Beliveau Y., "*Design, Construction and performance prediction of integrated solar roof collectors using finite element analysis*", Construction and Building Materials 2007:21(5): pp. 1069 - 1078.

[34] Matuska T., Sourek B., *Facade solar collectors*", Solar Energy 2006:80(11) 1443 - 1452

[35] Chow T. T., He W., Ji J., "*An experimental study of façade-integrated photovoltaic/water-heating system*", Applied Thermal Engineering 2007:27(1): pp. 37-45.

[36] Wei X., Yanhui L., Han Y., "*Implementation of integration of solar water heaters with buildings*", Construction Science and Technology 2005:17: pp. 18-19.

[37] Schuler A., Roecker C., Boudaden J., Oelhafen P., Scartezzini J.L., "*Potential of quarterwave interference stacks for coloured thermal solar collectors*", Solar Energy 2005:79(2): pp. 122-130.

[38] Tripanagnostopoulos Y., Souliotis M., Npusia T.H., "*Solar Collectors with coloured absorbers*", Solar Energy 2000:68(4): pp. 343-356.

[39] Zhai X.Q., Wang R, Z., "*Experiences on solar heating and cooling in China*", Renewable and Sustainable Energy Reviews 2008:12(4): pp. 1110-1128.

[40] Dalenback J. O., "*Solar Energy in building renovation*", Energy and Buildings 1996:24(1): pp. 39-50.

[41] Zinian H., Ning Z., Fang L., Shuling G., "*Design and performance of a solar absorption air conditioning and heat supply system*." Acta Energiae Solaris Sinica 1999:20(3): pp. 239-243.

[42] Jianhong L., Weibing M., Qing J., Zhibing H., Wenhui X., "*100kW Solar-powered air conditioning system*" Acta Energiae Solaris Sinica 1999:20(3): pp. 239-243.

[43] Jianhong L., Ning B., Weibing M., Donghai W., Xianhang L., Xinian J., "*Large Solar powered air conditioning heat pump system*" Acta Energiae Solaris Sinica 2006:27(2): pp. 152-158.

[44] Jiangong H., Guangming X., Lei F., "*Moderate and high temperature solar collectors and solar heating and cooling conference of China*", report no. 10-7. http://www.solar.sjtu.edu.cn>:2006.

[45] Epp B, "*Australia: Country's largest Solar Cooling System on Hospital*", http://www.solarthermalworld.org/content/australia-countrys-largest-solar-cooling-system-hospital, 13 September 2011.

[46] Sustainability Victoria, "*Solar-Assisted Cooling Project*", sustainability.vic.gov.au, March 2011

[47] WSP Lincolne Scott, "*Echuca Regional Hospital – Solar Cooling Project Q and A factsheet*", http://www.erh.org.au/solar-chiller.html, April 2011.

[48] Romanel C, Duarte Pereira E, Kissel J, Teixeira M. A., Orlando A. F, Leal J.E., "*Technical and Economic Assessment of Medium Sized Solar-Assisted Air-Conditioning in Brazil*", Dissertation presented to the Postgraduate Program in Urban and Environmental Engineering of the Departamento de Engenharia Civil do Centro Técnico Científico da PUC-Rio, as partial fulfillment of the requirements for the degree of Mestre, 25/01/2010.

[49] European Solar Thermal Industry Federation, "*Solar-Assisted Cooling*" - Key Issues for Renewable Heat in Europe (K4RES-H), August 2006.

[50] Balaras C. A., Grossman G., Henning H. M., Infante C.A., etc., "*Solar Air Conditioning in Europe – an Overview*", February 2005.

[51] Department of Minerals and Energy, "*Energy Outlook for South Africa: 2002*", Eskom Energy Research Institute, University of Cape Town.

[52] Statistics on the web: http://www.iea.org/stats/index.asp (Accessed July 2012).

[53] Department of Minerals and Energy (DME) South Africa, "*Energy Efficiency Strategy of the Republic of South Africa, March 2005*", March 2005.

[54] Department of Minerals and Energy (DME) South Africa, "*White Paper on Renewable Energy 2003*", 2003.

[55] Built Africa Holdings, "*The Current Energy Security Challenge and the Opportunity for Solar Water Heating*", DBSA/DME Workshop on Solar Water Heating, 13 February 2009.

[56] http://en.wikipedia.org/wiki/File:HeatIsland_Kanto_en.png (Accessed 28/07/2012).

[57] Perez-Lombard L., Ortiz J., Pout C., "*A review on buildings energy consumption information*", on 12th March 2007 downloaded from www.sciencedirect.com.

[58] Henning H.M., "*Solar Cooling and Air conditioning*", Renewable Energy Week, Fraunhofer-ISE, Brussels, January/ February 2007, IEA.

[59] Adams S., "*South African Consumer Attitudes towards Domestic Solar Power Systems*", University of Pretoria, 1st August 2011, page 5.

[60] Hoffman, A Pentair Company, "*White Paper: Apply Solar Shielding to Lessen Heat Load, Protect Enclosure Components*", downloaded from http://www.automation.com (Accessed 12/11/2012).

[61] Crepinsek Z., Goricanec D., Krope J., "*Comparison of the performances of absorption refrigeration cycles*", WSEAS Transactions on Heat and Mass Transfer, Issue 3, Volume 4, July 2009.

[62] Kevin D. Rafferty, P.E. "*Chapter 13, Absorption Refigeration*", Geo-Heat Center Klamath Falls. Viewed at http://geoheat.oit.edu (Accessed 30/09/2010).

[63] Hwang Y., "*Heat Driven Cooling: Absorption Closed Cycles and Machines*", University of Maryland, January 2010, viewed at http://www.iea-shc.org/task38/events accessed 28/09/2010.

[64] Moran M.J., Shapiro H.N., *"Fundamentals of Engineering Thermodynamics"*, sixth edition,

USA, John Wiley and Sons, 2010.

[65] Incropera F.P., DeWitt D.P., Bergman T.L., Lavine A.S., "*Fundamentals of Heat and Mass Transfer*", sixth edition, USA, John Wiley and Sons, 2007.

[66] Eicker U., "*Solar Technologies for Buildings*", Germany, 2001.

[67] Department of Energy, "*2008 Buildings Energy Data Book*", USA, March 2009.

[68] Dobson R.T., "*Solar Water Heating Theory*", Stellenbosch University and SAHPA (South African Heat Pipe Association), 24/10/2008 viewed at http://www.crses.sun.ac.za, (Accessed 22/10/2010).

[69] Adapted from "*Indoor Air Handlers*", 2010 McQuay Products catalogue, downloaded from http://www.mcquay.com/mcquaybiz/DocumentStorage accessed 12/11/2010.

[70] http://www.iklimnet.com/expert_hvac/ahu_energy.html "*Energy efficiency and Air Handling Units*" from "Ask the HVAC man", accessed 22/11/2010.

[71] http://en.wikipedia.org/wiki/Chaos_theory accessed 12/11/2010.

[72] Rosaler, Robert C. "*Cooling Towers: Design and Operation Considerations*" compiled using: The Standard Handbook of Plant Engineering, 2nd Edition, McGraw-Hill, New York, 1995 and Perry's Chemical Engineers' Handbook, 6th Edition, Green, Don W. et al, New York, McGraw-Hill, 1984.

[73] Cooling Tower Institute, *"Cooling Tower Performance Curves"* published in 1967

[74] Cengel Y. A., Boles M., "*Thermodynamics: An Engineering Approach*", Fourth Edition, New York, McGraw-Hill Higher Education, 2006.

[75] Yazaki, "*WFC-SC(H)10, 20 & 30 Version 8-1 Chiller and Chiller Heater – Specifications*", 2010, pp. 7-14.

[76] Statistics South Africa*, "Africa Symposia on Statistical Development"*, http://www.statssa.gov.za, accessed 20/03/2013.

APPENDIX A

Appendix A1: Published conference paper

Joseph J.S. and Inambao F.L., "Utilizing Solar Energy for Air Conditioning", Botswana Institution of Engineers (BIE), 12th Biennial Conference, 3rd -5th September 2011, pp 272-276.

Utilizing Solar Energy for Air Conditioning

Jerusha Joseph[a] and Dr. F.L Inambao[b]

[a,b] University of KwaZulu-Natal, School of Mechanical Engineering, Howard College, Durban, South Africa

Synopsis

The economy of a country describes how a country regulates its money. The availability and sustenance of ingredients that promote, sustain and create economic value are vital to ensure continuity of economic growth. To build up a destroyed economy, one has to address the causes/lack thereof of economic growth. Economic recovery cannot just be viewed from a monetary aspect, but from elements that promote monetary value. Innovation fuels the economy and the basis of the development of any country is to have access to usable energy for its technological processes that make commercial growth possible. One of the most abundant and under-utilized energy sources in Africa is solar energy. Technological development will lead to infrastructures that consume electrical energy and commercial buildings require air conditioning. Innovation first sees opportunity and the need for cooling coupled with the availability of solar energy calls for the harnessing of solar energy for air conditioning. This paper focuses on solar powered air conditioning (HVAC).

Introduction

Economic wellness should be viewed as an enterprise where success depends on efficiency and productivity of all staff and processes. One of the indicators used to measure success of a country's economy is its Gross Domestic Product (GDP). The Gross Domestic Product is calculated as the sum of Consumer Spending, Investment made by Industry, Excess of Exports over Imports and Government Spending. The eligibility and productivity potential of a country's GDP in this case can be measured by the Investment made by industry as these are the assets of the country. In the context of the GDP, Investment made by industry means the purchases made by industry in new productive facilities, or, the process of "buying new capital and putting it to use" (Gambs, John, *Economics and Man*, 1968, p. 168). This includes, for example, buying a new truck, building a new factory, or purchasing new software.

In essence, due to Africa being a third world country, much room is available for economic growth. Growth cannot be made without investment. Investment in industry cannot be made without materials and materials cannot be made without energy and human resources. Energy production should thus be viewed and handled as a life giving source of any economy. Life giving sources are always protected, used sparingly and sought after to ensure continued availability. A country's economic success in raw terms can sometimes be measured by its technological advancements for the purpose of sustenance of a vibrant economy through energy production, its availability and usage. This is evident from figure 1, where the World Energy use is classified into Developed economies and emerging economies.

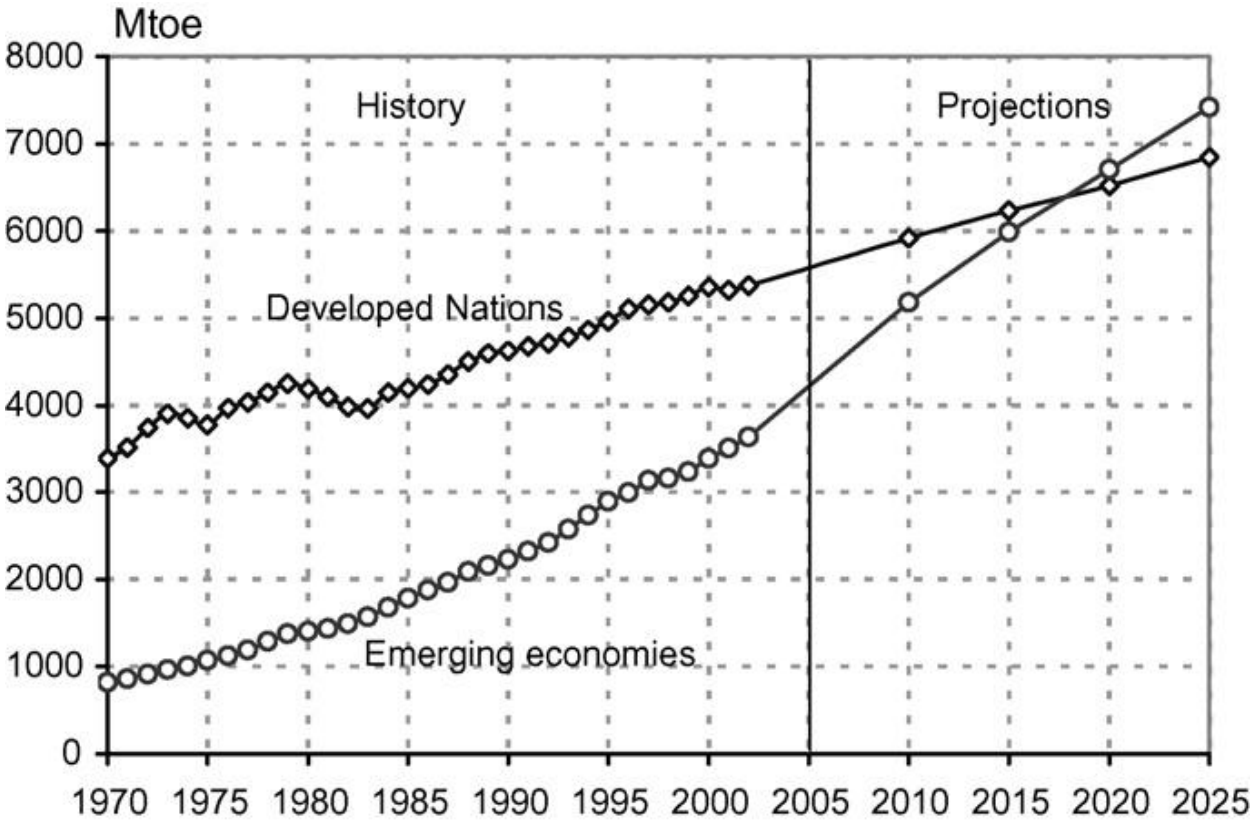

Figure 1: World Energy Use by region ["A review on buildings energy consumption information", by Luis Perez-Lombard (Spain), Jose Ortiz (UK), Christine Pout (UK) on 12th March 2007 downloaded from www.sciencedirect.com]

The characteristics of a first world country, for instance, the United States of America, are industries that it owns and its ability to trade. The physical characteristics of a first world country are the infrastructure like commercial buildings (in our interests) from which trade is facilitated and controlled. These buildings will be consumers of energy and from this one can plan that our future as we climb up the economic ladder will be similar. The statistics for 2006 USA Buildings End Use Energy splits (refer to figure 2) shows that Space heating and cooling contributed 37.5% of energy consumption in majority of the buildings. Similar analysis for Africa is not available presently, however looking at figure 1, one would visualize that Africa is not very far from the statistic shown in figure 2.

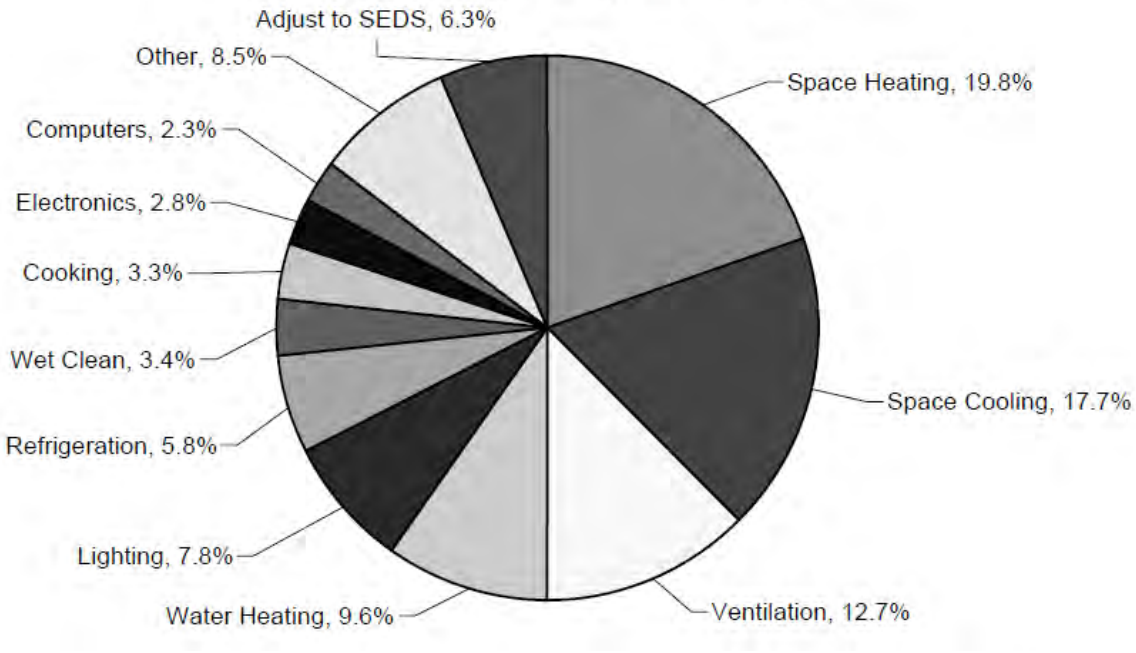

Figure 2: 2006 USA Buildings Energy End-Use splits ["2008 Buildings Energy Data Book", U.S Department of Energy, March 2009]

Among the first world and second world country economies, solar assisted HVAC systems are in use. In 2008, 450 to 500 solar cooling systems were realized worldwide with 400 of these being in Europe. About 60% of these systems use absorption chillers, 11% adsorption chillers and 29% are open systems (Desiccant and Evaporative Cooling Systems). [1]

The total amount of installations shows that this market is under-developed, especially in Africa. However, given our current energy crisis and the potential that exists in terms of solar insolation, this should change more sooner, than later.

For instance, the South African region daily solar radiation average is varies between 4.5 and 6.5 kWh/m^2 and when compared to the United States 3.6 kWh/m^2 and Europe's 2.5 kWh/m^2, the opportunity of the application of solar energy as a renewable resource is far from questionable. Refer to figure 3 to view the solar radiation distribution over the Southern part of Africa.

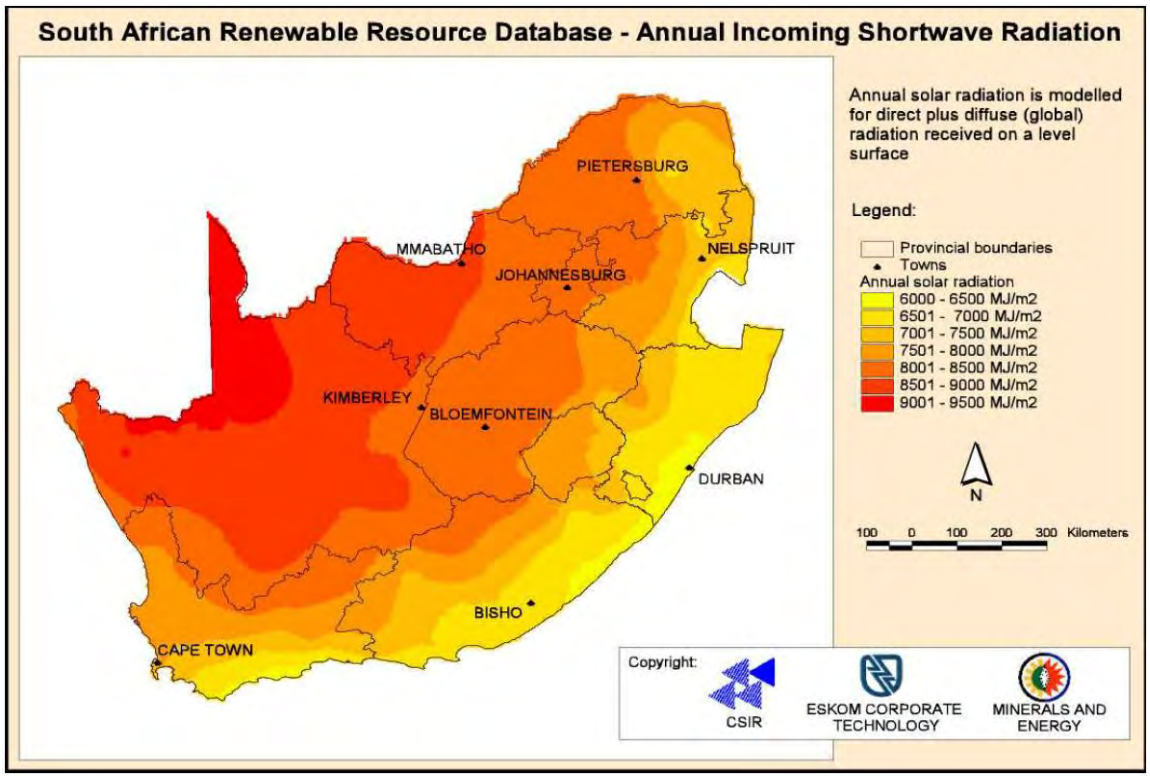

Figure 3: Annual Incoming Shortwave radiation for South African provinces (Eskom, CSIR, Minerals and Energy)

There are many types and forms of solar assisted HVAC systems; however the version discussed here moves away altogether from using a mechanical compression cycle in a compressor, which a energy hog in any air conditioning system to using a vapour absorption technology in the absorption chiller.

Solar Assisted HVAC: Absorption cycle air conditioning

The absorption cycle was invented by Ferdinand Carre when he sought to produce ice with heat input in 1846. The absorption cycle was used much in the 1920s in gas powered refrigerators/ice makers using the principle that absorbing ammonia in water causes the vapour pressure to decrease. This cycle is often viewed as chemical vapour-compression cycle with the compressor replaced by a generator, absorber and liquid pump.

The vapour absorption cycle uses two fluids and some quantity of heat input, rather than the electrical input as in the more familiar vapour compression cycle to achieve air conditioning. Both vapour compression and absorption air conditioning cycles accomplish the removal of heat through the evaporation of refrigerant at a low pressure and the rejection of heat through the condensation of the refrigerant at a higher pressure. The method of creating the pressure difference and circulating the refrigerant is the primary difference between the two cycles.

In the vapour compression cycle (refer to figure 4 and 5 following), a mechanical compressor creates the pressure difference necessary to circulate the refrigerant. The absorption cycle employs a secondary fluid or absorbent to circulate the refrigerant.

When a liquid evaporates, it absorbs heat. This is the principle on which all air conditioning is based. When a liquid condenses, it cools. The heat given up when a liquid condenses is called the latent heat of condensation. The absorbed heat is called the latent heat of evaporation.

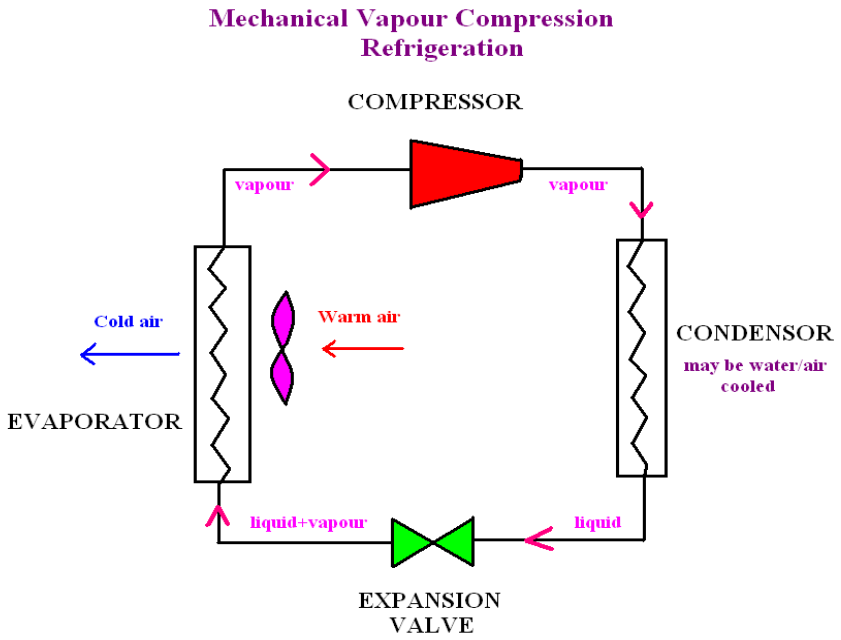

Figure 4: Single Stage Mechanical Vapour Compression Refrigeration

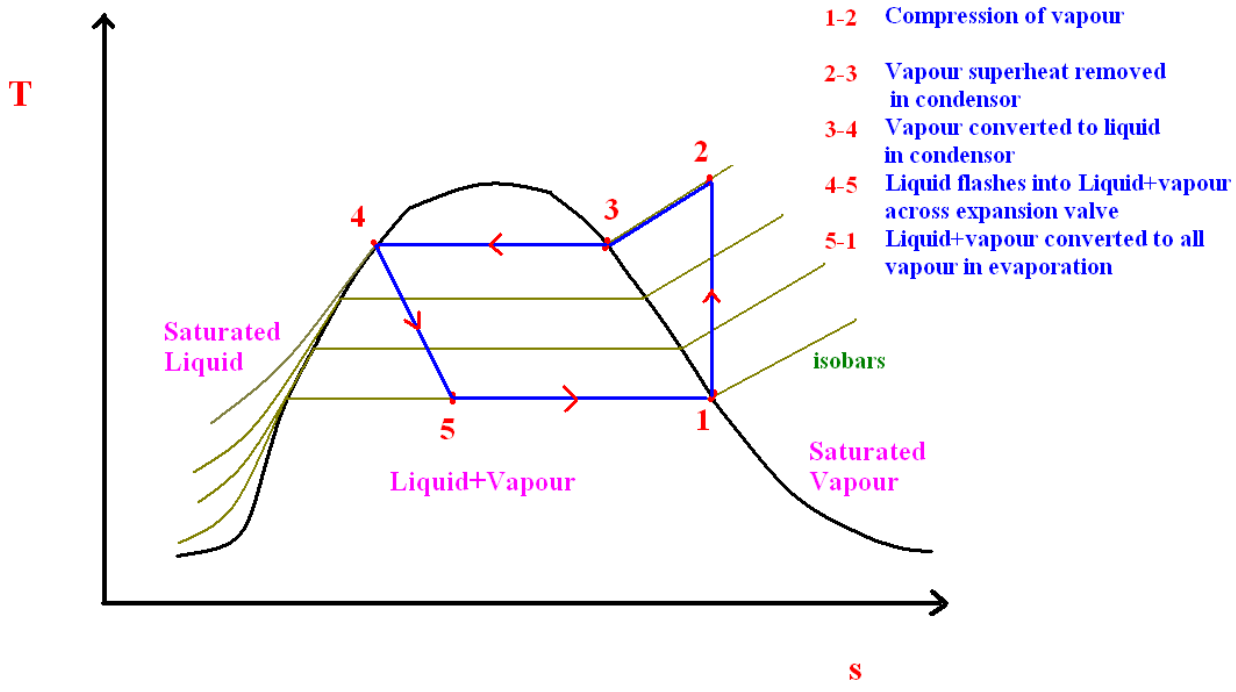

Figure 5: Temperature-Entropy Diagram of mechanical vapour compression cycle

The next principle in air conditioning is that the boiling point of a liquid is related to pressure. When a given body of water becomes hotter, the more it wants to become a gas, however the higher the pressure of the water, the more it wants to condense into a liquid.

Absorption cooling uses the affinity of some pairs of chemicals to dissolve in one another. Some examples are Lithium bromide and water (which will be used in this project), water and ammonia, and so on. The two factors governing this affinity are temperature and the concentration of the solution. The absorption chiller set up is shown in figure 6.

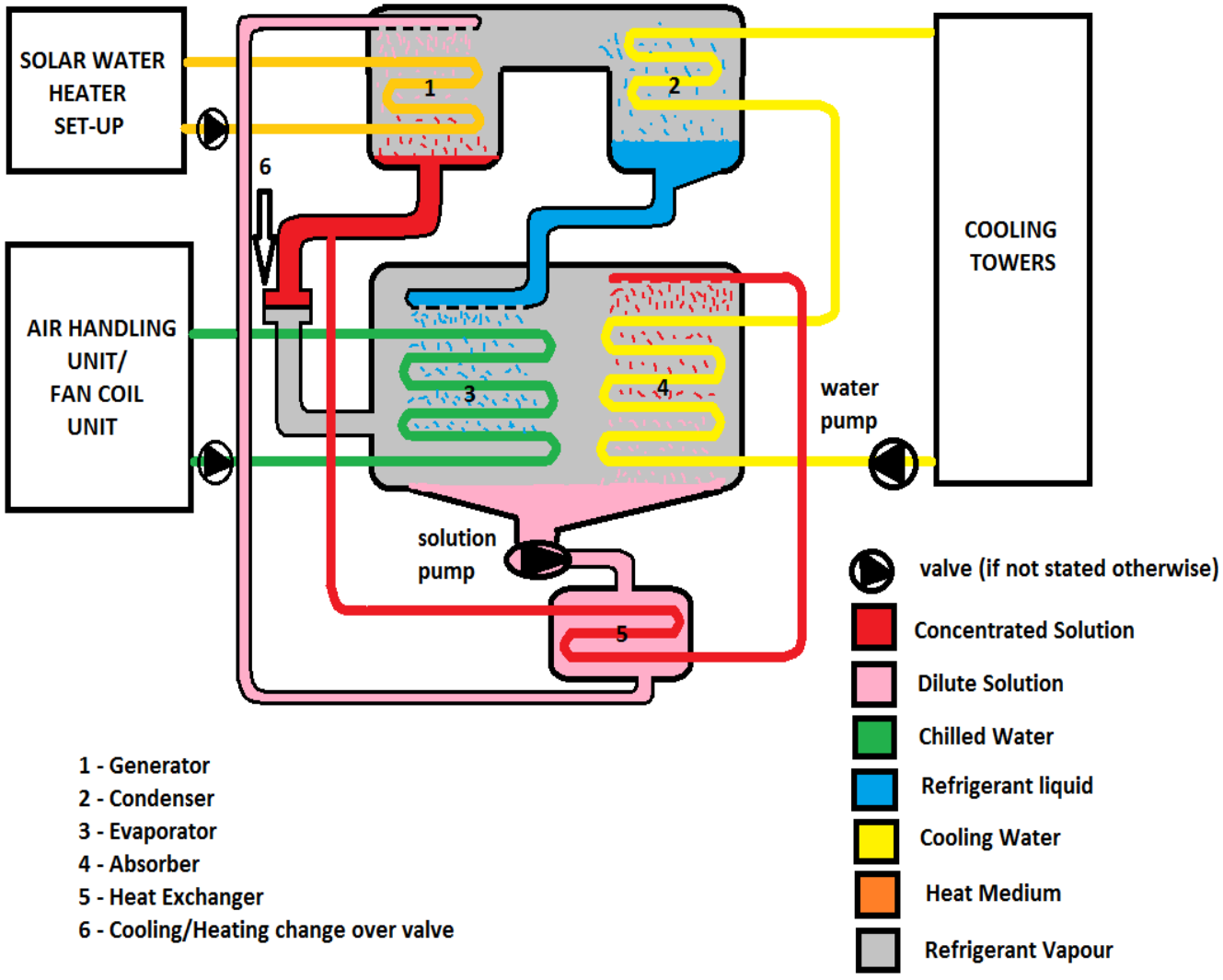

Figure 6: Chiller setup and relation to other components in an HVAC system

The temperature requirements for the cycle fall into the low-to-moderate temperature range, significant potential for electricity savings exist. The process occurs in two vessels or shells. The upper shell contains the generator and condenser and the lower shell, the absorber and evaporator. The heat supplied in the generator section is added to a solution of LiBr/H_20. This heat causes the refrigerant (water or H_20) to be boiled out of the solution in a distillation process.

The water vapour that results passes into the condenser section where a cooling medium is used to condense the vapour back to a liquid state. The water then flows down into the evaporator section where it passes over the heat exchanger containing the fluid to be cooled. By maintaining a very low pressure in the absorber-evaporator shell, the water boils at a very low temperature. [2] Refer to figure 7 for the pressure versus temperature diagram of the absorption cycle.

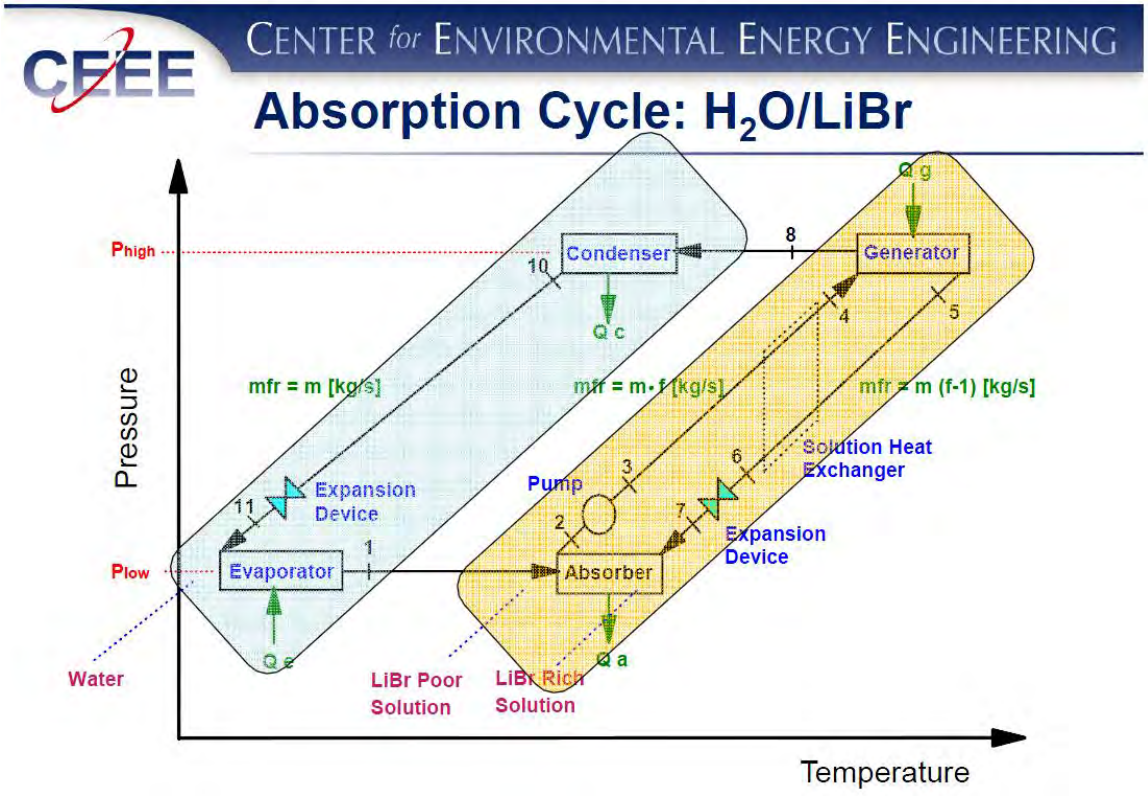

Figure 7: Diagram of Pressure versus Temperature for the absorption cycle ["Heat Driven Cooling: Absorption Closed Cycles and Machines", January 2010 by Yunho Hwang, PhD, University of Maryland viewed at: http://www.iea-shc.org/task38/events accessed 28/09/2010.]

This boiling causes the water to absorb heat from the medium to be cooled, lowering its temperature. Evaporated water then passes into the absorber section where it is mixed with a LiBr/H2O solution that is very low in water content. This strong solution (strong in LiBr) tends to absorb the vapour from the evaporator section to form a weaker solution. This is the absorption process that gives the cycle its name. The weak solution is then pumped to the generator section to repeat the cycle.

The difference between the vapour absorption air conditioning and vapour compression air conditioning is that the work input is different in that the former uses thermal energy as work input and the latter uses compressor energy as work input.

The absorption chiller will be the focus of attention when calculating the air conditioning efficiency. The performance efficiency of the HVAC system is called the coefficient of performance and is calculated according to equation (1). [3]

$$COP_{absorption} = \frac{output}{input} = \frac{Q_L}{Q_{gen} + W_{pump,in}} \cong \frac{Q_L}{Q_{gen}} \quad \text{..... (1)}$$

where Q_L is the energy of the refrigerated space

$W_{pump,in}$ is the work input (from the pump, as there is no compressor work involved)

Q_{gen} is the energy contribution from the generator (which is the solar water heater)

The maximum COP that an absorption system can have is determined by assuming totally reversible conditions, which yields (2)

$$COP_{rev,absorption} = \eta_{th,rev} COP_{R,rev} = \left(1 - \frac{T_o}{T_s}\right)\left(\frac{T_L}{T_o - T_L}\right) \quad \text{..... (2)}$$

Where T_o = thermodynamic temperature of environment

T_L = thermodynamic temperature of refrigerated space

T_s = thermodynamic temperature of heat source

The set up of the absorption chiller in relation to the rest of the air conditioning equipment can be seen in figure 8. The hot water required will be heated by the solar water heater to temperatures ranging from 60 to 90 degrees Celsius. This chiller will then be referred to as being "hot water fired".

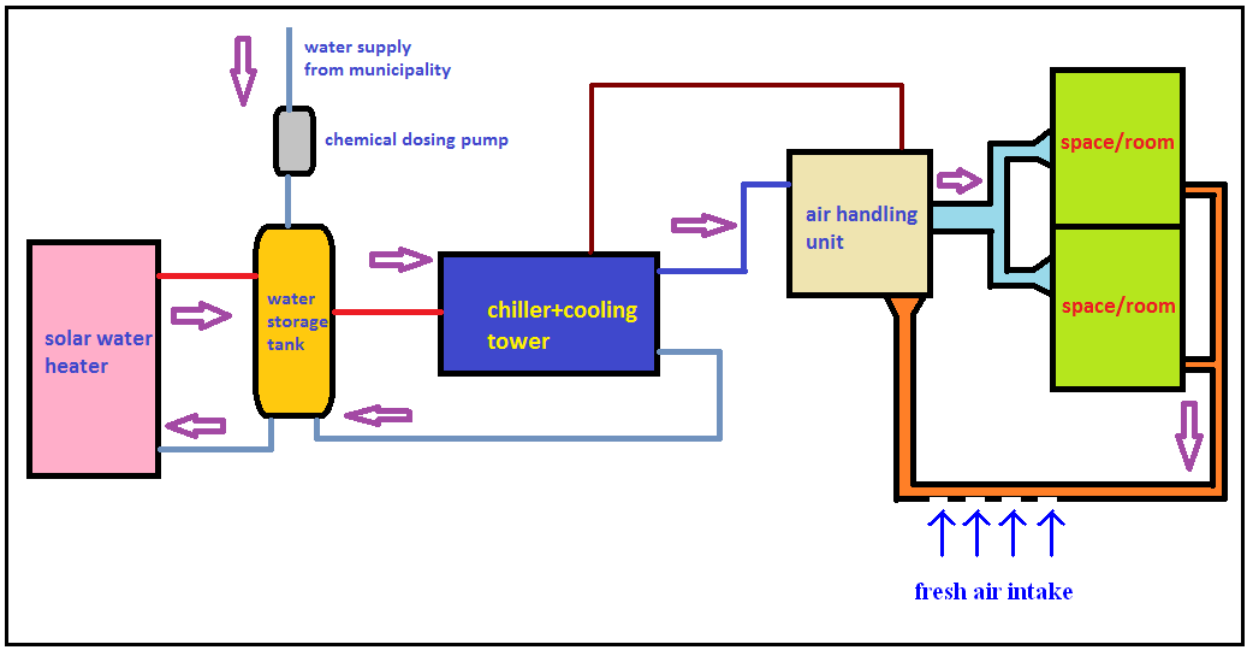

Figure 8: Indication of physical connection between components designed in the HVAC system

Conclusion

If one has to type in "world energy crisis" in an internet search engine, links that all communicate a similar message of key energy resources depletion will be listed. Two centuries ago, the Industrial Age was birthed due to the energy-rich hydrocarbon found in coal which replaced wood as a primary fuel source. This energy stored in coal

provided the power needed by investors and industrialists to energize machinery, process steel and propel steamships. The world's need for energy continued to increase and a hundred years ago, petroleum and natural gas was used as principal fuels. Atomic energy was used about 50 years ago when scientists trapped uranium to fuel nuclear reactors.

This was all well and good, but the definition of non-renewable indicates to us that the supply of these resources will come to an end, now sooner instead of later. This will mean no power, which will mean that our convenient, modern way of life will come to an end. The technological crash will lead to regress of this generation and those that will come after, to the primitive ages. However not all life will come to an end. The earth and its ecosystem will go on living efficiently – if human impact on them is not taken into consideration. Thus it can be confidently said that other forms of energy do exist – and like our discovery of non-renewable energy resources required infrastructure to release, capture and convert the energy into a form usable for our machinery, etc., so will renewable sources of energy require infrastructure to capture/convert this energy.

In 1948, Europe's destroyed economy began recovery due to four factors, i.e. the changes in government policies, growth in world trade, scientific and technological advances and foreign aid. During this period, most modern technologies had not spread to the rest of the world and thus, the opportunities for technological advances were almost endless. In December 2009, Washington, the CEO of the American Chemical Society says to the media that "Technological breakthrough will drive economic recovery. Innovation fuels the economy and science fuels innovation."

References:

[1] "Chilling out in the sun: Solar Cooling" from Renewable Energy World International Magazine, May/June 2010-Volume 13, Issue 3, viewed at www.renewableenergyworld.com

[2] "Chapter 13, Absorption Refrigeration" by Kevin D. Rafferty, P.E. Geo-Heat Center Klamath Falls. Downloaded from http://geoheat.oit.edu on 30/09/2010.

[3] "Thermodynamics: An Engineering Approach", Fourth Edition by Yunus A Cengel, Michael Boles.

APPENDIX B

Appendix B1: General Absorption Cooling System Layout

Appendix B2: Moot Hospital Absorption Plant Roof Layout

Appendix B3: Air Conditioning Equipment Layout

- Flow meter
- Temperature/Pressure release valve
- Pressure gauge
- Expansion tank
- Measure point
- Pressure measurment
- Temperature sensor
- NC / NO – Normally Closed / Open
- Valve
- Motor Valve
- Three-way valve
- Pressure reducing valve
- Non-return valve
- Circulation pump
- Strainer
- Air vent

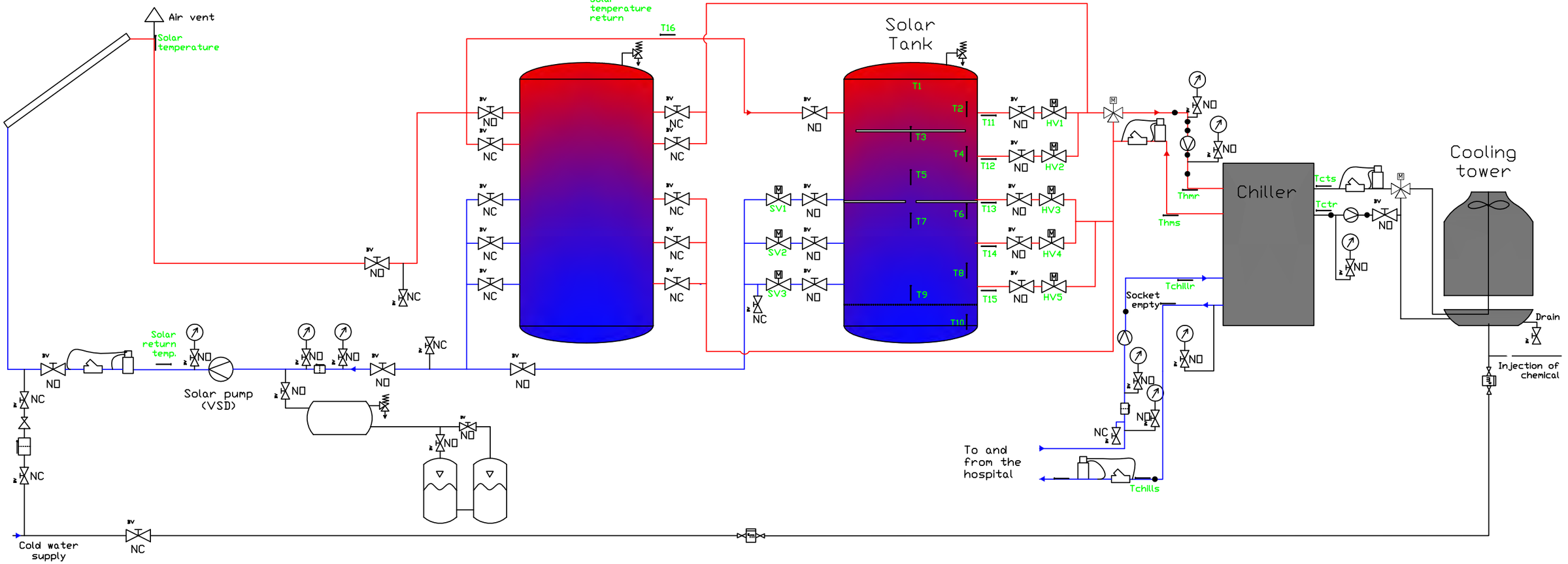

		REV	DATE:-
		0	03/07/2010
APPR:	H.M.	1	30/08/2010
CHECK:	H.M.		
DRAWN:	H.M.		

VOLTAS TECHNOLOGIES
Postnet Suite 5, Private BAg X11, Birnham Park 2015
Tel (+27) 011- 312 2430
Fax (+27) 011- 312 0502
e-mail: info@voltastechnolgies.co.za

PROJECT: MOOT HOSPITAL
CLIENT: NETCARE
DESCRIPTION: GENERAL SYSTEM LAYOUT WATER HEATING

DWG No MOOT01

storage tank

Cooling tower

storage tank

Chiller

NEW STRUCTURAL STEEL FRAMEWORK

Existing TH 1 A/C plantroom

Pipe support

Chilled water pipes to flight ref 1
Refer to DWG no 001/CH/ST

MU

FB

Existing Pot 200L

2467

NEW SOLAR PANELS
113m2 @ 7.5kg/m2

NEW SOLAR PANELS
113m2 @ 7.5kg/m2

NEW SOLAR PANELS
113m2 @ 7.5kg/m2

NEW SOLAR PANELS
113m2 @ 7.5kg/m2

NEW 300x300x300 CONCRETE
COLUMN HEADS WATERPROOFED
TO MATCH EXISTING

NEW STRUCTURAL STEEL
FRAMEWORK

Heat Exchanger (not to scale)
max. 120kg

Storage vessel 5000l
weight: 6000kg
Ø1450mm
height: 3210mm

Cooling tower
weight: 2000kg
Ø1900mm
height: 1900mm

Absorption Chiller
weight: 500kg
height: 2100mm
width: 1000mm
length: 1000mm

Pumps, inline vessel, expansion tanks, fittings, Piping, insulation and cladding on platform will be a load of max. 600kg (load will not be specifically on one point, but distributed over the total platform)

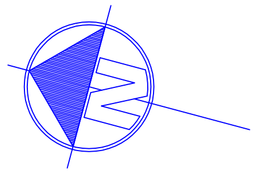

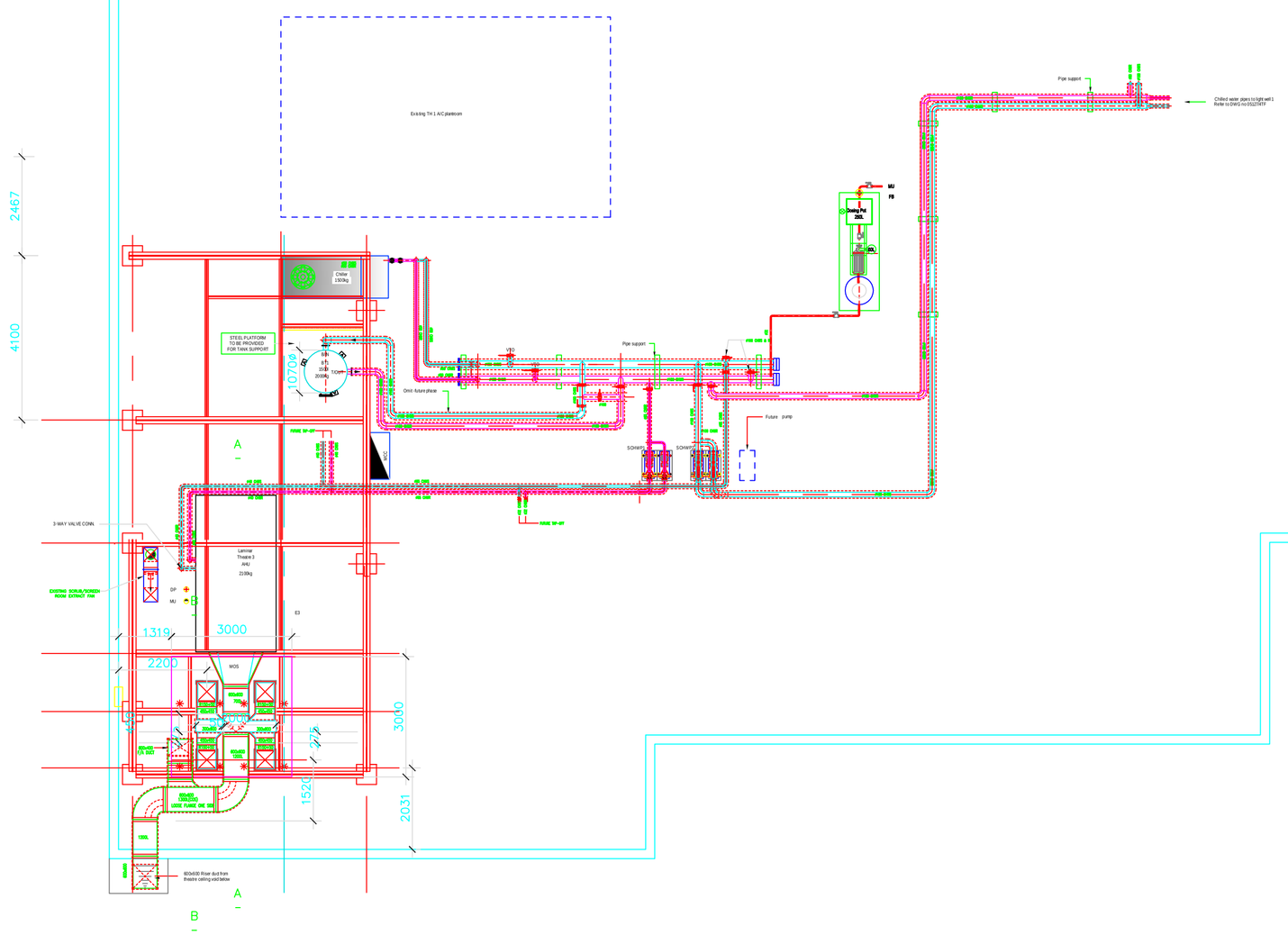

APPENDIX C1: CHILLER INSPECTION DATA

AROACE

WATER FIRED CHILLER

INSPECTION CERTIFICATE

DATE 4/15/2008

MODEL WFC-SC10

MFG/SERIAL NO. 81027029

ITEM	STANDARD	RESULTS
COOLING CAPACITY	35.2KW	OK
PRESSURE TEST WATER CIRCUIT	588.4KPA	OK
PRESSURE LOSS COOLING WATER	77.5KPA	OK
PRESSURE LOSS CHILLED WATER	51.0KPA	OK
PRESSURE LOSS HEAT MEDIUM	82.2KPA	OK
DIELECTRIC WITHSTAND	NO BREAKDOWN AT AC 2000V IN 1MIN	OK
INSULATION RESISTANCE	GREATER THAN 1MΩ	OK
HEAT MEDIUM INPUT	180.7MJ/H	OK
CONTROL SWITCH FUNCTION	FUNCTIONS CORRECTLY	OK
PHYSICAL APPEARANCE	NORMAL	OK

YAZAKI RESOURCES CO. LTD

HAMAMATSU FACTORY

QUALITY ASSURANCE DEPARTMENT

CHIEF ENGINEER: signed S TAKAGI

APPENDIX C2: PLANT COMMISSIONING DATA

[Taken from the BMS log files of the commissioning data of Pretoria's Netcare Moot Hospital's HVAC Absorption Cooling Plant]

[Site Information]			
Name	PlantVisorPRO version 1.52[Advanced]		
Identity	Supervisor1		
Phone			
Password			
[Parameters]			
Chiller And Cooling Tower	Chilled Water Return Temperature Calibration		0.0
Chiller And Cooling Tower	Chilled Water Supply Temperature Calibration		-0.2
Chiller And Cooling Tower	Chiller End Hour		11
Chiller And Cooling Tower	Chiller End Hour		11
Chiller And Cooling Tower	Chiller Manual		0
Chiller And Cooling Tower	Chiller Start Hour		7
Chiller And Cooling Tower	Chiller Start Minute		0
Chiller And Cooling Tower	Chilling Heating Pump Flow Alarm		-15.0
Chiller And Cooling Tower	Chilling Heating Pump Flow Alarm Delay		60
Chiller And Cooling Tower	Chilling Heating Pump Flow Calibration		0.0
Chiller And Cooling Tower	Chilling Heating Pump Manual		0
Chiller And Cooling Tower	Cooling Pump Tower Flow Alarm		-20.3
Chiller And Cooling Tower	Cooling Tower Fan Differential		2.0
Chiller And Cooling Tower	Cooling Tower Fan Manual		0
Chiller And Cooling Tower	Cooling Tower Fan Set Point		28.5
Chiller And Cooling Tower	Cooling Tower Fan VSD Change Amount		0.2
Chiller And Cooling Tower	Cooling Tower Fan VSD Change Rate		5
Chiller And Cooling Tower	Cooling Tower Fan VSD Manual Value		0
Chiller And Cooling Tower	Cooling Tower Pump Differential		1.0
Chiller And	Cooling Tower Pump Flow Alarm Delay		180

Cooling Tower			
Chiller And Cooling Tower	Cooling Tower Pump Flow Calibration		0.0
Chiller And Cooling Tower	Cooling Tower Pump Manual		0
Chiller And Cooling Tower	Cooling Tower Pump Set Point		50.0
Chiller And Cooling Tower	Cooling Tower Pump VSD Change Amount		0.2
Chiller And Cooling Tower	Cooling Tower Pump VSD Change Rate		5
Chiller And Cooling Tower	Cooling Tower Pump VSD Manual Value		0
Chiller And Cooling Tower	Cooling Tower Return Temperature Calibration		0.0
Chiller And Cooling Tower	Cooling Tower Supply Temperature Calibration		0.0
Chiller And Cooling Tower	Enable Chiller Manual		0
Chiller And Cooling Tower	Enable Chiller Time Scheduling		1
Chiller And Cooling Tower	Enable Chilling Heating Pump Manual		0
Chiller And Cooling Tower	Enable Cooling Tower Fan Manual		0
Chiller And Cooling Tower	Enable Cooling Tower Pump Manual		0
Chiller And Cooling Tower	Enable Heat Medium Pump Manual		0
Chiller And Cooling Tower	Enable Valve V10 Manual		0
Chiller And Cooling Tower	Existing Chiller Start 100% Set Point		8.3
Chiller And Cooling Tower	Existing Chiller Start 50% Set Point		6.8
Chiller And Cooling Tower	Existing Chiller Stop 100% Set Point		7.5
Chiller And Cooling Tower	Existing Chiller Stop 50% Set Point		6.5
Chiller And Cooling Tower	Existing Chiller Supply Temperature Calibration		0.0
Chiller And Cooling Tower	Heat Medium Pump Differential		1.0
Chiller And Cooling Tower	Heat Medium Pump Flow Alarm		-15.0
Chiller And Cooling Tower	Heat Medium Pump Flow Alarm Delay		60
Chiller And Cooling Tower	Heat Medium Pump Flow Calibration		0.0
Chiller And Cooling Tower	Heat Medium Pump Manual		0
Chiller And Cooling Tower	Heat Medium Pump Pump VSD Change Amount		0.2

Chiller And Cooling Tower	Heat Medium Pump Set Point		50.0
Chiller And Cooling Tower	Heat Medium Pump VSD Change Rate		5
Chiller And Cooling Tower	Heat Medium Pump VSD Manual Value		0
Chiller And Cooling Tower	Hot Water Return Temperature Calibration		0.0
Chiller And Cooling Tower	Hot Water Supply Temperature Calibration		-3.6
Chiller And Cooling Tower	Probe Alarm Delay		60
Chiller And Cooling Tower	Reset Alarms		0
Chiller And Cooling Tower	Solar Chiller Start Set Point (Daytime)		83.0
Chiller And Cooling Tower	Solar Chiller Start Set Point (Nighttime)		90.0
Chiller And Cooling Tower	Solar Chiller Stop Set Point (Daytime)		80.0
Chiller And Cooling Tower	Solar Chiller Stop Set Point (Nighttime)		86.0
Chiller And Cooling Tower	V10 Manual Value		0
Chiller And Cooling Tower	Valve V10 Set Point		28.0
Hot Water Tank	Ambient Humidity Calibration		20.0
Hot Water Tank	Ambient Temperature Calibration		0.0
Hot Water Tank	Collector 1 MAX		120.0
Hot Water Tank	Collector 1 MIN		80.0
Hot Water Tank	Control Procedure Time Check		10
Hot Water Tank	Delta T OFF		4.0
Hot Water Tank	Delta T ON		7.0
Hot Water Tank	Enable Solar Water Pump Manual		0
Hot Water Tank	Enable Valve HMV Manual		0
Hot Water Tank	Enable Valve HV1 Manual		1
Hot Water Tank	Enable Valve HV2 Manual		1
Hot Water Tank	Enable Valve HV3 Manual		1
Hot Water Tank	Enable Valve HV4 Manual		1
Hot Water Tank	Enable Valve HV5 Manual		1
Hot Water Tank	Enable Valve SV1 Manual		1
Hot Water Tank	Enable Valve SV2 Manual		1
Hot Water Tank	Enable Valve SV3 Manual		1
Hot Water Tank	Hot Mixing Valve Differential		4.0
Hot Water Tank	Hot Mixing Valve Set Point		90.0
Hot Water Tank	Hot Water High Activtion Set Point		95.0
Hot Water Tank	Hot Water High Deactivation Set Point		94.0
Hot Water Tank	Hot Water Tank 2 Bottom Temperature Calibration		0.0

Hot Water Tank	Hot Water Tank 2 Top Temperature Calibration		0.0
Hot Water Tank	Hot Water Tank Set Point		70.0
Hot Water Tank	Hot Water Tank Temperature 1 Calibration		0.0
Hot Water Tank	Hot Water Tank Temperature 10 Calibration		0.0
Hot Water Tank	Hot Water Tank Temperature 2 Calibration		0.0
Hot Water Tank	Hot Water Tank Temperature 3 Calibration		0.0
Hot Water Tank	Hot Water Tank Temperature 4 Calibration		0.0
Hot Water Tank	Hot Water Tank Temperature 5 Calibration		0.0
Hot Water Tank	Hot Water Tank Temperature 6 Calibration		0.0
Hot Water Tank	Hot Water Tank Temperature 7 Calibration		0.0
Hot Water Tank	Hot Water Tank Temperature 8 Calibration		0.0
Hot Water Tank	Hot Water Tank Temperature 9 Calibration		0.0
Hot Water Tank	Probe Alarm Delay		15
Hot Water Tank	Pump 10% Set Point		2.0
Hot Water Tank	Pump 100% Set Point		20.0
Hot Water Tank	Pump 20% Set Point		4.0
Hot Water Tank	Pump 30% Set Point		6.0
Hot Water Tank	Pump 40% Set Point		8.0
Hot Water Tank	Pump 50% Set Point		10.0
Hot Water Tank	Pump 60% Set Point		12.0
Hot Water Tank	Pump 70% Set Point		14.0
Hot Water Tank	Pump 80% Set Point		16.0
Hot Water Tank	Pump 90% Set Point		18.0
Hot Water Tank	Pump Start Time		5
Hot Water Tank	Reset Alarms		0
Hot Water Tank	Solar Pump End Hour		17
Hot Water Tank	Solar Pump End Minute		30
Hot Water Tank	Solar Pump Start Hour		7
Hot Water Tank	Solar Pump Start Minute		0
Hot Water Tank	Solar Water Flow Calibration		150.0
Hot Water Tank	Solar Water Pump Anti Freeze OFF Set Point		4.0
Hot Water Tank	Solar Water Pump Anti Freeze ON Set Point		2.0
Hot Water Tank	Solar Water Pump Manual		0
Hot Water Tank	Solar Water Pump VSD Manual Value		100
Hot Water Tank	Solar Water Return Temperature Calibration		0.0
Hot Water Tank	T11 Temperature Calibration		0.0
Hot Water Tank	T12 Temperature Calibration		0.0
Hot Water Tank	T13 Temperature Calibration		0.0
Hot Water Tank	T14 Temperature Calibration		0.0
Hot Water Tank	T15 Temperature Calibration		0.0
Hot Water Tank	T16 Temperature Calibration		0.0
Hot Water Tank	Valve HMV Manual Value		0
Hot Water Tank	Valve HV1 Manual Value		100
Hot Water Tank	Valve HV2 Manual Value		0

Hot Water Tank	Valve HV3 Manual Value		100
Hot Water Tank	Valve HV4 Manual Value		0
Hot Water Tank	Valve HV5 Manual Value		0
Hot Water Tank	Valve SV1 Manual Value		100
Hot Water Tank	Valve SV2 Manual Value		0
Hot Water Tank	Valve SV3 Manual Value		0
Power Analizer	Alarm reset	Alarm Res.	63 222
Power Analizer	Byte order in the words (=1 for correct system working) [*]	dat	1
Power Analizer	Counter reset	Counter Res.	63 222
Power Analizer	Current Tansformer (CT) ratio	Ct ratio	10
Power Analizer	Filter coefficient [*]	Filter coe	1
Power Analizer	Filter range [*]	Filter nrg	1
Power Analizer	Lower voltage threshold [*] [**]	Set vdown	0
Power Analizer	Max reset	Max Res.	63 222
Power Analizer	Neutral current threshold [*] [**]	Set an	0.00
Power Analizer	System type (0=3P	1=3P-n	2=2P
Power Analizer	Time period for currrent average (Admd) [*]	A int	1
Power Analizer	Time period for power average (Wdmd) [*]	P int	15
Power Analizer	Upper voltage threshold [*] [**]	Set vup	0

APPENDIX D1: Rising and setting times for the Sun (August 2010)

["*timeanddate.com*", http://www.timeanddate.com/worldclock/astronomy.html?accessed 11/01/2013]

			Length of day		Solar noon		
Date	**Sunrise**	**Sunset**	**This day**	**Difference**	**Time**	**Altitude**	**Distance (10^6 km)**
1 Aug 2010	06:46	17:42	10h 55m 50s	+ 1m 03s	12:14	46.3°	151.829
2 Aug 2010	06:45	17:42	10h 56m 55s	+ 1m 04s	12:14	46.6°	151.811
3 Aug 2010	06:45	17:43	10h 58m 00s	+ 1m 05s	12:13	46.8°	151.792
4 Aug 2010	06:44	17:43	10h 59m 07s	+ 1m 06s	12:13	47.1°	151.772
5 Aug 2010	06:43	17:44	11h 00m 15s	+ 1m 07s	12:13	47.4°	151.752
6 Aug 2010	06:43	17:44	11h 01m 23s	+ 1m 08s	12:13	47.6°	151.731
7 Aug 2010	06:42	17:44	11h 02m 33s	+ 1m 09s	12:13	47.9°	151.710
8 Aug 2010	06:41	17:45	11h 03m 43s	+ 1m 10s	12:13	48.2°	151.687
9 Aug 2010	06:40	17:45	11h 04m 55s	+ 1m 11s	12:13	48.5°	151.664
10 Aug 2010	06:40	17:46	11h 06m 07s	+ 1m 12s	12:13	48.8°	151.640
11 Aug 2010	06:39	17:46	11h 07m 20s	+ 1m 12s	12:12	49.1°	151.615
12 Aug 2010	06:38	17:47	11h 08m 33s	+ 1m 13s	12:12	49.4°	151.589
13 Aug 2010	06:37	17:47	11h 09m 48s	+ 1m 14s	12:12	49.7°	151.563
14 Aug 2010	06:37	17:48	11h 11m 03s	+ 1m 15s	12:12	50.0°	151.536
15 Aug 2010	06:36	17:48	11h 12m 19s	+ 1m 15s	12:12	50.3°	151.508
16 Aug 2010	06:35	17:49	11h 13m 36s	+ 1m 16s	12:12	50.6°	151.480
17 Aug 2010	06:34	17:49	11h 14m 53s	+ 1m 17s	12:11	50.9°	151.451
18 Aug 2010	06:33	17:49	11h 16m 11s	+ 1m 17s	12:11	51.2°	151.421
19 Aug 2010	06:32	17:50	11h 17m 29s	+ 1m 18s	12:11	51.6°	151.391
20 Aug 2010	06:31	17:50	11h 18m 48s	+ 1m 19s	12:11	51.9°	151.360
21 Aug 2010	06:31	17:51	11h 20m 08s	+ 1m 19s	12:10	52.2°	151.329
22 Aug 2010	06:30	17:51	11h 21m 28s	+ 1m 20s	12:10	52.6°	151.298
23 Aug 2010	06:29	17:52	11h 22m 49s	+ 1m 20s	12:10	52.9°	151.266
24 Aug 2010	06:28	17:52	11h 24m 11s	+ 1m 21s	12:10	53.2°	151.235
25 Aug 2010	06:27	17:52	11h 25m 32s	+ 1m 21s	12:09	53.6°	151.202
26 Aug 2010	06:26	17:53	11h 26m 55s	+ 1m 22s	12:09	53.9°	151.170
27 Aug 2010	06:25	17:53	11h 28m 18s	+ 1m 22s	12:09	54.3°	151.137
28 Aug 2010	06:24	17:54	11h 29m 41s	+ 1m 23s	12:09	54.6°	151.104
29 Aug 2010	06:23	17:54	11h 31m 05s	+ 1m 23s	12:08	55.0°	151.071
30 Aug 2010	06:22	17:54	11h 32m 29s	+ 1m 24s	12:08	55.3°	151.037
31 Aug 2010	06:21	17:55	11h 33m 53s	+ 1m 24s	12:08	55.7°	151.003

All times are in local time for Pretoria

APPENDIX D2: Rising and setting times for the Sun (September 2010)

["*timeanddate.com*", http://www.timeanddate.com/worldclock/astronomy.html?accessed 11/01/2013]

			Length of day		Solar noon		
Date	**Sunrise**	**Sunset**	**This day**	**Difference**	**Time**	**Altitude**	**Distance (10^6 km)**
1 Sep 2010	06:20	17:55	11h 35m 18s	+ 1m 24s	12:07	56.1°	150.969
2 Sep 2010	06:19	17:56	11h 36m 44s	+ 1m 25s	12:07	56.4°	150.934
3 Sep 2010	06:18	17:56	11h 38m 10s	+ 1m 25s	12:07	56.8°	150.899
4 Sep 2010	06:17	17:56	11h 39m 36s	+ 1m 25s	12:06	57.1°	150.864
5 Sep 2010	06:16	17:57	11h 41m 02s	+ 1m 26s	12:06	57.5°	150.827
6 Sep 2010	06:15	17:57	11h 42m 29s	+ 1m 26s	12:06	57.9°	150.791
7 Sep 2010	06:14	17:57	11h 43m 56s	+ 1m 26s	12:05	58.3°	150.753
8 Sep 2010	06:12	17:58	11h 45m 23s	+ 1m 27s	12:05	58.6°	150.716
9 Sep 2010	06:11	17:58	11h 46m 50s	+ 1m 27s	12:05	59.0°	150.677
10 Sep 2010	06:10	17:59	11h 48m 18s	+ 1m 27s	12:04	59.4°	150.639
11 Sep 2010	06:09	17:59	11h 49m 46s	+ 1m 28s	12:04	59.8°	150.599
12 Sep 2010	06:08	17:59	11h 51m 15s	+ 1m 28s	12:04	60.2°	150.559
13 Sep 2010	06:07	18:00	11h 52m 43s	+ 1m 28s	12:03	60.5°	150.519
14 Sep 2010	06:06	18:00	11h 54m 12s	+ 1m 28s	12:03	60.9°	150.478
15 Sep 2010	06:05	18:01	11h 55m 41s	+ 1m 28s	12:03	61.3°	150.437
16 Sep 2010	06:04	18:01	11h 57m 10s	+ 1m 29s	12:02	61.7°	150.396
17 Sep 2010	06:03	18:01	11h 58m 39s	+ 1m 29s	12:02	62.1°	150.355
18 Sep 2010	06:02	18:02	12h 00m 08s	+ 1m 29s	12:01	62.5°	150.313
19 Sep 2010	06:00	18:02	12h 01m 38s	+ 1m 29s	12:01	62.8°	150.271
20 Sep 2010	05:59	18:03	12h 03m 08s	+ 1m 29s	12:01	63.2°	150.229
21 Sep 2010	05:58	18:03	12h 04m 37s	+ 1m 29s	12:00	63.6°	150.187
22 Sep 2010	05:57	18:03	12h 06m 07s	+ 1m 29s	12:00	64.0°	150.145
23 Sep 2010	05:56	18:04	12h 07m 37s	+ 1m 29s	12:00	64.4°	150.104
24 Sep 2010	05:55	18:04	12h 09m 07s	+ 1m 30s	11:59	64.8°	150.062
25 Sep 2010	05:54	18:05	12h 10m 37s	+ 1m 30s	11:59	65.2°	150.020
26 Sep 2010	05:53	18:05	12h 12m 07s	+ 1m 30s	11:59	65.6°	149.978
27 Sep 2010	05:52	18:05	12h 13m 38s	+ 1m 30s	11:58	66.0°	149.937
28 Sep 2010	05:51	18:06	12h 15m 08s	+ 1m 30s	11:58	66.3°	149.895
29 Sep 2010	05:50	18:06	12h 16m 38s	+ 1m 30s	11:58	66.7°	149.853
30 Sep 2010	05:48	18:07	12h 18m 09s	+ 1m 30s	11:57	67.1°	149.812

All times are in local time for Pretoria

APPENDIX D3: Rising and setting times for the Sun (October 2010)

["*timeanddate.com*", http://www.timeanddate.com/worldclock/astronomy.html?accessed 11/01/2013]

			Length of day		Solar noon		
Date	**Sunrise**	**Sunset**	**This day**	**Difference**	**Time**	**Altitude**	**Distance (10^6 km)**
1 Oct 2010	05:47	18:07	12h 19m 39s	+ 1m 30s	11:57	67.5°	149.770
2 Oct 2010	05:46	18:07	12h 21m 09s	+ 1m 30s	11:57	67.9°	149.728
3 Oct 2010	05:45	18:08	12h 22m 39s	+ 1m 30s	11:56	68.3°	149.686
4 Oct 2010	05:44	18:08	12h 24m 10s	+ 1m 30s	11:56	68.7°	149.644
5 Oct 2010	05:43	18:09	12h 25m 40s	+ 1m 30s	11:56	69.1°	149.602
6 Oct 2010	05:42	18:09	12h 27m 10s	+ 1m 30s	11:55	69.4°	149.559
7 Oct 2010	05:41	18:10	12h 28m 40s	+ 1m 29s	11:55	69.8°	149.516
8 Oct 2010	05:40	18:10	12h 30m 10s	+ 1m 29s	11:55	70.2°	149.474
9 Oct 2010	05:39	18:11	12h 31m 39s	+ 1m 29s	11:55	70.6°	149.431
10 Oct 2010	05:38	18:11	12h 33m 09s	+ 1m 29s	11:54	71.0°	149.387
11 Oct 2010	05:37	18:12	12h 34m 39s	+ 1m 29s	11:54	71.3°	149.344
12 Oct 2010	05:36	18:12	12h 36m 08s	+ 1m 29s	11:54	71.7°	149.301
13 Oct 2010	05:35	18:13	12h 37m 37s	+ 1m 29s	11:54	72.1°	149.257
14 Oct 2010	05:34	18:13	12h 39m 06s	+ 1m 28s	11:53	72.5°	149.214
15 Oct 2010	05:33	18:14	12h 40m 34s	+ 1m 28s	11:53	72.8°	149.170
16 Oct 2010	05:32	18:14	12h 42m 03s	+ 1m 28s	11:53	73.2°	149.127
17 Oct 2010	05:31	18:15	12h 43m 31s	+ 1m 28s	11:53	73.6°	149.084
18 Oct 2010	05:30	18:15	12h 44m 58s	+ 1m 27s	11:52	73.9°	149.041
19 Oct 2010	05:29	18:16	12h 46m 26s	+ 1m 27s	11:52	74.3°	148.998
20 Oct 2010	05:28	18:16	12h 47m 53s	+ 1m 27s	11:52	74.7°	148.956
21 Oct 2010	05:27	18:17	12h 49m 20s	+ 1m 26s	11:52	75.0°	148.914
22 Oct 2010	05:27	18:17	12h 50m 46s	+ 1m 26s	11:52	75.4°	148.872
23 Oct 2010	05:26	18:18	12h 52m 12s	+ 1m 25s	11:52	75.7°	148.831
24 Oct 2010	05:25	18:18	12h 53m 37s	+ 1m 25s	11:52	76.1°	148.790
25 Oct 2010	05:24	18:19	12h 55m 02s	+ 1m 25s	11:51	76.4°	148.750
26 Oct 2010	05:23	18:20	12h 56m 27s	+ 1m 24s	11:51	76.8°	148.710
27 Oct 2010	05:22	18:20	12h 57m 51s	+ 1m 24s	11:51	77.1°	148.670
28 Oct 2010	05:22	18:21	12h 59m 15s	+ 1m 23s	11:51	77.4°	148.631
29 Oct 2010	05:21	18:22	13h 00m 38s	+ 1m 22s	11:51	77.8°	148.592
30 Oct 2010	05:20	18:22	13h 02m 00s	+ 1m 22s	11:51	78.1°	148.554
31 Oct 2010	05:19	18:23	13h 03m 22s	+ 1m 21s	11:51	78.4°	148.516

All times are in local time for Pretoria

APPENDIX D4: Rising and setting times for the Sun (November 2010)

["*timeanddate.com*", http://www.timeanddate.com/worldclock/astronomy.html?accessed 11/01/2013]

			Length of day		Solar noon		
Date	**Sunrise**	**Sunset**	**This day**	**Difference**	**Time**	**Altitude**	**Distance (10^6 km)**
1 Nov 2010	05:19	18:23	13h 04m 43s	+ 1m 21s	11:51	78.7°	148.478
2 Nov 2010	05:18	18:24	13h 06m 03s	+ 1m 20s	11:51	79.1°	148.440
3 Nov 2010	05:17	18:25	13h 07m 23s	+ 1m 19s	11:51	79.4°	148.402
4 Nov 2010	05:17	18:25	13h 08m 42s	+ 1m 18s	11:51	79.7°	148.365
5 Nov 2010	05:16	18:26	13h 10m 00s	+ 1m 18s	11:51	80.0°	148.328
6 Nov 2010	05:15	18:27	13h 11m 17s	+ 1m 17s	11:51	80.3°	148.291
7 Nov 2010	05:15	18:27	13h 12m 34s	+ 1m 16s	11:51	80.6°	148.254
8 Nov 2010	05:14	18:28	13h 13m 50s	+ 1m 15s	11:51	80.9°	148.218
9 Nov 2010	05:14	18:29	13h 15m 04s	+ 1m 14s	11:51	81.2°	148.181
10 Nov 2010	05:13	18:30	13h 16m 18s	+ 1m 13s	11:51	81.4°	148.145
11 Nov 2010	05:13	18:30	13h 17m 31s	+ 1m 12s	11:51	81.7°	148.109
12 Nov 2010	05:12	18:31	13h 18m 42s	+ 1m 11s	11:51	82.0°	148.074
13 Nov 2010	05:12	18:32	13h 19m 53s	+ 1m 10s	11:52	82.3°	148.039
14 Nov 2010	05:11	18:32	13h 21m 02s	+ 1m 09s	11:52	82.5°	148.004
15 Nov 2010	05:11	18:33	13h 22m 11s	+ 1m 08s	11:52	82.8°	147.970
16 Nov 2010	05:11	18:34	13h 23m 18s	+ 1m 07s	11:52	83.0°	147.936
17 Nov 2010	05:10	18:35	13h 24m 24s	+ 1m 05s	11:52	83.3°	147.903
18 Nov 2010	05:10	18:35	13h 25m 28s	+ 1m 04s	11:52	83.5°	147.871
19 Nov 2010	05:09	18:36	13h 26m 32s	+ 1m 03s	11:53	83.8°	147.839
20 Nov 2010	05:09	18:37	13h 27m 33s	+ 1m 01s	11:53	84.0°	147.808
21 Nov 2010	05:09	18:38	13h 28m 34s	+ 1m 00s	11:53	84.2°	147.778
22 Nov 2010	05:09	18:38	13h 29m 33s	+ 59s	11:53	84.4°	147.748
23 Nov 2010	05:08	18:39	13h 30m 30s	+ 57s	11:54	84.6°	147.719
24 Nov 2010	05:08	18:40	13h 31m 27s	+ 56s	11:54	84.8°	147.691
25 Nov 2010	05:08	18:41	13h 32m 21s	+ 54s	11:54	85.0°	147.664
26 Nov 2010	05:08	18:41	13h 33m 14s	+ 52s	11:55	85.2°	147.637
27 Nov 2010	05:08	18:42	13h 34m 05s	+ 51s	11:55	85.4°	147.611
28 Nov 2010	05:08	18:43	13h 34m 55s	+ 49s	11:55	85.6°	147.586
29 Nov 2010	05:08	18:43	13h 35m 43s	+ 47s	11:56	85.8°	147.561
30 Nov 2010	05:08	18:44	13h 36m 29s	+ 46s	11:56	85.9°	147.537

All times are in local time for Pretoria

APPENDIX D5: Rising and setting times for the Sun (December 2010)

["*timeanddate.com*", http://www.timeanddate.com/worldclock/astronomy.html?accessed 11/01/2013]

			Length of day		Solar noon		
Date	**Sunrise**	**Sunset**	**This day**	**Difference**	**Time**	**Altitude**	**Distance (10^6 km)**
1 Dec 2010	05:08	18:45	13h 37m 13s	+ 44s	11:56	86.1°	147.514
2 Dec 2010	05:08	18:46	13h 37m 56s	+ 42s	11:57	86.2°	147.491
3 Dec 2010	05:08	18:46	13h 38m 37s	+ 40s	11:57	86.4°	147.468
4 Dec 2010	05:08	18:47	13h 39m 15s	+ 38s	11:57	86.5°	147.446
5 Dec 2010	05:08	18:48	13h 39m 52s	+ 36s	11:58	86.7°	147.425
6 Dec 2010	05:08	18:49	13h 40m 27s	+ 34s	11:58	86.8°	147.404
7 Dec 2010	05:08	18:49	13h 41m 00s	+ 32s	11:59	86.9°	147.383
8 Dec 2010	05:08	18:50	13h 41m 31s	+ 30s	11:59	87.0°	147.363
9 Dec 2010	05:09	18:51	13h 41m 59s	+ 28s	12:00	87.1°	147.343
10 Dec 2010	05:09	18:51	13h 42m 26s	+ 26s	12:00	87.2°	147.324
11 Dec 2010	05:09	18:52	13h 42m 51s	+ 24s	12:00	87.3°	147.305
12 Dec 2010	05:09	18:53	13h 43m 13s	+ 22s	12:01	87.4°	147.287
13 Dec 2010	05:10	18:53	13h 43m 33s	+ 20s	12:01	87.4°	147.270
14 Dec 2010	05:10	18:54	13h 43m 51s	+ 18s	12:02	87.5°	147.253
15 Dec 2010	05:10	18:54	13h 44m 07s	+ 15s	12:02	87.6°	147.237
16 Dec 2010	05:11	18:55	13h 44m 21s	+ 13s	12:03	87.6°	147.222
17 Dec 2010	05:11	18:56	13h 44m 32s	+ 11s	12:03	87.6°	147.208
18 Dec 2010	05:11	18:56	13h 44m 41s	+ 09s	12:04	87.7°	147.194
19 Dec 2010	05:12	18:57	13h 44m 48s	+ 06s	12:04	87.7°	147.182
20 Dec 2010	05:12	18:57	13h 44m 53s	+ 04s	12:05	87.7°	147.170
21 Dec 2010	05:13	18:58	13h 44m 55s	+ 02s	12:05	87.7°	147.160
22 Dec 2010	05:13	18:58	13h 44m 55s	< 1s	12:06	87.7°	147.150
23 Dec 2010	05:14	18:59	13h 44m 53s	− 02s	12:06	87.7°	147.141
24 Dec 2010	05:14	18:59	13h 44m 49s	− 04s	12:07	87.7°	147.134
25 Dec 2010	05:15	19:00	13h 44m 42s	− 06s	12:07	87.7°	147.127
26 Dec 2010	05:15	19:00	13h 44m 33s	− 08s	12:08	87.6°	147.121
27 Dec 2010	05:16	19:00	13h 44m 22s	− 11s	12:08	87.6°	147.115
28 Dec 2010	05:17	19:01	13h 44m 09s	− 13s	12:09	87.6°	147.111
29 Dec 2010	05:17	19:01	13h 43m 53s	− 15s	12:09	87.5°	147.107
30 Dec 2010	05:18	19:01	13h 43m 36s	− 17s	12:10	87.4°	147.104
31 Dec 2010	05:18	19:02	13h 43m 16s	− 19s	12:10	87.4°	147.102

All times are in local time for Pretoria

APPENDIX D6: Rising and setting times for the Sun (January 2011)

["*timeanddate.com*", http://www.timeanddate.com/worldclock/astronomy.html?accessed 11/01/2013]

			Length of day		Solar noon		
Date	**Sunrise**	**Sunset**	**This day**	**Difference**	**Time**	**Altitude**	**Distance (10^6 km)**
1 Jan 2011	05:19	19:02	13h 42m 53s	− 22s	12:11	87.3°	147.101
2 Jan 2011	05:20	19:02	13h 42m 29s	− 24s	12:11	87.2°	147.100
3 Jan 2011	05:20	19:03	13h 42m 03s	− 26s	12:12	87.1°	147.099
4 Jan 2011	05:21	19:03	13h 41m 34s	− 28s	12:12	87.0°	147.099
5 Jan 2011	05:22	19:03	13h 41m 03s	− 30s	12:13	86.9°	147.100
6 Jan 2011	05:23	19:03	13h 40m 31s	− 32s	12:13	86.8°	147.101
7 Jan 2011	05:23	19:03	13h 39m 56s	− 34s	12:13	86.7°	147.103
8 Jan 2011	05:24	19:03	13h 39m 19s	− 36s	12:14	86.5°	147.105
9 Jan 2011	05:25	19:03	13h 38m 40s	− 38s	12:14	86.4°	147.109
10 Jan 2011	05:26	19:04	13h 38m 00s	− 40s	12:15	86.3°	147.112
11 Jan 2011	05:26	19:04	13h 37m 17s	− 42s	12:15	86.1°	147.117
12 Jan 2011	05:27	19:04	13h 36m 33s	− 44s	12:15	85.9°	147.122
13 Jan 2011	05:28	19:04	13h 35m 47s	− 46s	12:16	85.8°	147.127
14 Jan 2011	05:29	19:04	13h 34m 59s	− 48s	12:16	85.6°	147.134
15 Jan 2011	05:29	19:04	13h 34m 09s	− 49s	12:17	85.4°	147.142
16 Jan 2011	05:30	19:03	13h 33m 17s	− 51s	12:17	85.2°	147.150
17 Jan 2011	05:31	19:03	13h 32m 24s	− 53s	12:17	85.1°	147.159
18 Jan 2011	05:32	19:03	13h 31m 29s	− 54s	12:18	84.9°	147.169
19 Jan 2011	05:32	19:03	13h 30m 33s	− 56s	12:18	84.6°	147.181
20 Jan 2011	05:33	19:03	13h 29m 35s	− 57s	12:18	84.4°	147.193
21 Jan 2011	05:34	19:03	13h 28m 35s	− 59s	12:18	84.2°	147.206
22 Jan 2011	05:35	19:02	13h 27m 35s	− 1m 00s	12:19	84.0°	147.220
23 Jan 2011	05:36	19:02	13h 26m 32s	− 1m 02s	12:19	83.8°	147.235
24 Jan 2011	05:36	19:02	13h 25m 28s	− 1m 03s	12:19	83.5°	147.250
25 Jan 2011	05:37	19:02	13h 24m 23s	− 1m 05s	12:19	83.3°	147.267
26 Jan 2011	05:38	19:01	13h 23m 17s	− 1m 06s	12:20	83.0°	147.284
27 Jan 2011	05:39	19:01	13h 22m 09s	− 1m 07s	12:20	82.8°	147.302
28 Jan 2011	05:39	19:00	13h 21m 00s	− 1m 08s	12:20	82.5°	147.321
29 Jan 2011	05:40	19:00	13h 19m 50s	− 1m 10s	12:20	82.3°	147.340
30 Jan 2011	05:41	19:00	13h 18m 38s	− 1m 11s	12:20	82.0°	147.360
31 Jan 2011	05:42	18:59	13h 17m 26s	− 1m 12s	12:21	81.7°	147.380

All times are in local time for Pretoria

APPENDIX D7: Rising and setting times for the Sun (February 2011)

["*timeanddate.com*", http://www.timeanddate.com/worldclock/astronomy.html?accessed 11/01/2013]

			Length of day		Solar noon		
Date	**Sunrise**	**Sunset**	**This day**	**Difference**	**Time**	**Altitude**	**Distance (10^6 km)**
1 Feb 2011	05:43	18:59	13h 16m 13s	− 1m 13s	12:21	81.4°	147.401
2 Feb 2011	05:43	18:58	13h 14m 58s	− 1m 14s	12:21	81.1°	147.423
3 Feb 2011	05:44	18:58	13h 13m 42s	− 1m 15s	12:21	80.8°	147.445
4 Feb 2011	05:45	18:57	13h 12m 26s	− 1m 16s	12:21	80.5°	147.467
5 Feb 2011	05:45	18:57	13h 11m 08s	− 1m 17s	12:21	80.2°	147.490
6 Feb 2011	05:46	18:56	13h 09m 50s	− 1m 18s	12:21	79.9°	147.513
7 Feb 2011	05:47	18:55	13h 08m 31s	− 1m 19s	12:21	79.6°	147.537
8 Feb 2011	05:48	18:55	13h 07m 11s	− 1m 19s	12:21	79.3°	147.561
9 Feb 2011	05:48	18:54	13h 05m 50s	− 1m 20s	12:21	79.0°	147.585
10 Feb 2011	05:49	18:54	13h 04m 29s	− 1m 21s	12:21	78.7°	147.611
11 Feb 2011	05:50	18:53	13h 03m 06s	− 1m 22s	12:21	78.4°	147.636
12 Feb 2011	05:50	18:52	13h 01m 44s	− 1m 22s	12:21	78.0°	147.663
13 Feb 2011	05:51	18:51	13h 00m 20s	− 1m 23s	12:21	77.7°	147.690
14 Feb 2011	05:52	18:51	12h 58m 56s	− 1m 24s	12:21	77.3°	147.718
15 Feb 2011	05:52	18:50	12h 57m 31s	− 1m 24s	12:21	77.0°	147.746
16 Feb 2011	05:53	18:49	12h 56m 06s	− 1m 25s	12:21	76.7°	147.775
17 Feb 2011	05:54	18:48	12h 54m 40s	− 1m 25s	12:21	76.3°	147.805
18 Feb 2011	05:54	18:48	12h 53m 14s	− 1m 26s	12:21	76.0°	147.836
19 Feb 2011	05:55	18:47	12h 51m 47s	− 1m 26s	12:21	75.6°	147.868
20 Feb 2011	05:56	18:46	12h 50m 20s	− 1m 27s	12:21	75.3°	147.900
21 Feb 2011	05:56	18:45	12h 48m 52s	− 1m 27s	12:21	74.9°	147.933
22 Feb 2011	05:57	18:44	12h 47m 24s	− 1m 27s	12:21	74.5°	147.966
23 Feb 2011	05:57	18:43	12h 45m 56s	− 1m 28s	12:21	74.2°	148.000
24 Feb 2011	05:58	18:43	12h 44m 27s	− 1m 28s	12:21	73.8°	148.035
25 Feb 2011	05:59	18:42	12h 42m 58s	− 1m 29s	12:20	73.4°	148.070
26 Feb 2011	05:59	18:41	12h 41m 29s	− 1m 29s	12:20	73.1°	148.106
27 Feb 2011	06:00	18:40	12h 39m 59s	− 1m 29s	12:20	72.7°	148.142
28 Feb 2011	06:00	18:39	12h 38m 29s	− 1m 29s	12:20	72.3°	148.178

All times are in local time for Pretoria

APPENDIX D8: Rising and setting times for the Sun (March 2011)

["*timeanddate.com*", http://www.timeanddate.com/worldclock/astronomy.html?accessed 11/01/2013]

			Length of day		Solar noon		
Date	**Sunrise**	**Sunset**	**This day**	**Difference**	**Time**	**Altitude**	**Distance (10^6 km)**
1 Mar 2011	06:01	18:38	12h 36m 59s	− 1m 30s	12:20	71.9°	148.215
2 Mar 2011	06:02	18:37	12h 35m 28s	− 1m 30s	12:19	71.5°	148.251
3 Mar 2011	06:02	18:36	12h 33m 58s	− 1m 30s	12:19	71.2°	148.289
4 Mar 2011	06:03	18:35	12h 32m 27s	− 1m 30s	12:19	70.8°	148.326
5 Mar 2011	06:03	18:34	12h 30m 56s	− 1m 30s	12:19	70.4°	148.363
6 Mar 2011	06:04	18:33	12h 29m 25s	− 1m 31s	12:19	70.0°	148.401
7 Mar 2011	06:04	18:32	12h 27m 54s	− 1m 31s	12:18	69.6°	148.439
8 Mar 2011	06:05	18:31	12h 26m 22s	− 1m 31s	12:18	69.2°	148.477
9 Mar 2011	06:05	18:30	12h 24m 51s	− 1m 31s	12:18	68.8°	148.515
10 Mar 2011	06:06	18:29	12h 23m 19s	− 1m 31s	12:18	68.4°	148.553
11 Mar 2011	06:06	18:28	12h 21m 48s	− 1m 31s	12:17	68.1°	148.592
12 Mar 2011	06:07	18:27	12h 20m 16s	− 1m 31s	12:17	67.7°	148.630
13 Mar 2011	06:07	18:26	12h 18m 44s	− 1m 31s	12:17	67.3°	148.670
14 Mar 2011	06:08	18:25	12h 17m 13s	− 1m 31s	12:17	66.9°	148.709
15 Mar 2011	06:08	18:24	12h 15m 41s	− 1m 31s	12:16	66.5°	148.749
16 Mar 2011	06:09	18:23	12h 14m 09s	− 1m 31s	12:16	66.1°	148.789
17 Mar 2011	06:09	18:22	12h 12m 38s	− 1m 31s	12:16	65.7°	148.829
18 Mar 2011	06:10	18:21	12h 11m 06s	− 1m 31s	12:15	65.3°	148.870
19 Mar 2011	06:10	18:20	12h 09m 35s	− 1m 31s	12:15	64.9°	148.912
20 Mar 2011	06:11	18:19	12h 08m 03s	− 1m 31s	12:15	64.5°	148.953
21 Mar 2011	06:11	18:18	12h 06m 32s	− 1m 31s	12:15	64.1°	148.995
22 Mar 2011	06:12	18:17	12h 05m 00s	− 1m 31s	12:14	63.7°	149.038
23 Mar 2011	06:12	18:16	12h 03m 29s	− 1m 31s	12:14	63.3°	149.081
24 Mar 2011	06:12	18:14	12h 01m 58s	− 1m 31s	12:14	62.9°	149.124
25 Mar 2011	06:13	18:13	12h 00m 27s	− 1m 30s	12:13	62.5°	149.167
26 Mar 2011	06:13	18:12	11h 58m 56s	− 1m 30s	12:13	62.1°	149.211
27 Mar 2011	06:14	18:11	11h 57m 26s	− 1m 30s	12:13	61.8°	149.254
28 Mar 2011	06:14	18:10	11h 55m 55s	− 1m 30s	12:12	61.4°	149.298
29 Mar 2011	06:15	18:09	11h 54m 25s	− 1m 30s	12:12	61.0°	149.342
30 Mar 2011	06:15	18:08	11h 52m 55s	− 1m 30s	12:12	60.6°	149.385
31 Mar 2011	06:16	18:07	11h 51m 25s	− 1m 29s	12:12	60.2°	149.429

All times are in local time for Pretoria

APPENDIX D9: Rising and setting times for the Sun (April 2011)

["*timeanddate.com*", http://www.timeanddate.com/worldclock/astronomy.html?accessed 11/01/2013]

			Length of day		Solar noon		
Date	**Sunrise**	**Sunset**	**This day**	**Difference**	**Time**	**Altitude**	**Distance (10^6 km)**
1 Apr 2011	06:16	18:06	11h 49m 55s	− 1m 29s	12:11	59.8°	149.472
2 Apr 2011	06:17	18:05	11h 48m 26s	− 1m 29s	12:11	59.4°	149.516
3 Apr 2011	06:17	18:04	11h 46m 57s	− 1m 29s	12:11	59.0°	149.559
4 Apr 2011	06:17	18:03	11h 45m 28s	− 1m 28s	12:10	58.7°	149.602
5 Apr 2011	06:18	18:02	11h 43m 59s	− 1m 28s	12:10	58.3°	149.644
6 Apr 2011	06:18	18:01	11h 42m 31s	− 1m 28s	12:10	57.9°	149.687
7 Apr 2011	06:19	18:00	11h 41m 03s	− 1m 28s	12:10	57.5°	149.729
8 Apr 2011	06:19	17:59	11h 39m 35s	− 1m 27s	12:09	57.1°	149.771
9 Apr 2011	06:20	17:58	11h 38m 08s	− 1m 27s	12:09	56.8°	149.813
10 Apr 2011	06:20	17:57	11h 36m 41s	− 1m 26s	12:09	56.4°	149.855
11 Apr 2011	06:21	17:56	11h 35m 15s	− 1m 26s	12:08	56.0°	149.896
12 Apr 2011	06:21	17:55	11h 33m 48s	− 1m 26s	12:08	55.7°	149.938
13 Apr 2011	06:22	17:54	11h 32m 23s	− 1m 25s	12:08	55.3°	149.980
14 Apr 2011	06:22	17:53	11h 30m 57s	− 1m 25s	12:08	54.9°	150.021
15 Apr 2011	06:22	17:52	11h 29m 32s	− 1m 24s	12:07	54.6°	150.063
16 Apr 2011	06:23	17:51	11h 28m 08s	− 1m 24s	12:07	54.2°	150.104
17 Apr 2011	06:23	17:50	11h 26m 44s	− 1m 23s	12:07	53.9°	150.146
18 Apr 2011	06:24	17:49	11h 25m 21s	− 1m 23s	12:07	53.5°	150.188
19 Apr 2011	06:24	17:48	11h 23m 58s	− 1m 22s	12:06	53.2°	150.229
20 Apr 2011	06:25	17:47	11h 22m 35s	− 1m 22s	12:06	52.8°	150.271
21 Apr 2011	06:25	17:47	11h 21m 14s	− 1m 21s	12:06	52.5°	150.313
22 Apr 2011	06:26	17:46	11h 19m 52s	− 1m 21s	12:06	52.1°	150.354
23 Apr 2011	06:26	17:45	11h 18m 32s	− 1m 20s	12:06	51.8°	150.396
24 Apr 2011	06:27	17:44	11h 17m 12s	− 1m 20s	12:05	51.5°	150.437
25 Apr 2011	06:27	17:43	11h 15m 52s	− 1m 19s	12:05	51.2°	150.478
26 Apr 2011	06:28	17:42	11h 14m 34s	− 1m 18s	12:05	50.8°	150.519
27 Apr 2011	06:28	17:41	11h 13m 15s	− 1m 18s	12:05	50.5°	150.559
28 Apr 2011	06:29	17:41	11h 11m 58s	− 1m 17s	12:05	50.2°	150.600
29 Apr 2011	06:29	17:40	11h 10m 41s	− 1m 16s	12:05	49.9°	150.639
30 Apr 2011	06:30	17:39	11h 09m 26s	− 1m 15s	12:05	49.6°	150.679

All times are in local time for Pretoria

APPENDIX D10: Rising and setting times for the Sun (May 2011)

["*timeanddate.com*", http://www.timeanddate.com/worldclock/astronomy.html?accessed 11/01/2013]

			Length of day		Solar noon		
Date	**Sunrise**	**Sunset**	**This day**	**Difference**	**Time**	**Altitude**	**Distance (10^6 km)**
1 May 2011	06:30	17:38	11h 08m 10s	− 1m 15s	12:04	49.3°	150.717
2 May 2011	06:31	17:38	11h 06m 56s	− 1m 14s	12:04	49.0°	150.756
3 May 2011	06:31	17:37	11h 05m 43s	− 1m 13s	12:04	48.7°	150.793
4 May 2011	06:32	17:36	11h 04m 30s	− 1m 12s	12:04	48.4°	150.830
5 May 2011	06:32	17:36	11h 03m 18s	− 1m 11s	12:04	48.1°	150.867
6 May 2011	06:33	17:35	11h 02m 07s	− 1m 10s	12:04	47.8°	150.903
7 May 2011	06:33	17:34	11h 00m 57s	− 1m 09s	12:04	47.5°	150.938
8 May 2011	06:34	17:34	10h 59m 48s	− 1m 08s	12:04	47.2°	150.973
9 May 2011	06:34	17:33	10h 58m 40s	− 1m 07s	12:04	47.0°	151.008
10 May 2011	06:35	17:32	10h 57m 34s	− 1m 06s	12:04	46.7°	151.042
11 May 2011	06:35	17:32	10h 56m 28s	− 1m 05s	12:04	46.5°	151.075
12 May 2011	06:36	17:31	10h 55m 23s	− 1m 04s	12:04	46.2°	151.108
13 May 2011	06:36	17:31	10h 54m 19s	− 1m 03s	12:04	45.9°	151.141
14 May 2011	06:37	17:30	10h 53m 16s	− 1m 02s	12:04	45.7°	151.174
15 May 2011	06:37	17:30	10h 52m 15s	− 1m 01s	12:04	45.5°	151.206
16 May 2011	06:38	17:29	10h 51m 15s	− 1m 00s	12:04	45.2°	151.238
17 May 2011	06:38	17:29	10h 50m 16s	− 59s	12:04	45.0°	151.270
18 May 2011	06:39	17:28	10h 49m 18s	− 57s	12:04	44.8°	151.301
19 May 2011	06:39	17:28	10h 48m 21s	− 56s	12:04	44.6°	151.332
20 May 2011	06:40	17:27	10h 47m 26s	− 55s	12:04	44.3°	151.363
21 May 2011	06:40	17:27	10h 46m 32s	− 53s	12:04	44.1°	151.393
22 May 2011	06:41	17:27	10h 45m 40s	− 52s	12:04	43.9°	151.423
23 May 2011	06:41	17:26	10h 44m 49s	− 51s	12:04	43.7°	151.453
24 May 2011	06:42	17:26	10h 43m 59s	− 49s	12:04	43.6°	151.482
25 May 2011	06:42	17:26	10h 43m 10s	− 48s	12:04	43.4°	151.510
26 May 2011	06:43	17:25	10h 42m 24s	− 46s	12:04	43.2°	151.538
27 May 2011	06:43	17:25	10h 41m 38s	− 45s	12:04	43.0°	151.566
28 May 2011	06:44	17:25	10h 40m 54s	− 43s	12:04	42.9°	151.592
29 May 2011	06:44	17:25	10h 40m 12s	− 42s	12:05	42.7°	151.618
30 May 2011	06:45	17:24	10h 39m 31s	− 40s	12:05	42.6°	151.644
31 May 2011	06:45	17:24	10h 38m 52s	− 39s	12:05	42.4°	151.668

All times are in local time for Pretoria

APPENDIX D11: Rising and setting times for the Sun (June 2011)

["*timeanddate.com*", http://www.timeanddate.com/worldclock/astronomy.html?accessed 11/01/2013]

			Length of day		Solar noon		
Date	**Sunrise**	**Sunset**	**This day**	**Difference**	**Time**	**Altitude**	**Distance (10^6 km)**
1 Jun 2011	06:46	17:24	10h 38m 15s	− 37s	12:05	42.3°	151.692
2 Jun 2011	06:46	17:24	10h 37m 39s	− 35s	12:05	42.1°	151.715
3 Jun 2011	06:47	17:24	10h 37m 04s	− 34s	12:05	42.0°	151.737
4 Jun 2011	06:47	17:24	10h 36m 32s	− 32s	12:06	41.9°	151.758
5 Jun 2011	06:48	17:24	10h 36m 01s	− 30s	12:06	41.8°	151.778
6 Jun 2011	06:48	17:24	10h 35m 32s	− 29s	12:06	41.7°	151.798
7 Jun 2011	06:48	17:24	10h 35m 04s	− 27s	12:06	41.6°	151.817
8 Jun 2011	06:49	17:24	10h 34m 39s	− 25s	12:06	41.5°	151.835
9 Jun 2011	06:49	17:24	10h 34m 15s	− 23s	12:06	41.4°	151.853
10 Jun 2011	06:50	17:24	10h 33m 53s	− 22s	12:07	41.3°	151.869
11 Jun 2011	06:50	17:24	10h 33m 33s	− 20s	12:07	41.2°	151.886
12 Jun 2011	06:50	17:24	10h 33m 15s	− 18s	12:07	41.2°	151.902
13 Jun 2011	06:51	17:24	10h 32m 58s	− 16s	12:07	41.1°	151.917
14 Jun 2011	06:51	17:24	10h 32m 44s	− 14s	12:07	41.0°	151.932
15 Jun 2011	06:51	17:24	10h 32m 31s	− 12s	12:08	41.0°	151.946
16 Jun 2011	06:52	17:24	10h 32m 20s	− 10s	12:08	41.0°	151.960
17 Jun 2011	06:52	17:24	10h 32m 11s	− 09s	12:08	40.9°	151.973
18 Jun 2011	06:52	17:24	10h 32m 04s	− 07s	12:08	40.9°	151.986
19 Jun 2011	06:53	17:25	10h 31m 58s	− 05s	12:09	40.9°	151.998
20 Jun 2011	06:53	17:25	10h 31m 55s	− 03s	12:09	40.9°	152.010
21 Jun 2011	06:53	17:25	10h 31m 53s	− 01s	12:09	40.9°	152.021
22 Jun 2011	06:53	17:25	10h 31m 53s	< 1s	12:09	40.9°	152.032
23 Jun 2011	06:53	17:25	10h 31m 56s	+ 02s	12:09	40.9°	152.042
24 Jun 2011	06:54	17:26	10h 32m 00s	+ 04s	12:10	40.9°	152.051
25 Jun 2011	06:54	17:26	10h 32m 06s	+ 06s	12:10	40.9°	152.060
26 Jun 2011	06:54	17:26	10h 32m 14s	+ 07s	12:10	40.9°	152.068
27 Jun 2011	06:54	17:26	10h 32m 24s	+ 09s	12:10	41.0°	152.074
28 Jun 2011	06:54	17:27	10h 32m 35s	+ 11s	12:10	41.0°	152.081
29 Jun 2011	06:54	17:27	10h 32m 49s	+ 13s	12:11	41.1°	152.086
30 Jun 2011	06:54	17:27	10h 33m 04s	+ 15s	12:11	41.1°	152.090

All times are in local time for Pretoria

APPENDIX D12: Rising and setting times for the Sun (July 2011)

["*timeanddate.com*", http://www.timeanddate.com/worldclock/astronomy.html?accessed 11/01/2013]

			Length of day		Solar noon		
Date	**Sunrise**	**Sunset**	**This day**	**Difference**	**Time**	**Altitude**	**Distance (10^6 km)**
1 Jul 2011	06:54	17:28	10h 33m 21s	+ 17s	12:11	41.2°	152.093
2 Jul 2011	06:54	17:28	10h 33m 40s	+ 19s	12:11	41.3°	152.096
3 Jul 2011	06:54	17:29	10h 34m 01s	+ 20s	12:11	41.3°	152.097
4 Jul 2011	06:54	17:29	10h 34m 24s	+ 22s	12:12	41.4°	152.098
5 Jul 2011	06:54	17:29	10h 34m 48s	+ 24s	12:12	41.5°	152.098
6 Jul 2011	06:54	17:30	10h 35m 14s	+ 26s	12:12	41.6°	152.096
7 Jul 2011	06:54	17:30	10h 35m 42s	+ 27s	12:12	41.7°	152.095
8 Jul 2011	06:54	17:30	10h 36m 12s	+ 29s	12:12	41.8°	152.092
9 Jul 2011	06:54	17:31	10h 36m 43s	+ 31s	12:12	41.9°	152.089
10 Jul 2011	06:54	17:31	10h 37m 16s	+ 32s	12:13	42.1°	152.085
11 Jul 2011	06:54	17:32	10h 37m 51s	+ 34s	12:13	42.2°	152.080
12 Jul 2011	06:54	17:32	10h 38m 27s	+ 36s	12:13	42.3°	152.075
13 Jul 2011	06:54	17:33	10h 39m 05s	+ 37s	12:13	42.5°	152.069
14 Jul 2011	06:53	17:33	10h 39m 44s	+ 39s	12:13	42.6°	152.062
15 Jul 2011	06:53	17:34	10h 40m 25s	+ 41s	12:13	42.8°	152.056
16 Jul 2011	06:53	17:34	10h 41m 08s	+ 42s	12:13	42.9°	152.048
17 Jul 2011	06:53	17:34	10h 41m 52s	+ 44s	12:13	43.1°	152.040
18 Jul 2011	06:52	17:35	10h 42m 37s	+ 45s	12:13	43.3°	152.032
19 Jul 2011	06:52	17:35	10h 43m 24s	+ 46s	12:14	43.4°	152.023
20 Jul 2011	06:52	17:36	10h 44m 13s	+ 48s	12:14	43.6°	152.014
21 Jul 2011	06:51	17:36	10h 45m 03s	+ 49s	12:14	43.8°	152.004
22 Jul 2011	06:51	17:37	10h 45m 54s	+ 51s	12:14	44.0°	151.993
23 Jul 2011	06:50	17:37	10h 46m 46s	+ 52s	12:14	44.2°	151.982
24 Jul 2011	06:50	17:38	10h 47m 40s	+ 53s	12:14	44.4°	151.970
25 Jul 2011	06:50	17:38	10h 48m 35s	+ 55s	12:14	44.6°	151.957
26 Jul 2011	06:49	17:39	10h 49m 32s	+ 56s	12:14	44.8°	151.944
27 Jul 2011	06:49	17:39	10h 50m 30s	+ 57s	12:14	45.1°	151.929
28 Jul 2011	06:48	17:40	10h 51m 28s	+ 58s	12:14	45.3°	151.914
29 Jul 2011	06:48	17:40	10h 52m 28s	+ 1m 00s	12:14	45.5°	151.898
30 Jul 2011	06:47	17:41	10h 53m 30s	+ 1m 01s	12:14	45.8°	151.881
31 Jul 2011	06:47	17:41	10h 54m 32s	+ 1m 02s	12:14	46.0°	151.863

All times are in local time for Pretoria

APPENDIX D13: Rising and setting times for the Sun (August 2011)

["*timeanddate.com*", http://www.timeanddate.com/worldclock/astronomy.html?accessed 11/01/2013]

			Length of day		Solar noon		
Date	**Sunrise**	**Sunset**	**This day**	**Difference**	**Time**	**Altitude**	**Distance (10^6 km)**
1 Aug 2011	06:46	17:42	10h 55m 35s	+ 1m 03s	12:14	46.3°	151.845
2 Aug 2011	06:45	17:42	10h 56m 40s	+ 1m 04s	12:14	46.5°	151.825
3 Aug 2011	06:45	17:43	10h 57m 45s	+ 1m 05s	12:13	46.8°	151.805
4 Aug 2011	06:44	17:43	10h 58m 51s	+ 1m 06s	12:13	47.0°	151.784
5 Aug 2011	06:43	17:43	10h 59m 59s	+ 1m 07s	12:13	47.3°	151.762
6 Aug 2011	06:43	17:44	11h 01m 07s	+ 1m 08s	12:13	47.6°	151.740
7 Aug 2011	06:42	17:44	11h 02m 16s	+ 1m 09s	12:13	47.8°	151.717
8 Aug 2011	06:41	17:45	11h 03m 27s	+ 1m 10s	12:13	48.1°	151.693
9 Aug 2011	06:41	17:45	11h 04m 38s	+ 1m 11s	12:13	48.4°	151.669
10 Aug 2011	06:40	17:46	11h 05m 49s	+ 1m 11s	12:13	48.7°	151.644
11 Aug 2011	06:39	17:46	11h 07m 02s	+ 1m 12s	12:13	49.0°	151.619
12 Aug 2011	06:38	17:47	11h 08m 16s	+ 1m 13s	12:12	49.3°	151.593
13 Aug 2011	06:38	17:47	11h 09m 30s	+ 1m 14s	12:12	49.6°	151.567
14 Aug 2011	06:37	17:48	11h 10m 45s	+ 1m 14s	12:12	49.9°	151.541
15 Aug 2011	06:36	17:48	11h 12m 00s	+ 1m 15s	12:12	50.2°	151.514
16 Aug 2011	06:35	17:48	11h 13m 17s	+ 1m 16s	12:12	50.5°	151.487
17 Aug 2011	06:34	17:49	11h 14m 34s	+ 1m 17s	12:11	50.8°	151.459
18 Aug 2011	06:33	17:49	11h 15m 52s	+ 1m 17s	12:11	51.2°	151.432
19 Aug 2011	06:33	17:50	11h 17m 10s	+ 1m 18s	12:11	51.5°	151.403
20 Aug 2011	06:32	17:50	11h 18m 29s	+ 1m 18s	12:11	51.8°	151.375
21 Aug 2011	06:31	17:51	11h 19m 49s	+ 1m 19s	12:10	52.1°	151.345
22 Aug 2011	06:30	17:51	11h 21m 09s	+ 1m 20s	12:10	52.5°	151.316
23 Aug 2011	06:29	17:51	11h 22m 29s	+ 1m 20s	12:10	52.8°	151.286
24 Aug 2011	06:28	17:52	11h 23m 51s	+ 1m 21s	12:10	53.1°	151.255
25 Aug 2011	06:27	17:52	11h 25m 13s	+ 1m 21s	12:09	53.5°	151.223
26 Aug 2011	06:26	17:53	11h 26m 35s	+ 1m 22s	12:09	53.8°	151.191
27 Aug 2011	06:25	17:53	11h 27m 58s	+ 1m 22s	12:09	54.2°	151.159
28 Aug 2011	06:24	17:53	11h 29m 21s	+ 1m 23s	12:09	54.5°	151.125
29 Aug 2011	06:23	17:54	11h 30m 44s	+ 1m 23s	12:08	54.9°	151.091
30 Aug 2011	06:22	17:54	11h 32m 09s	+ 1m 24s	12:08	55.2°	151.057
31 Aug 2011	06:21	17:55	11h 33m 33s	+ 1m 24s	12:08	55.6°	151.022

All times are in local time for Pretoria

APPENDIX E1: WEATHER DATA FOR 2ND SEPTEMBER 2010, PRETORIA, SOUTH AFRICA

[http://www.underground.com/history, accessed 8/1/2013]

	Actual	Average	Record	
Temperature				
Mean Temperature	19 °C	-		
Max Temperature	30 °C	-	- ()	
Min Temperature	9 °C	-	- ()	
Cooling Degree Days	1			
Growing Degree Days	16 (Base 50)			
Moisture				
Dew Point	-1 °C			
Average Humidity	20			
Maximum Humidity	36			
Minimum Humidity	5			
Precipitation				
Precipitation	0.0 mm	-	- ()	
Wind				
Wind Speed	2 km/h ()			
Max Wind Speed	7 km/h			
Max Gust Speed	-			

T = Trace of Precipitation, MM = Missing Value Source: Averaged Metar Reports

APPENDIX E2: WEATHER DATA FOR 1ST DECEMBER 2010, PRETORIA, SOUTH AFRICA

[http://www.underground.com/history, accessed 8/1/2013]

Actual	Average	Record	
Temperature			
Mean Temperature	19 °C	-	
Max Temperature	30 °C	-	- ()
Min Temperature	17 °C	-	- ()
Cooling Degree Days	1		
Growing Degree Days	16 (Base 50)		
Moisture			
Dew Point	14 °C		
Average Humidity	58		
Maximum Humidity	75		
Minimum Humidity	34		
Precipitation			
Precipitation	0.0 mm	-	- ()
Wind			
Wind Speed	3 km/h ()		
Max Wind Speed	7 km/h		
Max Gust Speed	-		

T = Trace of Precipitation, MM = Missing Value Source: Averaged Metar Reports

APPENDIX E3: WEATHER DATA FOR 1ST MARCH 2011, PRETORIA, SOUTH AFRICA

[http://www.underground.com/history, accessed 8/1/2013]

Actual	Average	Record	
Temperature			
Mean Temperature	22 °C	-	
Max Temperature	28 °C	-	- ()
Min Temperature	17 °C	-	- ()
Cooling Degree Days	8		
Growing Degree Days	23 (Base 50)		
Moisture			
Dew Point	10 °C		
Average Humidity	40		
Maximum Humidity	62		
Minimum Humidity	14		
Precipitation			
Precipitation	0.0 mm	-	- ()
Wind			
Wind Speed	3 km/h ()		
Max Wind Speed	6 km/h		
Max Gust Speed	-		

T = Trace of Precipitation, MM = Missing Value Source: Averaged Metar Reports

APPENDIX E4: WEATHER DATA FOR 1ST JUNE 2011, PRETORIA, SOUTH AFRICA

[http://www.underground.com/history, accessed 8/1/2013]

Actual	Average	Record	
Temperature			
Mean Temperature	9 °C	-	
Max Temperature	15 °C	-	- ()
Min Temperature	3 °C	-	- ()
Degree Days			
Heating Degree Days	17		
Moisture			
Dew Point	-4 °C		
Average Humidity	34		
Maximum Humidity	50		
Minimum Humidity	9		
Precipitation			
Precipitation	0.0 mm	-	- ()
Wind			
Wind Speed	3 km/h ()		
Max Wind Speed	7 km/h		
Max Gust Speed	-		

T = Trace of Precipitation, MM = Missing Value Source: Averaged Metar Reports